The generation and evaluation of novel gut derived peptides for the treatment of Type 2 diabetes and obesity

By

Rachele Ann Perry, BSc (Hons) with DPP (Pathology)

School of Biomedical Sciences

Faculty of Life and Health Sciences

University of Ulster

A thesis presented for the degree of

Doctor of Philosophy

February 2019

(I confirm that the word count of this thesis is less than 100,000 words)

CONTENTS

Chapter 2: General Materials and Methods

ACKNOWLEDGEMENTS

I would like to take this opportunity to acknowledge and offer my sincerest thanks to Professor Victor Gault, to whom I will be eternally grateful for his unwavering support, advice and guidance, not only as his PhD student but back to my time as an undergraduate. I would also like to extend this gratitude to Dr Nigel Irwin who has been an invaluable addition to my PhD journey. I thank Professor Peter Flatt for the opportunity to complete my studies within the Diabetes Research Group and the other staff members for their encouragement throughout; Dr Charlotte Moffett, Dr Yasser Abdel-Wahab, Professor Stephen McClean, Professor Finbarr O'Harte, Professor Aine McKillop, Professor Neville McClenaghan and Professor Michael Conlon.

I also wish to acknowledge my fellow PhD students, both past and present; Neil, Andrew, Shruti, Vishal, Sarah, Ryan, Natalie, Prawej, Dipak, Galyna, Tak Ho Lo, Dr Chris McLaughlin, Dr Annie Hasib, Dr Michael Miskelly, Dr Dawood Khan, Dr Vadivel Parthsarathy, Dr Paul Millar, Dr Sagar Vyavahare and last but by no means least a very special thank you to my mentor Dr Ming T. Ng aka Tony. I would also like to thank Miss Leah Russell for her supporting role throughout my time in academia.

Finally, I would like to express my deepest gratitude to my parents and sister for their continued love, support and steadfast belief in my ability and to my dearest friends, especially Stephanie and Suzanne for their encouragement, patience and listening ear on this long journey, without which I may not have succeeded.

Summary

Type 2 diabetes mellitus (T2DM) is a leading non-communicable disease with increasing health, socio-economic implications and with pharmacological agents that fail to replicate the success of bariatric surgery. This thesis aims to evaluate the therapeutic potential of customised gastrointestinal (GIT)-derived peptide hormones, namely glucose-dependent insulinotropic polypeptide (GIP), xenin and neurotensin (NT) in the hope of advancing the therapeutic repertoire. GIP has important glucose-lowering endocrine and exocrine actions that become impaired in T2DM. Xenin is co-secreted with GIP and known to potentiate its biological actions. Thus, the biological and therapeutic potential of twice daily administration of a previously characterised GIP/xenin hybrid, (DAla^2)GIP/xenin-8-Gln, both alone and in combination with exendin-4 was assessed in high fat fed and *db/db* mouse models of T2DM. In HFF mice, treatment with (DAla^2)GIP-xenin-8-Gln in combination with exendin-4 was the most effective therapeutic strategy, although (DAla^2)GIP-xenin-8-Gln alone induced notable benefits in this model. Interestingly, in the *db/db* model, (DAla^2)GIP-xenin-8-Gln alone was much less efficacious than combined treatment with exendin-4, most likely linked to the disease severity and notable beta cell dysfunction. Further to this, NT has several antidiabetic actions and is known to facilitate fatty acid absorption. Xenin is structurally related to NT, with similar biological actions, thought to be partially mediated through NT receptors. Preliminary *in vitro* studies revealed that the novel acetyl-neurotensin(8-13)-xenin-8-Gln hybrid had antidiabetic attributes that warranted further *in vivo* assessment. Twice daily administration of acetyl-neurotensin(8-13)-xenin-8-Gln in combination with exendin-4 to HFF mice had positive glucose-lowering and insulinotropic effects with beneficial actions on lipid metabolism. Interestingly, GIP action has been linked to the exacerbation of obesity and T2DM, increasing insulin resistance and fat deposition. Thus, postulation that inhibiting GIP action could potentially halt the progression of obesity-related diabetes. However, to date there is no definitively characterised peptide-based GIP antagonist. Manipulation of the amino acid sequence, with N- and C- termini truncation, yielded Pro^3(3-30)GIP as a notable GIP receptor antagonistic that merits further testing. Overall, these data show that modified GIT peptides possess notable therapeutic efficacy with potential for translation to human T2DM and obesity.

Abbreviations

AAC	Area above the curve
ADP	Adenosine diphosphate
ANOVA	Analysis of variance
ATP	Adenosine triphosphate
AUC	Area under the curve
BMC	Bone mineral content
BMD	Bone mineral density
BMI	Body mass index
BSA	Bovine serum albumin
Ca^{2+}	Calcium
cAMP	Cyclic-AMP (3, 5'-cyclic monophosphate)
CNS	Central nervous system
CPM	Counts per minute
Da	Dalton(s)
(db/db)	Diabetic *(ob/ob)* mouse
DEXA	Dual-energy X-ray absorptiometry
dH_2O	Distilled water
DPP-IV	Dipeptidyl peptidase-4
DMSO	Dimethyl sulfoxide
ELISA	Enzyme linked immunosorbent assay
FBS	Foetal bovine serum
FFA	Free fatty acids
g	Gram(s)

GIP	Glucose-dependent insulinotropic polypeptide
GIPR	Glucose-dependent insulinotropic polypeptide receptor
GLP-1	Glucagon like peptide-1
GLUT	Glucose transporter
h	Hour(s)
HbA1c	Glycated haemoglobin
HBSS	Hanks balanced salt solution
HCl	Hydrochloric acid
HDL	High density lipoprotein
HEPES	N-2-hydroxyethyl-piperazine-N'-2-thane-sulphonic acid
HFF	High fat fed
HPLC	High performance liquid chromatography
IBMX	3-isobutyl-1 methylxanthine
IGT	Impaired glucose tolerance
i.p.	Intraperitoneal
K^+	Potassium
Kg	Kilogram(s)
KCl	Potassium chloride
KRBB	Krebs ringer bicarbonate buffer
l	Litre(s)
LDL	Low density lipoprotein
M	Molar
m/z	Mass-to-charge ratio
MALDI-TOF MS	Matrix-assisted laser desorption-Time of flight mass

	spectrometry
mg	Milligram
min	Minute(s)
ml	Millilitre(s)
mm	Millimetre(s)
mmol	Millimole(s)
n	Number of observations
ng	Nanogram(s)
nmol	Nanomole(s)
nM	Nanomolar
MALDI-ToF	Matrix assisted laser desorption ionisation time of flight spectrometry
OGTT	Oral glucose tolerance test
P	Probability
PAL	Palmitate
PBS	Phosphate buffered saline
PEG	Polyethylene glycol
PKA	Protein kinase A
PKC	Protein kinase C
RIA	Radioimmunoassay
RNA	Ribonucleic acid
rpm	Revolutions per minute
RT	Retention time
sec	Second(s)
S.E.M.	Standard error of the mean

t	Time
TCA	Tricarboxylic acid cycle
T2DM	Type 2 diabetes mellitus
TFA	Trifluoroacetic acid
U	Unit(s)
µg	Microgram(s)
µl	Microlitre(s)
v/v	Volume per volume
VLDL	Very low density lipoprotein
w/v	Weight per volume

DECLARATION

"I hereby declare that for 2 years following the date on which the thesis is deposited in the Library of the Ulster University, the thesis shall remain confidential with access or copying prohibited. Following expiry of this period I permit

1. the Librarian of the University to allow the thesis to be copied in whole or in part without reference to me on the understanding that such authority applies to the provision of single copies made for study purposes or for inclusion within the stock of another library.

2. The thesis to be made available through the Ulster Institutional Repository and/or EThOS under the terms of the Ulster eTheses Deposit Agreement which I have signed.

IT IS A CONDITION OF USE OF THIS THESIS THAT ANYONE WHO CONSULTS IT MUST RECOGNISE THAT THE COPYRIGHT RESTS WITH THE AUTHOR AND THAT NO QUOTATION FROM THE THESIS AND NO INFORMATION DERIVED FROM IT MAY BE PUBLISHED UNLESS THE SOURCE IS PROPERLY ACKNOWLEDGED."

Chapter 1

General Introduction

1.1 Peptide therapeutics

The area of gastrointestinal endocrinology involving the study of gastroenteropancreatic regulatory hormones/neuro peptides and the gut brain axis has become pivotal to scientific research and pharmaceutical development (Rehfeld 2015; Röder *et al.,* 2016). Research has focused on their locality, expression, secretory mechanisms, receptors, receptor binding and regulatory effects on: gastrointestinal motility, gastric acid secretion, pancreatic exocrine and carbohydrate metabolism to better understand their role under both normal and pathophysiological conditions (Rehfeld, 2012; 2015; Track, 1980). There is much interest in utilising these hormones as pharmacological agents, exploiting their pharmacokinetic and pharmacodynamic capabilities for the treatment of metabolic disease. As it is now understood, the gastrointestinal system is the largest endocrine organ, with gastrointestinal hormones extensively expressed outside the gut and neuropeptides expressed within the gut, thus it has vast potential as a major therapeutic target (Rehfeld, 2012; 2015).

1.2 The pancreas

The pancreas is a key regulatory organ located within the upper left side of the abdominal cavity, (behind the stomach) and comprises a head, body and tail (Figure 1.1). Its role as an organ within the body is to regulate metabolic homeostasis by secreting digestive enzymes and hormones (Röder *et al.,* 2016). Enzymes are secreted from exocrine cells into the accessory and pancreatic ducts and regulatory hormones are secreted from endocrine cells directly into the blood stream. Endocrine cells are located throughout exocrine tissue, where they cumulate together and assemble what is known as the Islets of Langerhans, which accounts for 1-2% of the whole organ and their secretions are key to regulating glucose homeostasis (Röder *et al.,* 2016). Islet architecture consists of five cell types all secreting different key hormones; alpha cells (15-20%) produce glucagon, beta cells (65-80%) produce insulin, ε cells produce ghrelin (<1%), gamma cells produce pancreatic polypeptide (PP) (3-5%) and delta cells produce somatostatin (3-10%) (Brereton *et al.,* 2015; Röder *et al.,* 2016).

Under normal conditions, it is primarily glucagon and insulin that are secreted by the pancreas to maintain glucose homeostasis within the ideal range (4-6 mmol/l). These two hormones achieve homeostasis by acting as a counterbalance to each other's

regulatory actions (Figure 1.2). In times of depleted blood glucose levels, glucagon is secreted from α-cells, and this triggers hepatic glycogenolysis and hepatic/renal gluconeogenesis elevating blood glucose levels. Conversely, when blood glucose levels become elevated β-cells are stimulated to secrete insulin by exocytosis (Figure 1.3). This enables insulin-dependent uptake of glucose by muscle and adipose tissue and therefore a lowering of blood glucose levels and initiation of glycogenesis and lipogenesis (Röder *et al.*, 2016).

Figure 1.1: The exocrine and endocrine function of the pancreas

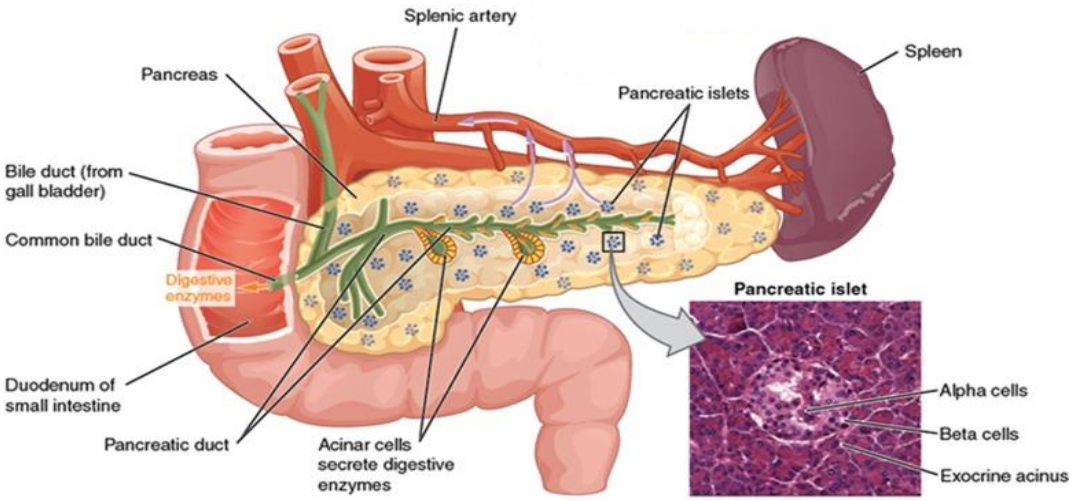

Pancreatic exocrine function involves secretion of digestive enzymes to the upper small intestine and endocrine function is to secrete several hormones from various cell types within the isles of Langerhans (Adapted from Röder *et al.*, 2016).

1.3 Type 2 diabetes mellitus an overview

Metabolic disturbances result in disease development and at the centre of gastroenteropancreatic dysregulation is T2DM (Röder *et al.*, 2016). T2DM is a chronic, non-communicable, multifactorial disease that is growing in prevalence. It occurs as a consequence of insulin resistance and impaired insulin secretion (Public Health England, 2018; Röder *et al.*, 2016). The former occurs when insulin progressively loses its efficacy on target muscle and adipose tissue. The latter

progresses because of a continuing decrease in glucose responsiveness causing glucose and lipid toxicity that results in a decrease in pancreatic beta cell mass (Kaku, 2010).

Figure 1.2: Glucose homeostasis

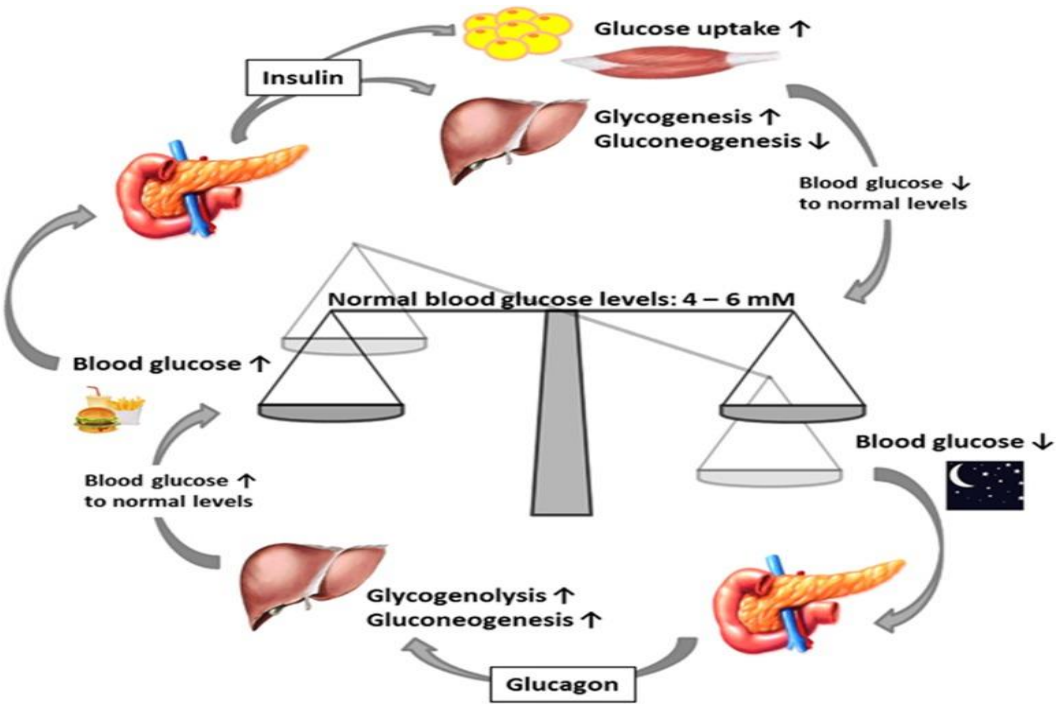

The mechanism of how blood glucose levels are balanced by glucose and insulin. Postprandially, blood glucose is high, insulin is secreted to initiate glucose uptake into muscle and adipose tissue and to promote glycogenesis. Conversely, when blood glucose is low, glucagon is secreted by the pancreas by glycogenolysis to increase endogenous blood glucose levels (Adapted from Röder *et al.*, 2016).

In the early stages of T2DM development, known as pre-diabetes, the body begins to compensate for increasing insulin resistance, by increasing the rate of insulin secretion (Dendup *et al.*, 2018). As a result, pancreatic beta cell mass increases and this is thought to be due to an increase in beta cell number but could also be linked to beta cell hypertrophy (Alarcon, 2016; Weir and Bonner-Weir, 2004). Eventually, the insulin produced has an inability to function normally, which is characterised by declining beta cell function, and over time this leads to prolonged, elevated blood glucose concentrations, a hyperglycaemic state (Röder *et al.*, 2016). This is

compounded by increased hepatic gluconeogenesis which in turn causes hepatic glucose production to increase thus exacerbating the hyperglycaemia (Redinger, 2007; Röder *et al.*, 2016).

Ultimately, the result is increased insulin resistance, decreased beta cell insulin secretion, and eventual beta cell exhaustion, thought to be induced by the increased stress, caused by inflammatory and oxidative states (Alarcon, 2016; Dendup *et al.*, 2018; Röder *et al.*, 2016). This tandem effect, the decline of beta cell function and insulin production, coupled with hyperglycaemia, exacerbates insulin resistance and T2DM (Alarcon, 2016; Dendup *et al.*, 2018; Weir and Bonner-Weir, 2004). The diagnostic criteria for T2DM is a fasting plasma of >7.0 mmol/l, an oral glucose tolerance of >11.1 mmol/l after 2 h and a haemoglobin A1c of 48 mmol/mol or 6.5% (Diabetes UK, 2018).

Figure 1.3: The insulin secretion cascade

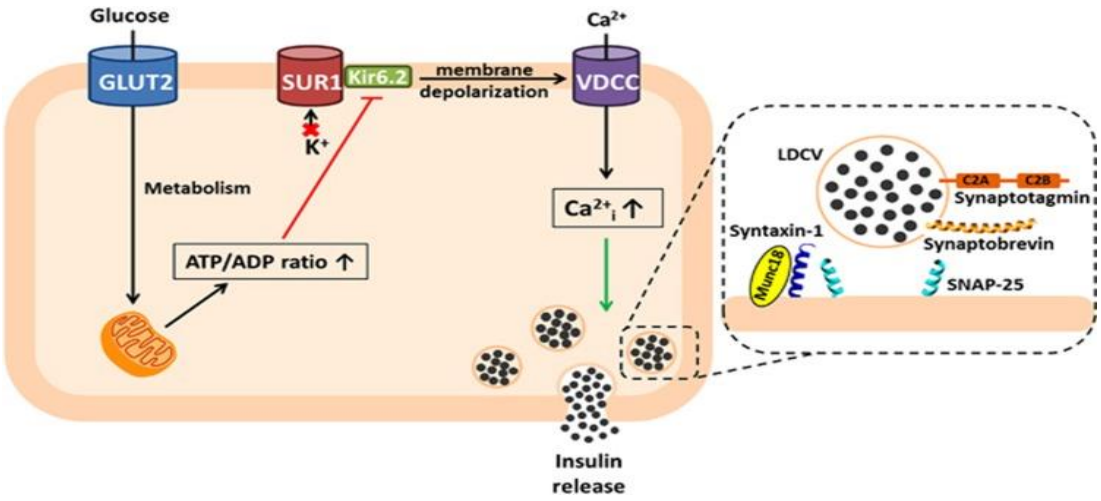

The mechanism for pancreatic beta cell insulin release. Uptake of exogenous glucose by GLUT2, undergoes glycolysis. The adenosine triphosphate (ATP) levels adjust the ATP/ADP ratio. This causes the ATP-sensitive K^+ channels to close and membrane depolarisation to occur opening the voltage-dependent Ca^{2+} channels as a response to the increase in intracellular calcium levels leading to vesicle fusion and ultimately insulin secretion (Adapted from Röder *et al.*, 2016).

There are several causative factors in development of T2DM. These risk factors include a genetic and/or ethnic predisposition and/or environmental factors such as a sedentary lifestyle, obesity, smoking, alcohol and aging (Figure 1.4; Public Health England, 2018). Globally, the prevalence of diabetes in 2015 was estimated to be 415 million adults and by 2040 this is expected to rise to 642 million (Dendup *et al.*, 2018). In the UK, 3.8 million people suffer from T2DM with 200,000 new cases diagnosed every year and a further 5 million at high risk of development (Public Health England, 2018). Furthermore, T2DM was listed by the World Health Organisation (WHO) as the sixth global cause of death in 2015 with approximately 1.6 million deaths from diabetes and related complications and/or diseases (Public Health England, 2018). Interestingly, this report also stated that diagnoses of T2DM is seven times more likely in obese adults than those of healthy weight and if recent trends continue, 1 in 3 people will be obese by 2034 and 1 in 10 will develop T2DM (Public Health England, 2018).

1.3.1 Obesity and T2DM

The primary causative factor of obesity in Western society is energy intake levels exceeding energy expenditure, resulting in the conversion of excess energy to fat. On a molecular level, excess circulating free fatty acids (FFA) are stored as triacylglycerol within adipocytes, which in turn cause a physiological accumulation of body fat mass. This simple mechanism of fat accumulation results in the manifestation of obesity and metabolic dysfunction (Redinger, 2007). Pathophysiologically, obesity is thought to result in metabolic dysfunction through the development of insulin resistance. The mechanism by which this occurs was first postulated by Randle *et al.*, (1963), where it was hypothesised that obesity-related insulin resistance was caused by the disruption of energy homeostasis, encompassing both dysregulation of lipid and glucose metabolism (Qatanani and Mitchell, 2007; Redinger, 2007). As obesity progresses, excess FFA are released from adipocytes due to enhanced lipolysis. This results in lipid toxicity causing insulin receptor dysfunction and a decrease in beta cell insulin secretion. An increase in macrophage activity along with the release of pro-inflammatory cytokines including TNF-α and IL1β, leads to a state of low grade inflammation, oxidative cellular stress and mitochondrial dysfunction (Boden, 2008; 2011; Greenberg and Obin, 2006).

1.3.2 The financial burden of T2DM

Financially T2DM is considered a major public health burden, as the NHS spends approximately 9% of its annual budget on the treatment of T2DM and associated diseases. In terms of monetary value this equates to approximately £8.8 billion (Public Health England, 2018). These figures are expected to rise over the next 25 years to 17% of the total annual budget (Diabetes UK, 2014; NHS, 2012). To the UK taxpayer, the total direct and indirect care costs are currently estimated at £23.7 billion and is expected to increase to £39.8 billion by 2035/6 (Diabetes UK, 2014).

Figure 1.4: Development of T2DM

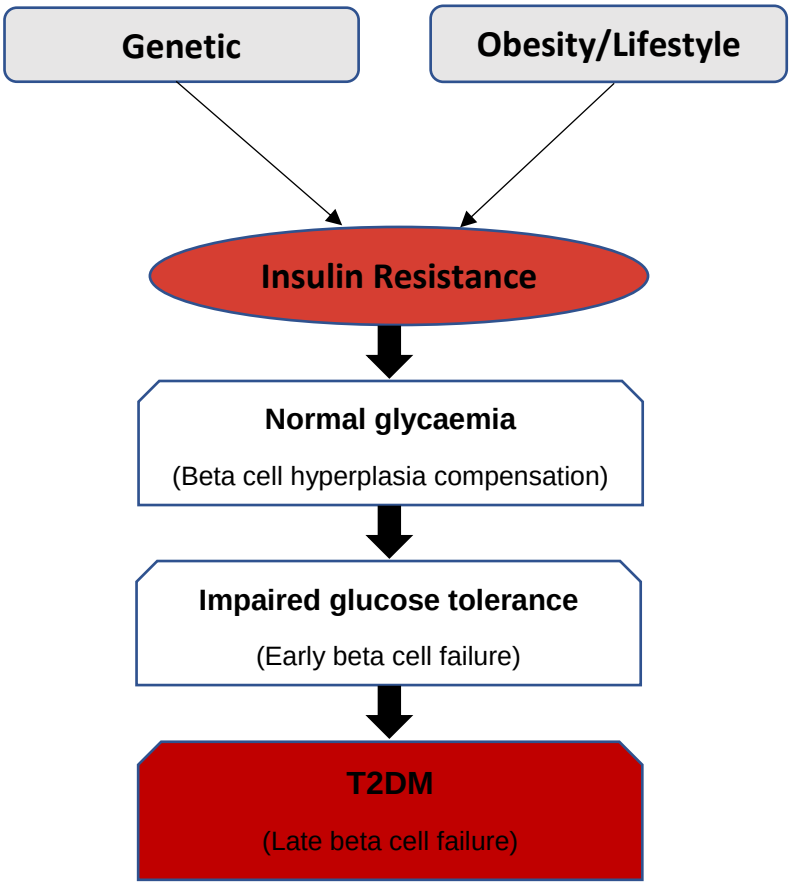

The aetiology and pathology of T2DM.

1.4 Current oral therapies for the treatment of T2DM

As diabetes progresses, the need for therapeutic intervention is essential for the individuals' well-being. The main objective is to increase insulin secretion, reduce hyperglycaemia and insulin resistance, along with energy regulation (Mayo Clinic, 2014). Treatment can range from implementation of dietary restriction and/or physical exercise to reduce BMI and waist circumference, improve glycaemic control and metabolic haemostasis. Often introduction of pharmaceutical therapeutics is necessary, as the majority of individuals fail to strictly adhere to non-pharmaceutical interventions (Chaudhury *et al.*, 2017; Olokoba *et al.*, 2012).

The range of pharmaceuticals available to treat diabetes is extensive and they target several of the pathophysiological mechanisms which lead to hyperglycaemia, and are given either alone or in combination. Some of these can be sub-divided into insulin sensitizers; biguanides and thiazolidinediones or insulin secretagogues; sulfonylureas, non-sulfonylureas alpha glucosidase inhibitors and incretin mimetics (Figure 1.5; Chaudhury *et al.*, 2017; Olokoba *et al.*, 2012).

Figure 1.5: Current T2DM therapeutics

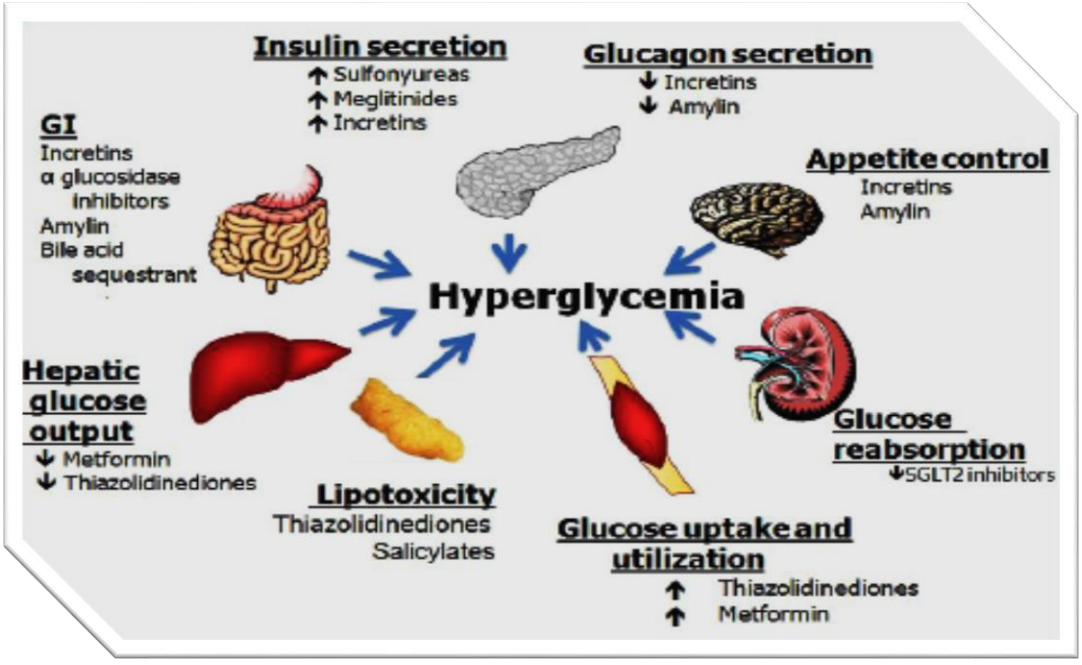

Current pharmaceutical agents for the treatment of T2DM sites of action (Adapted from Evans *et al.*, 2016).

1.4.1 Biguanides

There is currently only one biguanide available on the global market, known as metformin, (dimethylbiguanide). It is derived from *Galega officinalis* or more commonly known at goat's rue or French lilac (McCreight, Bailey and Pearson, 2016). Metformin is the initial treatment of choice for patients with obesity-diabetes (Evans *et al.,* 2016). Metformin does not stimulate insulin secretion, but rather works to increase insulin sensitivity and decrease gluconeogenesis, thus suppressing hepatic glucose production and increasing glucose uptake in skeletal muscle (Chaudhury *et al.,* 2017; Cheng and Fantus, 2005; Evans *et al.,* 2016).

Interestingly, a study by Zhou *et al.,* (2001) ascertained that metformin has another mechanism of action, as it activates the adenosine monophosphate-activated protein kinase (AMPK) enzyme found in muscle and liver tissue. Normal activation is by adenosine monophosphate which is a by-product of adenosine triphosphate and a cellular signal for increased energy (Chaudhury *et al.,* 2017; Cheng and Fantus, 2005). Activated AMPK causes phosphorylation and inhibition of acetyl-coenzyme A carboxylase, which acts as a catalyst to limit lipogenesis reducing the production of FFA (Chaudhury *et al.,* 2017). Hepatic AMPK can also reduce the transcription factor expression of sterol-regulatory-element-binding-protein-1 (SREBP-1), a known mediator of insulin resistance and dyslipidaemia pathogenesis (Zhou *et al.,* 2001). Additionally, Miller and colleagues (2013) have shown metformin to have another mechanism of action, reducing fasting glucose levels by antagonising glucagon action (Miller *et al.,* 2013). Metformin causes AMP and nucleotides to accumulate, thus inhibiting adenylate cyclase, reducing the activity of cyclic AMP and protein kinases A (PKA), and abolishing phosphorylation of PKA targets and hepatocytes are then obstructed from glucagon-dependent glucose output (Miller *et al.,* 2013).

Metformin is known to be a safe mono-pharmaceutical and when used in conjunction with other T2DM therapeutics and other prescribed medications. It has proven efficacy not only in reducing fasting plasma glucose but also fasting plasma insulin, triglycerides and free fatty acids (FFA) (Evans *et al.,* 2016). However, with any medication it can have adverse effects including gastrointestinal disturbance and cause vitamin B12 and folic acid deficiency, as well as fatal lactic acidosis due to severe renal insufficiency (Chaudhury *et al.,* 2017; Evans *et al.,* 2016).

1.4.2 Thiazolidinediones

Thiazolidinediones (TZDs) such as pioglitazone are also used to improve insulin sensitivity by increasing glucose uptake in adipose, liver and muscle tissue. The action of thiazolidinediones are thought to occur by modulating peroxisome proliferator-activated receptor gamma (PPARγ) on adipocytes, as these regulate the expression of genes involved with lipid and carbohydrate metabolism. This results in enhanced differentiation and a reduction in lipolysis and circulating adipo-cytokine levels (Chaudhury *et al.*, 2017; Evans *et al.*, 2016). There is also an improvement in lipogenesis and storage and therefore reduced FFA. This results in preserving beta cell integrity and function, which helps to improve insulin resistance and prevent beta cell exhaustion (Chaudhury *et al.*, 2017; Evans *et al.*, 2016). Thiazolidinediones can be used as a monotherapy or in combination with metformin and other therapeutics. However, in some countries, TZDs are not approved for use in combination with insulin due to reported adverse effects to include peripheral oedema and congestive heart failure (Chaudhury *et al.*, 2017; Evans *et al.*, 2016). Continued use of pioglitazone has also been linked to bladder cancer and usage restrictions have been enforced by US Food and Drugs Administration (FDA) and European Medicines Agency (EMA) in those at risk of development or with bladder cancer (Evans *et al.*, 2016).

1.4.3 Sulfonylureas

Sulfonylureas were initially developed in the 1950's and continue to be used as therapeutic agents for treatment of T2DM (Evans *et al.*, 2016). Sulfonylureas increase insulin release by directly targeting the beta cell and their mechanism of action is to cause depolarisation of the cell membrane through binding to the sulfonylurea receptor on the cell surface. This inhibits the potassium efflux and opens the calcium channels and thus insulin is released (Fowler, 2007). Furthermore, sulfonylureas can restrict gluconeogenesis, reduce lipogenesis and decrease the clearance rate of insulin by the liver (Chaudhury *et al.*, 2017). The first-generation sulfonylureas have now been replaced with second generation sulfonylureas that have improved safety profiles and these include glyburide and glipizide (Evans *et al.*, 2016; Fowler, 2007). This drug class can become self-limiting in those with late stage T2DM because there are

insufficient beta cells to elicit a therapeutic response (Evans *et al.*, 2016; Fowler, 2007). These pharmaceuticals are normally prescribed as a secondary or additional line of treatment but are contraindicated during pregnancy and in cases of hepatic and renal disease. Adverse effects include hypoglycaemia, hyponatremia and an increase in body weight (Chaudhury *et al.*, 2017; Evans *et al.*, 2016).

1.4.4 Non-sulfonylureas/meglitinides

Non-sulfonylureas also known as meglitinides, repaglinide and nateglinide work similar to sulfonylureas, binding to the receptor on the beta cell, although meglitinides have a reduced binding affinity and thus a reduced half-life. Meglitinides also have a reduced efficacy compared to sulfonylureas because the therapeutic effect is only initiated under high levels of hyperglycaemia (Chaudhury *et al.*, 2017; Fowler, 2007). The adverse effects are the same as those described in sulfonylureas, although episodes of hypoglycaemia are less likely due to shorter duration of action.

1.4.5 Alpha glucosidase inhibitors

Alpha glucosidase inhibitors, of which only acarbose is utilised within the UK, slow down the rate that carbohydrates are absorbed to reduce hyperglycaemic peaks. They block complex carbohydrates from enzymatic degradation in the small intestine by competitively binding to the α-glucosidase enzymes binding site on the oligosaccharide and thus prevent enzymatic hydrolysis (Evans *et al.*, 2016). Adverse effects include gastrointestinal issues including, but not limited to, flatulence caused by the increased level of carbohydrates within the colon, bloating and diarrhoea (Evans *et al.*, 2016).

1.4.6 Sodium-glucose cotransporter 2 (SGLT2) inhibitors

Sodium-glucose cotransporter 2 (SGLT2) inhibitors are a relatively new class of pharmaceutical agents for T2DM. SGLT2 inhibitors, such as dapagliflozin, have a

mechanism of action that is dependent on glucose not insulin. These drugs lower hyperglycaemia by preventing the kidney from reabsorbing glucose from within the proximal renal tubule by inhibiting SGLT2 (Chaudhury *et al.,* 2017). This mechanism allows for other therapies to be used in combination thus utilise their insulinotropic therapeutic effect in tandem. Insulin can also be utilised in combination with SGLT2 inhibitors (Ferrannini and Solini, 2012). SGLT2 inhibitors increase weight loss and reduce blood pressure but there is also associated adverse effects and these include; infections of genitourinary system, in some cases ketoacidosis and cancer. The efficacy of SGLT2 inhibitors can also be reduced when glomerular function is impaired (Chaudhury *et al.,* 2017; Ferrannini and Solini, 2012).

1.5 Bariatric surgery

Bariatric surgery is primarily used for obesity-diabetes in those with a BMI >30-35 kg/m^2 as it can significantly increase sustainable weight loss (Meek *et al*., 2016; Singh, Singh and Kota, 2015). Currently, the main three methods used are gastric banding, sleeve gastrectomy and *Roux-en-Y* gastric bypass (RYGB), the latter being the predominant choice (Figure 1.6; Meek *et al*., 2016; Singh, Singh and Kota, 2015). Gastric banding and sleeve gastrectomy methods both reduce the stomach capacity. The former utilises an adjustable silicone ring, forming a small pouch at the lower oesophagus and the latter involves the removal of a lateral section, with a reduced long-sleeve shape stomach remaining (Meek *et al*., 2016).

RYGB alters the passage of nutrients, as a small stomach pouch is constructed using staples and drained directly into the segmented jejunum, forming the Roux limb (Meek *et al*., 2016). Nutrients can then move down the alimentary limb, bypassing the remaining stomach and duodenum. The alimentary limb is then anastomosed with the distal biliopancreatic limb, creating the common limb where the nutrients are combined, for a shorter time with the biliopancreatic secretions. Time and nutritional absorption are dependent on the length of the common limb (Meek *et al*., 2016). Subsequently, with this alteration to the nutritional tract and absorption time, RYGB is demonstrated to resolve the associated disease pathologies of T2DM, inducing

euglycemia and normalising glycated haemoglobin leading to remission within a matter of days, in approximately 80% of patients (Singh *et al.*, 2015).

Figure 1.6: Types of bariatric surgery

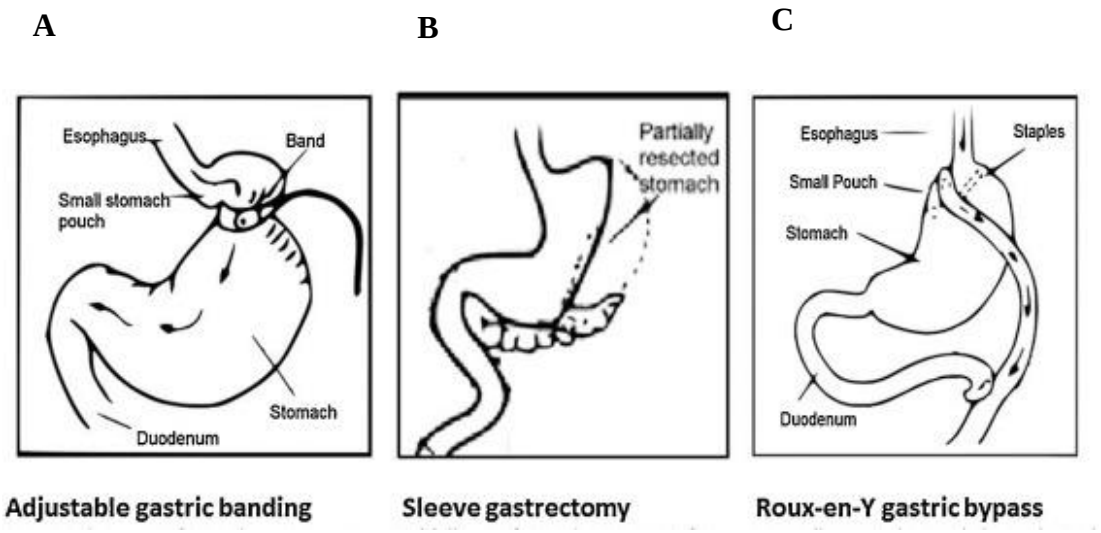

Gastric banding (A), the band can be altered to augment or decrease the effects. Sleeve gastrectomy (B), the stomach is permanently reduced by the removal of a lateral section. *Roux-en-Y* gastric bypass (C), a stomach pouch is constructed and joined to the jejunum along with the biliopancreatic limb to form the Y shape that ends with the common limb (Adapted from Meek *et al*., 2016).

There are several postulated mechanisms of action for the remission of T2DM (Figure 1.7), including the hindgut hypothesis (Cummings and colleagues (2004)) and the foregut hypothesis (Rubino and colleagues (2006)) amongst others (Meek *et al*., 2016; Pok and Lee, 2014; Singh *et al.*, 2015). The foregut hypothesis suggests that it is the exclusion of nutrients from the duodenum and proximal jejunum transit, inhibiting nutrient-induced secretion of a putative signal which augments insulin resistance and T2DM. One such candidate could be glucose-dependent insulinotropic polypeptide (GIP), that is recognised to be largely secreted from the duodenum and proximal jejunum (Campbell and Drucker, 2013). The hindgut hypothesis proposes that improved glucose control is gained by the accelerated transport of

nutrients to the distal small intestine, in turn inducing secretion of a physiological signal that improves glucose homeostasis (Pok and Lee, 2014). Indeed, glucagon like peptide-1 (GLP-1) is known to be predominantly secreted from the distal small intestine (Campbell and Drucker, 2013), and is therefore often linked to hindgut hypothesis.

Taken together, these hypotheses attribute the change in gut hormone secretion and action such as, but not limited to, GLP-1, peptide tyrosine tyrosine (PYY) and GIP, oxyntomodulin and pancreatic polypeptide (PP) (Meek *et al.,* 2016; Singh *et al.,* 2015). These changes in gut hormone secretion profile positively affect appetite and satiety as well as energy expenditure and are thought to attribute to sustaining the weight loss effect as well as improved glucose homeostasis (Meek *et al.,* 2016; Singh *et al.,* 2015; Troke, 2014).

However, initial improvement/remission is thought to be caused by dramatic reduction in plasma glucose levels following the surgery due to the acute negative calorie balance, thus within days there is normalisation of plasma glucose levels (Singh *et al.,* 2015). In addition, following the surgical re-direction of nutrients directly to the distal jejunum, which produces GLP-1 significantly increase its secretion and seems to augment the response to insulin, further contributing to alleviation of the disease pathologies (Singh *et al.,* 2015).

Furthermore, bariatric surgery has limitations in terms of its applicability to non-obese T2DM individuals (Singh *et al.,* 2015). Thus, the duodenal-jejunal bypass liner (DJBL), which is a non-surgical endoscopic method was developed to replicate the effect of RYGB, denoted as ‘metabolic surgery’ and has now been shown to exert significant improvements on glycaemic control (Singh *et al.,* 2015).

The adverse effects associated with bariatric surgery include an increased mortality rate, expense of surgery and post-surgical care, as well as acute complications. These occur in approximately 5-10% of cases and can result in leakages, obstructions and post-operative infections as well as other long-term complications such as internal hernias and nutritional deficiencies. Post-operatively, bariatric surgery has also been linked to having a detrimental effect on emotional well-being (Capozzi *et al.,* 2018; Pories, 2008; Singh *et al.,* 2015; Schauer *et al.,* 2017).

Figure 1.7: Suggested mechanisms for remission of T2DM

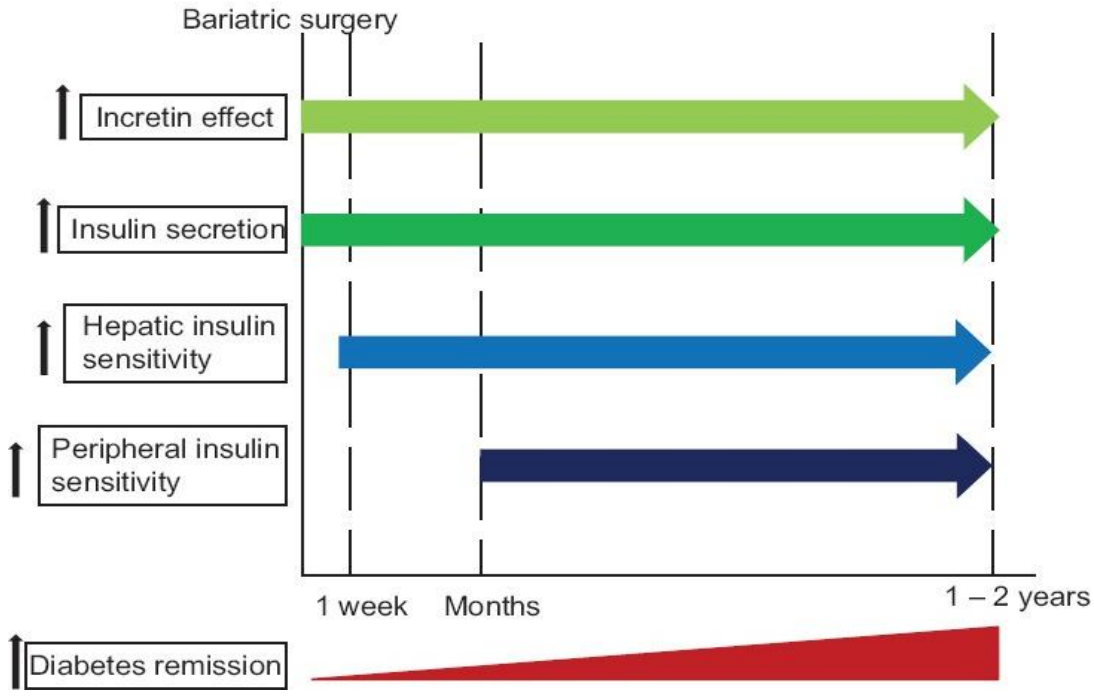

A timeline showing the suggested mechanisms of improving T2DM post-bariatric surgery (Adapted from Singh *et al.*, 2015).

1.6 Enteroendocrine hormones

Enteroendocrine hormones are recognised to play an important role in the control of metabolism and blood glucose levels (Campbell and Drucker, 2013; Psichas, Reimann and Gribble, 2015). Two of the major players in this regard, termed the incretin hormones, are GLP-1 and GIP (Campbell and Drucker, 2013). In addition, other notable enteroendocrine-derived regulators of metabolic state include, but not limited to, oxyntomodulin, PP, PYY, xenin, somatostatin and ghrelin. This enteroendocrine sensory system relates to the initial secretion of enteroendocrine hormones postprandially, which exert physiological responses to regulate glucose homeostasis, islet hormone secretion, lipid metabolism as well as appetite, gastrointestinal motility and body weight (Campbell and Drucker, 2013; Leckstrom *et al.*, 2009; Psichas, Reimann and Gribble, 2015).

Incretins are secreted by enteroendocrine cells located within the gastrointestinal tract in response to increased circulating glucose levels (Campbell and Drucker, 2013). Activation is initiated by orally ingested glucose, which in turn stimulates insulin secretion from pancreatic beta cells that express the specific G-protein coupled receptors for respective incretin hormone (Paschetta, Hvalrug and Musso, 2011). Thus, the 'incretin effect' is said to be the difference in insulin secretory response from an oral glucose load compared to a similar intravenously administered glucose challenge (Chaudhury *et al.,* 2017). Full proof of the incretin effect was not confirmed until 1964, when insulin concentrations could be determined by radioimmunoassay (RIA) (Creutzfeldt, 2004). Interestingly, enteroendocrine cells account for approximately 1% of intestinal epithelial cells yet it is estimated that 50-70% of total insulin secretion can be attributed to the incretin effect (Chaudhury *et al.,* 2017; Gault *et al.,* 2003; Psichas, Reimann and Gribble, 2015).

In contrast, if the incretin effect becomes dysregulated or impaired, the enteroendocrine system has no compensatory mechanism, this loss is an early indicator and characteristic of T2DM (Al-Sabah, 2015). Loss of incretin effect contributes to a defective response to both GLP-1 and GIP as well as impaired secretion of GLP-1 (Freeman, 2009). However, the insulinotropic response of GLP-1 can be restored through the administration of GLP-1 agonists, thus the impairment can be overcome and offers a valuable treatment option for T2DM. However, this is not the case with GIP, as T2DM progresses GIP beta cell insulinotropic response decreases. The mechanism underpinning this remains largely unclear, but studies have postulated that the progressing hyperglycaemia detrimentally affects GIP receptor (GIPR) signalling to a higher degree than that of the GLP-1 receptor (GLP-1R) (Al-Sabah, 2015). Furthermore, a study by Zhou and colleagues, (2007) using rat and human pancreatic islets under hyperglycaemic conditions revealed that GIPR expression, GIP-mediated cAMP, and insulin production were substantially decreased in T2DM (Al-Sabah, 2015).

GLP-1 and GIP action is also inhibited by the glycoprotein, CD26 better known as dipeptidyl peptidase-IV (DPP-IV). DPP-IV is a type II transmembrane protein with 4 domains; the cytoplasmic domain (1–6), the transmembrane domain (TMD) (7–28), the flexible stalk segment (29–39), and an extracellular domain (40–766) (Röhrborn,

Wronkowitz and Eckel, 2015). DPP-IV has multiple functions including acting as a binding partner for several peptides, and as an exopeptidase cleaving various substrates including incretin hormones, reducing their bioavailability. DPP-IV exerts its effects on incretin hormones by selectively cleaving their N-terminal amino acids in circulating plasma inhibiting their insulinotropic action, and ultimately their therapeutic efficacy (Röhrborn, Wronkowitz and Eckel, 2015; Seino and Yabe 2011).

1.6.1 Glucagon-like-peptide-1 (GLP-1)

GLP-1 is derived from post translational cleavage of the proglucagon gene by prohormone convertase PC 1/3 (Campbell and Drucker, 2013). This gene also encodes for glucagon-like peptide-2 and glucagon, with both peptides having a 50% homology to GLP-1 (Campbell and Drucker, 2013). There are two bioactive forms of GLP-1, amidated GLP-1(7-36) and non-amidated GLP-1(7-37), and both elicit metabolic actions (Seino and Yabe 2011). Enteroendocrine intestinal epithelial L-cells, located in the distal ileum and colon, secrete GLP-1 in response to nutritional ingestion as well as neural and endocrine factors (Campbell and Drucker, 2013; Psichas, Reimann and Gribble, 2015). Secretion is mediated by the automatic nervous system including the vagus nerve, neurotransmitters gastrin-releasing peptide (GRP) and acetyl choline as well as GIP (Baggio and Drucker, 2007; Campbell and Drucker, 2013). These activate protein kinase A (PKA), protein kinase C (PKC), calcium and mitogen-activated protein kinase (MAPK). Secretion occurs in a biphasic manner with the initial phase lasting 10-15 minutes and the secondary phase 30-60 minutes (Baggio and Drucker, 2007; Campbell and Drucker, 2013; Seino and Yabe 2011).

GLP-1R's belong to the class B family of G-protein coupled receptors (GPCRs), which have a large extracellular N-terminal domain (NTD) linked to a 7-transmembrane helical domain (Baggio and Drucker, 2007; Capozzi *et al.*, 2018; Seino, Fukushima and Yabe 2010). The N-terminal receptor domain is key for GLP-1R binding and the third intracellular loop is essential for coupling the receptor to specific G-proteins, crucial for signal and activation actions (Baggio and Drucker, 2007; Seino, Fukushima and Yabe 2010). The GLP-1R is expressed on pancreatic alpha, beta and delta cells, the lungs, kidneys, heart, stomach, intestines, skin, pituitary and nodose ganglion

neurons, and within regions of the central nervous system (CNS) mainly the hypothalamus and brain stem; hippocampus/cerebral cortex etc. (Baggio and Drucker, 2007; Campbell and Drucker, 2013; Seino, Fukushima and Yabe 2010).

Once receptor binding occurs, the biological actions of GLP-1 include: slowing gastric emptying, inhibiting glucagon production and increasing insulin secretion. In addition, GLP-1 suppresses appetite, lowers body weight and exhibits, anti-inflammatory properties (Capozzi *et al.,* 2018). Receptor binding on beta cells initiates insulin secretion by activating adenylate cyclase activity and production of cAMP. Other mechanisms are thought to include calcium and potassium ion channels, as well as intracellular energy homeostasis and exocytosis (Baggio and Drucker, 2007; MacDonald *et al.,* 2005; Seino and Yabe 2011). GLP-1 can also preserve islet morphology and restore glucose sensitivity of resistant beta cells by up-regulating glucose transporters and glucose kinase expression (Baggio and Drucker, 2007). This improves the ability of the beta cell to sense and respond to glucose. Furthermore, GLP-1 increases beta cell proliferation, neogenesis and prevention of apoptosis, via the phosphoinositide 3-kinase pathway (Baggio and Drucker, 2007; Seino, Fukushima and Yabe 2010). Native GLP-1 has a relatively short half-life of approximately one and a half minutes as it is subject to enzymatic degradation by DPP-IV (Röhrborn, Wronkowitz and Eckel, 2015; Tulaihi and Alhabib, 2017). Therefore, biologically active and enzymatically resistant GLP-1 receptor agonists have been developed for the treatment of T2DM.

1.6.2 GLP-1 receptor agonists

Injectable GLP-1 receptor agonists (GLP-1 RA), are analogues of GLP-1 that bind to its receptor and stimulate bioactive effects (Tulaihi and Alhabib, 2017). There are several variations available including; exenatide, lixisenatide, liraglutide, albiglutide and dulaglutide (Marín-Penalver *et al.,* 2016). They are classified by their therapeutic duration, either short-acting or long-acting, with half-lives ranging from 2.4 hours up to several days (Chaudhury *et al.,* 2017; Marín-Penalver *et al.,* 2016). The combined use of a DPP-IV inhibitor may also be warranted to further enhance the half-life and

therapeutic efficacy (Chaudhury *et al.*, 2017; Jackson *et al.*, 2010; Marín-Penalver *et al.*, 2016).

The first GLP-1 RA to be introduced to the market (2005), was the short-acting, twice daily synthetic analogue exenatide (Chaudhury *et al.*, 2017; Hansen, Vilsboll and Knop, 2010; Marín-Penalver *et al.*, 2016). It is identical to exendin-4, a 39 amino acid peptide derived from the venom of *Heloderma suspectum* lizard (Gila monster), and it shares a 53% sequence homology to native GLP-1 with potent agonist properties on the GLP-1R (Marín-Penalver *et al.*, 2016; Seino, Fukushima and Yabe 2010; Tulaihi and Alhabib, 2017). Short-acting GLP-1 RA provide brief receptor activation with therapeutic effects primarily directed towards postprandial hyperglycaemia and gastric emptying, with a lesser effect on fasting glucose (Marín-Penalver *et al.*, 2016). The long-acting, once daily GLP-1 RA liraglutide, and long-acting release (LAR) once weekly exenatide, as well as albiglutide and dulaglutide elicit their therapeutic effect by continuously activating the GLP-1R (Capozzi *et al.*, 2018; Chaudhury *et al.*, 2017; Freeman, 2009; Marín-Penalver *et al.*, 2016; Tulaihi and Alhabib, 2017). Thus, slowing gastric emptying, inhibiting glucagon production and increasing insulin production (Figure 1.8). Therapeutic effects, demonstrated by clinical data include improved glucose homeostasis and a reduction in body weight, essential for treating T2DM. Also noted was a reduction in systolic blood pressure and protection against cardiovascular events (Capozzi *et al.*, 2018; Chaudhury *et al.*, 2017).

Importantly, exendin-4 is resistant to DPP-IV degradation due to a glycine at position 2. Exendin-4, pre-clinically, was shown to have superior potency on lowering blood glucose levels attributed to extended circulating ability (Tulaihi and Alhabib, 2017). Exendin-4 (exenatide) was also shown to reduce glycated haemoglobin, improve beta cell function and decrease fasting and postprandial glucose levels in T2DM patients, with a potency estimated to be 5000 times greater than native GLP-1 (Seino, Fukushima and Yabe 2010).

More recently, studies utilising a GLP-1R antagonist exendin (9-39) propose GLP-1 has an energy intake reducing function subsequent to bariatric surgery (Capozzi *et al.*, 2018). GLP-1 concentrations are elevated to supraphysiological levels and appear to reduce appetite. Furthermore, GLP-1 is implicated as a major contributor to improved glycaemic control following bariatric surgery. However, it is postulated that

pharmacologically GLP-1 administered to supraphysiological levels would yield similar therapeutic effects but these concentrations are not well tolerated and result in adverse effects (Capozzi *et al.,* 2018; Nauck and Meier, 2018). GLP-1 RA are not prescribed to those that suffer or have a history of pancreatitis. Other adverse effects range from mild-to-moderate gastrointestinal disruption, nausea, vomiting and diarrhoea (Marín-Penalver *et al.,* 2016). Reactions at injection sites is another common problem with GLP-1 RA and can cause abscesses, cellulitis and necrosis. Additionally, the development of antibodies to GLP-1 RA can also occur (Marín-Penalver *et al.,* 2016).

Figure 1.8: Incretin mimetics: GLP-1 receptor agonists

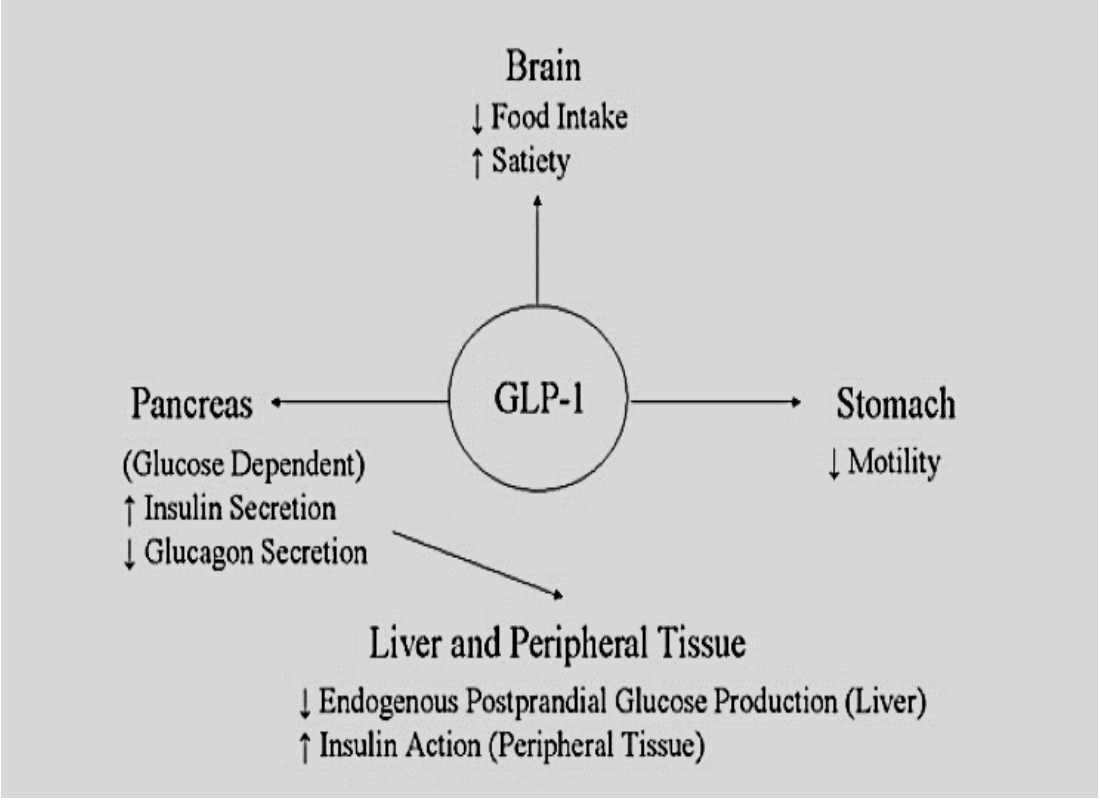

The pharmacological effects of GLP-1 receptor agonists in T2DM (Adapted from Evans *et al.,* 2016).

1.6.3 DPP-IV inhibitors

DPP-IV inhibitors are administered orally, usually once daily, and can be employed as a mono therapy, or alongside metformin, thiazolidinediones or sulfonylureas as a combination therapeutic (Nauck, 2016; Tulaihi and Alhabib, 2017). DPP-IV inhibitors main mechanism of action is to inhibit the enzymatic degradation of endogenous incretins GLP-1 and GIP (Capozzi *et al.*, 2018; Chaudhury *et al.*, 2017; Fowler, 2007). They act to reduce the serum activity of DPP-IV by >80%, thus increasing levels of biologically active GLP-1 (Nauck, 2016). The first approved DPP-IV inhibitor was the non-peptide heterocyclic compound sitagliptin in 2006, which is long-acting with a rapid onset (Nauck, 2016). With the subsequent introduction of vildagliptin and saxagliptin, which are long-acting, slow onset cyanopyrrolidines. Others include linagliptin, a methylxanthine and the newest to the market is alogliptin, a heterocyclic aminopiperidine (Chaudhury *et al.*, 2017; Nauck, 2016). Due to the variation in chemical structure their pharmacokinetic properties, bioavailability, half-life, plasma peak level and mode of excretion also differ (either renal or hepatic) (Nauck, 2016; Tulaihi and Alhabib, 2017).

Additionally, treatment with the DPP-IV inhibitor sitagliptin was shown to improve cardiac function and coronary artery perfusion (Chaudhury *et al.*, 2017). Adverse effects include acute pancreatitis and risk of hypoglycaemia, especially in those with reduced renal function. Certain medications are also contraindicated including warfarin and digoxin. Exenatide has been shown to increase the anticoagulant effect of warfarin and plasma levels of digoxin are increased by sitagliptin (Chaudhury *et al.*, 2017).

1.6.4 Glucose-dependent insulinotropic polypeptide (GIP)

Enteroendocrine K cells secrete GIP in response to ingestion of glucose and fat in an absorption dependent manner (Baggio and Drucker, 2007; Psichas, Reimann and Gribble, 2015). These cells are mainly located in the upper jejunum and duodenum (Campbell and Drucker, 2013). GIP is derived from the 153 amino acid proGIP

precursor and is processed by prohormone convertase 1 or 3 to yield a final peptide of 42 amino acids in length (Campbell and Drucker, 2013).

GIPR's, like GLP-1R, also belong to the class B family of GPCRs (Al-Sabah, 2015). It is the N-terminal region of GIP that binds to the receptors N-terminal domain (NTD), thus enabling a secondary interaction to occur between the N-terminus of the peptide and transmembrane domain (TMD). This activates the receptor and facilitates interaction and activation of the heterotrimeric G proteins by the TMD (Al-Sabah, 2015).

However, GIP is also subject to enzymatic degradation by DPP-IV, cleaving an N-terminal dipeptide to yield GIP(3-42) and thus the parent peptide has a half-life of approximately 5-7 minutes in humans and 2 minutes in rodents (Baggio and Drucker, 2007; Hansen *et al.,* 2015). Interestingly, there is a suggestion that GIP(3-42) may function as a GIPR antagonist (Gault *et al.,* 2002), albeit perhaps not at physiologically relevant concentrations (Deacon and Ahŕen, 2011; Gault *et al.,* 2002).

GIPR activation on pancreatic beta cells mediates glucose-induced insulin secretion, insulin biosynthesis and inhibition of beta cell apoptosis (Baggio and Drucker, 2007). GIPRs are also expressed on pancreatic alpha cells, adipose tissue (mediates lipid metabolism) and bone (enhances bone formation) with further distribution throughout a broad spectrum of tissue including adrenal cortex, endothelium and brain with pleiotropic effects (Al-Sabah, 2015; Baggio and Drucker, 2007).

Given the plethora of therapeutic targets that GIP may affect, there has been renewed interest in developing it into a viable therapeutic. Due to its relative large molecular weight (4983.6 Daltons), initial underpinning research focused on delineating the bioactive regions of GIP with the intent to develop a smaller molecule that retained the capabilities of native GIP (1-42) (Hinke *et al.,* 2004). Hinke and colleagues (2004) determined that GIP could be split into three bioactive regions. The N-terminal, amino acids 1-14, the mid-region amino acids 19-30 and the C-terminus amino acids 31-42. Interestingly, it was the N-terminal and mid-region segments of amino acids that were demonstrated in perfused rat pancreas to retain GIP insulinotropic bioactivity, with suggestion that the C-terminus segment processed only somatostatinotropic activity (Hinke *et al.,* 2004). Furthermore, a modified version of native GIP (1-14), with a reduced bond between Ala^2 and Glu^3 was shown to have a superior receptor potency

and DPP-IV resistance (Hinke *et al.*, 2004). Considering this, modified GIP analogues warrant further investigation as T2DM therapeutics.

However, chronic consumption of a high fat diet has been shown to induce hypersecretion of GIP (Paschetta, Hvalrug & Musso, 2011; Pathak *et al.*, 2015a). These elevated GIP concentrations have been linked to inducing obesity by upregulating lipogenesis due to GIPs direct role in lipid metabolism and insulin resistance. This could suggest that increased action or secretion of GIP can predispose to obesity (Paschetta, Hvalrug & Musso, 2011). Evidence to which was demonstrated, even under diminished insulin action, by Zhou and colleagues (2005). The study determined, utilising insulin receptor substrate (IRS)-1-deficient knockout mice that if the action of insulin was diminished GIP could switch from fat oxidation to fat accumulation. This would ultimately result in increased triglyceride storage and thus an inflammatory response (Zhou *et al.*, 2005). Conversely, a study by Varol *et al.*, (2014) reputed these conclusions. They postulated utilising several *in vivo* models and a long-acting GIP analogue, that GIP is in fact a suppressor of inflammation (Varol *et al.*, 2014). With the association of GIP and obesity, GIPR antagonism and/or disruption of GIP action has been at the forefront as a potential therapeutic for treating obesity-diabetes. There have been several *in vivo* studies, in dietary and genetically-induced obese rodent models, utilising GIP antagonism with promising outcomes including reduction of circulating triglycerides and body weight (Gault *et al.*, 2007; McClean *et al.*, 2007; Pathak *et al.*, 2015). To date, bariatric surgery is the only treatment option that delivers sustainable long-term weight loss in patients with obesity-diabetes (Troke *et al.*, 2014).

1.6.5 Neurotensin

Neurotensin (NT) is a 13 amino acid peptide hormone located in the CNS and gastrointestinal tract where it acts as a neurotransmitter and regulatory hormone, respectively (Boules *et al.*, 2013). NT is synthesised from a precursor (pro-NT/NN) that contains NT and a neurotensin-like peptide, neuromedin N (NN) (Kitabgi, 2006). Pro-NT/NN is cleaved by pro-protein convertases (PC), primarily pro-hormone convertases PC1, PC2 and PC5-A, giving rise to NT and NN (Kitabgi, 2006). NT is

expressed in neuronal synaptic vesicles within the CNS and in neuroendocrine cells within the gastrointestinal tract (Mazella *et al.,* 2012). NT has also been located on organs such as the liver, heart, lungs spleen and pancreas (Boules *et al.,* 2013).

NT mediates its physiological effects through three NT receptors (NTRs). These are known as NTSR1, NTSR2 and NTSR3 (Boules *et al.,* 2013; Mazella *et al.,* 2012). NTSR1 and NTSR2 are neuropeptide receptors, coupled to GPCRs with a 7-transmembrane helical domain. NTSR3 or sortilin is non-coupled to GPCRs type I receptor, has a single transmembrane domain, and is structurally unrelated to NTSR1 or NTSR2 (Boules *et al.,* 2013; Mazella *et al.,* 2012).

NT has been implicated as an important regulator of body weight, both centrally and peripherally, as it has been shown to mediate peripheral fat absorption from the intestinal tract and appetite via the CNS (Schroeder and Leinninger, 2018). Recently, it has been shown that disruption to NT signalling can cause a significant decrease in central NT expression within the ventromedial hypothalamus (VMH) in obese rodents when compared to lean counterparts and suggested that this loss could contribute to the pathogenesis of obesity (Schroeder and Leinninger, 2018).

This is supported by several studies that demonstrate reduced levels of NT, primarily within the lateral hypothalamic area (LHA), in high-fat fed (HFF) rats and genetically obese mice (Schroeder and Leinninger, 2018). This suggests a commonality cross-over on regulation of food intake and body weight between the signalling actions of NT and leptin (Schroeder and Leinninger, 2018). In addition, a ten-day study by Feifel and colleagues (2010) in genetically obese *ob/ob* mice showed that an agonist of the NTR1 could supress food intake and induce weight loss. Furthermore, circulating levels of NT are significantly increased following bariatric surgery and weight loss, further suggesting that NT contributes to decreasing food intake and therefore regulation of body weight (Schroeder and Leinninger, 2018).

1.6.6 Xenin

Xenin is a peptide hormone that is synthesised and secreted from the same cell type as GIP, enteroendocrine K cells within human gastric mucosa, primarily that of the

duodenum and jejunum (Feurle *et al.,* 1998; Kerbel *et al.,* 2018). It is also located within the pancreas, liver, stomach, kidneys, heart, lungs and hypothalamus (Craig, Gault and Irwin, 2018; Feurle *et al.,* 1998; Parthsarathy *et al.,* 2016). Biologically active xenin is 25 amino acids long and derived from the N-terminal of coatomer protein alpha (COPA), which is a 35 amino acid precursor known as proxenin (Feurle *et al.,* 1992; Feurle *et al.,* 1998; Kerbel *et al.,* 2018). Proxenin is cleaved by aspartic proteinases including pepsin and cathepsin E, removing 10 C-terminal amino acids, thus xenin 25 (Craig, Gault and Irwin, 2018; Feurle *et al.,* 1992; Kerbel *et al.,* 2018).

Xenin-25 is structurally related to neurotensin. As such, the C-terminus of xenin-25 and neurotensin share a free non-amidated C-terminal isoleucine, the only difference is the substitution of amino acids arginine for lysine and tyrosine for tryptophan, the N-terminus and mid-sequence share no homologies (Craig, Gault and Irwin, 2018). Indeed, there has been no specific xenin receptor identified to date, and it is thought that its biological actions may be mediated in part through activation of neurotensin receptors, as well as cholinergic nerve fibres (Craig, Gault and Irwin, 2018; Feurle *et al.,* 2002).

Circulating levels of xenin are increased postprandially and xenin exerts effects on metabolism such as reducing the rate of gastrointestinal transit and gastric emptying (Anlauf *et al.,* 2000). Xenin also has the ability to suppress appetite and modulate lipid metabolism by increasing lipolysis and decreasing lipogenesis within adipose tissue and therefore affects energy balance (Anlauf *et al.,* 2000; Bhavya *et al.,* 2018).

Secretions of the endocrine and exocrine pancreas are also affected by xenin. Several studies have demonstrated that xenin-25 and the naturally occurring bioactive fragment, xenin-8, activate the secretion of insulin, glucagon and PP (Craig, Gault and Irwin, 2018; Gault *et al.,* 2015; Taylor *et al.,* 2010). Interestingly, xenin-25 can act independently as an insulinotropic agent stimulating pancreatic beta cell insulin release with the ability to increase the proliferation of pancreatic beta cells (Khan *et al.,* 2017). In addition, it was initially postulated that xenin-25 directly mediates release of insulin and glucagon, because it has no regulatory effect on somatostatin release (Craig, Gault and Irwin, 2018).

Further to this, under normal and elevated glycaemic conditions, xenin-25 has been shown to induce insulin release and enhance the biological actions of GIP and GLP-1 (Martin *et al.,* 2012; Taylor *et al.,* 2010). As previously discussed, the loss of GIP action is a major consequence of T2DM (Al-Sabah, 2015), therefore it would seem logical that xenin-25 has potential as an antidiabetic agent. The only thing to incumbent exploitation of xenin-25 is the biological half-life, like the incretins, xenin is subject to enzymatic degradation (Martin *et al.,* 2012; Taylor *et al.,* 2010). Xenin-25 is vulnerable to enzymatic degradation carried out by trypsin-like enzymes and serine proteases as it contains lysine and arginine residues, thus the native peptide lacks stability (Parthsarathy *et al.,* 2016). Therefore, recent research has been directed towards developing stable, biologically active and enzymatically resistant peptide analogues of xenin (Parthsarathy *et al.,* 2016).

Novel enzymatically resistant derivatives of xenin-25 include xenin-25-Gln, which has Glutamine (Gln) amino acid substitution at all Lysine (Lys) and Arginine (Arg) amino acids have been shown to maintain biological activity and be resistant against enzymatic degradation (Parthsarathy *et al.,* 2016). Xenin-25-Gln improves blood glucose levels, insulin secretion and glucose tolerance along with enhancing insulin sensitivity and GIP-stimulated insulin-release when used to treat high fat fed diabetic mice (Parthsarathy *et al.,* 2016). Fragmented forms of xenin-25 have also been utilised in the search for potential therapeutics. These include the mentioned C-terminally truncated bioactive metabolite xenin-8, which reportedly has the equivalent metabolic benefits as xenin-25, as well as the truncated analogue xenin-8-Gln. As with xenin-25-Gln, xenin-8-Gln is substituted with a Gln at amino acids Lys and Arg. Xenin-8-Gln were shown to be resistant to enzymatic degradation and elicit a significant insulin secretory effect in high-fat fed mice, similar to that of xenin-25-Gln, with xenin-8-Gln having a slightly superior effect (Martin *et al.,* 2012; Martin *et al.,* 2016). Moreover, this fragment displayed insulin-induced reductions of blood glucose levels in high-fat fed mice, not exhibited by xenin-25[Lys^{13}PAL] (Martin *et al.,* 2012; Martin *et al.,* 2016). Furthermore, an analogue xenin-6, the last 6 C-terminal residues of xenin-25, with a reduced pseudopeptide bond between the amino acid residues Lys and Arg, has been demonstrated to retain impressive xenin-like bioactivity (Feurle *et al.,* 2002).

1.7 Peptide therapeutics

Peptides are deemed to be extremely beneficial as therapeutics and offer several advantages in comparison to other pharmaceuticals including small molecules and biologics. They are highly potent, extremely selective, with low toxicity and have superior efficacious properties (Fosgerau and Hoffmann, 2015). Peptides are also relatively easy and fairly economical to produce (Fosgerau and Hoffmann, 2015). Peptide technology is continually advancing to improve their utility as a therapeutic including; peptides with cell penetrating abilities, multiple functions and peptide drug conjugates alongside alternative administration routes (Fosgerau and Hoffmann, 2015).

1.7.1 Novel approaches utilising peptides

Currently, at the forefront of pharmaceutical peptide technology is the development of single receptor agonists into unimolecular dual and triple receptor agonists. These unimolecular peptides have the potential to offer an expansive and bespoke treatment for T2DM and/or obesity as they combine multiple hormones with complimenting glucose regulating and anorectic effects (Capozzi *et al.,* 2018; Sadry and Drucker, 2013). Further support of this multi-targeted rationale is the efficacious utility of bariatric surgery to treat metabolic syndromes. The success of bariatric surgery is linked to alteration of several gastrointestinal hormones to reverse disease pathology. This multiple hormone modulation has yet to be successfully pharmacologically replicated and presently unimolecular dual and triple agonists offer the best opportunity to do so (Capozzi *et al.,* 2018).

The enteroendocrine system is the largest regulatory endocrine organ within the body and by extension, there are multiple mechanisms available for exploitation. This bring into question the current rational and efficacy of single target therapeutics. Therefore, the potential for extending the scope from a single target to dual or triple target therapeutic seems a logical step. As with the development of any novel pharmaceutical, the development and testing of novel unimolecular peptide therapeutics must take into consideration the broad tissue dissemination and pleiotropic effects of parent peptides (Al-Sabah, 2015). In addition, understanding of

peptide structure/function, knowledge of receptor and ligand binding specificity are required to maximise potency and efficacy, and reduce potential adverse effects.

Studies employing unimolecular peptide mimetics such as GLP-1/GIP dual receptor agonist show they are biphasic. Initially, the principle strategy of these types of dual agonists was to augment the glycaemic control and body weight reducing ability of GLP-1 and facilitate re-sensitivity to GIP to further modulate glycaemic control and body weight (Capozzi *et al.,* 2018; Finan *et al.,* 2013). Alone GIPR agonists were shown to have no effect on body weight or fat mass and dual receptor agonism had superior efficacious effects than the GLP-1R agonist alone (Capozzi *et al.,* 2018; Finan *et al.,* 2013). Furthermore, recent studies by Finan *et al.,* (2015) and Bhat *et al*., (2013), demonstrated that monomeric tri-agonist peptides had superior efficacious effects on glycaemic control and decreased body weight in relevant *in vivo* models of obesity and T2DM. Currently, several of these unimolecular dual and triple agonists are undergoing clinical trial phases with promising preliminary results for the treatment of obesity and T2DM (Capozzi *et al.,* 2018).

1.8 Hypothesis

Modulation of endogenous enteroendocrine and neuroendocrine peptide hormones yields superior therapeutic efficacy than parent peptide hormones to treat type 2 diabetes and obesity.

1.9 Thesis aims

Aims and objectives:

1. To assess the *in vivo* metabolic and therapeutic efficacy of a GIP-xenin hybrid peptide alone or in combination with a GLP-1 RA in a mouse model of diet-induced obesity-diabetes.

2. To evaluate the glucose-regulatory, insulinotropic activity and satiety enhancing properties of a GIP-xenin hybrid peptide alone or in combination with a GLP-1 RA in a genetically-induced mouse model of T2DM with established beta cell dysfunction.

3. To characterise a novel neurotensin-xenin hybrid peptide and investigate its gluco-regulatory, insulinotropic and antidiabetic activity in a pre-clinical model of diet-induced obesity-T2DM mouse model.

4. To design, synthesise and characterise novel N- and C- terminally truncated GIP peptides as specific and efficacious GIP receptor antagonists.

Chapter 2

General materials and methods

2.1 Peptides

All peptides used throughout this thesis were purchased from Synpeptide Company, Ltd (Shanghai, China). Peptides used in Chapter 3-5 (Table 2.1) were procured at >95% purity. Peptides used in Chapter 6 (Table 2.1) were procured in crude form and subsequently purified in-house, as described in Section 2.2.2.

2.2 Peptide purification and characterisation

2.2.1 Materials

Acetonitrile (HPLC grade), trifluoroacetic acid (TFA) (sequencing grade) and α-cyano-4-hydroxycinnamic acid were purchased from Sigma-Aldrich (Poole, Dorset, UK). Distilled water (18.2 MΩ-cm purity) was used in all experiments and obtained from an Elga PURELAB Ultra system (Elga, Celbridge, Ireland).

2.2.2 Purification of crude synthetic peptides

All crude peptides in Chapter 6 (Table 6.1) were purified to a single homogenous peak by reverse-phase high performance liquid chromatography (RP-HPLC) on a Surveyor Plus Liquid Chromatograph/HPLC (Thermo Finnigan, San Jose, California, USA), using a Jupiter Proteo analytical column (250 x 4.6 mm, Phenomenex, Torrance, California, USA), equilibrated with 0.1% (v/v) TFA/water, flow rate 6 ml/min. Peptides were re-suspended in 0.1% (v/v) (TFA)/H_2O and 0.1% TFA in 70% acetonitrile/H_20 (2:1 ratio) and injected into the column. Eluting solvent, acetonitrile (70%), was increased using linear gradients with percentage raised from 0-30% (v/v) over 13 min and 70% (v/v) over 53 min. Absorbance was measured at 214 nm. Peaks for each run were analysed using Thermo Electron ChromQuest data collection software (Version 3) and eluted peptides manually collected. Peptide aliquots (3-4 ml), were concentrated using a Savant SPD2010 SpeedVac concentrator and freeze dried (-55 ˚C) by a FreeZone Benchtop Freeze Dry System (Labconco, Kansas City, Missouri, USA).

2.2.3 Confirmation of peptide purity

Peptide purity (Chapters 3-6) was confirmed by RP-HPLC as described in Section 2.2.2 with the exception that peptides were re-suspended in distilled water and a 1 ml solution, (900 µl of 0.1% (v/v) TFA/water and 100 µl of peptide) was injected into the column. Chapters 3-5 used a Jupiter C-18 analytical column (250 x 4.6 mm) equilibrated with 0.1% (v/v) TFA/water, flow rate 1 ml/min, percentage acetonitrile raised from 0-40% (v/v) over 10 min, to 60% (v/v) over 40 min and to 70% (v/v) over 5 min. Chapter 6 used an Aeris XB-C18 HPLC column (Phenomenex), equilibrated with 0.1% TFA/water flow rate 1 ml/min and percentage acetonitrile raised from 0-30% (v/v) over 10 min and to 70% (v/v) over 30 min. Retention times were recorded and sample fractions were collected for MALDI-TOF analysis (Section 2.2.4).

2.2.4 Confirmation of molecular mass

Molecular mass of peptides was confirmed by matrix-assisted laser desorption ionisation time of flight mass spectrometry (MALDI-TOF MS) using a Voyager-DE Biospectrometry Workstation (PerSeptive Biosystems, Farmingham, MA, USA). Each peptide was combined with a matrix solution, 10 mg/ml cyano-4-hydroxycinnamic acid in acetonitrile/ethanol, 1:1 ratio, suspension (1.5µ l) and applied to a stainless-steel sample plate and allowed to dry at room temperature. The plate was inserted into plate holder and the mass spectra recorded as a mass-to-charge (m/z) ratio against relative peak intensity. The experimental molecular mass of each peptide was then compared to their respective theoretical mass using a peptide calculator.

2.3 Metabolic degradation

2.3.1 Materials

All reagents used in RP-HPLC and MALDI-TOF were purchased from Sigma Aldrich (Poole, Dorset, UK) as stated previously in Section 2.2.1. Purified water used in these experiments was obtained from an Elga PURELAB Ultra system. All other chemicals used were purchased from BDH chemicals (Poole, Dorset, UK). Murine plasma was obtained from overnight fasted male Swiss mice aged 10-12 weeks.

2.3.2 Plasma degradation

Murine plasma was collected as described in Section 2.10. The plasma degradation profile of peptides was determined by method described by Taylor *et al*. (2010). In brief, 10 µl plasma was incubated with 100 µl of peptide (100 µl of 1 mg/ml) and 390 µl Triethanolamine-HCl (50 mmol/l, pH 7.8) at 37ºC with gentle agitation for 0, 2, 4 and 6 hour(s). The enzymatic reactions were terminated by addition of 50 µl TFA/water 10% (v/v). Degradation products were then separated from intact peptide using RP-HPLC (Section 2.2.3) and fractions collected were subsequently characterised by MALDI-TOF MS (Section 2.2.4).

2.4 Cell culture

2.4.1 Materials

DMEM and RPMI-1640 tissue culture media, foetal bovine serum (FBS), penicillin, streptomycin, gentamicin, trypsin/EDTA and Hanks Buffered Saline Solution (HBSS) were all purchased from Gibco Life Technologies Ltd. (Paisley, Strathclyde, UK). All other chemicals including trypan blue were purchased from Sigma Aldrich.

2.4.2 Culture of pancreatic BRIN-BD11 cells

BRIN-BD11 cells are an insulin-secreting, clonal pancreatic beta cell line, secreting insulin in a glucose-dependent manner. They express incretin receptors and are derived from electrofusion of New England Deaconess Hospital (NEDH) rat pancreatic islet cells and immortal rat insulinoma RINm5F cells (McClenaghan *et al.,* 1996a). Culturing took place under sterile conditions using vented 20-175 cm^2 tissue culture flasks (Nalgene Labware, Thermo Scientific Corporation, Denmark), pre-warmed RPMI-1640 growth media supplemented with 10% (v/v) FBS and 1% (v/v) antibiotics (100 U/ml penicillin and 0.1 mg/ml streptomycin), maintained at 37°C and 5% CO_2, in a LEEC incubator (Laboratory technical engineering, Nottingham, UK) as previously described by McClenaghan *et al.,* (1996a). Sub-culturing at 70-80% cell confluency was employed before experimentation. Culture media was decanted, cells

washed (10 ml HBSS) and detached by incubating (3-4 min) with 3 ml 0.025% (w/v) trypsin/EDTA and viewed using an Olympus CX41 phase contrast microscope (Olympus, Southend-on-Sea, UK) at 100X magnification. Culture media (7-8 ml) was added to re-suspend, then pipetted into a 50 ml sterilin tube (Sterilin Ltd., Hounslow, UK) and centrifuged for 5 min at 900 rpm. Supernatant was decanted, and the pellet resuspended by culture media of a known volume and cells stained and counted using trypan blue and Neubauer haemocytometer (Scientific Supplies Co., UK). Routine sub-culture, cell suspension (1 ml) and culture media (25 ml) was added to the flask and maintained at 37º C until confluent.

2.5 Insulin secretion from BRIN-BD11 cells

2.5.1 Materials

All reagents used in culturing BRIN-BD11 cells were purchased from Gibco Life Technologies Ltd. as stated in Section 2.4.1. Trypan blue, thimerosal, iodogen (1,3,4,6-tetrachloro-3α,6α-diphenylglycoluril), bovine insulin, BSA, fraction V, sequencing grade TFA, dextran T-70 and activated charcoal and HPLC grade acetonitrile were all purchased from Sigma Aldrich. Disodium hydrogen orthophosphate (Na_2HPO_4) and sodium dihydrogen orthophosphate ($NaH_2PO_4.2H_2O$) were purchased from VWR International Ltd. (Lutterworth, Leicestershire, UK). Radiolabelled sodium iodide ($Na^{125}I$) was purchased from Perkin Elmer (UK). Rat insulin standard was purchased from Novo Industria (Copenhagen, Denmark). Dichloromethane (DCM) was purchased from Rathburn (Walkersburn, Scotland, UK). All other chemicals used were of highest purity and purchased from BDH chemicals. Water was obtained from an Elga PURELAB Ultra system.

2.5.2 Acute *in vitro* insulin secretion studies in BRIN-BD11 cells

The insulin secreting activity of peptides were assessed using BRIN-BD11 cells, obtained and quantified as outlined in section 2.4.2, (passage used was between 18 and 40). The protocol as described by McClenaghan and colleagues (1996b) was followed for insulin secretion experiments. In brief, cells were seeded and allowed to attach

overnight at 37°C in 24 well tissue culture plates (150,000 cell/well). After 18 hours, culture media was decanted and cells pre-incubated with 1 ml of Krebs–Ringer bicarbonate buffer (KRBB- 115 mmol/l NaCl, 4.7 mmol/l KCl, 1.2 mmol/l $MgSO_4$, 1.28 mmol/l $CaCl_2$, 1.2 mmol/l KH_2PO_4, 25 mmol/l HEPES and 8.4% $NaHCO_3$, containing 0.5% (w/v) BSA, pH 7.4) supplemented with 1.1 mmol/l glucose for 40 min at 37°C. Subsequently, the buffer was decanted and buffer containing glucose (3.3 to 16.7 mmol/l) in the presence of test peptides (10^{-12} to 10^{-6} mol/l), were added to wells and incubated for 20 min at 37°C. Once complete, 950 µl of the assay buffer from each well was collected and stored at -20°C for measurement of insulin by radioimmunoassay (RIA) (Section 2.5.4). In a separate set of experiments, BRIN-BD11 cells were incubated at 5.6 mmol/l glucose with test peptides in the presence or absence of appropriate receptor antagonists (receptor antagonists used are detailed in corresponding Chapters), and insulin measured by RIA (Section 2.5.4).

2.5.3 Iodination of bovine insulin for RIA

A modified protocol based on the method previously described by Fraker and Speck Jr (1978), was followed for iodination of bovine insulin. In brief, 100 µl of iodogen solution (1,3,4,6-tetrachloro-3α,6α-diphenylglycoluril), 1 mg of iodogen in 10 ml of dichloromethane, was added to Eppendorf tubes. Tubes were incubated at 37°C until a thin coating formed. Bovine insulin solution; 1 mg of insulin to 1 ml of 10 mmol/l HCL and diluted to 125 µg/ml (1:8 dilution) in 500 mmol/l phosphate buffer (pH 7.4). Bovine insulin (20 µl) and sodium iodide ($Na^{125}I$ 100 mCi/ml stock, Perkin Elmer, Cambridge, UK) (5 µl) were added to iodogen coated tube and kept on ice with gentle agitation every 3-4 min for 15 min, and the reaction stopped by transferring to a clean Eppendorf tube. The reaction tube was washed with 300 µl of 50 mmol/l sodium phosphate buffer and added to the reaction mixture. The iodinate was separated by RP-HPLC on a Vydac C- 8 (250 x 4.6 mm) analytical column. Flow rate; 1.0 ml/min with 0.12% (v/v) TFA/water and the acetonitrile concentration in the eluting solvent was increased from 0% to 56% over 60 min and to 70% in 5 min (Figure 2.1). Fractions (1 ml) were collected using a fraction collector (Frac-100, LKB), aliquoted (5 µl) into LP3 tubes and counts measured on a gamma counter (Perkin Elmer Wallac Wizard 1470 Automatic Gamma Counter). Fractions with the highest counts were diluted with

1 ml of 40 mmol/l sodium phosphate buffer (pH 7.4) containing 1 g/100 ml BSA and 0.02 g/100 ml thimerosal. Binding capacity was determined by a series of antibody dilutions (1:25,000-1:45,000), and fractions were kept at 4ºC.

2.5.4 Insulin RIA with modified dextran-coated charcoal

Determination of insulin concentration by using a modified dextran-coated charcoal radioimmunoassay established by Flatt and Bailey (1981). In brief, stock RIA buffer, 40 mmol/l disodium hydrogen orthophosphate (containing 0.3% (w/v) sodium chloride and 0.02% (w/v) thimerosal) was prepared and pH adjusted to 7.4 with 40 mmol/l sodium dihydrogen orthophosphate and stored at 4°C. Working RIA buffer was prepared by adding 0.5% (w/v) BSA to stock RIA buffer. Unknown samples (200 µl) were aliquoted in duplicate and insulin standards in triplicate (200 µl) into LP3 tubes. Insulin standards ranged from 0.039 to 20 ng/ml and prepared by serial dilution of frozen stock rat insulin. Antibody, guinea pig anti-porcine from frozen stock was diluted (1:25000 to 1:45000) with working RIA buffer (100 µl) added to all unknown samples and insulin standards except for control tubes. I^{125}-labeled tracer was added to working RIA buffer (10,000 counts per min (CPM) in 100 µl) and 100 µl was added to each tube and incubated at 4°C for 48 h. After 48 h incubation period, 1 ml of working DCC (1:5, stock DCC and working RIA buffer) was added to all tubes (except total), incubated for 20 min at 4°C, then centrifuged at 2500 rpm for 20 min at 4ºC and supernatant decanted. The radioactivity of each pellet was measured by a gamma counter and insulin concentration of unknown samples determined by rat insulin standard curve, generated using a spline-curve fitting algorithm.

2.6 *In vitro* beta cell proliferation and apoptosis

2.6.1 Materials

All reagents used in culturing BRIN-BD11 cells were purchased from Gibco Life Technologies Ltd. as stated in Section 2.4.1. Paraformaldehyde (PFA), phosphate buffered saline (PBS), sodium citrate, TWEEN® 20, BSA, streptozotocin (STZ) and glycerol were all purchased from Sigma Aldrich. Anti-Ki-67 (Abcam, ab15580)

primary antibody and goat anti-rabbit Alexa Fluor® 568 (Abcam, ab175471) secondary antibody was purchased from Abcam (Cambridge, UK). ApoLive-Glo™ Multiplex assay (Madison, Wisconsin, USA). Water was obtained from an Elga PURELAB Ultra system.

2.6.2 Assessment of *in vitro* beta cell proliferation

BRIN-BD11 cells were used to assess the effects of test peptides on beta cell proliferation. Cells were seeded at 40,000 cell/well onto a glass cover slip within a 12 well tissue culture plate. Cells were incubated in RPMI media (section 2.4.2) containing test peptides (10^{-8} to 10^{-6} mol/l) and GLP-1 (10^{-6} mol/l) (positive control) at 37^{o}C for 18 h. Following incubation period, cells were washed (PBS x 2) and fixed using 4% paraformaldehyde at room temperature for 30 min. Citrate buffer (sodium citrate and 0.05% TWEEN® 20), 1 ml at 90°C for 20 min, was used for antigen retrieval. Once cooled (20 min) and citrate buffer decanted, cells were washed (PBS x 2) and 300 µl of 1.1% BSA was added for 45 minutes to block tissue. The species specific (rat) primary antibody; rabbit anti-Ki67 (1:250; Abcam ab16667), was added, 200 µl/well and incubated for 2 h at 37°C. Cell were washed (PBS x 2) and a secondary antibody; goat anti-mouse IgG (1:400; Alexa Fluor® 594 Abcam ab150116) was added, 200 µl/well and incubated for 45 min at 37°C. After the final wash (PBS x 2), glass cover slips were removed and mounted onto glass slides using anti-fade mounting medium (1:1 glycerol and PBS). Slides were imaged using a fluorescent microscope (Olympus System Microscope, model BX51; Southend-on-Sea, UK) and photographed by DP70 camera adapter system. Analysis of cell proliferation frequency was expressed as percentage of total cells analysed, with approximately 150 cells analysed per replicate.

2.6.3 Determination of *in vitro* apoptosis

BRIN-BD11 cells seeded at 20,000 cells per well were incubated in RPMI media (section 2.4.2) containing test peptides (10^{-8} to 10^{-6} mol/l) and allowed to attach overnight. The following day determination of apoptosis, via the activation of

biomarkers, caspase 3 and 7 was initiated by a luminogenic, tetrapeptide sequence DEVD Caspase-Glo® 3/7 substrate. This caused cell lysis with subsequent caspase cleavage of the substrate that generated luminescence proportional to the amount of caspase activity. Assessment of apoptosis was by ApoLive-Glow™ Multiplex assay kit as directed by manufacturer (Promega, Madison, Wisconsin, USA).

2.7 Cyclic AMP production in BRIN-BD11 cells

2.7.1 Materials

The enzyme immunoassay kit for cAMP production was purchased from Bio-Techne (R&D Systems, Abingdon, UK) and all chemicals and reagents used are previously described in section 2.4.1.

2.7.2 Measurement of *in vitro* cAMP production

Cells were seeded and allowed to attach overnight (75,000 cells per well). The assay was performed the following day. Cells were treated with KRB buffer (pH 7.4) in the presence of test peptides at a range of concentrations, 0.1% BSA, 200 µmol/L IBMX and 5.6 mmol/l glucose for 60 min at 37^{o}C. Following incubation, supernatant was removed, wells were washed with ice cold PBS and cell lysis buffer added (200 µl). To ensure complete cell lysis, plates were frozen at -80^{o}C for 30 min and thawed using the orbital plate shaker at 37^{o}C (this was repeated until all cells were lysed). The contents were then centrifuged at 600 rpm for 2 min and supernatant stored at -20^{o}C for assessment of cAMP production by a cAMP Parameter® kit per manufacture instructions (R&D Systems, Abingdon, UK).

2.8 *Ex vivo* insulin secretion studies from isolated murine islets

2.8.1 Materials

Tissue culture medium (RPMI 1640), FBS, penicillin, streptomycin, gentamicin, trypsin/EDTA and HBSS were all purchased from Gibco Life Technologies Ltd. All other chemicals including trypan blue were purchased from Sigma Aldrich.

2.8.2 Isolation of islets by collagenase digestion

Pancreata from lean Swiss mice (12-14 weeks), were harvested and islets isolated by a modified collagenase digestion protocol described by Lacy and Kostinosky (1967). The collagenase and wash solution were prepared from stock HBSS by dissolving 136.9 mmol/l NaCl, 5.4 mmol/l KCl, 1.3 mmol/l $CaCl_2$, 0.4 mmol/l $MgSO_4.7H_2O$, 0.5 mmol/l $MgCl_2.6\ H_2O$, 0.4 mmol/l $Na_2HPO_4.H_2O$, 0.4 mmol/l KH_2PO_4, 5.6 mmol/l glucose, 0.06 mmol/l phenol red and 4.2 mmol/l $NaHCO_3$ in distilled water. The collagenase solution was prepared by adding 1.4 mg/ml collagenase to stock HBSS (5 ml required per pancreas) and wash buffer. Stock HBSS with the addition of 0.1% BSA was prepared on the day of islet isolation. Once pancreata were harvested they were placed into tubes containing ice-cold collagenase solution and minced to aid with initial digestion. Digestion was further enhanced by placing harvested pancreata in a shaking water bath at 37^{o}C for 8-12 min, the tubes were then forcefully shaken to dislocate islets from exocrine tissue. Tubes were then filled with ice-cold wash buffer and centrifuged for 2 min at 1200 rpm, the supernatant discarded, and remaining pellet resuspended in wash buffer (15 ml). This was repeated three times followed by filtering to ensure removal of unwanted tissue. The filtrate was then processed in the same way and the pellet obtained. It was re-suspended in pre-warmed RPMI-1640 media (supplemented with 10% BSA and 1% penicillin/streptomycin), transferred into petri-dishes allowing culture of islets at 37°C and 5% CO_2, in a LEEC incubator for a period of 2-3 days prior to use.

2.8.3 Insulin secretion from isolated murine islets

After 48 h culture, islets (n=20) were collected using a microscope and placed into 1.5 ml Eppendorf tubes, then centrifuged for 5 min at 1200 rpm to remove excess media. Acute insulin secretion studies then followed a modified method of *in* vitro insulin

secretion described in section 2.5.2. Islets were preincubated in 1 ml KRBB at 1.1 mmol/l glucose for 1 h and decanted after centrifugation for 5 min at 1200 rpm. Test solutions at 16.7 mmol/l glucose with a range of concentrations of peptides (10^{-8} to 10^{-6} mol/l) were then added and incubated for 1 h. Following incubation, tubes were centrifuged and 950 µl of the supernatant from each tube collected, aliquoted into 200 µl duplicates and stored at -20ºC until measurement of insulin by dextran-coated charcoal RIA (Section 2.5.4).

2.9 Animal models

Several animal models of obesity, insulin resistance and diabetes were utilised in this thesis to assess the biological actions and therapeutic potential of modified peptides *in vivo*. All animal experimentation was completed in accordance with the UK Animals (Scientific Procedures) Act 1986 and EU Directive 2010/63EU for animal experiments. Studies were also approved by University of Ulster Research Ethics Committee and all necessary steps were taken to reduce any potential suffering. Project licence number: 2804 and Personal licence number: 1692. All long-term *in vivo* studies were blinded and remained so throughout the biochemical and statistical analysis.

2.9.1 Normal lean model

National Institutes of Health (NIH) Swiss albino male mice, derived from a nucleus colony, were purchased from Envigo, Huntingdon, UK. The animals were housed at Ulster University's Behavioural and Biomedical Research Unit (BBRU) in an air-conditioned room (22 ± 2 °C) under a 12 h light and 12 h dark cycle. Animals were aged matched, individually housed and had free access to drinking water and standard laboratory chow (10% fat, 30% protein, 60% carbohydrate; percentage of total energy 12.99 KJ/g; Trouw Nutrition, Cheshire, UK). This murine model was used for acute animal studies and chronic studies, a model that represented normal glycaemic control.

2.9.2 High fat fed model

Male Swiss mice were purchased from Envigo and housed in the BBRU as described in section 2.9.1. Animals were aged matched, individually housed and had free access to drinking water and a high fat diet (45% fat, 20% protein, and 35% carbohydrate; percentage of total energy 26.15 kJ/g; Special Diet Services, Essex, UK). High fat feeding commenced for a minimum of three months to cause diet-induced obesity-diabetes. The diet progressively induced an increase in body weight and hyperglycaemia compared to age-matched controls fed standard laboratory chow. Prior to beginning chronic treatment regimen, mice were grouped based on body weight and blood glucose. This murine model is widely utilised for assessment of novel obesity-diabetes therapeutic agents (Winzell and Ahrén, 2004).

2.9.3 Diabetic (*db/db*) model

Male diabetic mice (*db/db*) (BKS.Cg-+ Leprdb/+ Leprdb/OlaHsd, were purchased from Envigo, and housed in the BBRU as described in section 2.9.1. Animals were aged matched, individually housed and had free access to drinking water and standard laboratory chow. Mice were grouped based on body weight and blood glucose. This murine model was employed as a genetic representation of obesity-diabetes exhibiting disease characteristics including; weight gain, beta cell dysfunction, hyperglycaemia and hyperinsulinemia (King, 2012).

2.10 Acute *in vivo* studies

2.10.1 Acute effects of peptides on glucose tolerance in lean mice

Fasted lean mice (10-12 weeks) had blood glucose measured immediately before and after intraperitoneal injection of glucose alone (18 mmol/kg body weight) or in combination with test peptides (50-100 nmol/kg bw detailed in individual chapters) at various time points (0, 15, 30 and 60 min). Final volume of 5 ml/kg body weight was administered for each test solution.

2.10.2 Delayed effects of peptides on glucose tolerance in lean mice

Fasted lean mice (10-12 weeks) had blood glucose measured before and after intraperitoneal injection of glucose alone (18 mmol/kg body weight) at various time points (0, 15, 30 and 60 min). Prior to this (-30 min), blood glucose was measured followed by an intraperitoneal injection of saline alone or in combination with test peptides (100 nmol/kg bw detailed in individual chapters). A final volume of 5 ml/kg body weight was administered for each test solution.

2.10.3 Biochemical Analysis

An incision to the tail vain of conscious mice was used to obtain blood samples for biochemical analysis. Blood glucose was measured directly by Ascencia Contour glucose meter (Bayer, Newbury, UK). Blood samples for plasma glucose or insulin were collected into fluoride micro-centrifuge tubes (Sarstedt, Numbrecht, Germany) and centrifuged (Beckman Instruments, Galway, Ireland) at 13000 rpm for 3 min at 4 °C with plasma aliquoted into Eppendorf tubes and stored at -20ºC until subsequent biochemical analysis. Plasma insulin was determined by diluting 20 µl of plasma with 180 µl of working RIA buffer (1:10 dilution) and measured using RIA (Section 2.5.4). Plasma glucose was evaluated using the GOD-PAP method determined by a glucose assay kit (GL 364, Randox Laboratories Ltd., UK) as directed by manufacturer.

2.11 Long-term *in vivo* studies

The high fat fed (HFF) and *db/db* animal models were used for long term studies. Grouping and maintenance of mice are detailed in Sections 2.9.2 and 2.9.3.

2.11.1 Treatment and monitoring regime of long-term peptide administration

Twice daily intraperitoneal injections (09:00 and 17:00 h) were administered with either saline alone (0.9% (w/v) NaCl) or in combination with peptides (25 nmol/kg) for the assessment duration. Prior to treatment, to customise the mice to injection and

handling anxiety, twice daily injections (4-6 days) of saline alone were administered. Assessment of non-fasting glucose and insulin levels (Section 2.5.4) were monitored every 3-4 days (from day -6 or -4 onwards), along with cumulative energy intake and body weight.

2.11.2 Glucose profile

Prior to cessation of treatment, a 24 h glucose profile on non-fasted mice was evaluated. Twice daily injection continued (Section 2.11.1) with values measured prior (0 h) to first daily injection and 4, 8, 12 and 24 h afterwards.

2.11.3 HbA1c analysis

Following cessation of treatment, HbA1c concentrations were assessed using whole blood and A1cNow$^{®+}$ kits (PTS diagnostics, Indiana, USA), as directed by manufacturer.

2.11.4 Glucose tolerance test

Mice were fasted (10 h) prior to oral or intraperitoneal administration of glucose (18 mmol/kg bw). Glucose and insulin were measured (Section 2.5.4), before (0 h) and after time points 15, 30, 60, 90 and 120 min.

2.11.5 GIP tolerance test

Mice were fasted (10 h) prior to intraperitoneal administration of glucose (18 mmol/kg bw) in combination with native GIP(1-42) (25 nmol/kg bw). Glucose and insulin were measured (Section 2.5.4), before (0 h) and after time points 15, 30, 60 and 90 min.

2.11.6 Insulin sensitivity test

Assessed on non-fasted mice, intraperitoneal administration of bovine insulin (25 or 50 U/kg body weight). Glucose was measured (Section 2.5.4), at various time points (0, 15, 30, and 60 min).

2.11.7 Pancreatic insulin secretion from *ex vivo* isolated mouse islets

Insulin secretion from isolated islets was assessed on cessation of treatment and measured as stated in Section 2.8, using known insulin secretagogues; 7.68 mmol/l calcium chloride, 20 mmol/l potassium chloride, 200 µmol/l IBMX and 10 nmol/l PMA.

2.11.8 Pancreatic insulin content

Tissue was excised, snap frozen and stored following treatment cessation until assay. Pancreas was thawed, washed with cold PBS, weighed and homogenised in extraction buffer (20 mmol/l Tris HCl, 150 mmol/l NaCl, 1 mmol/l EDTA, 1 mmol/l EGTA and 0.5% Triton X 100, 0.1% protease inhibitor, pH 7.5) using a handheld VWR VDI 12 homogeniser (VWR, UK). Contents were centrifuged for 5 min at 1300 rpm and supernatant collected. Insulin content was then measured form extracted content, 20 µl was diluted with 180 µl of working RIA buffer (1:10 dilution) and measured using RIA (Section 2.5.4).

2.11.9 Bone mineral density and body composition analysis by dual energy X-ray absorption (DXA)

Lean mass and total fat percentage as well as bone mineral content (BMC) and bone mineral density (BMD) were analysed by the Piximus Densitometer (GE Medical Systems, LUNAR, USA). Instrument was calibrated using a phantom provided by the manufacturer. Mice were sedated using isoflurane and culled by cervical dislocation before being placed on specimen tray for analysis.

2.11.10 Lipid profile analysis

Following the cessation of treatment terminal blood was collected. Analysis of total triglycerides, high-density and total cholesterol was determined by Hitachi Automated Analyzer 912 (Boehringer Ingelheim, Mannheim, Germany) within Ulster University's NICHE department. The low-density cholesterol was calculated using Friedwald equation: total cholesterol - HDL - (triglycerides / 5).

2.11.11 Immunohistochemistry analysis

Following pancreatic excision, tissue was sectioned longitudinally and fixed in 4% parafolmaldehyde at 4ºC. Tissue was then processed by automated tissue processor (Leica TP1020, Leica Microsystems, Nussloch, Germany) and embedded in paraffin wax. Tissue sections were cut (5 µm) by a manual microtome (Shandon finesse 325, Thermo scientific, UK) and positioned on poly-L-lysine coated glass slides (VWR International, Pennsylvania, USA). Tissue, prior to staining, was deparaffinised by xylene (Sigma Aldrich) and rehydrated using a series concentration of ethanol (100%, 95%, 85%, 70% and 50%; Sigma Aldrich) with subsequent antigen retrieved by exposing tissue to sodium citrate buffer (10 mmol/l sodium citrate, 0.05% Tween 20, pH 6.0) for 20 min at 95ºC. The sections were then blocked (2% BSA for 30 min) and incubated with species specific (mouse) primary antibodies; rabbit anti-glucagon antibody (1:400; Abcam, ab92517) and mouse anti-insulin antibody (1:1000; Abcam, ab6995) for 2 h at 37ºC. Following washing with PBS sections were incubated with respective secondary antibodies; goat anti-mouse IgG (1:400; Alexa Fluor 594® Abcam ab150116), and goat anti-rabbit IgG (1:400; Alexa Fluor® 488 Abcam ab150077), for 1 h at 37ºC. Subsequent to washing with PBS, sections were incubated with DAPI (4,6-diamidino-2-phenylindole), a nuclear stain for 10 min at room temperature. Following a final washing step, slides were mounted with anti-fade (PBS supplemented with 1:1 (v/v) glycerol). Imaging was carried out using a fluorescent microscope (Olympus system microscope, model BX51), under a FITC (488 nm) or TRITC filter (594 nm) and imaged using a DP70 camera adapter system. Subsequent analysis of islet parameters was carried out using Cell^{F} image analysis software (Olympus Soft Imaging Solutions, GmbH).

2.12 Statistical analysis

GraphPad PRISM (Version 5) was used for statistical analysis. The results are expressed as mean ± SEM. Data was compared by one-way ANOVA followed by Student-Newman-Keuls *post-hoc* test or two-way ANOVA followed by Bonferroni post-tests, and unpaired student *t*-test where appropriate. Incremental insulin and glucose area under the curve (AUC) and area above the curve (AAC) were calculated using trapezoidal rule with baseline subtraction. Significant difference was considered between data sets with $P<0.05$.

Table 2.1 Structure of peptides in Chapters 3, 4, 5 and 6

Name	Purity	Sequence
(DAla^2)GIP/Xenin-8-Gln	>95%	Y[DA]EGTFISDYSIAMHPQQPWIL-OH
Exendin-4	>95%	HGEGTFTSDLSKQMEEEAVRLFIEWLKNGGPSSGAPPPS - NH2
Neurotensin	>95%	pELYENKPRRPYIL-OH
Xenin-8-Gln	>95%	HPQQPWIL-OH
Neurotensin(8-13)	>95%	RRPYIL-OH
Acetyl-neurotensin(8-13)	>95%	Ac- RRPYIL-OH
Acetyl-neurotensin(8-13)-xenin-8-Gln	>95%	Ac-RRPYIL-HPQQPWIL-OH
Human GIP(1-42)	Crude	YAEGTFISDYSIAMDKIHQQDFVNWLLAQKGKKNDWKHNITQ
Human GIP(1-30)	Crude	YAEGTFISDYSIAMDKIHQQDFVNWLLA QK-NH_2
Mouse GIP(1-30)	Crude	YAEGTFISDYSIAMDKIRQQDFVNWLLA QR-NH2
Human GIP(3-30)	Crude	EGTFISDYSIAMDKIHQQDFVNWLLAQ K-NH_2
Mouse GIP(3-30)	Crude	EGTFISDYSIAMDKIRQQDFVNWLLAQR-NH_2
Human Pro^{3}GIP(3-30)	Crude	PGTFISDYSIAMDKIHQQDFVNWLLAQK-NH_2
Human GIP(3-42)	Crude	EGTFISDYSIAMDKIHQQDFVNWLLAQKGKKNDWKHNITQ
Human GIP(5-30)	Crude	TFISDYSIAMDKIHQQDFVNWLLAQK-NH_2
Human GIP(5-42)	Crude	TFISDYSIAMDKIHQQDFVNWLLAQKGKKNDWKHNITQ

Figure 2.1 HPLC separation of iodinated bovine Insulin

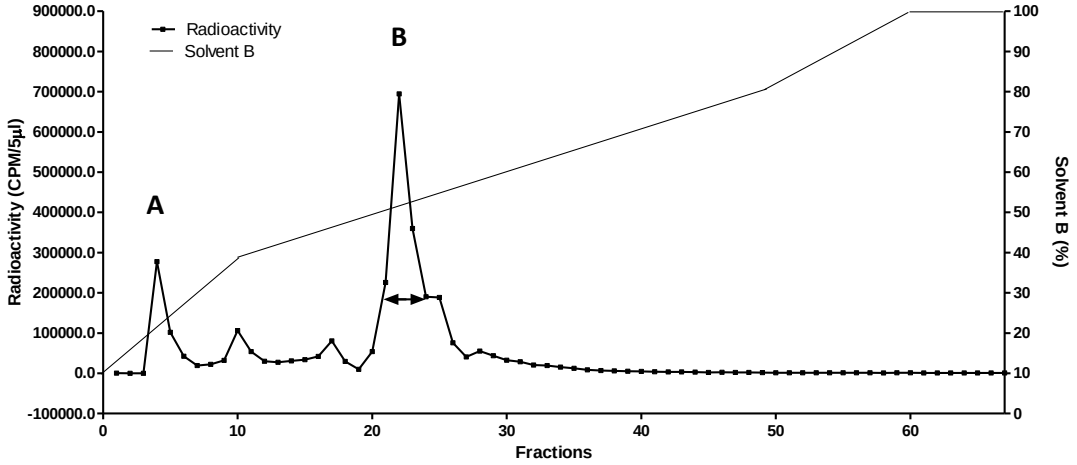

Iodinated I^{125}-bovine insulin was separated by reverse-phase HPLC and eluting solvent B (70% acetonitrile, increased using linear gradients with percentage raised over time). Fractions were collected every minute by an automated fraction collector. The radioactivity level of fractions (5 µl) was determined on a gamma counter. Peak A correlates with fractions 5-6, containing unbound sodium iodide ($Na^{125}I$) and peak B correlates with fractions 21-25, containing the iodinated insulin.

Chapter 3

Investigating the biological actions and therapeutic efficacy of a GIP-xenin-8-Gln hybrid peptide on high fat fed induced obesity-diabetes

3.1 Summary

The regulatory enteroendocrine hormone GIP, secreted from enteroendocrine K cells in response to glucose and fat has important biological actions including glucose homeostasis, insulin biosynthesis and secretion, beta cell proliferation and anti-apoptotic protection, as well as regulation of energy balance and bone turnover. However, under hyperglycaemic conditions of T2DM these beneficial actions become impaired and unlike the action of its sister incretin, GLP-1, cannot be restored by exogenous administration. However, the related regulatory enteroendocrine hormone xenin, also secreted from K-cells, can potentiate the biological actions of GIP under both normal glycaemia and T2DM. The current study has compared the biological actions and therapeutic efficacy of the hybrid peptide (DAla^2)GIP/xenin-8-Gln either alone or in combination with exendin-4. *In vitro* assessment revealed that (DAla^2)GIP-xenin-8-Gln activated insulin secretion via GIPR cell signalling pathway and the GIP component is essential for activation of the adenylate cyclase pathway. (DAla^2)GIP-xenin-8-Gln also demonstrated significant ($P<0.01$ to $P<0.001$) beta cell proliferative and protective effects. *In vivo*, twice-daily administration of (DAla^2)GIP/xenin-8-Gln in combination with exendin-4 improved ($P<0.05$ to $P<0.001$) glycaemic control and insulinotropic action and reduced ($P<0.001$) HbA1c concentrations. An improved ($P<0.05$) sensitivity to GIP and insulin was also noted, especially in the group treated with (DAla^2)GIP/xenin-8-Gln in combination with exendin-4, with *ex vivo* isolated islets confirming improved ($P<0.05$ to $P<0.001$) insulin secretory action. Additionally, there was positive effects on islet morphology, where both treatment groups increased pancreatic beta cell area and decreased alpha cell area ($P<0.05$ to $P<0.01$), also in keeping with *in vitro* proliferation and apoptosis studies. Neither treatment group had any effects on body weight or energy intake. Interestingly, the percentage fat mass, total cholesterol and triglycerides were reduced ($P<0.05$ to $P<0.01$) by both treatment groups. Together, their data suggest that further evaluation of (DAla^2)GIP/xenin-8-Gln either alone or in combination with exendin-4 is warranted for the potential treatment of T2DM.

3.2 Introduction

GIP secreted from enteroendocrine K cells in response to glucose and fat, contributes equivalently to the incretin effect under normal physiological conditions together with its sister incretin hormone, GLP-1 (Baggio and Drucker, 2007; Paschetta, Hvalryg and Musso, 2011). The biological actions of GIP encompass endocrine and exocrine effects, and these include but are not limited to: insulin biosynthesis and secretion, beta cell proliferation and anti-apoptotic protection, as well as regulation of appetite, satiety and bone turnover (Baggio and Drucker, 2007; Mabilleau *et al.*, 2018; Paschetta, Hvalryg and Musso, 2011; Senio, Fukushima and Yabe, 2010). However, with the onset of T2DM resulting from persisting insulin resistance, impaired insulin secretion and loss of beta cell mass, GIP fails to yield a potent insulinotropic effect even though circulating levels have increased (Kaku, 2010). This impaired GIP incretin action is thought to be due to loss of sensitivity or down regulation of the GIP receptor (GIPR) on the pancreatic beta cell due to elevated hyperglycaemia, which further exacerbates resistance to GIP action (Paschetta, Hvalryg and Musso, 2011; Senio, Fukushima and Yabe, 2010).

Interestingly, the biological actions of GLP-1 are also believed to be partially compromised in T2DM (Nauck, 2016). However, unlike GLP-1 action, which can be restored though elevation of circulating levels via administration of GLP-1 agonists, this is not the case for native GIP (Nauck, 2016; Paschetta, Hvalryg and Musso, 2011). Elevated levels of GIP fail to elicit a notable biological response on insulin secretion in T2DM (Gault, 2018; Paschetta, Hvalryg and Musso, 2011). Therefore, the therapeutic prospect of formulating an enzymatically stable, long-acting GIP agonist would appear somewhat redundant for T2DM (Paschetta, Hvalryg and Musso, 2011; Pathak *et al*., 2015a), however several such GIP analogues have been synthesised and characterised over the years (Gault, 2018).

GIP is not the only gut hormone to be secreted from enteroendocrine K cells. Xenin, a 25 amino acids peptide hormone with glucose homeostasis and energy balancing capabilities, is co-secreted with GIP in response to feeding (Craig, Gault and Irwin, 2018). Furthermore, xenin has been demonstrated to potentate the biological actions of GIP under both normal glycaemia and hyperglycaemic conditions (Chowdhury *et al.*, 2013; Craig, Gault and Irwin, 2018; Martin *et al.*, 2012). With that said, the

biological half-life of these two gut hormones must also be considered when formulating a potential new pharmaceutical agent. GIP substituted with a D-alanine in position 2 termed ($DAla^2$)GIP(1-42) was demonstrated to have improved enzymatic resistance to DPP-IV, increased GIP stimulated cAMP production and glucose tolerance (Hinke *et al.,* 2002). Furthermore, the N-terminally truncated form of GIP, GIP(1-14), demonstrated similar biological actions as the parent peptide, ($DAla^2$)GIP(1-42) (Hinke *et al.,* 2004), highlighting that smaller bioactive regions of GIP could be useful for generating GIP-based drugs.

Interestingly, xenin has a naturally occurring bioactive fragment, the C-terminally truncated xenin-8 (Feurle *et al.,* 1997; Silvestre *et al.,* 2003). Xenin-8 processes nearly all the biological capabilities of xenin-25, except possible induction of satiety (Craig, Gault and Irwin, 2018; Martin *et al.,* 2014). Moreover, a modified xenin-8-Gln analogue, with Gln substitution of the Lys^{21} and Arg^{22} amino acid residues, has been shown to improve insulin sensitivity, glucose tolerance and most importantly to augment the glucose-lowering and insulinotropic responses of GIP in high fat fed (HFF) mice (Martin *et al.,* 2016).

The advantage of these fragmented, biologically active and enzymatically resistant analogues is the opportunity to formulate them into monomeric peptide therapeutics (Fosgerau and Hoffmann, 2015). Thus, combining individual peptides biological action(s) into a single therapeutic entity. This has been achieved to good effect with a number of other gut-derived peptide hormones (Fosgerau and Hoffmann, 2015). The dual agonism approach has been shown to exhibit synergistic beneficial effects in the treatment of T2DM (Finan, 2015; Sadry and Drucker, 2013). As such, this rationale is in keeping with a recent review by Skow and colleagues (2016) on the improved efficacy of a dual action, monomeric GLP-1 and GIP receptor agonist in the treatment of T2DM (Skow, Bergmann and Knop, 2016). Therefore, a GIP-xenin hybrid peptide with dual receptor agonism and augmentation abilities has the potential to revive sensitivity to GIP and mediate the biological activities of both hormones in T2DM. Similar actions have been documented in a review by Irwin and Flatt (2015), with hybrid peptides including GIP-oxyntomodulin, cholecystokinin-8-GLP-1 and gastrin-GLP-1. All denoted hybrid peptides exhibited remarkable improvements over either parent peptide alone (Irwin and Flatt, 2015).

Employing this knowledge, our laboratory previously created a novel GIP/xenin hybrid peptide utilising the biologically active and enzymatically resistant regions of GIP and xenin, to create (DAla^2)GIP-xenin-8-Gln (Hasib *et al.,* 2017). (DAla^2)GIP-xenin-8-Gln was shown to be capable of activating GIP and xenin based cellular pathways, to restore GIP action in T2DM and impart notable therapeutic benefits in an animal model of T2DM (Hasib *et al.,* 2017). The aim of this study was two-fold, to initially extend the scope of what is known surrounding this hybrid peptide through *in vitro* evaluation of insulinotropic and cAMP activity, as well as pancreatic beta cell proliferation and anti-apoptotic actions. Secondly, to build on previous work, the antidiabetic benefits of (DAla^2)GIP-xenin-8-Gln was examined in HFF mice following a treatment with (DAla^2)GIP-xenin-8-Gln alone and in combination with exendin-4.

3.3 Materials and Methods

3.3.1 Peptides

All peptides were purchased from Syn Peptide Shanghai, China. Purity was confirmed by RP-HPLC and characterised by MALDI-TOF MS, (Sections 2.1, 2.2.3, and 2.2.4). For all experimental materials and methods please refer to Section 2.1, and relevant subsections.

3.3.2 Acute effects of peptides alone and in the presence of receptor antagonists on *in vitro* insulin secretion from BRIN-BD11 cells

The *in vitro* insulin secretory activity of test peptides on BRIN-BD11 cells is as described in Section 2.5.2. BRIN-BD11 cells were incubated with test peptides (10^{-6}–10^{-12} mol/l) alone or in the presence of specific GIP or neurotensin receptor antagonists namely: GIP(6-30)-CexGluPAL (Pathak *et al.,* 2015b), SR488692 (neurotensin-1) and SR142984 (non-specific neurotensin) (at 10^{-7} mol/l or 10^{-6} mol/l) for 20 min. Following test incubations, insulin was measured by RIA (Sections 2.5.2 and 2.5.4).

3.3.3 *In vitro* proliferation

Effects of test peptides on cell proliferation in BRIN-BD11 was conducted as described in Section 2.6.2. Cells were incubated in RPMI media (Section 2.4.2) containing test peptides (10^{-8} to 10^{-6} mol/l). The primary antibody, anti-Ki-67 (1:250) and the secondary antibody, goat anti-rabbit Alexa Fluor® 594 (1:400), were used to detect proliferating beta cells by fluorescent microscopy.

3.3.4 *In vitro* apoptosis

The effects of test peptides on BRIN-BD11 cell apoptosis was conducted as described in Section 2.6.3. The cells were incubated in RPMI media (section 2.4.2) containing test peptides (10^{-8} to 10^{-6} mol/l) and apoptosis initiated by adding the caspase-3/7 substrate reagent that results in cell lysis, followed by caspase cleavage of the substrate and detection of beta cell apoptosis by luminescence.

3.3.5 *In vitro* cyclic AMP

Effects of peptides on *in vitro* cyclic AMP production was examined using BRIN-BD11 cells described in Section 2.7.2. Briefly, test peptides (10^{-9} to 10^{-6} mol/l) were incubated for 60 mins, and cAMP generation assessed using a cAMP Parameter® ELISA kit.

3.3.6 Animals

The long-term study utilised HFF male Swiss mice, as described in Section 2.9.2. Prior to experimentation, mice were maintained on high fat diet for 10 weeks, resulting in overt obesity and hyperglycaemia.

3.3.7 Long-term *in vivo* study in HFF mice

Twice daily intraperitoneal injections (09:00 and 17:00 h) of either saline vehicle (0.9% (w/v) NaCl), (DAla^2)GIP-xenin-8-Gln alone or in combination with exendin-4 (all peptides at 25 nmol/kg bw) for 32 days is described in Section 2.11.1. Assessed metabolic parameters included: circulating glucose and insulin, body weight and cumulative energy intake, monitored every 3-4 days (Sections 2.11.1). End of treatment assessment parameters included glucose tolerance (18 mmol/kg bw), HbA1c, blood glucose profile, GIP tolerance (25 nmol/kg bw), insulin sensitivity (25 U/kg), insulin content, islet insulin secretory response, percentage fat mass, circulating triglycerides and cholesterol as well as islet morphology, as described in more detail within Sections 2.8.2, 2.8.3 and 2.11.2.

3.3.8 Biochemical analysis

Blood/plasma glucose, plasma and pancreatic insulin were assayed as described in Sections 2.5.4 and 2.10

3.3.9 Statistical analysis

As described in Section 2.12

3.4 Results

3.4.1 Effects of (D-Ala^2)GIP-xenin-8-Gln alone, and in the presence of GIP and neurotensin receptor antagonists, on insulin secretion from BRIN-BD11 cells

Figure 3.1 (A-C) demonstrates that (D-Ala^2)GIP-xenin-8-Gln significantly ($P<0.01$ and $P<0.001$) increases insulin secretion from BRIN-BD11 cells at 5.6 mmol/l glucose in a dose dependent manner. In the presence of the antagonist GIP(6-30)-CexGluPAL (10^{-7} and 10^{-6} mol/l), (D-Ala^2)GIP-xenin-8-Gln induced insulin secretion was significantly ($P<0.05$ to $P<0.001$) inhibited at all concentrations (10^{-12} to 10^{-6} mol/l) examined (Figure 3A). Similarly, an inhibitory effect on (D-Ala^2)GIP-xenin-8-Gln insulinotropic response (10^{-9} mol/l to 10^{-6} mol/l, $P<0.05$ to $P<0.01$) was demonstrated

in the presence of neurotensin 1 antagonist (Figure 3.1B). However, the non-specific neurotensin antagonist had no significant effect on (D-Ala^2)GIP-xenin-8-Gln insulin secretory ability at 5.6 mmol/l glucose, except at 10^{-9} mol/l and 10^{-6} mol/l concentrations where there was a moderate reduction (Figure 3.1C).

3.4.2 Effects of (D-Ala^2)GIP, xenin-8-Gln and (D-Ala^2)GIP-xenin-8-Gln on BRIN-BD11 cell proliferation

Culturing of BRIN-BD11 cells in the presence of GLP-1, exendin-4, (D-Ala^2)GIP and (D-Ala^2)GIP-xenin-8-Gln (at 10^{-6} mol/l or 10^{-8}mol/l) for 18 hours significantly ($P<0.01$ and $P<0.001$) increased proliferation frequency in comparison to the untreated control culture (Figure 3.2A). However, xenin-8-Gln alone had no effect on beta cell proliferation (Figure 3.2A). The hybrid peptide, (D-Ala^2)GIP-xenin-8-Gln (10^{-6} mol/l), induced a significant ($P<0.001$) elevation of proliferation frequency ($P<0.001$) compared to either parent peptide alone (Figure 3.2A). Figure 3.2B shows representative images of proliferating cells under each culture condition.

3.4.3 Effects of (D-Ala^2)GIP, xenin-8-Gln and (D-Ala^2)GIP-xenin-8-Gln on BRIN-BD11 cell apoptosis

BRIN-BD11 cells cultured in the presence of exendin-4, (D-Ala^2)GIP, xenin-8-Gln, xenin-8, xenin-25, (D-Ala^2)GIP-xenin-8-Gln (10^{-6}mol/l or 10^{-8}mol/l) for 18 hours demonstrated a significant ($P<0.05$ to $P<0.001$) protective effect against capase-3/7 activated apoptosis compared to untreated control culture (Figure 3.3).

3.4.4 Effects of (D-Ala^2)GIP-xenin-8-Gln on intracellular cAMP production alone and in the presence of GIP or neurotensin antagonists in BRIN-BD11 cells

BRIN-BD11 cells had increased ($P<0.01$- $P<0.001$) cAMP production at 5.6 mmol/l glucose in the presence of (D-Ala^2)GIP-xenin-8-Gln (Figure 3.4). The neurotensin 1 antagonist (10^{-9}mol/l to 10^{-6} mol/l) had no impact on (D-Ala^2)GIP-xenin-8-Gln induced cAMP formation (Figure 3.4). In contrast, GIP(6-30)-CexGluPAL (10^{-9}mol/l to 10^{-6} mol/l) had a significant inhibitory ($P<0.01$ and $P<0.001$) effect on (D-Ala^2)GIP-

xenin-8-Gln induced cAMP production (Figure 3.4). Importantly, neither GIP(6-30)-CexGluPAL nor the neurotensin 1 receptor antagonist affected basal cAMP accumulation in BRIN-BD11 cells (Figure 3.4).

3.4.5 Effects of twice-daily administration of (D-Ala^2)GIP-xenin-8-Gln alone or in combination with exendin-4 on cumulative energy intake, body weight and percentage fat mass in HFF mice

Following twice daily administration of all treatments for 32 days there was no significant effect on cumulative energy intake (Figure 3.5A). Although not significant, there was a progressive decline in body weight from day 4 in both treatment groups (Figure 3.5B). This reduction is also reflected in percentage fat mass, where all treatment groups had significantly reduced ($P<0.05$) percentage fat mass in comparison to saline control (Figure 3.5C).

3.4.6 Effects of twice-daily administration of (D-Ala^2)GIP-xenin-8-Gln alone or in combination with exendin-4 on non-fasted glucose and insulin in HFF mice

From the fourth day of treatment there was a progressive decline in non-fasting blood glucose in mice treated with (D-Ala^2)GIP-xenin-8-Gln in combination with exendin-4, with a significant decrease ($P<0.05$) on days 11 and 14 (Figure 3.6A). (D-Ala^2)GIP-xenin-8-Gln alone mice were also observed to have a non-significant progressive decrease in non-fasted blood glucose concentrations (Figure 3.6A). Plasma insulin concentrations of (D-Ala^2)GIP-xenin-8-Gln in combination with exendin-4 mice progressively increased ($P<0.05$ to $P<0.001$) from the fourth treatment day and remained significantly elevated throughout the study, compared to saline controls (Figure 3.6B). (D-Ala^2)GIP-xenin-8-Gln alone treatment lead to a non-significant elevation of circulating insulin when compared to saline treated control HFF mice.

3.4.7 Effects of twice daily administration of (D-Ala^2)GIP-xenin-8-Gln alone or in combination with exendin-4 on 24 hour blood glucose profile and % HbA1c in HFF mice

After administration of the twice daily peptide treatment regimens over the 32 day treatment period a 24 hour profile was conducted (Figure 3.7A). All treatment groups had sustained lower, albeit not significantly, blood glucose levels compared to the saline control HFF mice (Figure 3.7A). However, HbA1c was significantly reduced ($P<0.001$) on day 32 in both treatment groups of mice (Figure 3.7B).

3.4.8 Effects of twice-daily administration of (D-Ala^2)GIP-xenin-8-Gln alone or in combination with exendin-4 on oral glucose tolerance in HFF mice

The 32 day administration of (D-Ala^2)GIP-xenin-8-Gln alone had no significant effect on glycaemic response post oral glucose load in comparison to saline control (Figure 3.8A). Corresponding glucose-induced plasma insulin concentrations were non-significantly elevated in (D-Ala^2)GIP-xenin-8-Gln treatment group, when compared to saline treated mice (Figure 3.8B). However, (D-Ala^2)GIP-xenin-8-Gln in combination with exendin-4 significantly ($P<0.05$) reduced the glycaemic excursion and elevated insulin secretion in comparison to the saline control (Figure 3.8AB).

3.4.9 Effects of twice-daily administration of (D-Ala^2)GIP-xenin-8-Gln alone or in combination with exendin-4 on GIP tolerance test in HFF mice

(D-Ala^2)GIP-xenin-8-Gln in combination with exendin-4 significantly ($P<0.05$) augmented the glucose-lowering action of GIP in terms of AUC (Figure 3.9A). In addition, the rise in blood glucose levels following combined glucose and GIP injection at observation points 15 and 30 min was significantly ($P<0.05$) reduced by 32 days treatment with (D-Ala^2)GIP-xenin-8-Gln in combination with exendin-4 (Figure 3.9A). Interestingly, GIP-induced elevation of plasma insulin was not significantly different between groups (Figure 3.9B).

3.4.10 Effects of twice-daily administration of (D-Ala^2)GIP-xenin-8-Gln alone or in combination with exendin-4 on insulin sensitivity and pancreatic insulin content in HFF mice

Following twice daily administration of (D-Ala^2)GIP-xenin-8-Gln in combination with exendin-4 for 32 days in HFF mice, glucose levels were significantly ($P<0.05$) reduced in response to exogenous insulin, both at 15 and 30 min post-injection and in terms of AAC (Figure 3.10A). (D-Ala^2)GIP-xenin-8-Gln alone had no significant effect on insulin sensitivity (Figure 3.10A). There was a significant ($P<0.01$ and $P<0.001$) reduction in pancreatic insulin in both treatment groups compared with saline control (Figure 3.10B).

3.4.11 Effects of twice daily administration of (D-Ala^2)GIP-xenin-8-Gln alone or in combination with exendin-4 on insulin secretory response of isolated islets in HFF mice

Islets from HFF mice were isolated by collagenase digestion in day 32 and exposed to $CaCl_2$, KCl, IBMX and PMA to assess insulin secretory performance (Figure 3.11). In response to either 3.3 or 16.7 mM glucose, there was no significant difference in insulinotropic responses between all groups of mice (Figure 3.11). However, in the presence of $CaCl_2$, KCl, IBMX and PMA, there was a significant increase in insulin secretion ($P<0.05$ and $P<0.001$) from islets of both treatment groups, barring islets from (D-Ala^2)GIP-xenin-8-Gln treated mice exposed to IBMX (Figure 3.11).

3.4.12 Effects of twice daily administration of (D-Ala^2)GIP-xenin-8-Gln alone or in combination with exendin-4 on total cholesterol, triglycerides, HDL and LDL in HFF mice

Following 32 days of twice daily administration of both treatment regimens, there was a significant decrease in total cholesterol ($P<0.01$ and $P<0.001$) and triglycerides ($P<0.001$) compared to saline controls (Figure 3.12A,B). Furthermore, (D-Ala^2)GIP-xenin-8-Gln decreased ($P<0.01$) HDL and LDL (Figure 3.12C,D). Treatment with (D-Ala^2)GIP-xenin-8-Gln in combination with exendin-4 also lowered ($P<0.05$) LDL compared to saline treated controls (Figure 3.12D).

3.4.13 Effects of twice daily administration of (D-Ala^2)GIP-xenin-8-Gln alone or in combination with exendin-4 on pancreatic islet histology in HFF mice

Pancreatic islet area was not different between all groups of HFF mice (Figure 3.13A). However, (D-Ala^2)GIP-xenin-8-Gln alone and in combination with exendin-4 increased ($P<0.05$) beta cell area when compared to saline treated control (Figure 3.13B). Furthermore, alpha cell area was decreased ($P<0.05$) by (D-Ala^2)GIP-xenin-8-Gln alone and in combination with exendin-4 (Figure 3.13C). Representative images of islets from all groups of mice are shown in Figure 3.14A-C.

3.5 Discussion

Current T2DM therapeutics, although somewhat effective, have numerous limitations related to their efficacy and/or adverse effects (Capozzi *et al.,* 2018; Irwin and Flatt, 2015). These approved therapies all preferentially target a single receptor, ion channel, transporter or enzyme (Capozzi *et al.,* 2018). Therefore, current research has been revised, focusing on the multiple targets contributing to T2DM, by employing synergistic hybrid peptides that target more than one cell signalling pathway (Capozzi *et al.,* 2018; Irwin and Flatt, 2015). In T2DM, hyperglycaemia and hyperlipidaemia contribute to desensitisation of the insulinotropic effects of GIP, arbitrated by decreased expression and/or down regulation of GIPR (Irwin and Flatt, 2015; Pathak *et al.,* 2014). Using this combined knowledge, previous work from our laboratory lead to the generation of (DAla^2)GIP-xenin-8-Gln (Hasib *et al.,* 2017). This hybrid peptide was shown to target two separate pathways and to restore GIP action in T2DM (Hasib *et al.,* 2017), highlighting it as an exciting potential new T2DM therapeutic that requires more investigation.

In the current study, characterisation of the predominant pathway used to employ biological activity of (DAla^2)GIP-xenin-8-Gln was determined by utilising two neurotensin receptor antagonists, the commercially available SR488692 (neurotensin-1) and SR142984 (non-specific neurotensin), as well as a GIPR specific, GIP(6-30)Cex-K^{40}[Pal] (Pathak *et al.,* 2015b). The *in* vitro activation of insulin action by (DAla^2)GIP-xenin-8-Gln was demonstrated to be favourable to GIPR cell signalling pathway rather than xenin. This concurs with previous studies demonstrating the bioactive region of GIP to be the N-terminus and xenin the C-terminus (Hinke *et al.,*

2004; Craig, Gault and Irwin, 2018). Assessment of cAMP production by (DAla^2)GIP-xenin-8-Gln in clonal beta cells again revealed that the GIP component of (DAla^2)GIP-xenin-8-Gln was critical for activation of the adenylate cyclase pathway. This is in keeping with published literature that xenin does not alter cAMP accumulation in cells (Taylor *et al.,* 2010), and previous research with (DAla^2)GIP-xenin-8-Gln (Hasib *et al.,* 2017).

Building on this knowledge, and to further elucidate the beta cell actions of DAla^2)GIP-xenin-8-Gln, proliferation and anti-apoptotic effects were evaluated using clonal BRIN-BD11 beta cells. The proliferative abilities of (DAla^2)GIP were notable but xenin-8-Gln alone had no effect. Considering the latter, and the very significant beta cell proliferative actions of (DAla^2)GIP-xenin-8-Gln, this is suggestive of xenin-8-Gln and its ability to augment the biological actions of GIP (Martin *et al.,* 2016). The anti-apoptotic benefits of (DAla^2)GIP-xenin-8-Gln compared to (DAla^2)GIP were less pronounced, although both compounds did elicit notable apoptosis preventive effects in keeping with the action of GIP (Martin *et al.,* 2013; Varol *et al.,* 2014). Also, a recent study with xenin-25 suggests that this hormone may also be involved in beta cell proliferation and protection against apoptosis (Khan *et al.,* 2017). These positive observations, along with corresponding recent literature on (DAla^2)GIP-xenin-8-Gln (Hasib *et al.,* 2017), prompted the next set of experiments to determine whether the antidiabetic benefits of (DAla^2)GIP-xenin-8-Gln could be enhanced through concurrent administration with the clinically approved GLP-1 mimetic, exendin-4. The premise being that (DAla^2)GIP-xenin-8-Gln would lead to upregulation of GIP activity and responsiveness, with exendin-4 activating the other arm of the incretin effect. Thus, together the two treatments would positively modulate the overall incretin effect that is known to be compromised in T2DM (Capozzi *et al.,* 2018).

As expected, chronic 32 day treatment with (DAla^2)GIP-xenin-8-Gln in HFF mice resulted in sustained improvements in glycaemic control and insulinotropic action. (DAla^2)GIP-xenin-8-Gln caused a progressive decrease in non-fasted circulating blood glucose. This beneficial action was further enhanced, albeit non-significantly, when administered in combination with the known GLP-1 agonist exendin-4 (Fusco *et al.,* 2017). This correlated well with reduced HbA1c concentrations in all treated mice. More interestingly, circulating insulin levels were elevated by both treatments,

but the combination group clearly induced much higher circulating insulin levels. This might imply that the combined action of (DAla^2)GIP-xenin-8-Gln and exendin-4 is having a positive effect at the level of the beta cell (Hasib *et al.*, 2017; Pathak *et al.*, 2018a). All effects were largely independent of changes in body weight or energy intake, which is possibly a little surprising as exendin-4 is believed to induce satiety and lower body weight (Shah and Vella, 2014). However, a similar lack of effect of exendin-4 has previously been noted in this same strain of mice (Hasib *et al.*, 2018a). These observations are also in line with the described loss of satiety action of xenin-8-Gln when compared to xenin-25 (Craig, Gault and Irwin, 2018; Martin, 2016).

GIP has been demonstrated to regulate lipid metabolism including adipocyte size, storage and inflammatory response (Freeman, 2009; Varol *et al.*, 2014). A study using (DAla^2)GIP by Varol and colleagues (2014) suggested that obesity-diabetes was related to adipose tissue inflammation by GIP resulting in dysregulation of lipid metabolism and storage, correlating with a study by Pathak and colleagues (2015). The study concluded that (DAla^2)GIP repressed this inflammatory response thus resolving the lipid dysregulation and in turn improved insulin sensitivity (Pathak *et al.*, 2015a). In the present study, this is supported by a reduction in triglyceride and total cholesterol levels in all treatment groups, with the combination of (D-Ala^2)GIP-xenin-8-Gln and exendin-4 also lowering LDL levels. Indeed, recent evidence suggests that GLP-1 receptor signalling could be inherently involved in lipid metabolism (Kooijman *et al.*, 2015). Conversely, other aspects such as locomotor activity, energy expenditure, feeding behaviour and/or patterns could factor here, and warrant further assessment (Freeman, 2009; Pathak *et al.*, 2015a; Varol *et al.*, 2014).

Glucose tolerance following 32 days treatment was not significantly improved by any of the treatments in HFF mice. However and more importantly, there was a distinct improvement in the sensitivity to both GIP and insulin, especially in the group of mice treated with (D-Ala^2)GIP-xenin-8-Gln in combination with exendin-4. This corroborates the idea that xenin can restore GIP action in T2DM (Hasib *et al.*, 2017; Parthsarathy *et al.*, 2016), and that the effect can be enhanced by GLP-1. Furthermore, secretory data derived directly from *ex vivo* isolated islets, following 32 days treatment in HFF mice confirms that insulin secretion and beta cell signalling pathways are enhanced by combined (DAla^2)GIP-xenin-8-Gln and exendin-4 treatment. This is in

line with the notable beta cell benefits of GIP, GLP-1 and xenin (Fusco *et al.*, 2017; Gault, 2018; Khan *et al.*, 2017).

Moreover, it is well understood that islet structure is altered by T2DM conditions as they undergo morphological changes. The beta cell mass is disrupted, and alpha cell mass has been shown to increase and to contribute to disease aetiology (Brereton *et al.*, 2015). Therefore, it is pivotal for positive effects on islet cell architecture with the introduction of treatment interventions. Moreover, in this study there were positive effects on the pancreatic beta cell area as it was significantly augmented in this group of HFF mice. The beta cell mass was greatly increased by treatment with either (DAla^2)GIP-xenin-8-Gln alone or in combination with exendin-4, in HFF mice. This was also in keeping with the proliferation and apoptosis studies and previous observations (Hasib *et al.*, 2017). Additionally, the alpha cell mass was also reduced by treatment with either (DAla^2)GIP-xenin-8-Gln alone or in combination with exendin-4, in HFF mice. Interestingly, for both treatment groups, the overall islet area was similar to the saline treated control suggesting that they both positively altered the beta to alpha cell ratio by upregulating islet beta cells.

This study has shown (DAla^2)GIP-xenin-8-Gln, a dual agonist monomeric therapeutic, had beneficial effects on the pathologies associated with T2DM. This was represented by notable positive effects in an established *in vivo* model of T2DM induced by high fat feeding. Moreover, the work confirms (DAla^2)GIP-xenin-8-Gln can augment GIP action in diet induced T2DM (Hasib *et al.*, 2017). Furthermore, the therapeutic efficacy of (DAla^2)GIP-xenin-8-Gln was notably enhanced by exendin-4. This was particularly evident in terms of benefits on beta cell area, beta cell secretory responsiveness and circulating insulin levels in HFF mice, strongly suggesting the beta cell effects are key to these actions. There is clearly a need for further investigations into the therapeutic efficacy and applicability of this treatment approach, especially in a model of T2DM that exhibits clear beta cell dysfunction.

Figure 3.1 Effects of (D-Ala^2)GIP-xenin-8-Gln alone and in the presence of a GIP and neurotensin receptor antagonists on insulin secretion from BRIN-BD11 cells

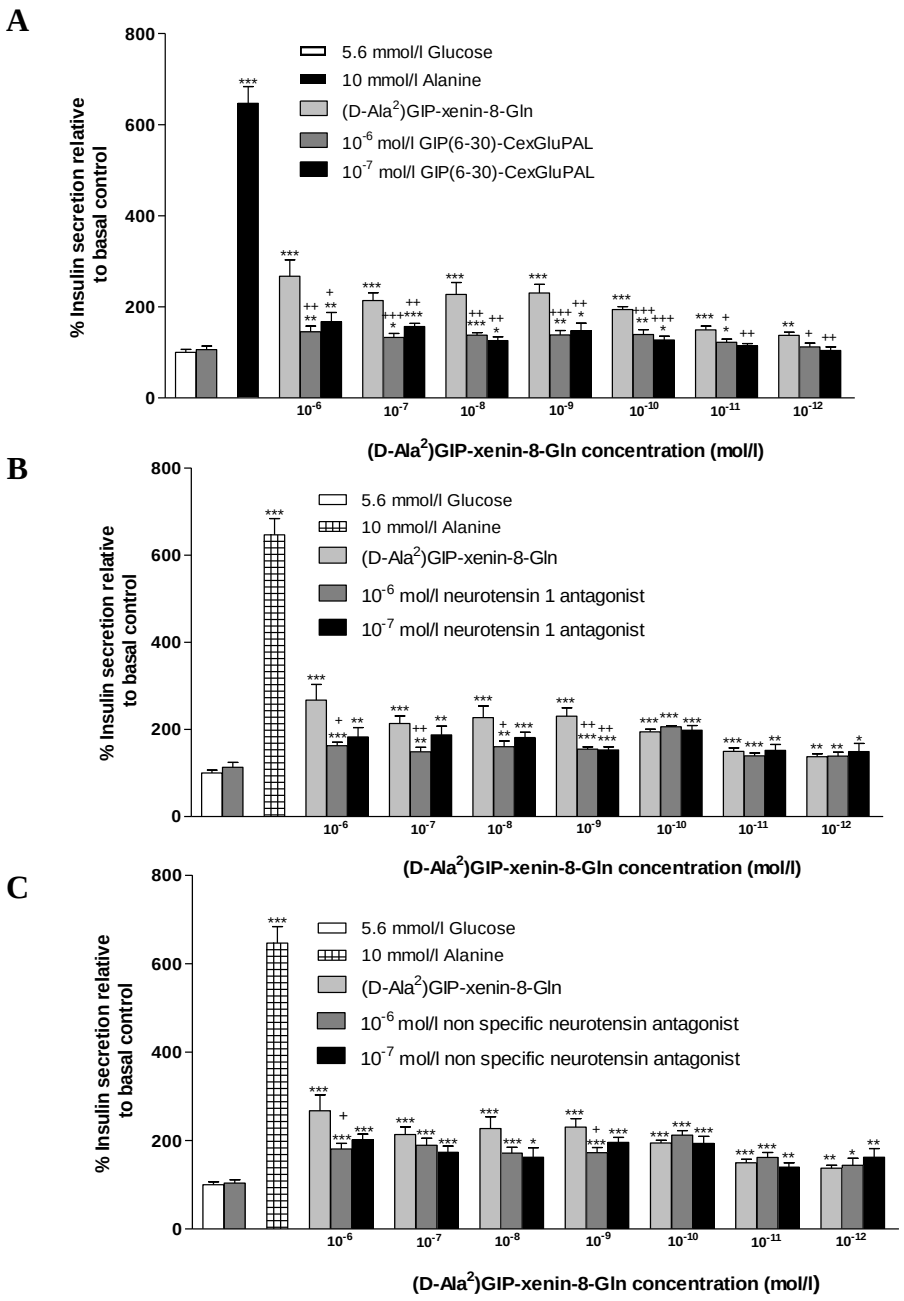

BRIN-BD11 cells were incubated (20 min) with GIP hybrid (10^{-12} to 10^{-6} mol/l) in the presence of 5.6 mmol/l glucose and a GIP (A) neurotensin 1 (B) or non-specific neurotensin (C) receptor antagonist. Insulin was measured by RIA. Values are mean ± SEM (n=8) for insulin release. *P<0.05, **P<0.01 and ***P<0.001 compared to 5.6 mmol/l glucose alone. $^{+}$P<0.05, $^{++}$P<0.01 and $^{+++}$P<0.001 compared to respective (D-Ala^2)GIP-xenin-8-Gln.

Figure 3.2 Effects of (D-Ala^2)GIP, xenin-8-Gln and (D-Ala^2)GIP-xenin-8-Gln on BRIN-BD11 cell proliferation

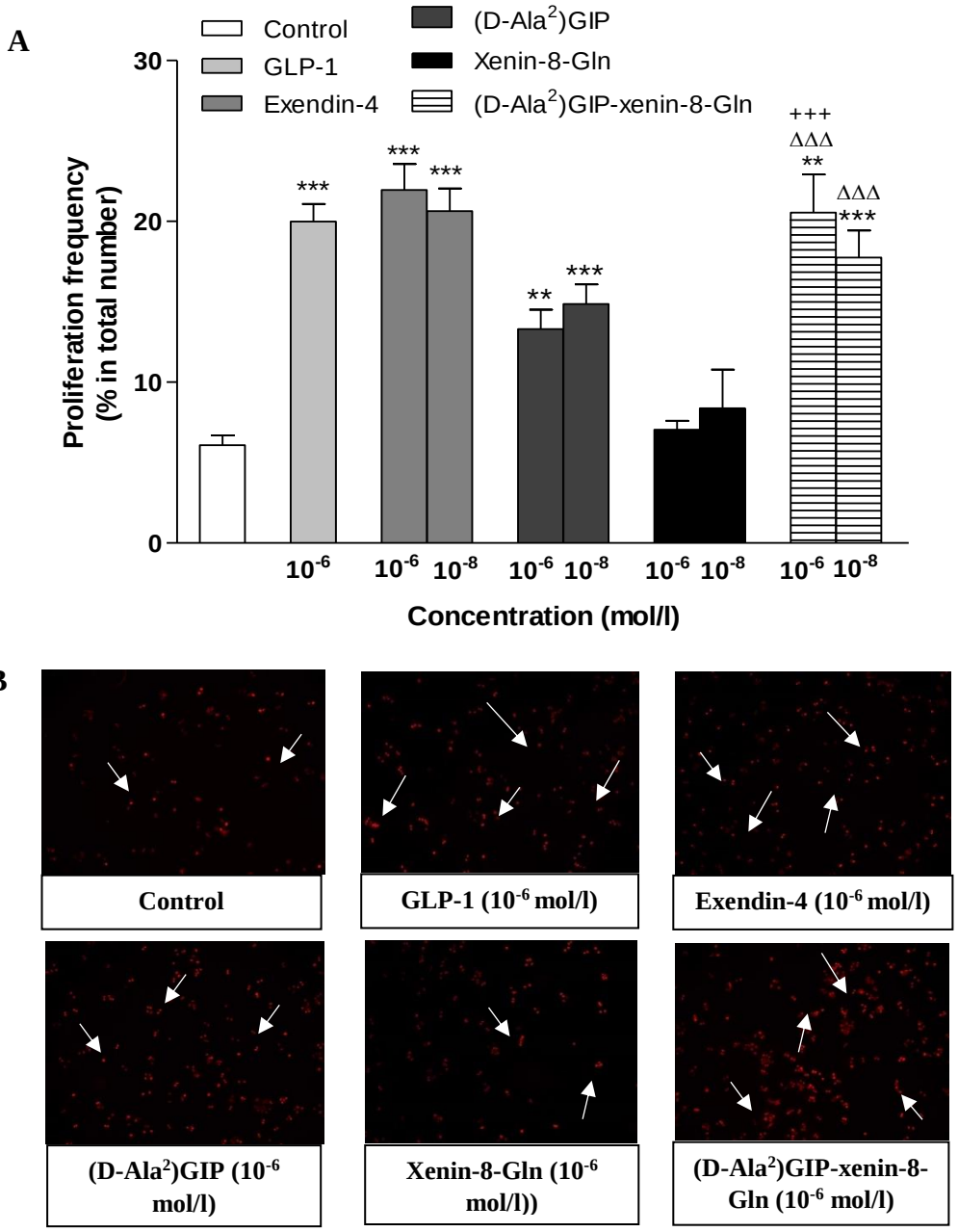

Proliferation frequency in BRIN-BD11 cells cultured with GLP-1, exendin-4, (D-Ala^2)GIP, xenin-8-Gln and (D-Ala^2)GIP-xenin-8-Gln (A) (at 10^{-6} or 10^{-8} mol/l) for 18 h. Representative images (B) showing proliferating beta cells in the presence (18 h) of GLP-1, exendin-4, (D-Ala^2)GIP, xenin-8-Gln and (D-Ala^2)GIP-xenin-8-Gln. Arrows indicate proliferating cells. Values are mean ± SEM (n=4). **P<0.01 and ***P<0.001 compared to control culture. $^{+++}$P<0.001 compared to respective (D-Ala^2)GIP. $^{\Delta\Delta\Delta}$P<0.001 compared to respective xenin-8-Gln.

Figure 3.3 Effects of (D-Ala^2)GIP, xenin-8-Gln and (D-Ala^2)GIP-xenin-8-Gln on BRIN-BD11 cell apoptosis

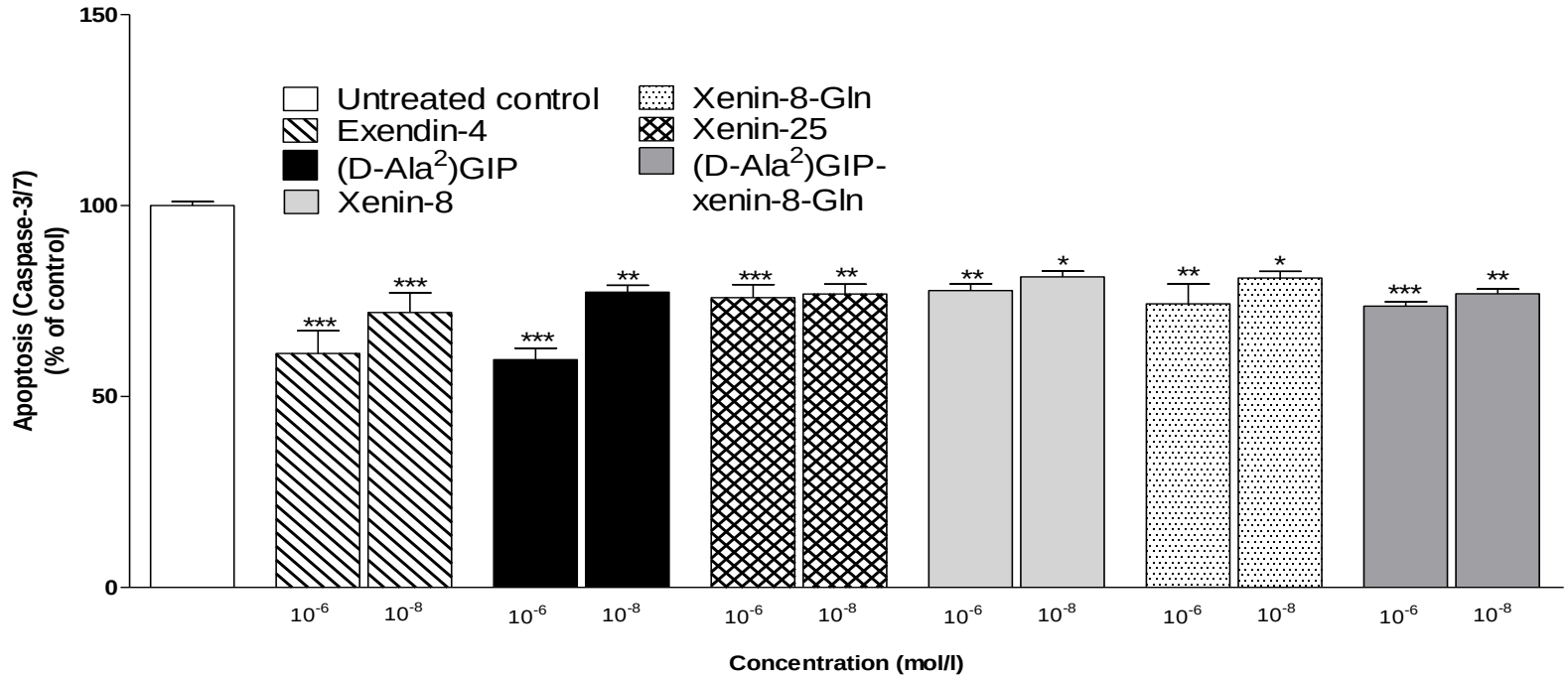

Apoptosis frequency in BRIN-BD11 cells cultured with exendin-4, (D-Ala^2)GIP, xenin-8-Gln, xenin-8, xenin-25, (D-Ala^2)GIP-xenin-8-Gln (at 10^{-6} or 10^{-8} mol/l) for 18 h. Caspase-3/7 activation was detected by luminescence. Values are mean ± SEM (n=3). *P<0.05, **P<0.01 and ***P<0.001 compared to un-treated control culture.

Figure 3.4 Effects of (D-Ala^2)GIP, xenin-8-Gln and (D-Ala^2)GIP-xenin-8-Gln on intracellular cAMP production alone and in the presence of GIP or neurotensin receptor antagonists in BRIN-BD11 cells

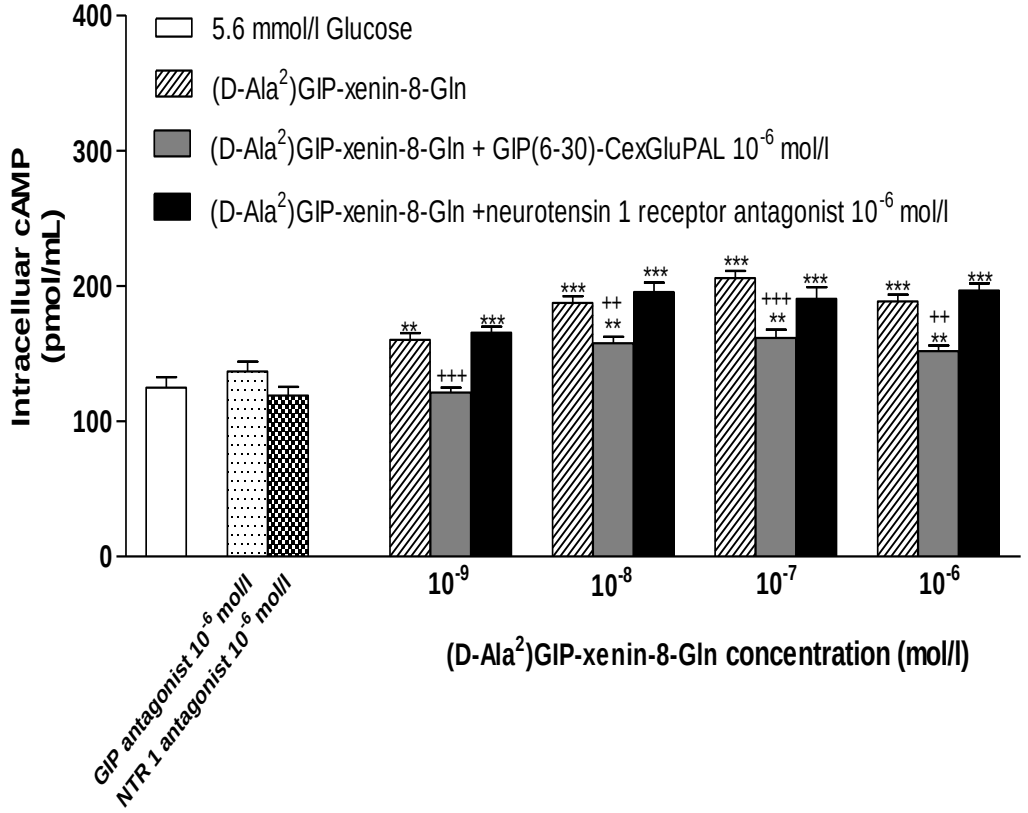

BRIN-BD11 cells were exposed to 5.6 mmol/l glucose control (with 100µm IBMX) and various concentrations (10^{-9} to 10^{-6} mol/l) of (D-Ala^2)GIP-xenin-8-Gln in the presence of 5.6 mmol/l glucose with GIP(6-30)-CexGluPAL or neurotensin 1 receptor antagonist. Values are mean ± SEM (n=4) for cAMP production. **P<0.01 and ***P<0.001 compared to 5.6 mmol/l glucose alone. $^{++}$P<0.01 and $^{+++}$P<0.001 compared to (D-Ala^2)GIP-xenin-8-Gln.

Figure 3.5 Effects of twice-daily administration of (D-Ala^2)GIP-xenin-8-Gln alone and in combination with exendin-4 on cumulative energy intake, body weight and percentage fat mass in HFF mice

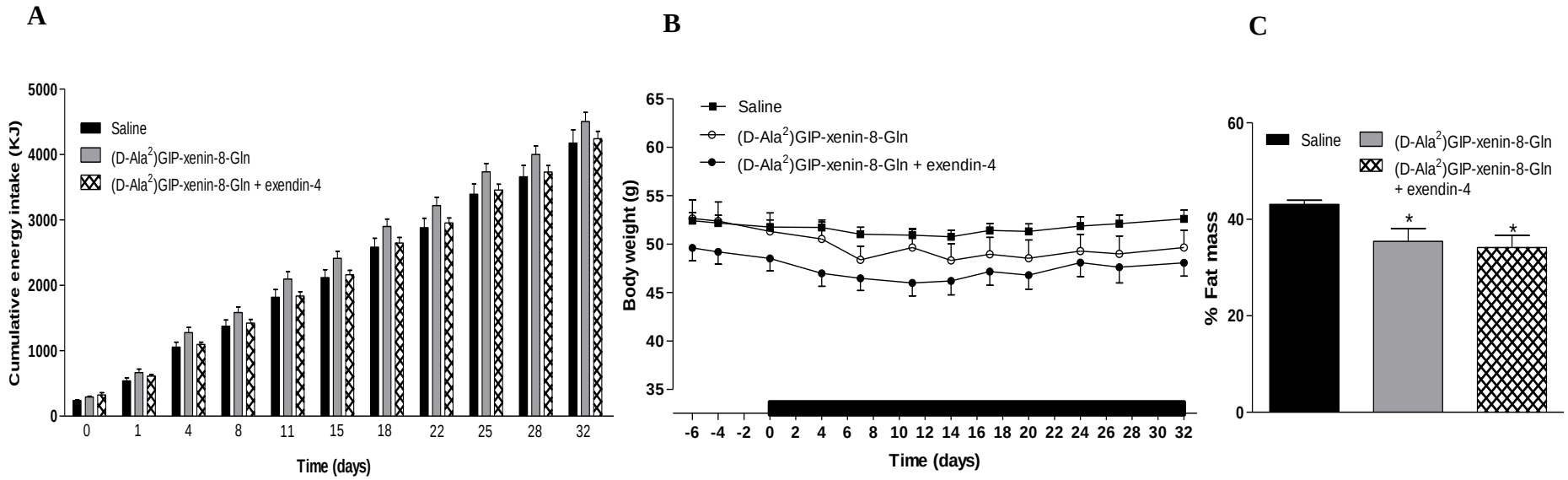

Variables were measured for 6 days before and 32 days during (indicated by black horizontal line), twice-daily treatment with saline, (D-Ala^2)GIP-xenin-8-Gln or (D-Ala^2)GIP-xenin-8-Gln in combination with exendin-4 (each at 25 nmol/kg bw). Values represent mean ± SEM (n=6-8). *P<0.05 in comparison with saline control.

Figure 3.6 Effects of twice-daily administration of (D-Ala^2)GIP-xenin-8-Gln alone and in combination with exendin-4 on non-fasting blood glucose and plasma insulin in HFF mice

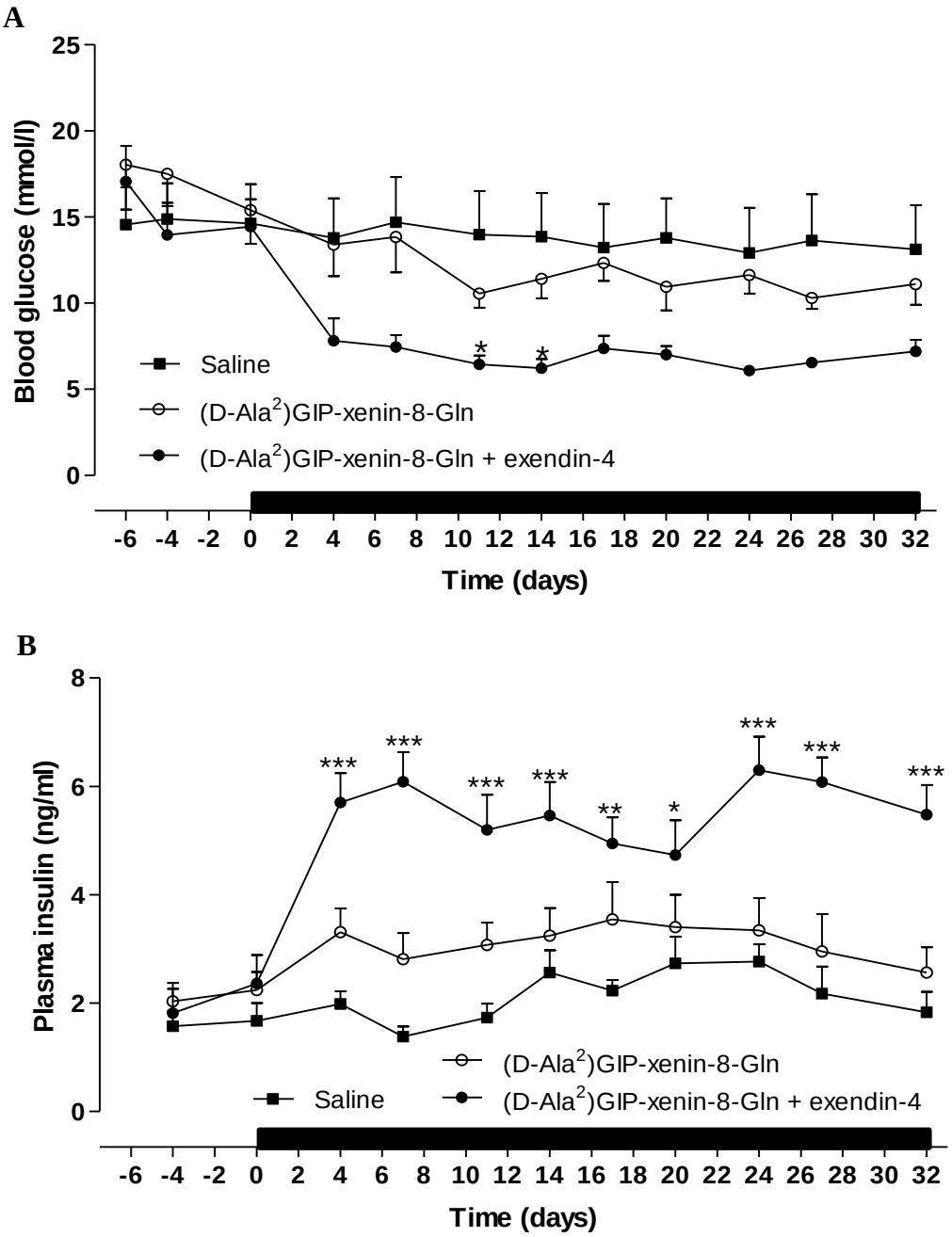

Blood glucose (A) and plasma insulin (B) was measured for 6 days before and 32 days during (indicated by black horizontal line) twice-daily treatment with saline, (D-Ala^2)GIP-xenin-8-Gln or (D-Ala^2)GIP-xenin-8-Gln in combination with exendin-4 (each at 25 nmol/kg bw). Values represent mean ± SEM (n=6-8). *P<0.05, **P<0.01 and ***P<0.001 compared with saline control.

Figure 3.7 Effects of twice daily administration of (D-Ala^2)GIP-xenin-8-Gln alone and in combination with exendin-4 on 24 hour blood glucose profile and % HbA1c in HFF mice

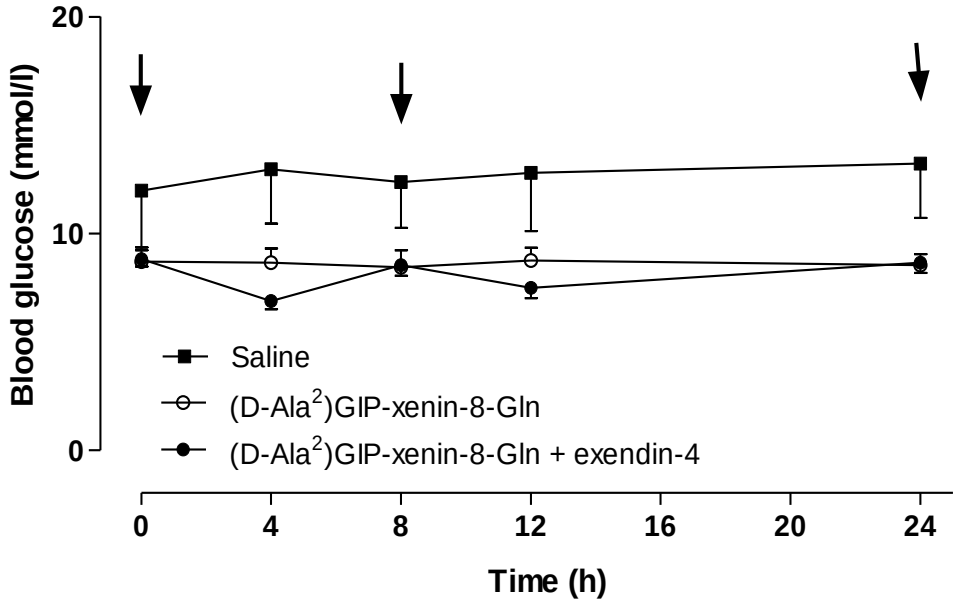

B

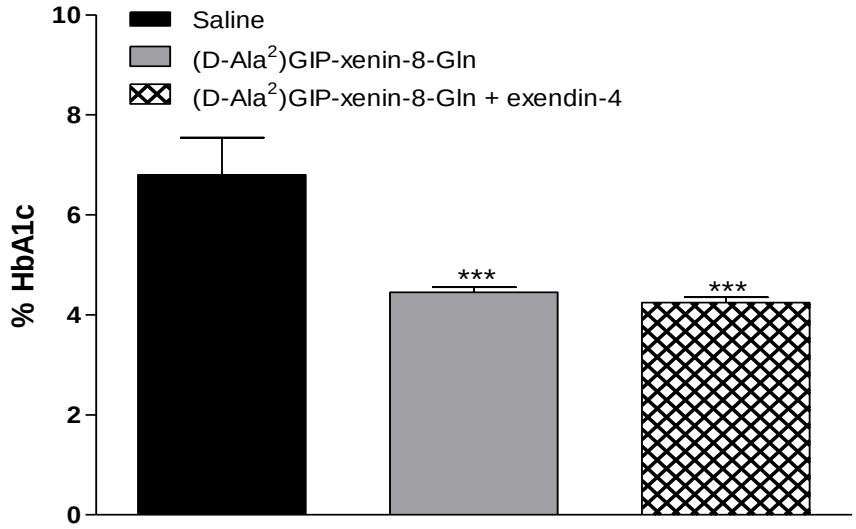

The 24 hour blood glucose profile (A) and %HbA1c (B) were assessed following 32 days of twice daily intraperitoneal administration of saline, (D-Ala^2)GIP-xenin-8-Gln or (D-Ala^2)GIP-xenin-8-Gln in combination with exendin-4 (each at 25 nmol/kg bw). Arrows indicate timing of treatment administration. Values represent mean ± SEM (n=6-8). ***P<0.001 compared with saline control.

Figure 3.8 Effects of twice-daily administration of (D-Ala^2)GIP-xenin-8-Gln alone and in combination with exendin-4 oral glucose tolerance in HFF mice

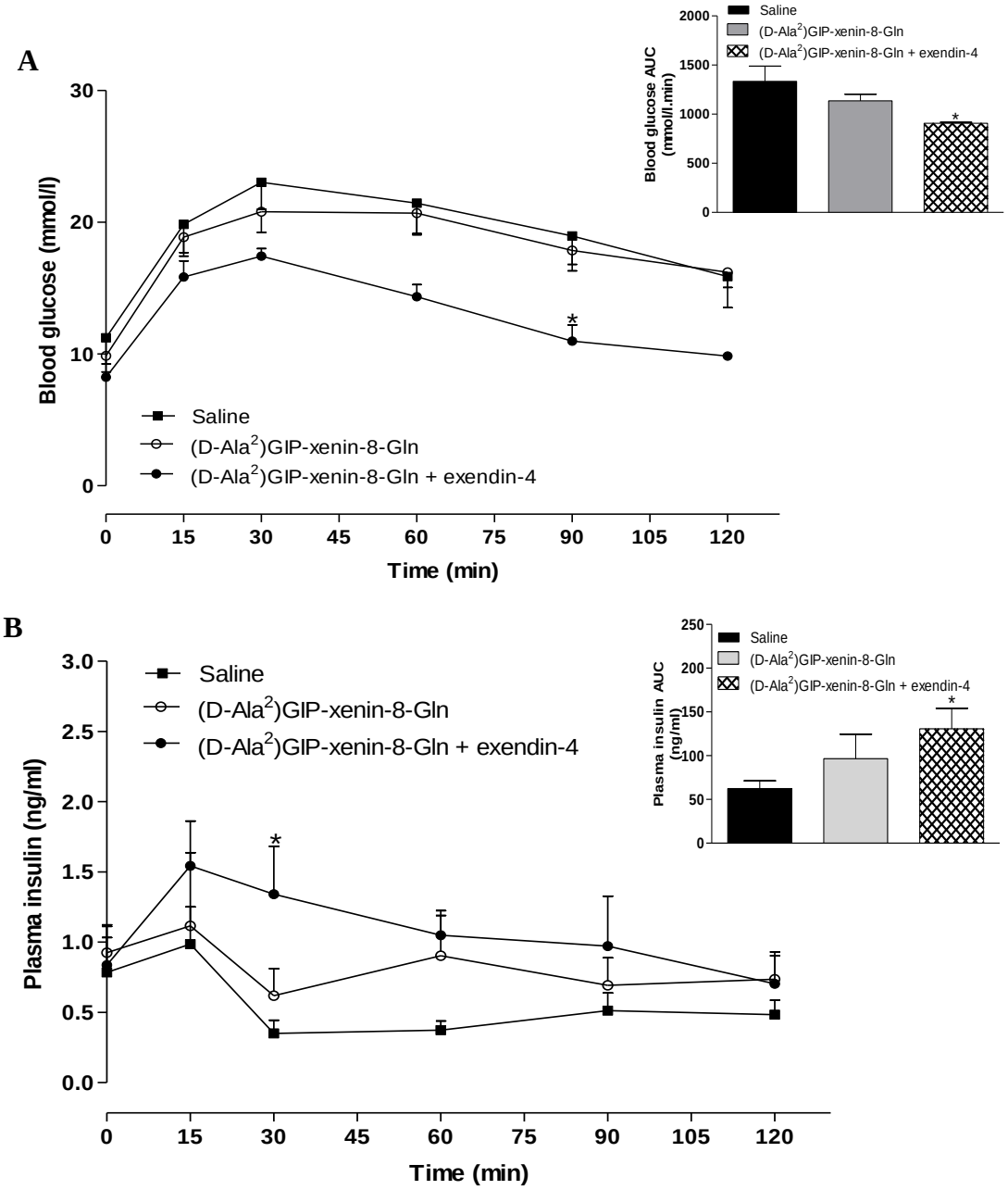

Test were performed following 32 days of twice-daily intraperitoneal administration of saline, (D-Ala^2)GIP-xenin-8-Gln or (D-Ala^2)GIP-xenin-8-Gln in combination with exendin-4 (each at 25 nmol/kg bw). Mice were fasted for 10 h previously. Blood glucose (A) and plasma insulin (B) was measured prior to and after oral administration of glucose (18 mmol/kg bw). Blood AUC values for 0-120 min are also included. Values represent mean ± SEM (n=6-8). *P<0.05 and **P<0.01 compared with saline control.

Figure 3.9 Effects of twice-daily administration of (D-Ala^2)GIP-xenin-8-Gln alone and in combination with exendin-4 on GIP tolerance test in HFF mice

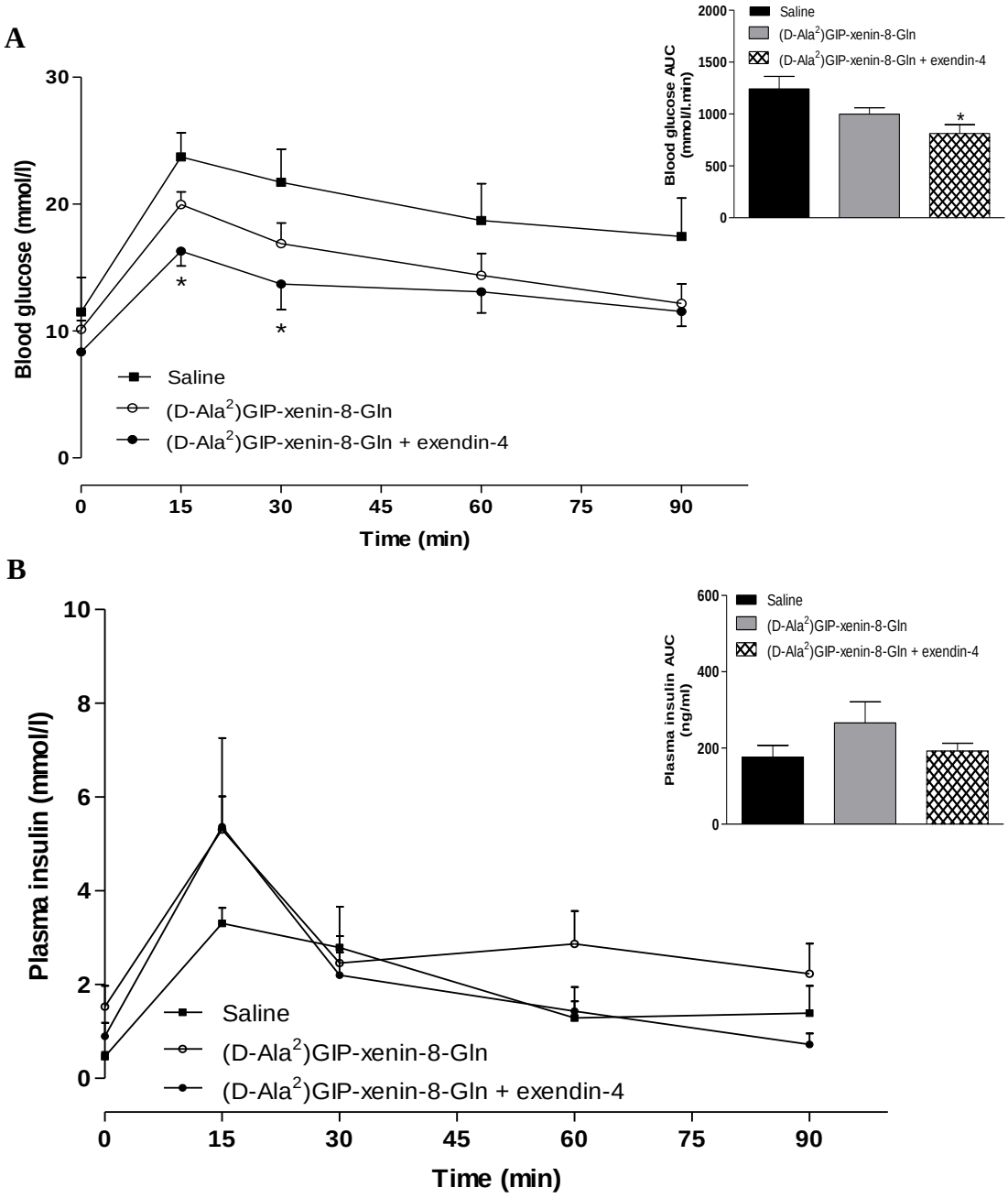

Test were performed following 32 days of twice-daily intraperitoneal administration of saline, (D-Ala^2)GIP-xenin-8-Gln or (D-Ala^2)GIP-xenin-8-Gln in combination with exendin-4 (each at 25 nmol/kg bw). Mice were fasted for 10 h previously. Blood glucose (A) and plasma insulin (B) was measured prior to and after intraperitoneal administration of glucose (18 mmol/kg bw) in combination with GIP (25 nmol/kg bw). Blood AUC values for 0-90 min are also included. Values represent mean ± SEM (n=6-8). *P<0.05 compared with saline control.

Figure 3.10 Effects of twice-daily administration of (D-Ala^2)GIP-xenin-8-Gln alone and in combination with exendin-4 on insulin sensitivity and pancreatic insulin content in HFF mice

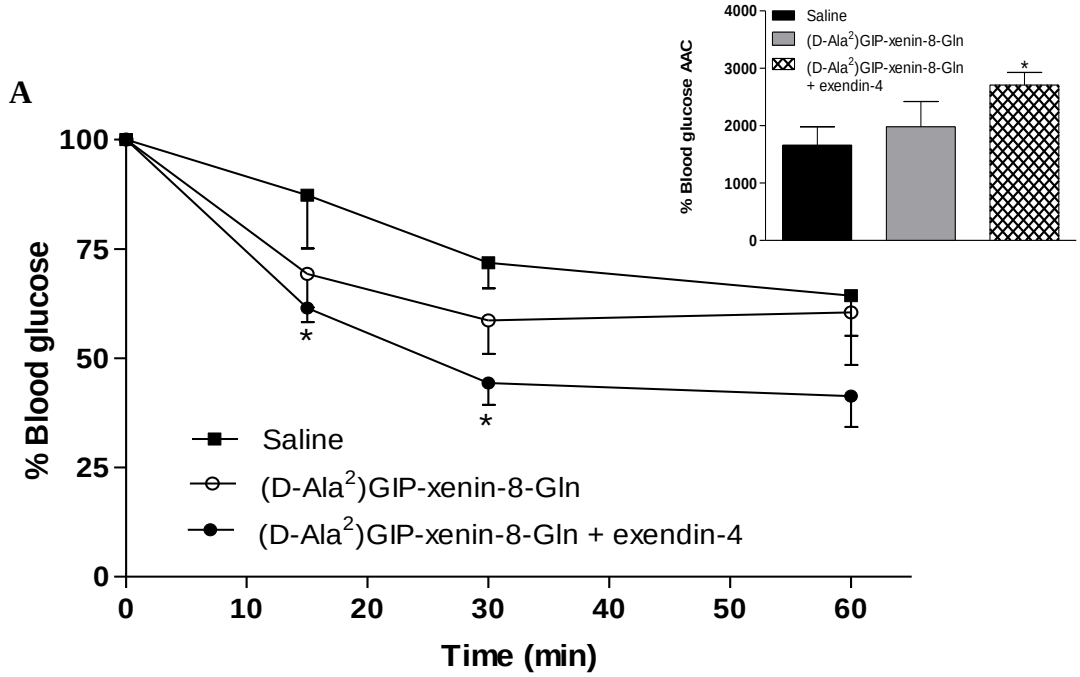

Test were performed following 32 days of twice-daily intraperitoneal administration of saline, (D-Ala^2)GIP-xenin-8-Gln or (D-Ala^2)GIP-xenin-8-Gln in combination with exendin-4 (each at 25 nmol/kg bw). Plasma glucose (A) was measured prior to and after i.p. administration of insulin (25 U/kg bw). Plasma AAC values for 0-60 min are also included. Pancreatic insulin content (B) was measured by RIA following pancreatic hormone extraction. Values represent mean ± SEM (n=6-8). *P<0.05, **P<0.01 and ***P<0.01 compared with saline control.

Figure 3.11 Effects of twice daily administration of (D-Ala^2)GIP-xenin-8-Gln alone and in combination with exendin-4 on insulin secretory responsiveness of isolated islets from HFF mice

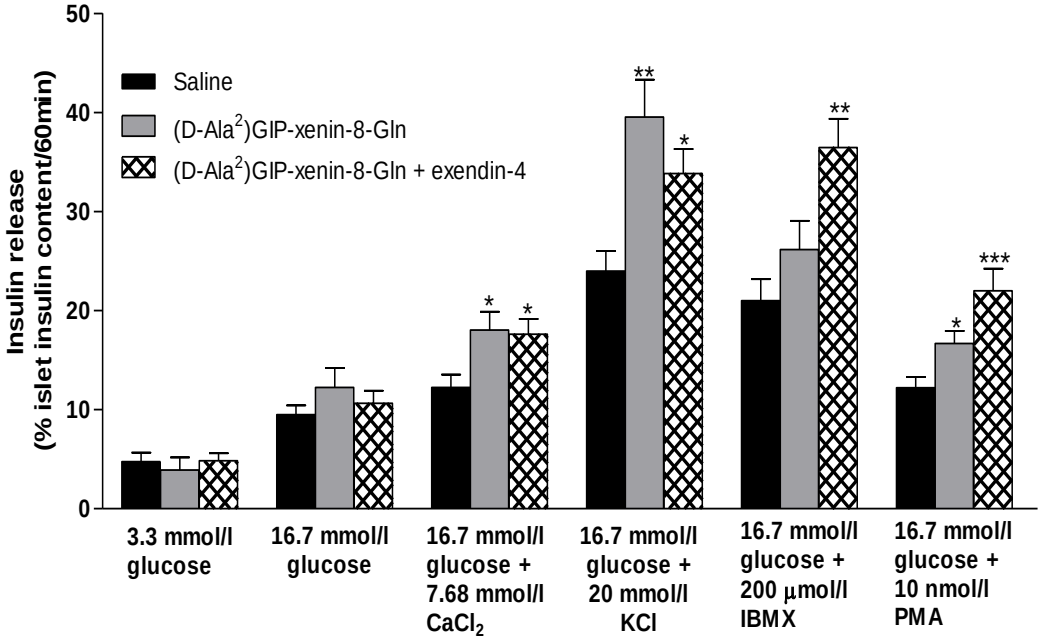

Effects of 32 days twice-daily i.p. administration of exendin-4, (D-Ala^2)GIP-xenin-8-Gln or a combination of both peptides (each at 25 nmol/kg bw) on pancreatic beta cell insulin secretory responsiveness in HFF mice. Pancreatic islets were isolated by standard collagenase digestion procedures. Values are mean ± SEM for (n=6-8). *P<0.05, **P<0.01 and ***P<0.01 compared with 16.7 mmol/l glucose control.

Figure 3.12 Effects of twice daily administration of (D-Ala^2)GIP-xenin-8-Gln alone and in combination with exendin-4 on total cholesterol, triglycerides, HDL and LDL in HFF mice

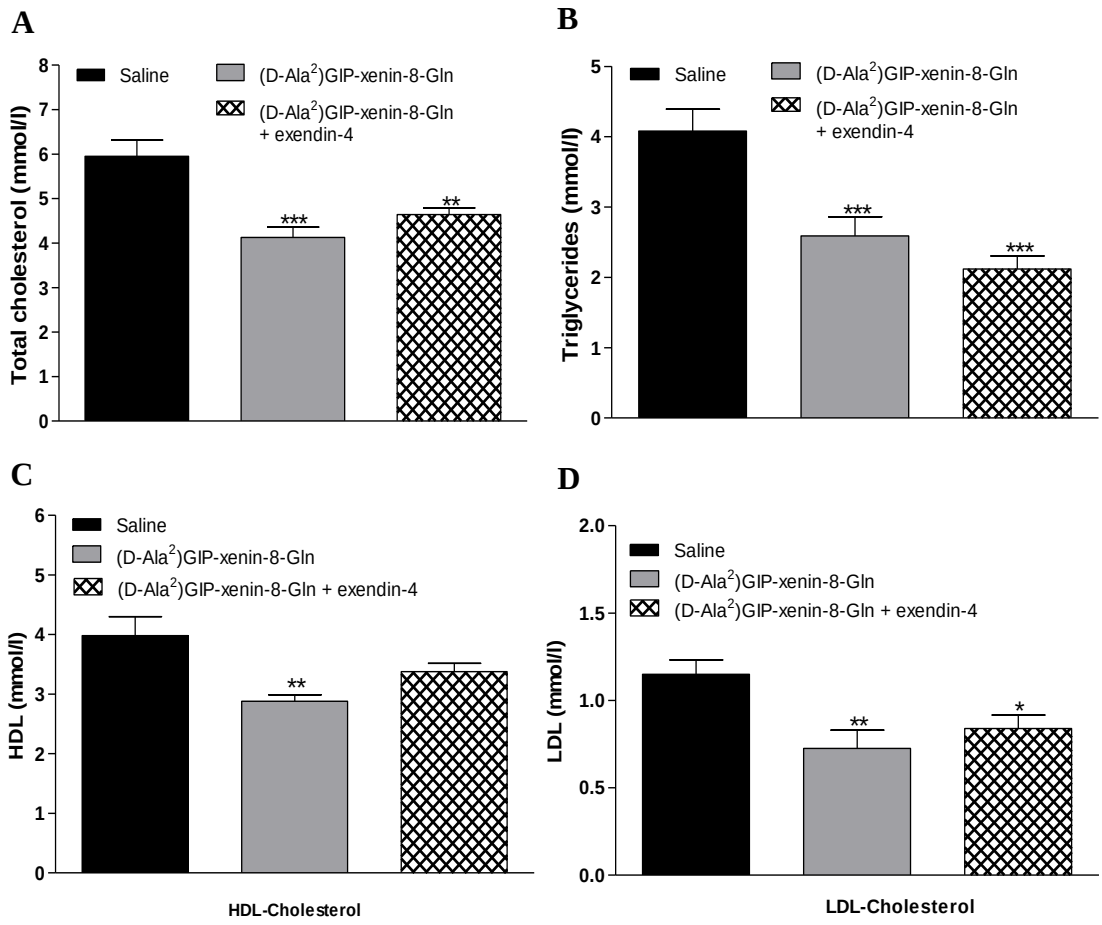

Effects of 32 days twice-daily i.p. administration of saline, (D-Ala^2)GIP-xenin-8-Gln or (D-Ala^2)GIP-xenin-8-Gln in combination with exendin-4 (each at 25 nmol/kg bw) on total cholesterol (A), triglycerides (B), HDL (C) and LDL (D) in HFF mice. LDL was calculated as total cholesterol - HDL - (triglycerides/5). Values are mean ± SEM (n=6-8). *P<0.05, **P<0.01 and ***P<0.001 compared with saline control.

Figure 3.13 Effects of twice daily administration of (D-Ala^2)GIP-xenin-8-Gln alone and in combination with exendin-4 on pancreatic islet histology in HFF mice

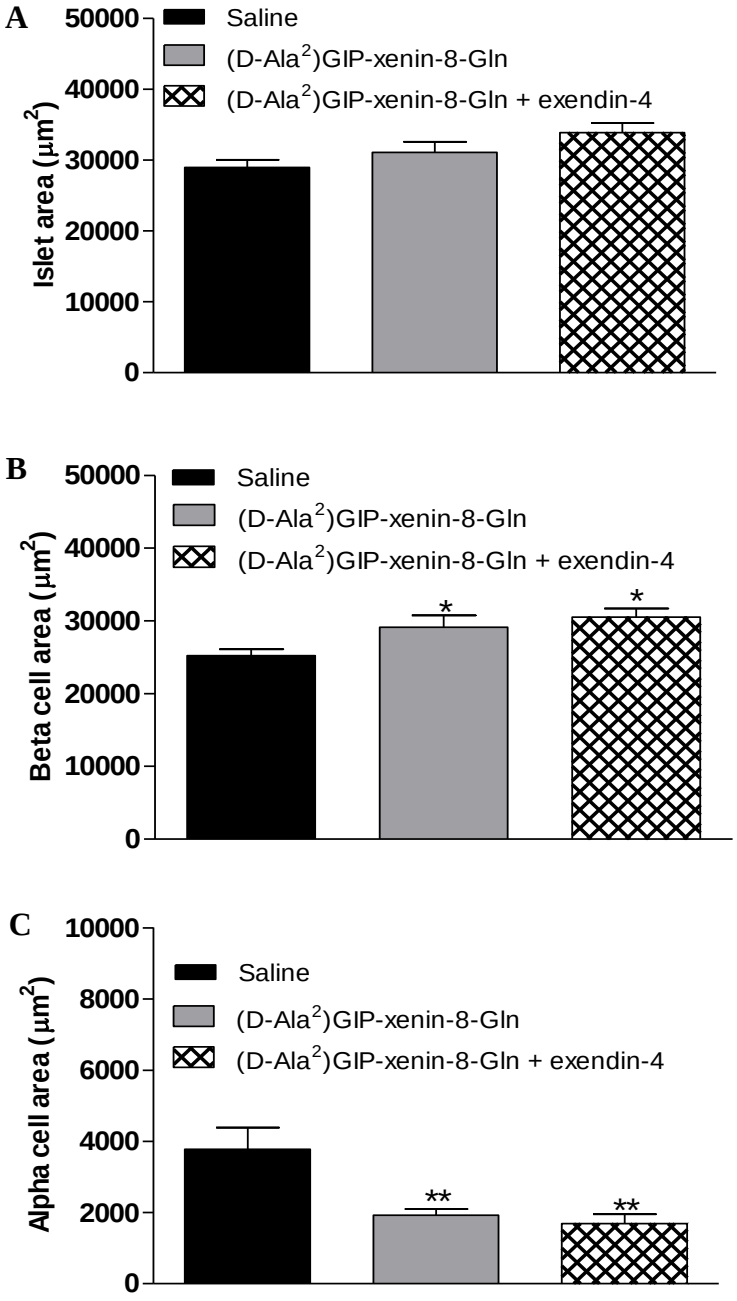

Effects of 32 days twice-daily i.p. administration of saline, (D-Ala^2)GIP-xenin-8-Gln or (D-Ala^2)GIP-xenin-8-Gln in combination with exendin-4 (each at 25 nmol/kg bw) on islet area (A), beta cell area (B), and alpha cell area (C) in HFF mice. Values are mean ± SEM (n=6-8). *P<0.05 and **P<0.01 compared with saline control.

Figure 3.14 Effects of twice daily administration of (D-Ala^2)GIP-xenin-8-Gln alone and in combination with exendin-4 on pancreatic islet histology in HFF mice

A

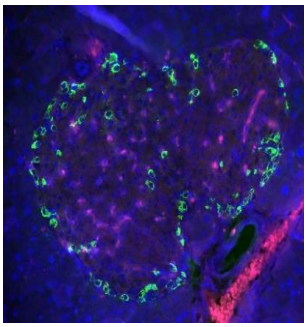

B

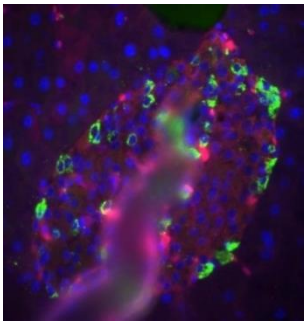

C

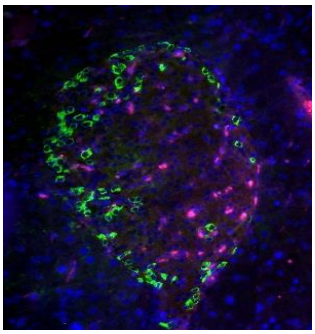

Images were captured by an Olympus System Microscope BX51 (Olympus instruments, UK) and a DP70 camera adapter. Cell^F image analysis software was used to assess parameters, magnification was X40. Insulin (red), glucagon (green) and DAPI (blue) in pancreatic tissue harvested from HFF mice treated for 32 days twice-daily with saline (A), (D-Ala^2)GIP-xenin-8-Gln (B) or a combination of both peptides (C) (each at 25 nmol/kg bw).

Chapter 4

Investigation of the antidiabetic and therapeutic potential of GIP-xenin-8-Gln in diabetic *db/db* mice

4.1 Summary

Previously, the HFF mouse model of obesity-induced T2DM was utilised to investigate the therapeutic, antidiabetic effects of the (D-Ala^2)GIP-xenin-8-Gln hybrid. However, no single animal model can fully replicate the complex aetiology of human T2DM. Therefore, the *db/db* mouse model, a genetically induced model of metabolic abnormalities including; dyslipidaemia, obesity, with well recognised beta cell dysfunction, representative of a severe manifestation of T2DM, was used to further investigate and evaluate the (D-Ala^2)GIP-xenin-8-Gln hybrid. Twice daily intraperitoneal administration of (DAla^2)GIP-xenin-8-Gln in *db/db* mice revealed no therapeutic effect on circulating glucose when treated with (DAla^2)GIP-xenin-8-Gln alone. However, in combination with exendin-4, (DAla^2)GIP-xenin-8-Gln improved glycaemic control throughout the observation period. Interestingly, only days 1 and 8 saw circulating insulin levels increased ($P<0.05$- $P<0.01$), suggesting that extrapancreatic glucose-lowering action of GIP, xenin and GLP-1 could be important. The daily plasma glucose levels corresponded with improved glucose profile (24h) and decreased percentage glycated haemoglobin (HbA1c) levels. Cumulative energy intake but not body weight was also significantly lowered by exendin-4 and (DAla^2)GIP-xenin-8-Gln in combination with exendin-4 ($P<0.05$ and $P<0.001$). Additionally, the percentage fat mass was also reduced in all treatment groups with (DAla^2)GIP-xenin-8-Gln showing the greatest reduction ($P<0.05$ to $P<0.001$) suggestive of (DAla^2)GIP-xenin-8-Gln having an influencing effect on body balancing factors. Glucose excursion was also improved by (DAla^2)GIP-xenin-8-Gln in combination with exendin-4 ($P<0.05$). However, sensitivity to insulin and GIP was unaffected. Furthermore, the pancreatic insulin content and islet morphology correlates with progressive disease manifestation. The results suggest that at the latter stages of T2DM, even with pharmacological intervention of (DAla^2)GIP-xenin-8-Gln alone or in combination with exendin-4, the progression of T2DM is difficult to halt and perhaps only applicable to earlier stages of disease manifestation, when beta cell function is more apparent.

4.2 Introduction

The progression to the development of T2DM is denoted by five distinct phases marked by progressing pancreatic beta cell dysfunction (Weir and Bonner-Weir, 2004). Phase one is compensation when insulin levels are increased along with beta cell mass due to increasing insulin resistance. Phase two is stable adaption with glucose levels increased, impaired glucose tolerance (IGT), loss of beta cell mass and increasing dysfunction. Phase three, unstable early decompensation and increasingly amplified hyperglycaemia within a brief time frame due to increasing insulin resistance and/or diminished beta cell mass. Phase four, stable decompensation: severe beta cell dedifferentiation. Phase five, severe decompensation: beta cell mass is extremely reduced resulting in overt diabetes (Weir and Bonner-Weir, 2004).

Phases one to three are characteristic of early stage diabetes or what is termed pre-diabetes and this infers the risk to development of diabetes (Fonseca, 2009; Weir and Bonner-Weir, 2004). T2DM has both genetic and environmental aetiologies and is a key element in the metabolic syndrome. Other characteristics include: high blood pressure, cholesterol, triglycerides and obesity that may also contribute to the pathogenesis of T2DM as well as the onset of beta cell dysfunction (O'Brien, Sakowski and Feldman, 2014). Therefore, it is of utmost importance to choose *in vivo* models that are representative of the various elements involved with the human condition (O'Brien, Sakowski and Feldman, 2014).

In the previous chapter, HFF mouse model of obesity-induced T2DM was utilised to investigate the therapeutic, antidiabetic effects of (D-Ala^2)GIP-xenin-8-Gln. This is a well-established experimental model pioneered by Surwit *et al.,* 1988, and is considered to be clinically relevant for investigation of diet-induced dysregulation of metabolic syndromes. However, no single animal model can completely mimic the complex aetiology of human T2DM. Therefore, in this chapter we continue the investigation of (D-Ala^2)GIP-xenin-8-Gln and its therapeutic effects in the *db/db* mouse model, a genetically induced model of T2DM that originated from the Jackson Laboratory in 1966. This model results from an autosomal recessive mutation on chromosome four that prevents the expression of the leptin receptor and compromises leptin signalling (Faita *et al.,* 2018; King, 2012). Leptin is a hormone that regulates food intake and energy expenditure, the consequences of dysregulation can result in

an altered metabolism and endocrine function (Srinivasan and Ramarao, 2007). The *db/db* model is also considered a valid animal model for investigating metabolic abnormalities including; dyslipidaemia, obesity and T2DM. This model is characterised by hyperinsulinemia at around two weeks, obesity at three to four weeks, high levels of cholesterol and triglycerides as well as the development of persistent hyperglycaemia at approximately four to six weeks that is sustained over its life span. This is propelled by peripherally impaired insulin action and progressing failure of the pancreatic beta cell (Faita *et al.,* 2018; Katsuda *et al.,* 2013; King, 2012). This model is well recognised as a T2DM model of beta cell dysfunction (Faita *et al.*, 2018), unlike HFF mice.

Thus, rationale for assessing the therapeutic effects of (D-Ala^2)GIP-xenin-8-Gln in two *in vivo* models of T2DM is because the HFF model is primarily representative of IGT and early T2DM, perceived by the development of insulin resistance and insufficient islet compensation. (Winzell and Ahren, 2004). Whereas *db/db* is considered a severe diabetes model with early on-set insulin resistance, a subsequent insulin secretory defect that results in profound hyperglycaemia and eventually ketosis (Katsuda *et al.,* 2013; King, 2012). Therefore it is essential to uncover the potential therapeutic applicability of the (D-Ala^2)GIP-xenin-8-Gln hybrid in both rodent models. The aim of this study was to assess the therapeutic effectiveness of the (D-Ala^2)GIP-xenin-8-Gln hybrid in the genetic *db/db* model of T2DM and to ascertain if there are any differences in its efficacious qualities or robustness as an antidiabetic therapeutic when the disease severity, aetiology and/or pathophysiology is altered compared to HFF mice (Chapter 3).

4.3 Materials and Methods

4.3.1 Peptides

All peptides were purchased from Syn Peptide Shanghai, China. Purity was confirmed by RP-HPLC and characterised by MALDI-TOF MS, previously described in Sections 2.1, 2.2.3, and 2.2.4. For all experimental materials and methods please refer to Section 2.1 and the relevant subsections.

4.3.2 Animals

The long-term study utilised male diabetic (*db/db*) mice (BKS.Cg-+ Leprdb/+ Leprdb/OlaHsd, 6-8 weeks), as described in Section 2.9.3.

4.3.3 Long-term *in vivo* study in *db/db* mice

Twice daily intraperitoneal injections (09:00 and 17:00 h) were administered with either saline alone (0.9% (w/v) NaCl), exendin-4, (DAla^2)GIP-xenin-8-Gln alone or in combination with exendin-4 (all peptides at 25 nmol/kg bw) for 29 days described in Section 2.11.1. Assessed metabolic parameters included: blood glucose, plasma insulin, body weight and cumulative energy intake, monitored every 3-4 days as described in Sections 2.11.1. End of treatment assessment parameters included glucose tolerance (18 mmol/kg bw), HbA1c, blood glucose profile, GIP tolerance, insulin sensitivity (50 U/kg), insulin content, percentage fat mass and islet morphology described in Sections 2.8.2, 2.8.3 and 2.11.2

4.3.4 Biochemical analysis

Blood/plasma glucose, plasma and pancreatic insulin were assayed as described in Sections 2.5.4 and 2.10

4.3.5 Statistical analysis

As described in Section 2.12

4.4 Results

4.4.1 Effects of twice-daily administration of exendin-4, (D-Ala^2)GIP-xenin-8-Gln or a combination of both peptides on cumulative energy intake, body weight and percentage fat mass in *db/db* mice

Following twice daily administration of all treatments for 29 days there was a significant lowering ($P<0.05$ to $P<0.001$) on cumulative energy intake compared to saline control (Figure 4.1A). Although not significant, there was a progressive decline in body weight in all groups (Figure 4.1B). However, percentage fat mass was significantly reduced (1.2-1.3 fold decrease; $P<0.05$ and $P<0.01$) in all treatment groups compared to saline treated control, with (D-Ala^2)GIP-xenin-8-Gln having the most significant decrease (1.3 fold decrease) (Figure 4.1C).

4.4.2 Effects of twice-daily administration of exendin-4, (D-Ala^2)GIP-xenin-8-Gln or a combination of both peptides on non-fasted glucose and insulin in *db/db* mice

Throughout the treatment period, non-fasted glucose was observed to be significantly decreased ($P<0.001$) when compared to saline treated control (Figure 4.2A). Treatment with (D-Ala^2)GIP-xenin-8-Gln alone resulted in a significant decrease until day 8 ($P<0.001$) but reverted to levels similar to that of saline treated control group from day 8 onwards (Figure 4.2A). Non-fasted insulin concentrations were significantly increased ($P<0.05$ and $P<0.01$) by exendin-4 on days 11 and 18, with (D-Ala^2)GIP-xenin-8-Gln in combination with exendin-4 only increasing ($P<0.01$) insulin on day 1 and 8, compared to saline control (Figure 4.2B).

4.4.3. Effects of twice daily administration of exendin-4, (D-Ala^2)GIP-xenin-8-Gln or a combination of both peptides on 24 hour blood glucose profile and % HbA1c in *db/db* mice

After twice daily administration of the peptide treatment regimens for 29 days (D-Ala^2)GIP-xenin-8-Gln and (D-Ala^2)GIP-xenin-8-Gln in combination with exendin-4 significantly reduced ($P<0.05$) glucose levels at both 4 and 8 hour time points compared to saline control (Figure 4.3A). Moreover, exendin-4 further reduced ($P<0.001$) glucose levels at the same time points when compared to saline (Figure 4.3A). The % HbA1c was reduced ($P<0.05$) in all exendin-4 treated *db/db* mice when compared to (D-Ala^2)GIP-xenin-8-Gln alone but all were still elevated ($P<0.001$) compared to lean controls (Figure 4.3B).

4.4.4 Effects of twice-daily administration of exendin-4, (D-Ala^2)GIP-xenin-8-Gln or a combination of both peptides on glucose and insulin in response to an oral glucose challenge in *db/db* mice

Twice daily administration of all treatment groups demonstrated limited effects on glycaemic response on post oral glucose load (Figure 4.4A). Glucose was unaffected by the treatment groups, except (D-Ala^2)GIP-xenin-8-Gln in combination with exendin-4, which had reduced ($P<0.05$) glucose at 15 min time point with a significantly lower ($P<0.05$) overall AUC (Figure 4.4A). (D-Ala^2)GIP-xenin-8-Gln had significantly lower ($P<0.05$) glucose-induced insulin secretion at time point 0 min after 10 hours fasting, and this remained reduced ($P<0.05$) at the 15 min time point compared to saline controls (Figure 4.4B). Exendin-4 had significantly reduced ($P<0.001$) insulin at the 15 min time point only, (D-Ala^2)GIP-xenin-8-Gln in combination with exendin-4 reduced ($P<0.05$) insulin at the same time point compared to saline control (Figure 4.4B). The AUC demonstrates that exendin-4 is the only treatment group to significantly effect insulin response as it reduced ($P<0.05$) AUC values (Figure 4.4B).

4.4.5 Effects of twice-daily administration of exendin-4, (D-Ala^2)GIP-xenin-8-Gln or a combination of both peptides on glucose and insulin in response to GIP in *db/db* mice

Glucose and GIP was administered in combination to assess GIP tolerance following twice daily peptide administration for 29 days. Interestingly, in terms of individual values all treatments had no significant effect on either glucose or insulin levels when compared to saline treated controls (Figure 4.5A-B). However, AUC values for exendin-4 show that overall, exendin-4 reduced ($P<0.05$) glucose and the corresponding insulin levels ($P<0.01$) when compared to (D-Ala^2)GIP-xenin-8-Gln treatment alone (Figure 4.5A-B).

4.4.6 Effects of twice-daily administration of exendin-4, (D-Ala^2)GIP-xenin-8-Gln or a combination of both peptides on insulin sensitivity and pancreatic insulin content in *db/db* mice

Following 29 days, twice daily administration of exendin-4 or (D-Ala^2)GIP-xenin-8-Gln alone had no effect on insulin sensitivity (Figure 4.6A). However, there was a significant effect by (D-Ala^2)GIP-xenin-8-Gln in combination with exendin-4, which decreased ($P<0.05$) glucose at the 15 min time point compared to saline controls (Figure 4.6A). In addition, ACC shows that none of the treatment groups had a significant overall effect on insulin sensitivity (Figure 4.6A). Pancreatic insulin content was not significantly different across the treatment groups compared to saline controls (Figure 4.6B). However, all *db/db* mice had reduced ($P<0.05$) pancreatic insulin content when compared to lean mice (Figure 4.6B).

4.4.7 Effects of twice daily administration of exendin-4, (D-Ala^2)GIP-xenin-8-Gln or a combination of both peptides on pancreatic histology in *db/db* mice

Pancreatic islet area was unaffected by any of the treatment groups in comparison to saline treated controls (Figure 4.7A). In all *db/db* mice treated with exendin-4, pancreatic islet area was not significantly different from lean control mice (Figure 4.7A). Pancreatic beta cell area was unaffected by all treatment groups compared to saline treated *db/db* control (Figure 4.7B). In comparison to lean mice beta cell area of all the *db/db* groups was significantly reduced ($P<0.05$ to $P<0.01$) (Figure 4.7B). Interestingly, there was no significant change in alpha cell area (Figure 4.7C). Representative images of islets from all groups of mice are shown in Figure 4.7A-E.

4.5 Discussion

This study investigated the therapeutic utility of (DAla^2)GIP-xenin-8-Gln using a preclinical genetic *db/db in vivo* model useful for studying novel pharmacological targets to treat T2DM and other metabolic syndromes. This model presents with age-dependent progression of diabetes, early insulin resistance followed by defective insulin secretion that ultimately results in extreme hyperglycaemia and is considered to replicate a fairly, severe manifestation of T2DM (Faita *et al.*, 2018; King, 2012; Winzell and Ahren, 2004). In the previous chapter (DAla^2)GIP-xenin-8-Gln was shown to have efficacious potential for treatment of obesity-diabetes as demonstrated in HFF mice (Chapter 3). Qualities included an enhanced glycaemic control and

insulinotropic effect along with potential restoration of GIP action which is lost as T2DM progresses (Hasib *et al.,* 2017; Kaku, 2010). This present study was designed to investigate if such benefits would be achievable in a genetically induced, later stage rodent model of T2DM.

The chronic 29 day treatment regimen, with twice daily intraperitoneal administration of (DAla^2)GIP-xenin-8-Gln in *db/db* mice revealed no therapeutic effect on non-fasted glucose when treated alone. However, with the addition of exendin-4, (DAla^2)GIP-xenin-8-Gln markedly improved glycaemic control throughout the observation period. However, circulating insulin levels were only increased on day 1 and 8 of treatment, which was unexpected suggesting that the recognised extrapancreatic glucose-lowering action of GIP, xenin and GLP-1 could be important (Al-Sabah, 2015; Baggio and Drucker, 2007; Capozzi *et al.,* 2018; Parthsarathy *et al.,* 2016; Psichas Reimann and Gribble, 2015). The blood profile (24h) and percentage glycated haemoglobin (HbA1c) levels emulated the daily glucose levels as (DAla^2)GIP-xenin-8-Gln in combination with exendin-4 yielded greater glycaemic control. Moreover, even though glucose levels were reduced by peptide therapy, they remained at a significantly elevated level when compared to non-diabetic controls, this was in keeping with the described disease progression of profound hyperglycaemia in *db/db* mice (Faita *et al.,* 2018; Katsuda *et al.,* 2013; King, 2012).

(DAla^2)GIP-xenin-8-Gln in combination with exendin-4 had significant lowering effects on cumulative energy intake but not on body weight over the 29 day period. Moreover, throughout the treatment period the body weight of all *db/db* mice began to progressively decrease. When considering the decrease in body weight it is important to consider if its relevance is in relation to pharmacological intervention or if it is phenotypical to the *in vivo* model, as weight loss is characteristic of the *db/db* breed at the latter stage of the disease (Srinivasan and Ramarao, 2007). Other factors that must also be considered but not limited to, when interpreting information and data include the age of said mice and the rate/stage of disease progression, as this can vary between colonies (Srinivasan and Ramarao, 2007). However, exendin-4 is well known to reduce body weight (Kanoski, Hayes and Skibicka, 2016) and there are suggestions that GIP and xenin may also decrease body weight (Al-Sabah, 2015; Anlauf *et al.,* 2000; Campbell and Drucker, 2013; Craig, Gault and Irwin, 2018; Parthsarathy *et al.,* 2016). Interestingly, the percentage fat mass was also reduced in all treatment groups

but not the saline group. (DAla^2)GIP-xenin-8-Gln elicited the greatest reduction closely followed by the exendin-4 and (DAla^2)GIP-xenin-8-Gln in combination with exendin-4 treatment groups. This is suggestive that (DAla^2)GIP-xenin-8-Gln may have an influencing effect on body balancing factors such as fat mass in *db/db* mice. Indeed, both GIP and xenin are known to play a role in lipid metabolism (Campbell and Drucker, 2013; Craig, Gault and Irwin, 2018). Further studies examining actions at adipocytes using *in vitro* models and *ex vivo* imaging would be important.

The oral glucose challenge following the treatment period revealed improvement in glucose excursion in *db/db* mice treated with (DAla^2)GIP-xenin-8-Gln in combination of exendin-4. However, sensitivity to insulin and GIP was unaffected by treatment with (DAla^2)GIP-xenin-8-Gln alone or in combination with exendin-4. This is perhaps not surprising given the severe hyperglycaemia in this model. Similarly, the bolus of GIP administered may not have been high enough to elicit a basal response in these mice given the severity of beta cell dysfunction (Gault *et al.*, 2002: King *et al.*, 2012).

In agreement, the pancreatic insulin content had no marked difference between the treatment groups, although insulin content was significantly reduced compared to the lean control highlighting the extreme level of beta cell dysfunction of this breed (Faita *et al.*, 2018; Katsuda *et al.*, 2013). Islet morphology also correlates with the progressive disease manifestation where pancreatic islets undergo atrophy and beta cell necrosis (Faita *et al.*, 2018; Katsuda *et al.*, 2013). None of the pharmacological interventions were able to fully prevent or protect against decline or death in either islets or beta cells, although exendin-4 alone and in combination with (DAla^2)GIP-xenin-8-Gln did appear most effective in this regard. However, overall islet and beta cell areas of the treatment groups was similar to that of the saline treated control (Katsuda *et al.*, 2013). Although it is important to note this *in vivo* monogenetic model is absent of the inflammatory mechanism as well as other genetic and environmental factors that are apparent within the human manifestation of T2DM. Therefore, the complex interactions that lead to the diseased state in humans is not replicated fully by this model (Faita *et al.*, 2018; Katsuda *et al.*, 2013; Winzell and Ahren, 2004).

Together these results suggest that at the end stages of disease, even with the pharmacological intervention of (DAla^2)GIP-xenin-8-Gln alone or in combination with exendin-4, the progression of T2DM is difficult to halt (Paschetta, Hvalryg and

Musso, 2011; Senio, Fukushima and Yabe, 2010). Thus, the postulation that restoration of GIP sensitivity dramatically improves T2DM is perhaps only applicable to earlier stages of disease manifestation, when beta cell function is more apparent (Al-Sabah, 2015; Irwin and Flatt, 2015). We were disappointed to some degree with the results using the *db/db* model, especially given positive effects using HFF mice. This was the first time we used this particular strain which appeared to exhibit a much more severe diabetes phenotype than we had initially expected. On reflection, we may well have initiated treatment earlier or if time and other resources had been available, we would have conducted a dose-finding pilot.

To conclude, the data from this study largely correlates with the previous chapter, noting the ability of the monomeric, multi-targeting analogue, (DAla^2)GIP-xenin-8-Gln to have a positive effect on regulating energy balance in T2DM. This is most likely attributed to the biological action of xenin as it is the hormone with established appetite suppression and lipid metabolism modulating abilities, thought to be mediated by neurotensin receptors. Neurotensin, as a hormone and neurotransmitter, has also been shown to have protective effects on beta cells and modulate energy balance (Craig, Gault and Irwin, 2018; Mazella *et al.*, 2012). Therefore, there may well be the possibility that xenin or neurotensin derived entities could represent an alternative area of study for development of novel antidiabetic therapeutics and forms the substance of the following chapter.

Figure 4.1 Effects of twice-daily administration of exendin-4, (D-Ala^2)GIP-xenin-8-Gln or a combination of both peptides on cumulative energy intake, body weight and percentage fat mass in *db/db* mice

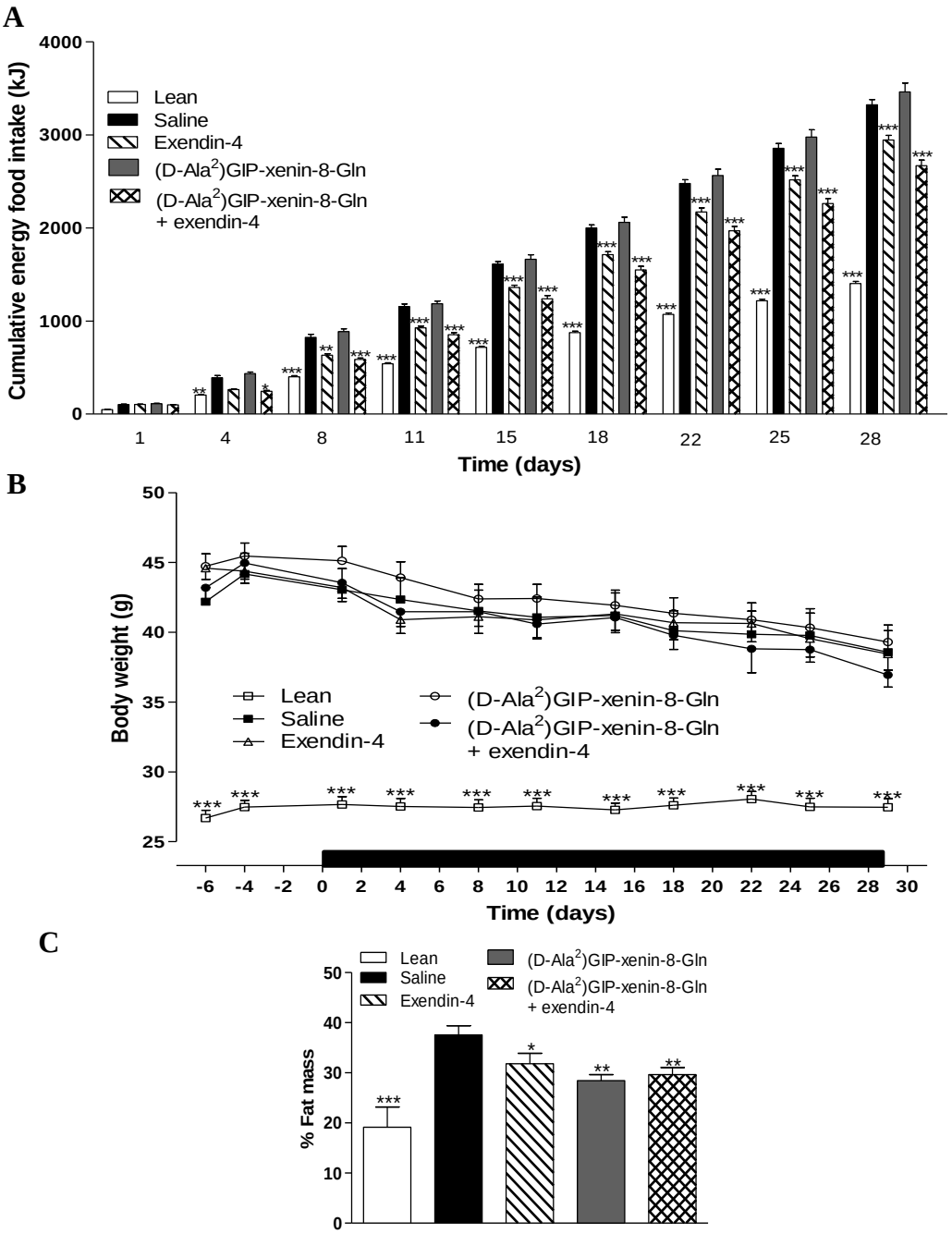

Variables were measured for 6 days before and 29 days during (indicated by black horizontal line (B)) twice-daily treatment with saline, exendin-4, (D-Ala^2)GIP-xenin-8-Gln or in combination of exendin-4 (each at 25 nmol/kg) on cumulative energy intake (A) and body weight (B) and percentage fat mass measured by DEXA, after 29 days (C). Values represent mean ± SEM (n=6-8). *P<0.05, **P<0.01 and ***P<0.001 in comparison with saline control.

Figure 4.2 Effects of twice-daily administration of exendin-4, (D-Ala^2)GIP-xenin-8-Gln or a combination of both peptides on non-fasted plasma glucose and insulin in *db/db* mice

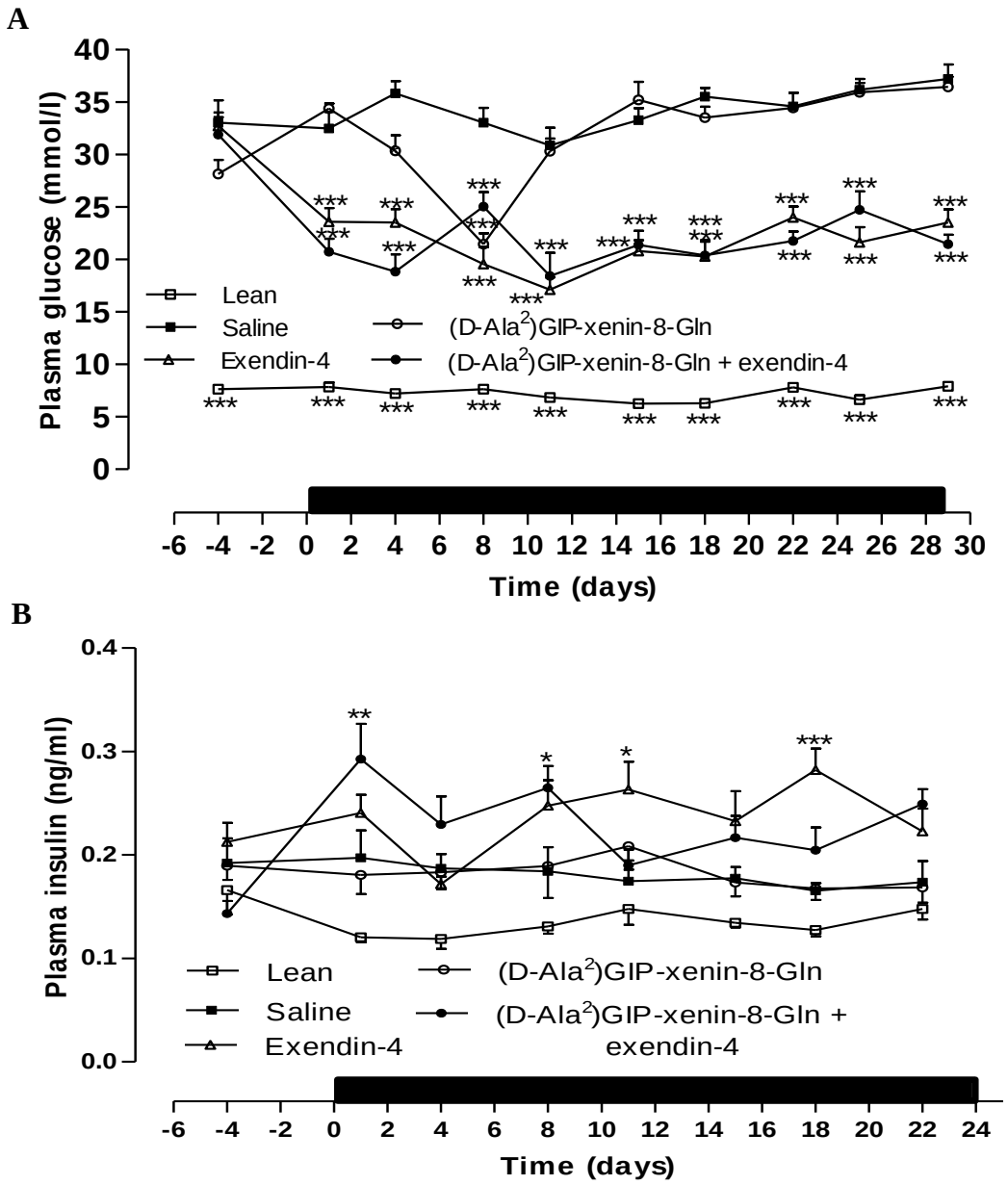

Blood glucose (A) and plasma insulin (B) was measured for 6 days before and 29 days during (indicated by black horizontal line) twice-daily treatment with saline, exendin-4, (D-Ala^2)GIP-xenin-8-Gln or in combination of exendin-4 (each at 25 nmol/kg bw). Values represent mean ± SEM (n=6-8). *P<0.05, **P<0.01 and ***P<0.001 compared with saline control.

Figure 4.3. Effects of twice daily administration of exendin-4, (D-Ala^2)GIP-xenin-8-Gln or a combination of both peptides on 24 hour blood glucose profile and % HbA1c in *db/db* mice

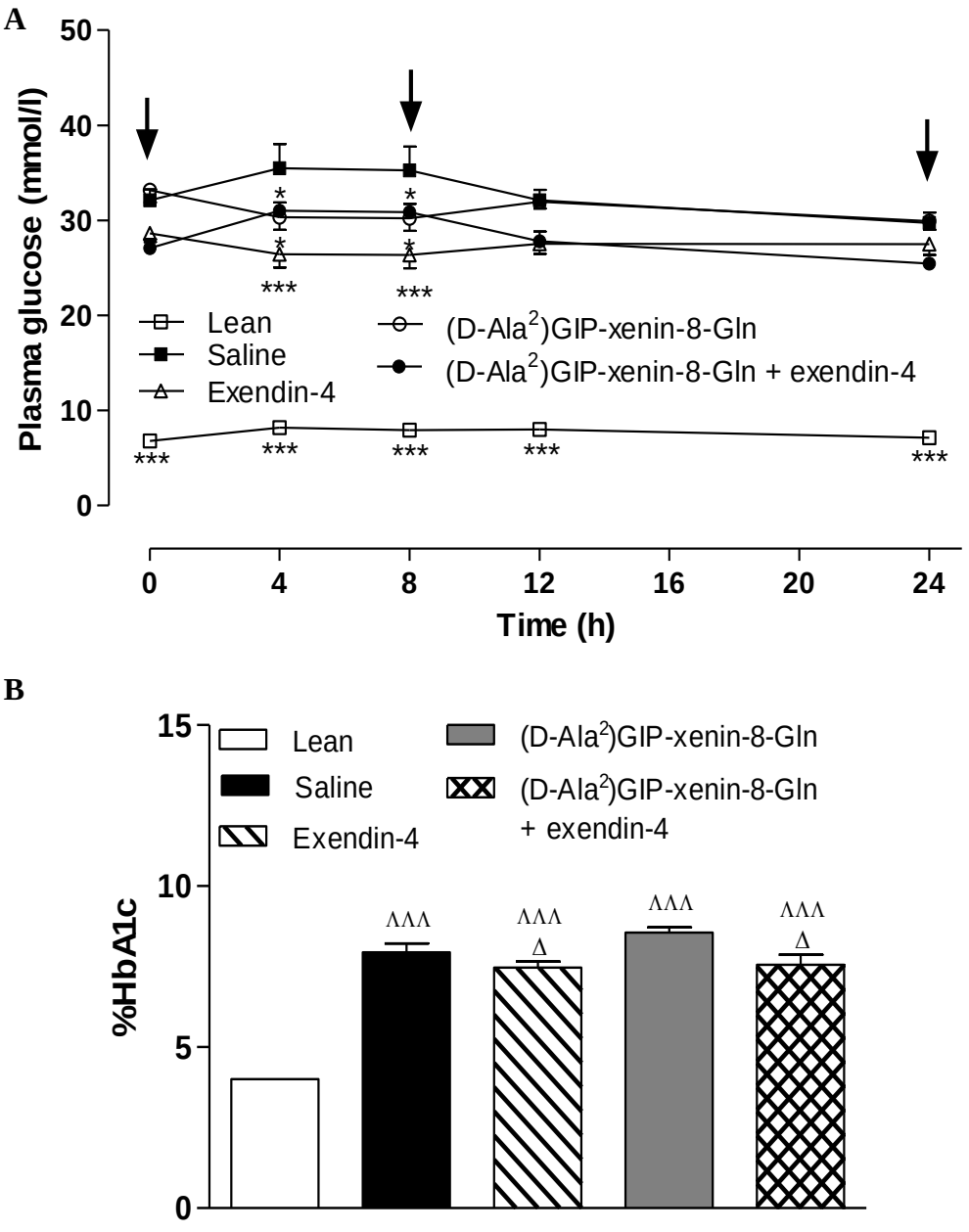

The 24 hour blood glucose profile (A) and % HbA1c (B) were assessed following 29 days of twice daily intraperitoneal administration of saline, exendin-4, (D-Ala^2)GIP-xenin-8-Gln or in combination of exendin-4 (each at 25 nmol/kg bw). Arrows are indicative of treatment administration. Values represent mean ± SEM (n=6-8). *P<0.05, **P<0.01 and ***P<0.001 compared with saline control or $^{\Delta}$P<0.05 compared with (D-Ala^2)GIP-xenin-8-Gln or $^{\Lambda\Lambda\Lambda}$P<0.001 compared to lean control.

Figure 4.4 Effects of twice-daily administration of exendin-4, (D-Ala^2)GIP-xenin-8-Gln or a combination of both peptides on plasma glucose and plasma insulin in response to an oral glucose challenge in *db/db* mice

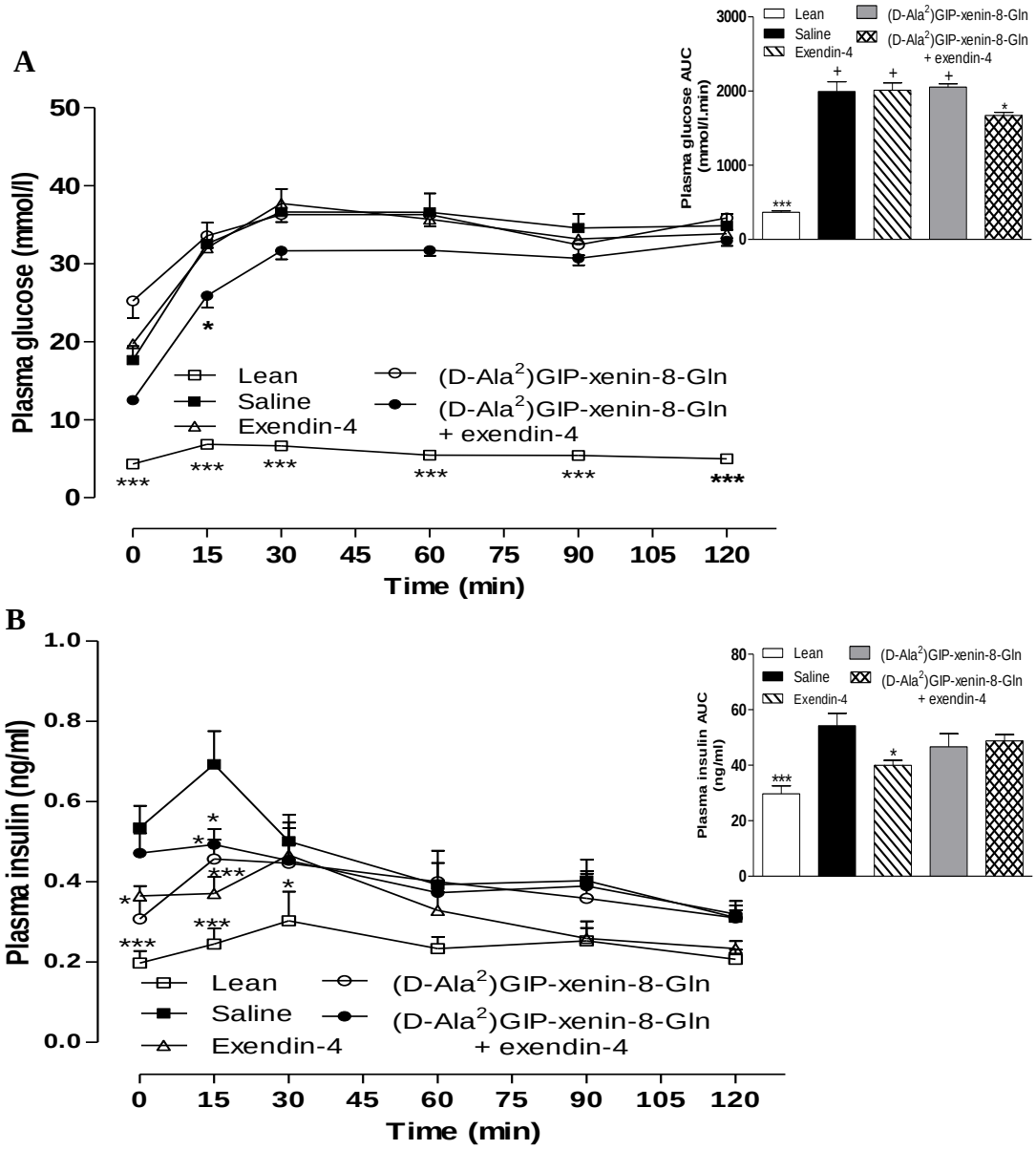

Test were performed following 29 days of twice-daily intraperitoneal administration of saline, exendin-4, (D-Ala^2)GIP-xenin-8-Gln or in combination of exendin-4 (each at 25 nmol/kg bw). Mice were fasted for 10 h previously. Plasma glucose (A) and plasma insulin (B) was measured prior to and after oral administration of glucose alone (18 mmol/kg bw). Plasma AUC values for 0-120min are also included. Values represent mean ± SEM (n=6-8). *P<0.05, **P<0.01 and ***P<0.001 with saline control or $^{+}$P<0.05 compared with (D-Ala^2)GIP-xenin-8-Gln in combination with exendin-4.

Figure 4.5 Effects of twice-daily administration of exendin-4, (D-Ala^2)GIP-xenin-8-Gln or a combination of both peptides on plasma glucose and plasma insulin in response to GIP in *db/db* mice

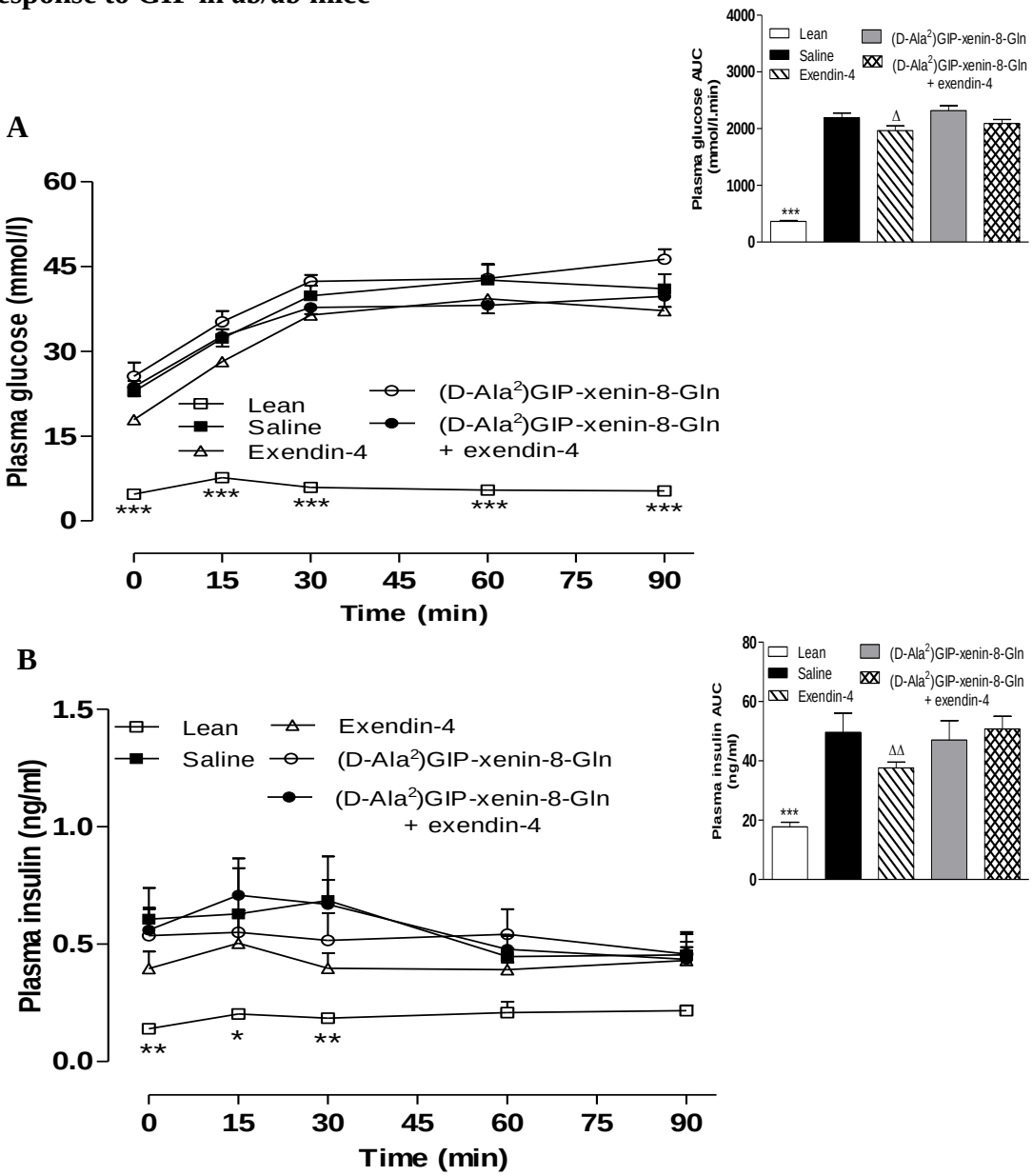

Test were performed following 29 days of twice-daily intraperitoneal administration of saline, exendin-4, (D-Ala^2)GIP-xenin-8-Gln or in combination of exendin-4 (each at 25 nmol/kg bw). Mice were fasted for 10 h previously. Plasma glucose (A) and plasma insulin (B) was measured prior to and after intraperitoneal administration of glucose (18 mmol/kg bw) in combination with GIP (25 nmol/kg bw). Plasma AUC values for 0-90min are also included. Values represent mean ± SEM (n=6-8). *P<0.05, **P<0.01 and ***P<0.001 with saline control or $^{\Delta}$P<0.05 and $^{\Delta\Delta}$P<0.01 compared with (D-Ala^2)GIP-xenin-8-Gln.

Figure 4.6 Effects of twice-daily administration of exendin-4, (D-Ala^2)GIP-xenin-8-Gln or a combination of both peptides on insulin sensitivity and pancreatic insulin content in *db/db* mice

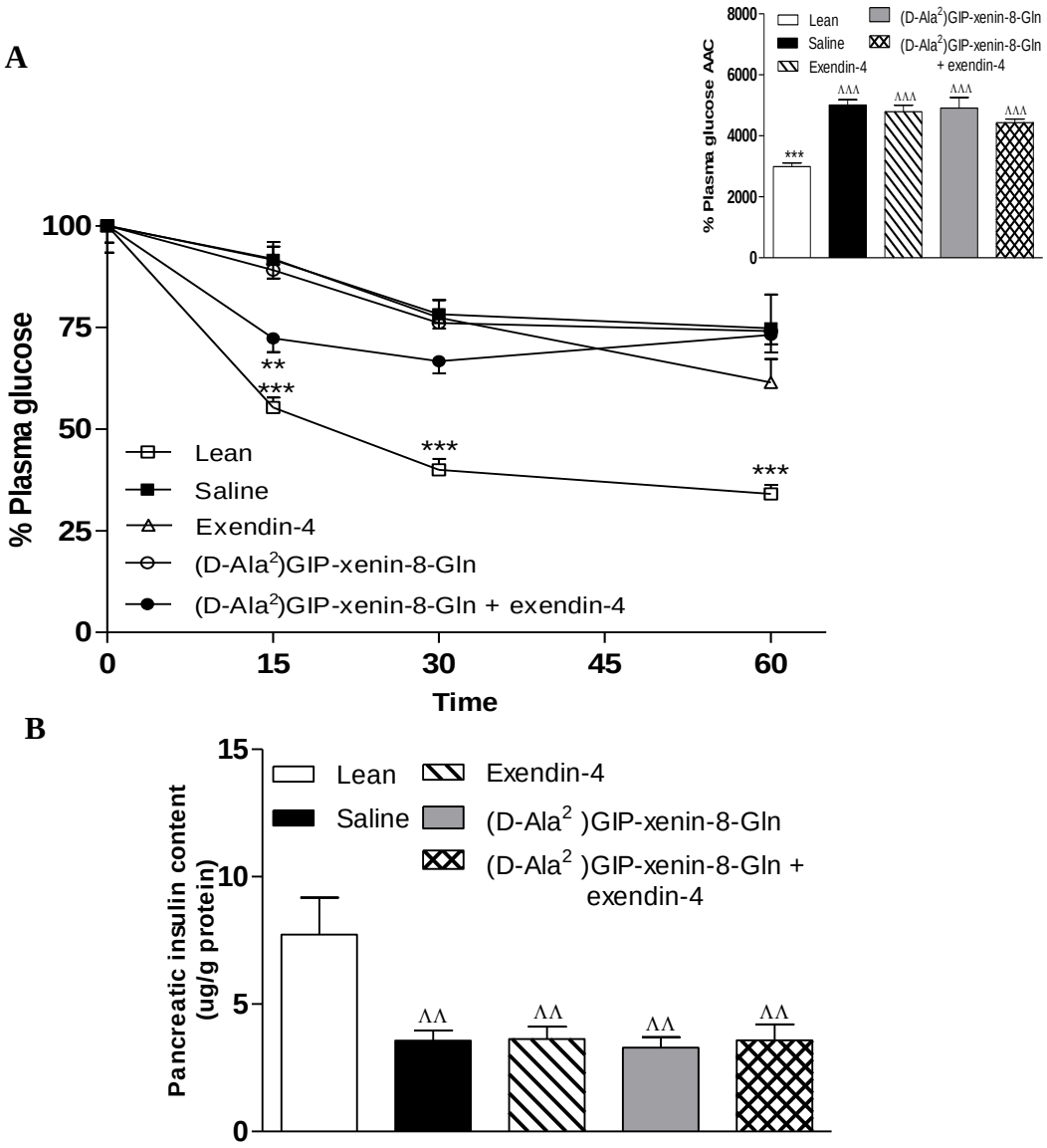

Test were performed following 29 days of twice-daily intraperitoneal administration of saline, exendin-4, (D-Ala2)GIP-xenin-8-Gln or in combination of exendin-4 (each at 25 nmol/kg bw). Plasma glucose (A) was measured prior to and after i.p. administration of insulin (50 U/kg bw). Plasma AAC values for 0-60min are also included. Pancreatic insulin content (B) was measured by RIA following pancreatic hormone extraction. Values represent mean ± SEM (n=6-8). **P<0.01 and ***P<0.001 compared with saline control or $^{\wedge\wedge}$P<0.01 and $^{\wedge\wedge\wedge}$P<0.001 compared to lean control.

Figure 4.7 Effects of twice daily administration of exendin-4, (D-Ala^2)GIP-xenin-8-Gln or a combination of both peptides on pancreatic histology in *db/db* mice

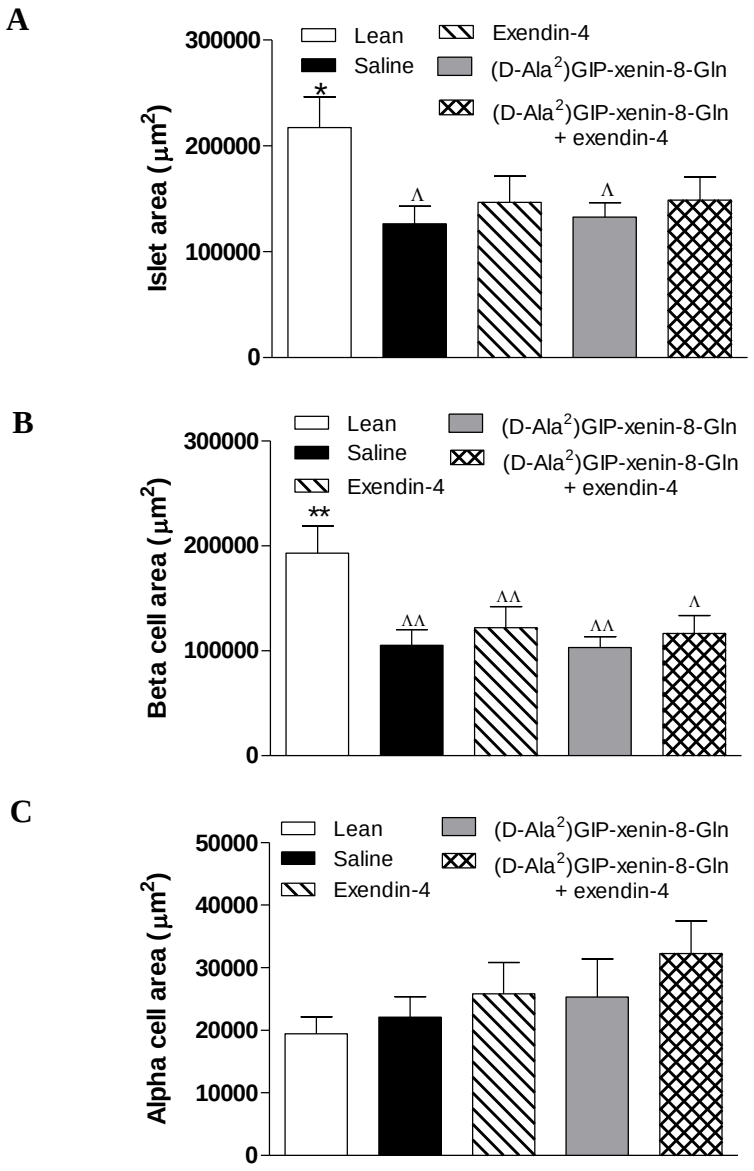

Effects of twice-daily i.p. administration of exendin-4, (D-Ala^2)GIP-xenin-8-Gln or a combination of both peptides (each at 25 nmol/kg bw) following 29 day administration on islet area (A), beta cell area (B), and alpha cell area (C) in *db/*db mice. Values are mean ± SEM (n=6-8). *P<0.05 and **P<0.01 compared with saline treated control. $^{\Lambda}$P<0.05, $^{\Lambda\Lambda}$P<0.01 compared to lean control.

Figure 4.8 Effects of twice daily administration of exendin-4, (D-Ala^2)GIP-xenin-8-Gln or a combination of both peptides on pancreatic histology in *db/db* mice

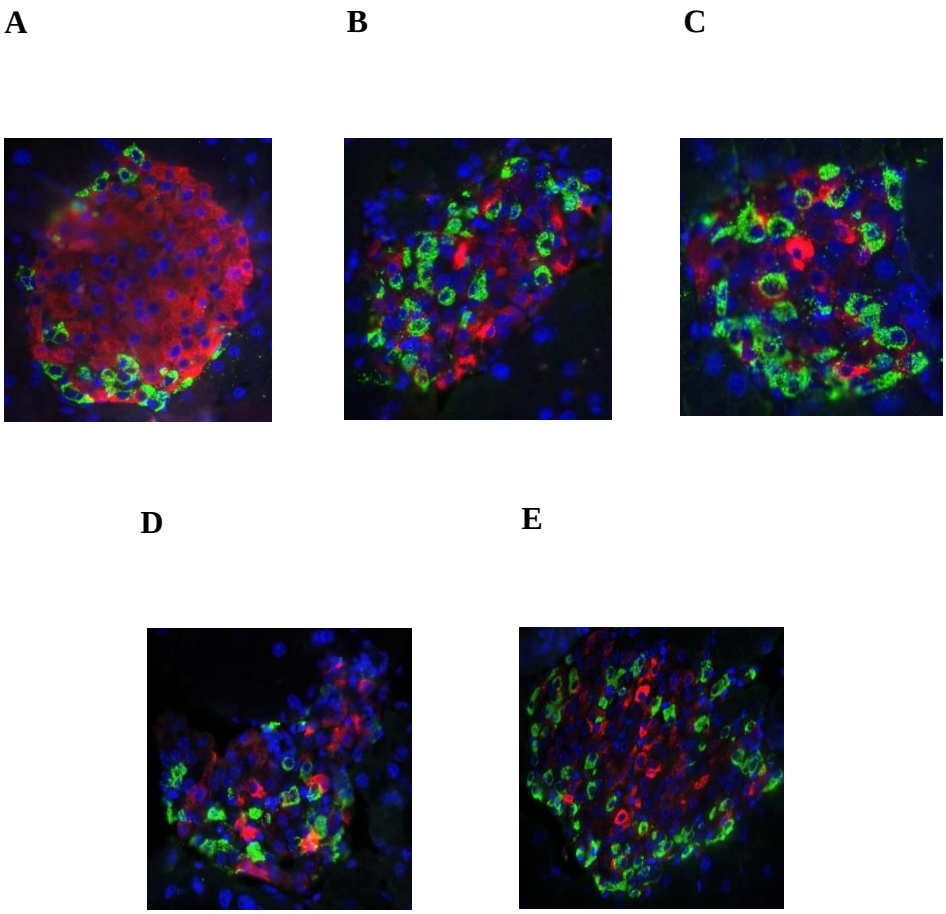

Images were captured by an Olympus System Microscope BX51 (Olympus instruments, UK) and a DP70 camera adapter. Cell^F image analysis software was used to assess parameters, magnification was X40. Insulin (red), glucagon (green) and DAPI (blue) in pancreatic tissue harvested from lean, (A) saline (B), exendin-4 (C), (D-Ala^2)GIP-xenin-8-Gln (D) or a combination of both peptides (E) (each at 25 nmol/kg bw).

Chapter 5

Assessing the biological actions and application as an antidiabetic therapeutic of a novel neurotensin-xenin hybrid peptide

5.1 Summary

Xenin based molecules appear to have notable antidiabetic potential and as such warrant further appraisal as a pharmacological therapeutic. In this study xenin-8-Gln was fused to a biologically active fragment of neurotensin (NT), acetyl-neurotensin(8-13). Xenin is also said to mediate its biological actions via NTRs. It seems NT, like xenin, has biological actions within the endocrine system and that all three NTRs are involved in mediating glycaemic control, insulinotropic action, along with body balancing factors and protective effects. Thus, combining the biologically active fragments of NT and xenin may have therapeutic potential. Acetyl-neurotensin(8-13)-xenin-8-Gln was chosen over the native peptide as it showed superior receptor binding and enhanced bioactivity with *in vitro* insulin secretion increased ($P<0.01$ to $P<0.01$). Acetyl-neurotensin(8-13)-xenin-8-Gln showed significant ($P<0.001$) beta cell proliferation and protection against apoptosis in BRIN-BD11 cells. Twice daily treatment of acetyl-neurotensin(8-13)-xenin-8-Gln in HFF mice resulted in a sustained improvement in glycaemic control and insulin secretion but was significantly ($P<0.05$ to $P<0.001$) enhanced when in combination with exendin-4, also reflected in blood glucose profile and glycated haemoglobin (HbA1c) levels ($P<0.05$ to $P<0.01$). Glucose excursion had marked improvements ($P<0.05$) with acetyl-neurotensin(8-13)-xenin-8-Gln in combination with exendin-4 as well as notably improved ($P<0.05$ to $P<0.001$) response to exogenous GIP and insulin sensitivity, reinforced by pancreatic insulin content. Additionally, islet and beta cell areas were unaffected by acetyl-neurotensin(8-13)-xenin-8-Gln but were significantly increased ($P<0.05$ to $P<0.01$) when in combination with exendin-4. In relation to energy balance, acetyl-neurotensin(8-13)-xenin-8-Gln only in combination with exendin-4 had weight reducing effects and yielded the greatest reduction ($P<0.05$ and $P<0.001$) in triglyceride levels. The data shows acetyl-neurotensin(8-13)-xenin-8-Gln has improved therapeutic efficacy in combination with exendin-4 and appears to enhance the therapeutic range of exendin-4 in several biological actions including glycaemic control, insulinotropic action and fat reduction. Thus, acetyl-neurotensin(8-13)-xenin-8-Gln combination with exendin-4, may have the potential as a T2DM-obesity therapeutic.

5.2 Introduction

As noted in previous chapters (Chapters 3,4), and in recent literature (Gault *et al.,* 2015; Hasib *et al.,* 2017; Hasib *et al.,* 2018a; Hasib *et al.,* 2018b; Martin *et al.,* 2016; Parthsarathy *et al.,* 2016), xenin based molecules have notable antidiabetic potential. To further examine and appraise the pharmacological therapeutic potential of xenin, we have designed another novel hybrid peptide. On this occasion the modified biologically active region of xenin, xenin-8-Gln was fused to the biologically active fragment of neurotensin (NT), namely acetyl-neurotensin(8-13)-xenin-8-Gln. The truncated neurotensin fragment, neurotensin(8-13), was selected over the native thirteen amino acid parent peptide because it has shown superior receptor binding and enhanced bioactivity (Martin, 2016; Schroeder and Leinninger, 2018). The premise for this novel hybrid is of a similar nature to the previous (D-Ala^2)GIP-xenin-8-Gln (Chapter 3). However, in this case xenin-8-Gln was linked to the structurally similar NT analogue, as both entities are believed to utilise the neurotensin receptor (NTR) to mediate their biological actions. (Craig, Gault and Irwin, 2018; Martin *et al.,* 2012).

A number of studies indicate that NT, as a neurotransmitter or as a circulating hormone, has a role within the endocrine system influencing glucose homeostasis and energy balance (Mazella *et al.,* 2012; Schroeder and Leinninger, 2018). Satiety is the key in energy balance and is primarily regulated by leptin secreted from adipocytes, which controls food intake by acting as a hormone directly on satiety regions within the hypothalamus (Mazella *et al.,* 2012; Schroeder and Leinninger, 2018). Recent studies have postulated that leptin may be controlled by NTSR1 expressing neurons as the effects of leptin were impaired in NTSR1-deficient mice (Mazella *et al.,* 2012). Additionally, a study by Leinninger and colleagues (2011) revealed that NT neurons control leptin actions including the mesolimbic dopamine system, secretion of orexin and energy balance (Leinninger *et al.,* 2011; Mazella *et al.,* 2012). Moreover, NT has been implicated in the control of nutrient absorption particularly in conjunction with fatty acid (FA) rich food. Studies have determined that postprandially, the ingestion of FA substantially increases circulating levels of NT (Mazella *et al.,* 2012). As such, NT is secreted from the gut in response to fat ingestion and this stimulates secretions from the pancreas to facilitate lipid digestion (Mazella *et al.,* 2012).

Furthermore, NT has a role in glucose homeostasis, including regulating the release of endocrine pancreatic hormones and at low glucose levels stimulates glucagon and insulin release (Mazella *et al.,* 2012). These endocrine actions have been confirmed in several studies (Coppola *et al.,* 2008; Grunddal *et al.,* 2016; Khan *et al.,* 2017; Mazella *et al.,* 2012). NT can directly mediate endocrine actions on the pancreas as this tissue expresses all three NTSRs (Khan *et al.,* 2017; Mazella *et al.,* 2012). It is postulated that NTSR2 initiates the effect of NT on insulin secretion, but the impact of NTSR3/sortilin has also been investigated (Mazella *et al.,* 2012). This suggests that NTSR2 and NTSR3/sortilin beta cell pathways may work in tandem. Indeed, the literature confirms that within beta cells, NTSR2 and NTSR3/sortilin form heterodimers (Mazella *et al.,* 2012). Interestingly, NT predominantly via NTSR2 has protective effects on beta cells against external cytotoxic agents including interlukin-1 beta via the PI3 kinase pathway (Mazella *et al.,* 2012). This protective effect is significant as beta cell death is a major factor in T2DM pathology (Khan *et al.,* 2017; Mazella *et al.,* 2012). Taken together, it is clear that NT, either as a neurotransmitter or circulating hormone, has an important role in the control of energy balance and glucose homeostasis (Mazella *et al.,* 2012).

As noted previously (Chapter 3,4), xenin derivatives have shown the ability to improve insulin sensitivity, augment insulinotropic response and decrease the overall glycaemic excursion in HFF models of obesity-T2DM. Xenin signalling can also regulate lipid metabolism via the NTR1 by acting directly on adipose tissue to stimulate lipolysis (Bhavya, Lew and Mizuno, 2018; Martin *et al.,* 2016). Moreover, it seems that all three NTRs have a profound involvement in mediating glycaemic control, insulinotropic action, along with body balancing factors and protective effects, which are mediated by NT and xenin collectively, both centrally and peripherally (Bhavya, Lew and Mizuno, 2018; Martin *et al.,* 2016; Mazella *et al.,* 2012). Therefore, combining the biologically active fragments of NT and xenin to assemble a monomeric hybrid peptide, may result in an advantageous therapeutic, with improved practicality over individual agonists of either peptide (Irwin and Flatt, 2015).

Within this study the biological actions and stability of the novel hybrid peptide acetyl-neurotensin(8-13)-xenin-8-Gln were appraised. Acetyl-neurotensin(8-13)-xenin-8-Gln was investigated both *in vitro* and *in vivo* to assess its potential as a T2DM

therapeutic. Given our previous negative experience with *db/db* mice and possible complications of leptin deficiency in application with NT, we decided to evaluate effects in HFF mice.

5.3 Materials and Methods

5.3.1 Peptides

All peptides (Table 1) were purchased from Syn Peptide Shanghai, China. Purity was confirmed by RP-HPLC and characterised by MALDI-TOF MS, all previously described in Sections 2.1, 2.2.3, and 2.2.4. For all experimental materials and methods please refer to Section 2.1 and the relevant subsections.

5.3.2 Plasma degradation

The effect of murine plasma on peptide stability was assessed as described previously in section 2.3.2.

5.3.3 Acute effects of peptides alone in the presence of GLP-1 or GIP on *in vitro* insulin secretion from BRIN-BD11 cells

The *in vitro* insulin secretory activity of peptides in BRIN-BD11 cells was conducted as described in Section 2.5.2. BRIN-BD11 cells were incubated (20 min) with test peptides (10^{-6} – 10^{-12} mol/l) alone at 5.6 and 16.7 mol/l glucose and in the presence of GLP-1or GIP (10^{-7} mol/l). Following test incubations (20 min), insulin secretion was measured by RIA as previously described in Sections 2.5.2 and 2.5.4.

5.3.4 *In vitro* proliferation

Effects of test peptides on cell proliferation in BRIN-BD11 cells was conducted as described in Section 2.6.2. Cells were incubated with test peptides (10^{-8} to 10^{-6} mol/l) for 18 hours. The primary antibody, anti-Ki-67 (1:250) and the secondary antibody, goat anti-rabbit Alexa Fluor® 594 (1:400) were used to detect proliferating beta cells by fluorescent microscopy.

5.3.5 *In vitro* apoptosis

The effects of test peptides on protection of BRIN-BD11 from cytokine-induced apoptosis was examined is as described in Section 2.6.3. Cells were incubated with test peptides (10^{-8} to 10^{-6} mol/l) for 18 hours and apoptosis initiated by adding caspase-3/7 substrate reagent (ApoLive-Glow™ Multiplex assay) that results in cell lysis, followed by caspase cleavage of the substrate and detection of beta cell apoptosis by luminescence.

5.3.6 *In vitro* cyclic AMP

Effects of peptides on cAMP production was examined using BRIN-BD11 cells (Section 2.7.2). Briefly, test peptides (10^{-9} to 10^{-6} mol/l) were incubated with cells for 60 mins, and cAMP measured using a cAMP Parameter® ELISA kit.

5.3.7 Animals

The long-term study utilised HFF male Swiss mice, as described in Section 2.9.2. Prior to experimentation, mice were maintained on high fat diet for 10 weeks, resulting in overt obesity and hyperglycaemia.

5.3.8 Long-term *in vivo* study in high fat fed mice

Twice daily intraperitoneal (i.p.) injections (09:00 and 17:00 h) of either saline vehicle (0.9% (w/v) NaCl), exendin-4, acetyl-neurotensin(8-13)-xenin-8-Gln alone or in combination with exendin-4 (all peptides at 25 nmol/kg) were administered for 32 days (Section 2.11.1). Assessed metabolic parameters during the study included: circulating glucose and insulin, body weight and cumulative energy intake, monitored every 3-4 days (Sections 2.11.1). End of treatment assessment parameters included: glucose tolerance (18 mmol/kg bw), HbA1c, blood glucose profile, GIP tolerance (25 nmol/kg bw), insulin sensitivity (25 U/kg), pancreatic insulin content, percentage fat mass, circulating triglycerides and cholesterol as well as islet morphology, as described in more detail within Sections 2.8.2, 2.8.3 and 2.11.2.

5.3.9 Biochemical analysis

Blood/plasma glucose, plasma and pancreatic insulin were assayed as described in Sections 2.5.4 and 2.10

5.3.10 Statistical analysis

As described in Section 2.12

5.4 Results

5.4.1 Peptide characterisation of native neurotensin, xenin-8-Gln, neurotensin(8-13), acetyl-neurotensin(8-13) and acetyl-neurotensin(8-13)-xenin-8-Gln and stability in the presence of mouse plasma

Following RP-HPLC on a C-18 analytical column, all peptides showed homogenous well-resolved peaks indicating a high degree of purity. Table 5.1 represents retention times which corresponded well with the purity information supplied by manufacturer. The experimental mass detected for each peptide corresponded to theoretical mass (Table 5.1), confirming successful synthesis. Moreover, the hybrid peptide acetyl-

neurotensin(8-13)-xenin-8-Gln showed improved stability under plasma degradation for up to 8 hours (Table 5.1).

5.4.2 Acute effects of neurotensin on insulin release from BRIN-BD11 cells

Figure 5.1 (A-D) demonstrates the abilities of neurotensin to increase insulin secretion from BRIN-BD11 cells at various concentrations of glucose. Neurotensin increased ($P<0.001$) insulin secretion at 3.3 mmol/l glucose in a dose dependent manner compared to respective glucose control (Figure 5.1A). At 5.6 mmol/l glucose neurotensin only enhanced ($P<0.05$) insulin secretion at 10^{-6} mol/l when compared to control (Figure 5.1B). At higher glucose levels (11.1 and 16.7 mmol/l), neurotensin inhibited ($P<0.05$ to $P<0.01$) insulin secretion, especially at the higher concentrations examined (Figure 5.1C-D).

5.4.3 Acute effects of neurotensin on insulin release from BRIN-BD11 cells in the presence of GIP and GLP-1

When neurotensin was combined with GIP or GLP-1 at 5.6 mmol/l glucose, the levels of secreted insulin were significantly increased ($P<0.001$), compared glucose alone (Figure 5.2A-B). However, neurotensin did not augment GIP-induced insulin secretion (Figure 5.2A), and the insulin secretory ability of GLP-1 was actually reduced by neurotensin at 10^{-8} and 10^{-6} mol/l concentrations (Figure 5.2B).

5.4.4 Acute effects of xenin-8-Gln on insulin release from BRIN-BD11 cells

Figure 5.3 (A-D) demonstrates the ability of xenin-8-Gln to increase insulin secretion from BRIN-BD11 cells at various concentrations of glucose. Xenin-8-Gln increased ($P<0.05$ to $P<0.01$) insulin secretion at 11.1 and 16.7 mmol/l glucose in a dose dependent manner (Figure 5.3C-D), and this is also demonstrated at 5.6 mmol/l glucose, as higher concentrations (10^{-8} mol/l to 10^{-6} mol/l) of xenin-8-Gln increased ($P<0.05$ to $P<0.001$) insulin secretion (Figure 5.3B).

5.4.5 Acute effects of xenin-8-Gln on insulin release from BRIN-BD11 cells in the presence of GIP and GLP-1

When xenin-8-Gln was combined with GIP or GLP-1 at normal physiological levels of glucose (5.6 mmol/l) the levels of secreted insulin were significantly increased ($P<0.001$) compared glucose alone (Figure 5.4A-B). Xenin-8-Gln also enhanced ($P<0.05$ to $P<0.01$) the secretory ability of GIP at higher concentrations (10^{-8} mol/l to 10^{-6} mol/l) compared to respective control (Figure 5.4A). However, this enhancement ability was not demonstrated in combination with GLP-1 (Figure 5.4B).

5.4.6 Acute effects of acetyl-neurotensin(8-13) on insulin release from BRIN-BD11 cells

Acetyl-neurotensin(8-13) significantly increased ($P<0.05$ to $P<0.001$) insulin secretion from BRIN-BD11 cells at lower glucose levels (3.3 mmol/l) in a dose dependent manner when compared to respective control (Figure 5.5A). This increase ($P<0.05$ to $P<0.01$) was also shown at normal physiological glucose (5.6 mmol/l) (Figure 5.5B), but only at higher peptide concentrations (10^{-8} mol/l to 10^{-6} mol/l). Conversely, at higher glucose concentrations (11.1 and 16.7 mmol/l) acetyl-neurotensin(8-13) induced insulin secretion decreased in a dose dependent manner, as such the higher the concentration (10^{-12} mol/l to 10^{-6} mol/l) the less insulin secreted (Figure 5.5C-D). Insulin secretion was significantly decreased ($P<0.05$ to $P<0.001$) at 16.7 mmol/l glucose by acetyl-neurotensin(8-13) (at 10^{-10} mol/l to 10^{-6} mol/l) compared to glucose control (Figure 5.5D).

5.4.7 Acute effects of acetyl-neurotensin(8-13) on insulin release from BRIN-BD11 cells in the presence of GIP and GLP-1

Acetyl-neurotensin(8-13) combined with GIP or GLP-1 at normal physiological levels of glucose (5.6 mmol/l) significantly increased ($P<0.001$) levels of secreted insulin when compared to the 5.6 mmol/l glucose control (Figure 5.6A-B). However, when compared to GLP-1 (at 10^{-6} mol/l) the level of insulin secretion was significantly diminished ($P<0.05$) compared to the GLP-1 control (Figure 5.6B).

5.4.8 Acute effects of acetyl-neurotensin(8-13)-xenin-8-Gln on insulin release from BRIN-BD11 cells

Acetyl-neurotensin(8-13)-xenin-8-Gln) enhanced ($P<0.05$ to $P<0.001$) insulin secretion from BRIN-BD11 cells at all glucose concentrations (3.3, 5.6, 11.1 and 16.7 mmol/l) tested, but only at higher peptide concentrations (10^{-8} mol/l to 10^{-6} mol/l) (Figure 5.7A-D).

5.4.9 Acute effects of acetyl-neurotensin(8-13)-xenin-8-Gln on insulin release from BRIN-BD11 cells in the presence of GIP and GLP-1

Acetyl-neurotensin(8-13)-xenin-8-Gln combined with GIP or GLP-1 at normal physiological levels of glucose (5.6 mmol/l) significantly increased ($P<0.001$) the levels of secreted insulin when compared to the 5.6 mmol/l glucose control (Figure 5.8A-B). When compared to GIP, at higher (10^{-12} mol/l to 10^{-6} mol/l) concentrations of acetyl-neurotensin(8-13)-xenin-8-Gln insulin secretion was significantly increased ($P<0.001$), compared to the GIP control (Figure 5.8A).

5.4.10 Effects of neurotensin analogues and neurotensin-xenin-8-Gln hybrids on insulin release from lean mouse islets

Isolated islets from lean mice incubated with acetyl-neurotensin(8-13), neurotensin-xenin-8-Gln or acetyl-neurotensin(8-13)-xenin-8-Gln (10^{-8} mol/l or 10^{-6} mol/l) at 3.3 mmol/l glucose stimulated a significant increase ($P<0.05$ to $P<0.01$) of insulin secretion when compared to the glucose control (Figure 5.9A). However, xenin-8-Gln had no effect, and neurotensin elicited a response ($P<0.05$) only at a higher peptide concentration (10^{-6} mol/l) from isolated islets at 3.3 mmol/l glucose (Figure 5.9A). All concentrations of xenin-8-Gln, neurotensin-xenin-8-Gln and acetyl-neurotensin(8-13)-xenin-8-Gln employed stimulated a significant increase ($P<0.05$ to $P<0.001$) of insulin secretion from islets at 16.7 mmol/l glucose and compared to neurotensin and acetyl-neurotensin(8-13) (Figure 5.9B).

5.4.11 The effects of xenin-8-Gln, neurotensin(8-13), acetyl-neurotensin(8-13) and acetyl-neurotensin(8-13)-xenin-8-Gln on BRIN-BD11 cell proliferation

Culturing of BRIN-BD11 cells in the presence of exendin-4, acetyl-neurotensin(8-13), xenin-25 and acetyl-neurotensin(8-13)-xenin-8-Gln (A) (at 10^{-6} mol/l or 10^{-8}mol/l) for 18 hours significantly increased ($P<0.001$) the proliferation frequency in comparison to the control culture (Figure 5.10A-B). Xenin-8-Gln alone exhibited no enhancing effects, but when combined with acetyl-neurotensin(8-13) as a hybrid, namely acetyl-neurotensin(8-13)-xenin-8-Gln, beta cell proliferation was dramatically ($P<0.01$ to $P<0.001$) increased (Figure 5.10A). However, this increase was significantly less ($P<0.001$) when compared to exendin-4. Representative images under each culture condition are shown in Figure 5.10B.

5.4.12 The effects of exendin-4, xenin-8, xenin-8-Gln, neurotensin(8-13), acetyl-neurotensin(8-13) and acetyl-neurotensin(8-13)-xenin-8-Gln on BRIN-BD11 cell apoptosis

BRIN-BD11 cells cultured in the presence of exendin-4, neurotensin, xenin-8, xenin-8-Gln, neurotensin(8-13), acetyl-neurotensin(8-13), xenin-25 and acetyl-neurotensin(8-13)-xenin-8-Gln (at 10^{-6} or 10^{-8} mol/l) for 18 hours all demonstrated a significant ($P<0.01$ to $P<0.001$) protective effect against capase-3/7 activated apoptosis in comparison to the untreated control culture (Figure 5.11).

5.4.13 Effects of twice-daily administration of exendin-4, acetyl-neurotensin(8-13)-xenin-8-Gln or a combination of both peptides on cumulative energy intake, body weight and percentage fat in HFF mice

Following twice daily administration of all treatments, barring exendin-4 alone, there was no significant effect on cumulative energy intake over the 32 days in HFF mice (Figure 5.12A). However, there was a significant decrease ($P<0.05$ to $P<0.001$) in body weight in all exendin-4 treated mice from the fourth day of treatment (Figure 5.12B). The percentage body fat mass also reflects this reduction ($P<0.05$ and $P<0.001$) in both exendin-4 and acetyl-neurotensin(8-13)-xenin-8-Gln in combination with exendin-4 treated groups when compared to the HFF controls (Figure 5.12C).

5.4.14 Effects of twice-daily administration of exendin-4, acetyl-neurotensin(8-13)-xenin-8-Gln or a combination of both peptides on non-fasted glucose and insulin in HFF mice

From the fourth day of treatment there was a significant decrease ($P<0.05$ to $P<0.001$) in non-fast glucose in all exendin-4 treatment groups (Figure 5.13A). Acetyl-neurotensin(8-13)-xenin-8-Gln induced a progressive decrease in glucose, but not significantly (Figure 5.13A). Non-fasted plasma insulin concentrations of exendin-4 alone and acetyl-neurotensin(8-13)-xenin-8-Gln in combination with exendin-4 progressively increased ($P<0.05$ and $P<0.001$) from the fourth day of treatment (Figure5.13B). Treatment with acetyl-neurotensin(8-13)-xenin-8-Gln alone had no significant effect on non-fasted insulin over the treatment period, in comparison to HFF control mice (Figure 5.13B).

5.4.15 Effects of twice daily administration of exendin-4, acetyl-neurotensin(8-13)-xenin-8-Gln or a combination of both peptides on 24 hour blood glucose profile and %HbA1c in HFF mice

Following administration over the 32 day treatment period, a 24 hour profile was conducted (Figure 5.14A). Non-fasted glucose levels demonstrated that exendin-4 alone and acetyl-neurotensin(8-13)-xenin-8-Gln in combination with exendin-4 treatment modalities induced a sustained lowering of blood glucose over the observation period, compared to HFF controls (Figure 5.14A). Acetyl-neurotensin(8-13)-xenin-8-Gln treatment maintained a reduced level compared to the HFF control mice, but this was not significant (Figure 5.14A). Moreover, this correlated with end of treatment percentage HbA1c levels, as treatment with exendin-4 alone and in combination with acetyl-neurotensin(8-13)-xenin-8-Gln resulted in significantly reduced ($P<0.01$) HbA1c concentrations in comparison to HFF controls (Figure 5.14B).

5.4.16 Effects of twice daily administration of exendin-4, acetyl-neurotensin(8-13)-xenin-8-Gln or a combination of both peptides on glucose and insulin in response to an oral glucose challenge in HFF mice

Only administration of acetyl-neurotensin(8-13)-xenin-8-Gln in combination with exendin-4 demonstrated a significant ($P<0.05$) improvement in glycaemic response post oral glucose load (Figure 5.15A). This was also reflected by overall AUC, as acetyl-neurotensin(8-13)-xenin-8-Gln in combination with exendin-4 significantly lowered ($P<0.05$) overall glycaemic excursion in comparison to acetyl-neurotensin(8-13)-xenin-8-Gln, but not compared to controls (Figure 5.15B). However, none of the treatment groups had any significant effects on glucose-induced insulin secretion (Figure 5.15B).

5.4.17 Effects of twice daily administration of exendin-4, acetyl-neurotensin(8-13)-xenin-8-Gln or a combination of both peptides on glucose and insulin in response to GIP tolerance test in HFF mice

Exendin-4 alone and in combination with acetyl-neurotensin(8-13)-xenin-8-Gln augmented the glucose-lowering action of GIP, as they maintained reduced glucose levels throughout assessed time points, although this effect was not significant (Figure 5.16A). However, the AUC revealed an overall significant reduction ($P<0.05$) in glucose levels by acetyl-neurotensin(8-13)-xenin-8-Gln in combination with exendin-4 compared with saline controls (Figure 5.16A). GIP-induced elevations of insulin for all HFF groups was not significantly different (Figure 5.16B).

5.4.18 Effects of twice-daily administration of exendin-4, acetyl-neurotensin(8-13)-xenin-8-Gln or a combination of both peptides on insulin sensitivity and pancreatic insulin content in HFF mice

Twice daily administration of exendin-4 and acetyl-neurotensin(8-13)-xenin-8-Gln had no significant effect on individual glucose levels in response to exogenous insulin (Figure 5.17A). However, in acetyl-neurotensin(8-13)-xenin-8-Gln in combination with exendin-4 mice glucose levels were significantly reduced ($P<0.05$) at the 60 min time point, as well as AUC, when compared to controls and acetyl-neurotensin(8-13)-xenin-8-Gln mice (Figure 5.17A). Pancreatic insulin content revealed that there was a significant ($P<0.001$) reduction in insulin concentrations by exendin-4 and acetyl-neurotensin(8-13)-xenin-8-Gln in combination with exendin-4 treatment, when

compared to saline controls and acetyl-neurotensin(8-13)-xenin-8-Gln alone (Figure 5.17B).

5.4.19 Effects of twice daily administration of exendin-4, acetyl-neurotensin(8-13)-xenin-8-Gln or a combination of both peptides on bone mineral density and bone mineral content in HFF mice

There was no significant effect on bone mineral density (BMD) or bone mineral content (BMC) post twice daily administration of exendin-4, acetyl-neurotensin(8-13)-xenin-8-Gln and acetyl-neurotensin(8-13)-xenin-8-Gln in combination with exendin-4 (Figure 5.18A-B).

5.4.20 Effects of twice daily administration of exendin-4, acetyl-neurotensin(8-13)-xenin-8-Gln or a combination of both peptides on total cholesterol, triglycerides, HDL and LDL in HFF mice

Following 32 days twice daily administration of exendin-4 alone and in combination with acetyl-neurotensin(8-13)-xenin-8-Gln there was a significant decrease ($P<0.01$ and $P<0.001$) in circulating total and LDL-cholesterol (Figure 5.19A,D), with a decrease ($P<0.05$ and $P<0.01$) in HDL levels in all treatment groups (Figure 5.19C). However, there was only a decrease ($P<0.01$) in LDL in mice treated with acetyl-neurotensin(8-13)-xenin-8-Gln in combination with exendin-4 (Figure 5.19B).

5.4.21 Effects of twice daily administration of exendin-4, acetyl-neurotensin(8-13)-xenin-8-Gln or a combination of both peptides on pancreatic histology in HFF mice

Islet and beta cell area were increased ($P<0.001$) in all the HFF groups compared to lean controls (Figure 5.20A-B). Pancreatic islet area after 32 days treatment revealed that there was a significant increase ($P<0.05$-$P<0.001$) in islet area with acetyl-neurotensin(8-13)-xenin-8-Gln in combination with exendin-4 (Figure 5.20A). Additionally, there was an elevation of beta cell area by acetyl-neurotensin(8-13)-xenin-8-Gln in combination with exendin-4, with cell area significantly ($P<0.01$-

P<0.001) enhanced in this treatment group compared to both lean and saline controls (Figure 5.20B). Moreover, both the islet and beta cell areas were significantly (P<0.05-P<0.01) increased by acetyl-neurotensin(8-13)-xenin-8-Gln in combination with exendin-4 compared to acetyl-neurotensin(8-13)-xenin-8-Gln alone (Figure 5.20A-B). There was no significant effect on alpha cell area by any of the treatment regimens (Figure 5.20C). Representative islet images for all groups are shown in Figure 5.21A-E.

5.5 Discussion

With the mediation of xenin and NT's biological activity primarily underpinned by the activation of NTRs, it was essential to establish if this was maintained by the hybrid peptide analogue acetyl-neurotensin(8-13)-xenin-8-Gln. A recent study by Khan and colleagues (2017) involving the assessment of NTRs expression within the endocrine pancreas, supports the applicability of the initial *in vitro* assessment of insulin secretory activity, as well as beta cell growth and survival, of xenin-8-Gln, NT and NT-xenin analogue(s) in the BRIN-BD11 cell line and isolated mouse islets (Khan *et al.*, 2017).

The work by Khan and colleagues (2017), which was focused on the native forms of both peptides, correlates and corroborates the insulinotropic data generated in this study. Xenin-8-Gln can elicit superior insulin secretion at both low and high glucose concentrations, but it remains that NT and NT analogues can only enhance insulin secretion at lower glucose concentrations in BRIN-BD11 cells and mouse islets (Devader *et al.*, 2013; Khan *et al.*, 2017). However, the monomeric NT-xenin analogue, acetyl-neurotensin(8-13)-xenin-8-Gln overcomes this inability to increase insulin secretion at higher glucose concentrations. It appears that combining the modified biologically active fragment of xenin with acetylation of the active fragment of NT, not only extends the DPP-IV half-life of the peptide but enhances the insulinotropic abilities in BRIN-BD11 cells, and importantly with further insulin secretory superiority evidenced in isolated islets.

Additionally, studies on the proliferative and protective effects of xenin and NT have noted xenin to increase proliferation. Both xenin and NT protect against streptozotocin induced cellular stress in BRIN-BD11 cells and NT has been shown to

exhibitprotective effects against caspase-3 activity (Coppola *et al.,* 2008; Devader *et al.,* 2013; Khan *et al.,* 2017). In line with this published literature on NT (Khan *et al.,* 2017), acetyl-neurotensin(8-13)-xenin-8-Gln demonstrated significant beta cell proliferation and offered protection against beta cell apoptosis, via inhibition of the caspase 3/7 pathway. This suggests that the hybrid peptide may have beneficial effects on maintaining and/or increasing beta cell mass, with obvious positive implications for the treatment of diabetes (Halban *et al.,* 2014).

With such promising *in vitro* results further assessment of acetyl-neurotensin(8-13)-xenin-8-Gln biological capabilities *in vivo* was warranted. Thus, a chronic 32 day investigation of acetyl-neurotensin(8-13)-xenin-8-Gln antidiabetic activity was conducted in the HFF mouse model of T2DM. The choice of animal model in which to study the biological effects of acetyl-neurotensin(8-13)-xenin-8-Gln was crucial to fully corroborating the efficacy of the hybrid peptide for the treatment of T2DM. This choice was of the utmost importance because of the studies linking NT to the control of the hormone leptin, as it acts directly on specific areas of the hypothalamus controlling food intake and energy expenditure (Mazella *et al.,* 2012; Srinivasan and Ramarao, 2007). Therefore, the use of other genetic models of T2DM such as the previously utilised *db/db* model, which has a mutation on chromosome 4 inhibiting the expression of the leptin receptor, would restrict the full exploration of the true potential of the hybrid peptide (Faita *et al.,* 2018; Mazella *et al.,* 2012; Schroeder and Leinninger, 2018).

Twice daily treatment of acetyl-neurotensin(8-13)-xenin-8-Gln in HFF mice resulted in a sustained improvement in glycaemic control and insulin secretion. Acetyl-neurotensin(8-13)-xenin-8-Gln, although not significant, caused a progressive decrease in circulating glucose levels than those of the HFF saline treated control, similar to that seen with other xenin derived hybrid peptides (Hasib *et al.,* 2017; Hasib *et al.,* 2018a; Hasib *et al.,* 2018b; Martin *et al.,* 2016). Moreover, this action was significantly enhanced when administered in combination with the GLP-1 agonist exendin-4, suggesting the utility of its bioactivity to further reduce glucose levels (Fusco *et al.,* 2017). This enhanced anti-diabetic action of xenin in combination with GLP-1 has also been demonstrated by Hasib and colleagues in HFF using a GIP-xenin hybrid peptide (Hasib *et al.,* 2018b).

In addition, the blood glucose profile and HbA1c levels also confirm that acetyl-neurotensin(8-13)-xenin-8-Gln in combination with exendin-4 had a superior glucose lowering ability than the hybrid peptide alone. Moreover, the glucose tolerance test, following 32 days treatment with acetyl-neurotensin(8-13)-xenin-8-Gln in combination with exendin-4 showed marked improvements in the glucose excursion. This was also noted in response to exogenous GIP injection, along with improved insulin sensitivity. This is reinforced by pancreatic insulin content, which revealed that exendin-4 and acetyl-neurotensin(8-13)-xenin-8-Gln in combination with exendin-4 had significantly less insulin per µg/g protein, but insulin sensitivity was superior. Furthermore, the islet and beta cell areas were unaffected by acetyl-neurotensin(8-13)-xenin-8-Gln alone but were significantly increased with acetyl-neurotensin(8-13)-xenin-8-Gln in combination with exendin-4, which had similar effects to exendin-4 alone. This is suggestive that while acetyl-neurotensin(8-13)-xenin-8-Gln does not enhance the action of exendin-4 it does not diminish its therapeutic action. These observations are in line with positive beta cell architecture effects of GLP-1 in numerous type 2 diabetes animal model studies (Moffett *et al.,* 2015; Vasu *et al.,* 2014). This data collectively suggests that like results from previous Chapters and published literature, NT receptor signalling can augment sensitivity to GIP, and impart clear antidiabetic actions, positive attributes that are retained, or even enhanced by this NT-xenin hybrid (Al-Sabah, 2015; Hasib *et al.,* 2017; Hasib *et al.,* 2018b; Irwin and Flatt, 2015).

In relation to energy balance, both NT and xenin have been shown to play a role in satiety, as both have anorexigenic abilities (Bhavya, Lew and Mizuno, 2018; Cooke *et al.,* 2012). Initial studies indicated that this effect was influenced primarily via intracerebroventricularly (i.c.v.) administration, but more recently intraperitoneal (i.p.) administration has been shown to also facilitate these actions (Cooke *et al.,* 2012; Ratner *et al.,* 2018). The anorectic actions of NT through leptin are thought to be mediated via the ventral tegmental area (VTA) by the NT neurons located within the lateral hypothalamic area (LHA), as 15-30% of these NT neurons co-express the leptin receptor (Schroeder and Leinninger, 2018). Similarly, xenin is also thought to partially exert its influence over food intake via the hypothalamus (Kim *et al.,* 2016). Both native peptides are believed to bind to the NTR1, located within the hypothalamus to induce their anorexic effects (Kim *et al.,* 2016; Ratner *et al.,* 2018).

Taking this into account, a recent study on a PEGylated NT peptide that induced a prolonged decrease in food intake (Ratner *et al.*, 2018), along with the augmentative ability of a xenin hybrid, meant the potential for the dual receptor agonist, acetyl-neurotensin(8-13)-xenin-8-Gln to effect energy balance was likely. However, acetyl-neurotensin(8-13)-xenin-8-Gln alone or in combination with exendin-4 had no impact on cumulative energy intake over the 32 day treatment period in HFF mice. Thus, the discrepancy could be related to dose of peptide employed, as xenin appears to impact feeding only at high concentrations (Taylor *et al.*, 2010), or perhaps the need for central administration (Cooke *et al.*, 2012). In addition, lack of effect on feeding is paralleled by no significant body weight reduction in HFF mice. Indeed, it is only when in combination with exendin-4 that acetyl-neurotensin(8-13)-xenin-8-Gln had any weight reducing effects, probably linked to GLP-1 receptor effects on the hypothalamus (Kanoski, Hayes and Skibicka, 2016). Interestingly, GLP-1's ability to reduce body weight loss via anorectic and orexigenic endocrine signals may be related to regulation of the expression of neuropeptides including NT (Dalvi *et al.*, 2012; Good, 2012; Kanoski, Hayes and Skibicka, 2016).

In contrast to the findings on food intake and body weight, where exendin-4 exerted superior body balancing effects, it was acetyl-neurotensin(8-13)-xenin-8-Gln in combination with exendin-4 that yielded the greatest reduction in percentage fat mass and triglyceride levels. Both xenin and NT have been linked with direct effects on adipocytes, and to play a role in lipid metabolism. Systemically, xenin has been shown to stimulate lipolysis on adipose tissue, and this is thought to be mediated by NTR1 as NTR1 mRNA is expressed on mouse adipose tissue (Bhavya, Lew and Mizuno, 2018). Furthermore, NT secreted from the intestine in response to postprandial fat ingestion has been shown to facilitate the absorption of fat. This influences the circulating levels of leptin as fat initiates the secretion of leptin from adipocytes (Barchetta *et al.*, 2018; Mazella *et al.*, 2012). Systemically leptin then initiates enteroendocrine cells to release their gastrointestinal peptides such as GLP-1 and GIP, thus working synergistically to regulate energy balance (Barchetta *et al.*, 2018). This suggests that the superior reduction of percentage fat mass by acetyl-neurotensin(8-13)-xenin-8-Gln in combination with exendin-4 can be attributed to several mechanisms, with multiple hormone receptor pathways working in concert to elicit this effect.

In conclusion, this data reveals that acetyl-neurotensin(8-13)-xenin-8-Gln has improved therapeutic efficacy in combination with GLP-1R agonist exendin-4. In combination it also appears to improve the therapeutic range of exendin-4 in several biological actions including glycaemic control, insulinotropic action and fat reduction. Therefore, this novel hybrid with complementary effects in combination with GLP-1, may have the potential to treat not only T2DM but obesity related diabetes.

Table 5.1 Peptide characterisation of native neurotensin, xenin-8-Gln, neurotensin(8-13), acetyl-neurotensin(8-13) and acetyl-neurotensin(8-13)-xenin-8-Gln and stability in the presence of mouse plasma

Peptides	Name	Primary Sequence	Theoretical Mass (Da)	Experimental Mass (Da)	Retention Time (Min)	Percentage degradation (%)		
						2 (h)	4 (h)	8 (h)
1	Neurotensin	pELYENKPRRPYIL-OH	1672.9	1672.9	14.9	1.5	21.2	31.1
2	Xenin-8-Gln	HPQQPWIL-OH	1018.1	1018.1	16.1	-	-	-
3	Neurotensin(8-13)	RRPYIL-OH	817.0	817.0	13.0	46.7	79.3	83.9
4	Acetyl-neurotensin(8-13)	Ac- RRPYIL-OH	859.0	859.0	14.4	1.8	6.6	10.4
5	Acetyl-neurotensin(8-13)-xenin-8-Gln	Ac-RRPYIL-HPQQPWIL-OH	1859.1	1859.1	19.2	0	0	8.32

Peptide sequences of native neurotensin, xenin-8-Gln, neurotensin(8-13), acetyl-neurotensin(8-13) and acetyl-neurotensin(8-13)-xenin-8-Gln. Purification of peptides confirmed by RP-HPLC, retention times recorded using ChromQuest software. Molecular mass confirmed using MALDI-ToF, Voyager-DE BioSpectrometry Workstation and m/z ratio *vs* peak intensity. Plasma stability assessed by percentage peptide degraded.

Figure 5.1 Acute effects of neurotensin on insulin release from BRIN-BD11 cells

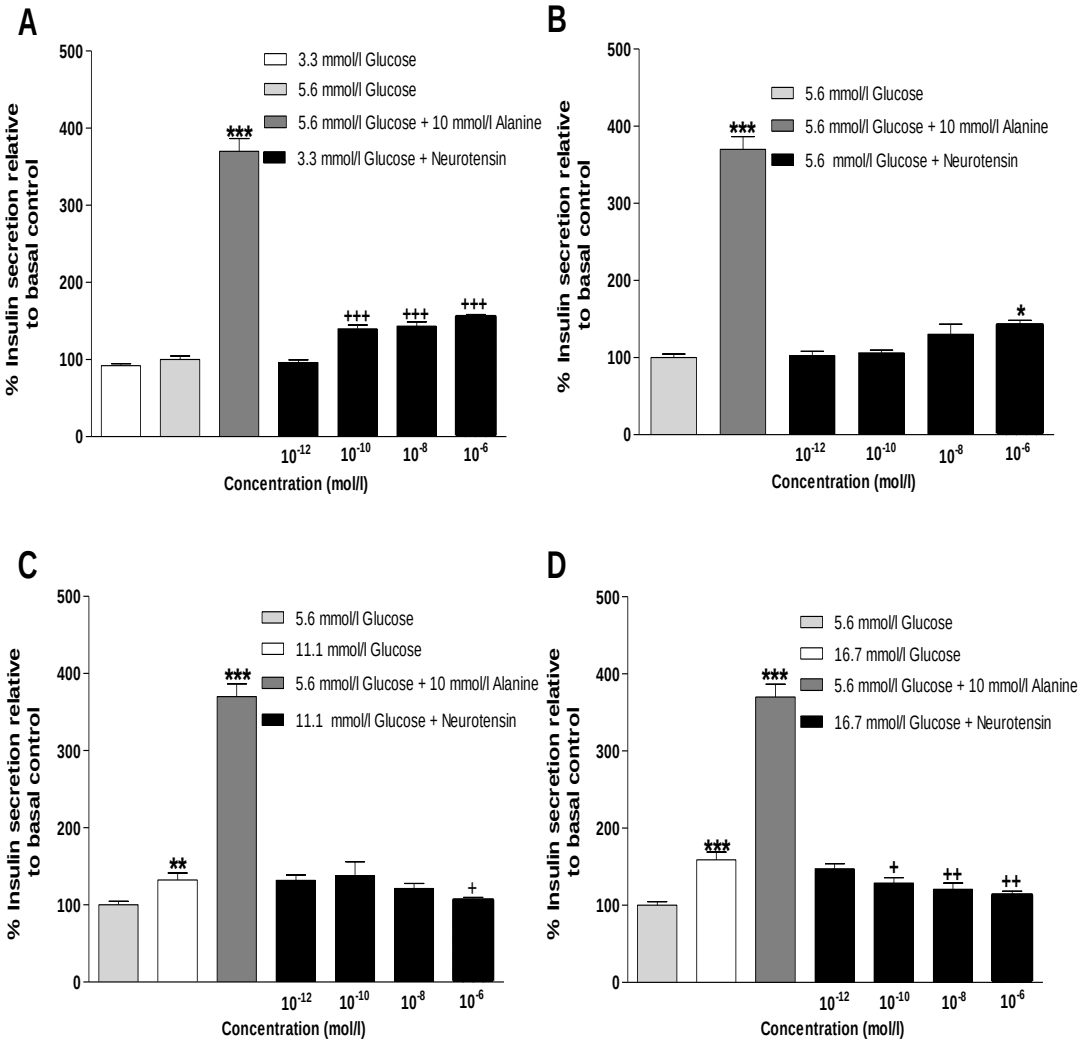

BRIN-BD11 cells were incubated (20 min) with test peptide (10^{-12} to 10^{-6} mol/l) in the presence of (A) 3.3, (B) 5.6, (C) 11.1 and (D) 16.7 mmol/l glucose. Insulin was measured by RIA. Values are mean ± SEM (n=8) for insulin release. *P<0.05, **P<0.01 and ***P<0.001 compared to 5.6 mmol/l glucose control. $^{+}$P<0.05, $^{++}$P<0.01 and $^{+++}$P<0.001 compared to respective glucose control.

Figure 5.2 Acute effects of neurotensin in the presence of GIP and GLP-1 on insulin release from BRIN-BD11 cells

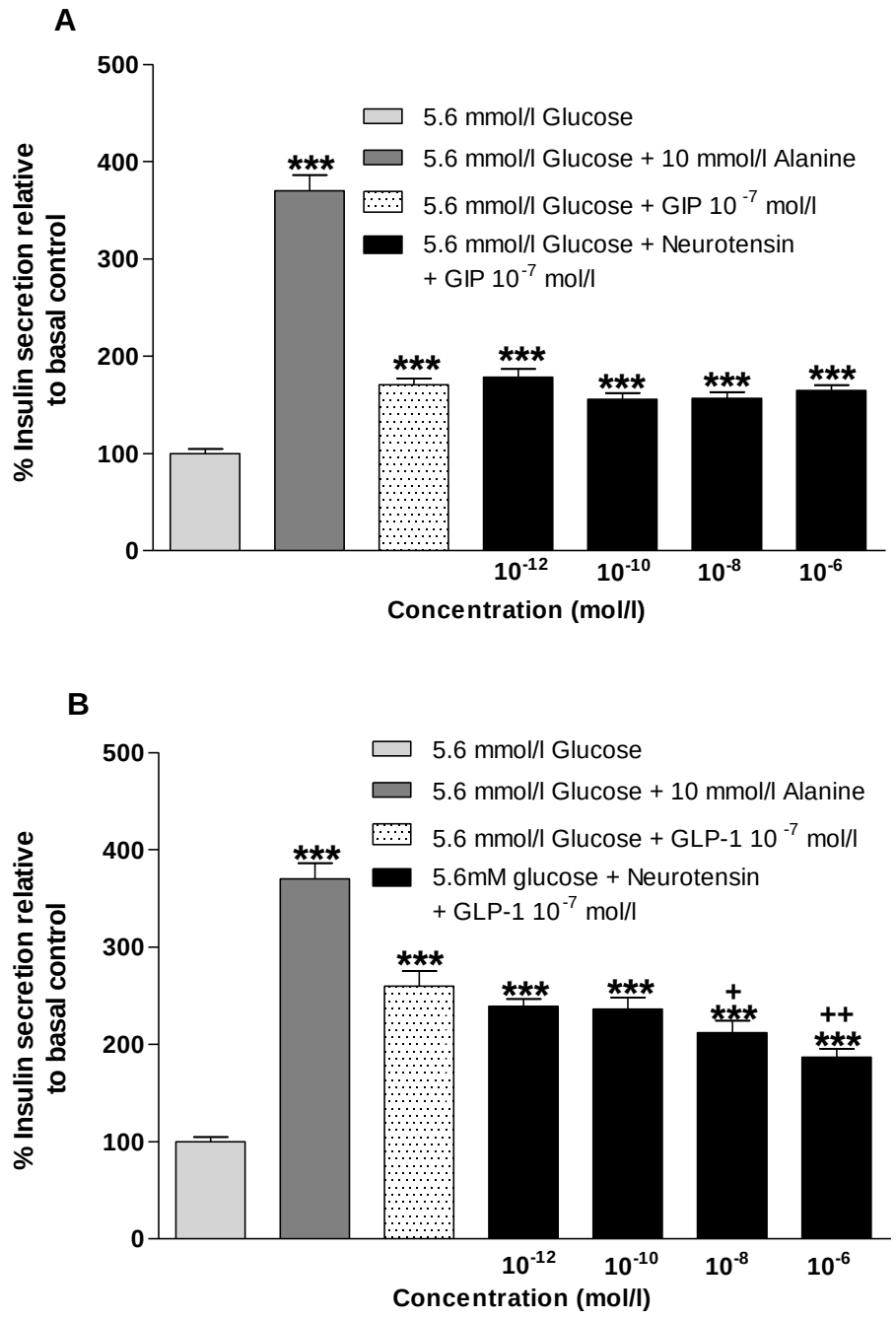

BRIN-BD11 cells were incubated (20 min) with test peptide (10^{-12} to 10^{-6} mol/l) in the presence of (A) GIP and (B) GLP-1 (both at 10^{-7} mol/l) at 5.6 mmol/l glucose. Insulin was measured by RIA. Values are mean ± SEM (n=8) for insulin release. ***P<0.001 compared to 5.6 mmol/l glucose alone. $^{+}$P<0.05 and $^{++}$P<0.01 compared to respective GIP or GLP-1 control.

Figure 5.3 Acute effects of xenin-8-Gln on insulin release from BRIN-BD11 cells

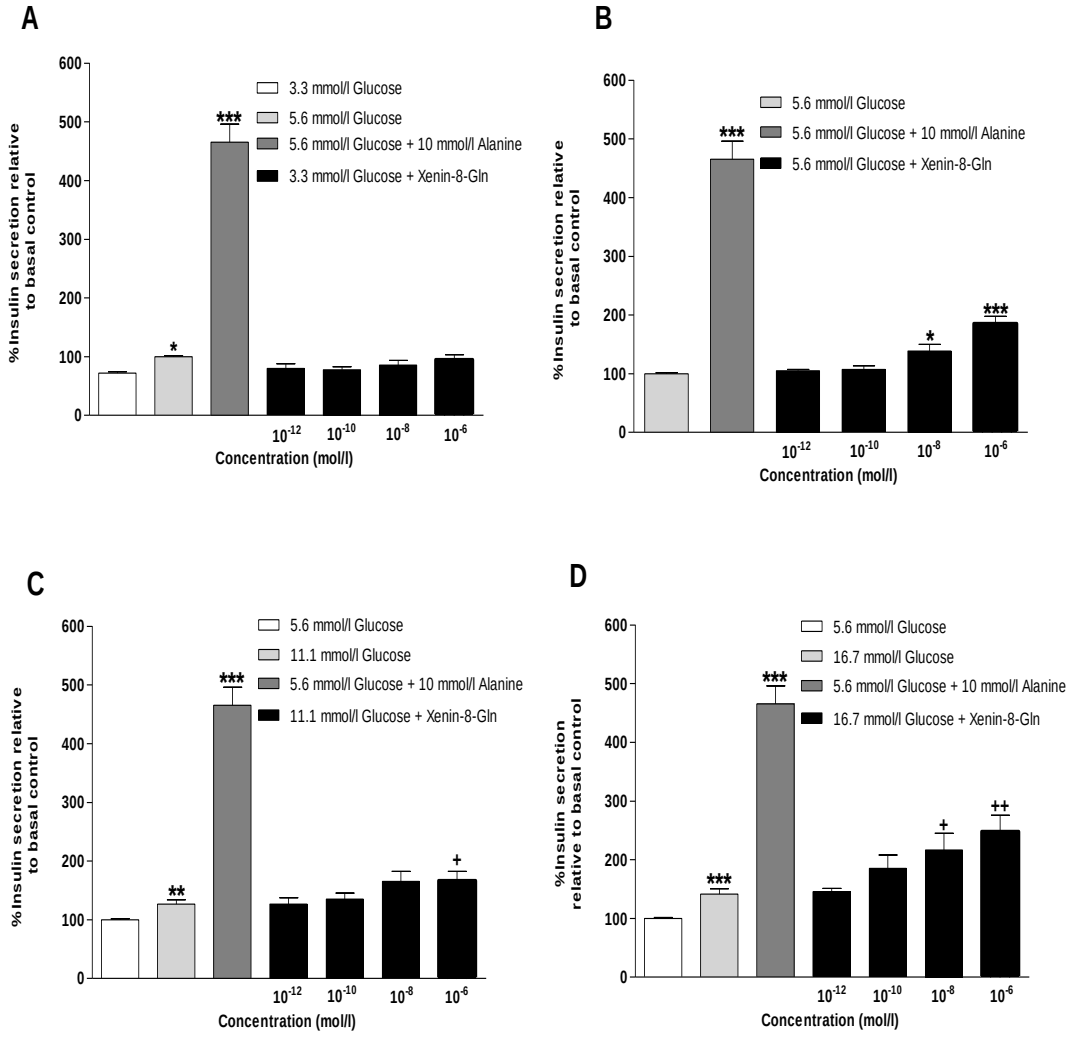

BRIN-BD11 cells were incubated (20 min) with test peptide (10^{-12} to 10^{-6} mol/l) in the presence of (A) 3.3, (B) 5.6, (C) 11.1 and (D) 16.7 mmol/l glucose. Insulin was measured by RIA. Values are mean ± SEM (n=8) for insulin release. *P<0.05, **P<0.01 and ***P<0.001 compared to 5.6 mmol/l glucose control. $^{+}$P<0.05, $^{++}$P<0.01 and compared to respective glucose control.

Figure 5.4 Acute effects of xenin-8-Gln in the presence of GIP and GLP-1 on insulin release from BRIN-BD11 cells

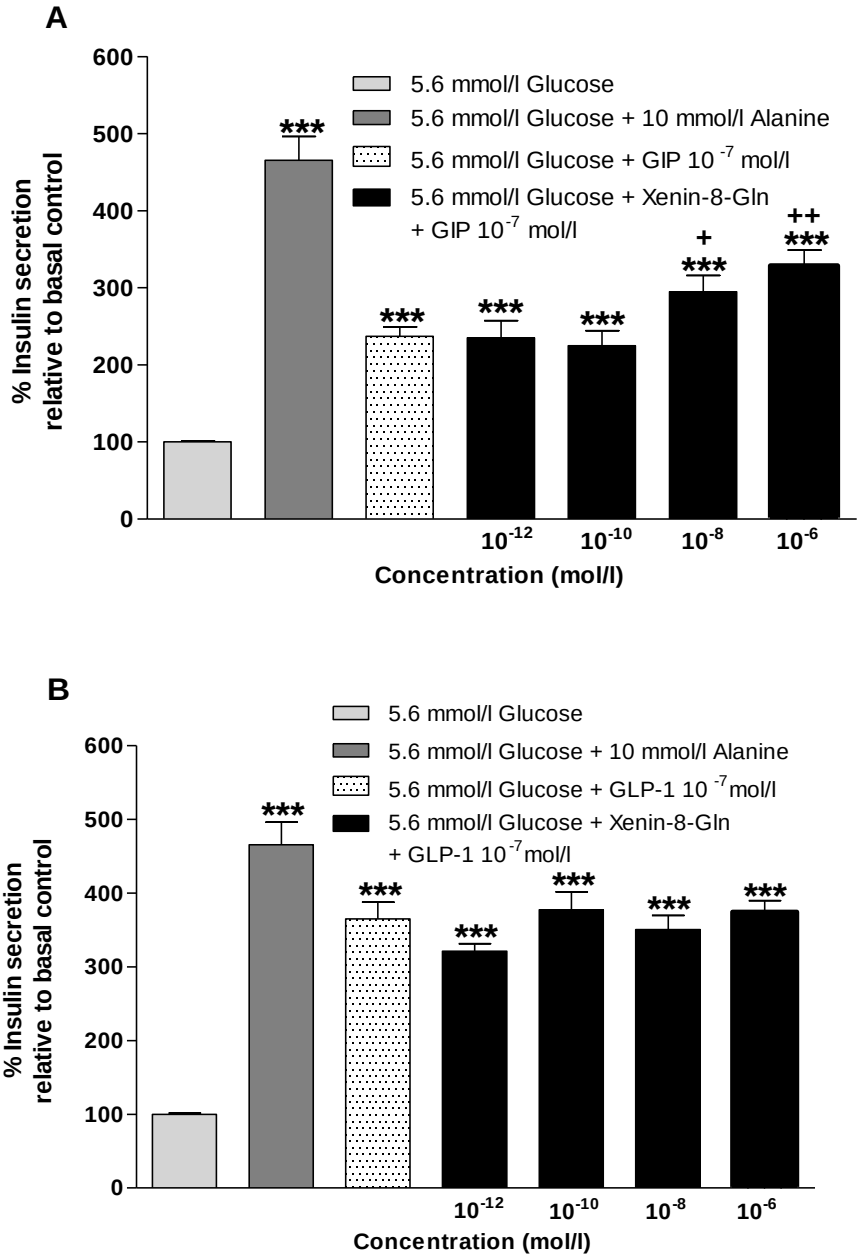

BRIN-BD11 cells were incubated (20 min) with test peptide (10^{-12} to 10^{-6} mol/l) in the presence of (A) GIP and (B) GLP-1 (both at 10^{-7} mol/l) at 5.6 mmol/l glucose. Insulin was measured by RIA. Values are mean ± SEM (n=8) for insulin release. ***P<0.001 compared to 5.6 mol/l glucose alone. $^{++}$P<0.01 and $^{+++}$P<0.001 compared to respective GIP or GLP-1 control.

Figure 5.5 Acute effects of acetyl-neurotensin(8-13) on insulin release from BRIN-BD11 cells

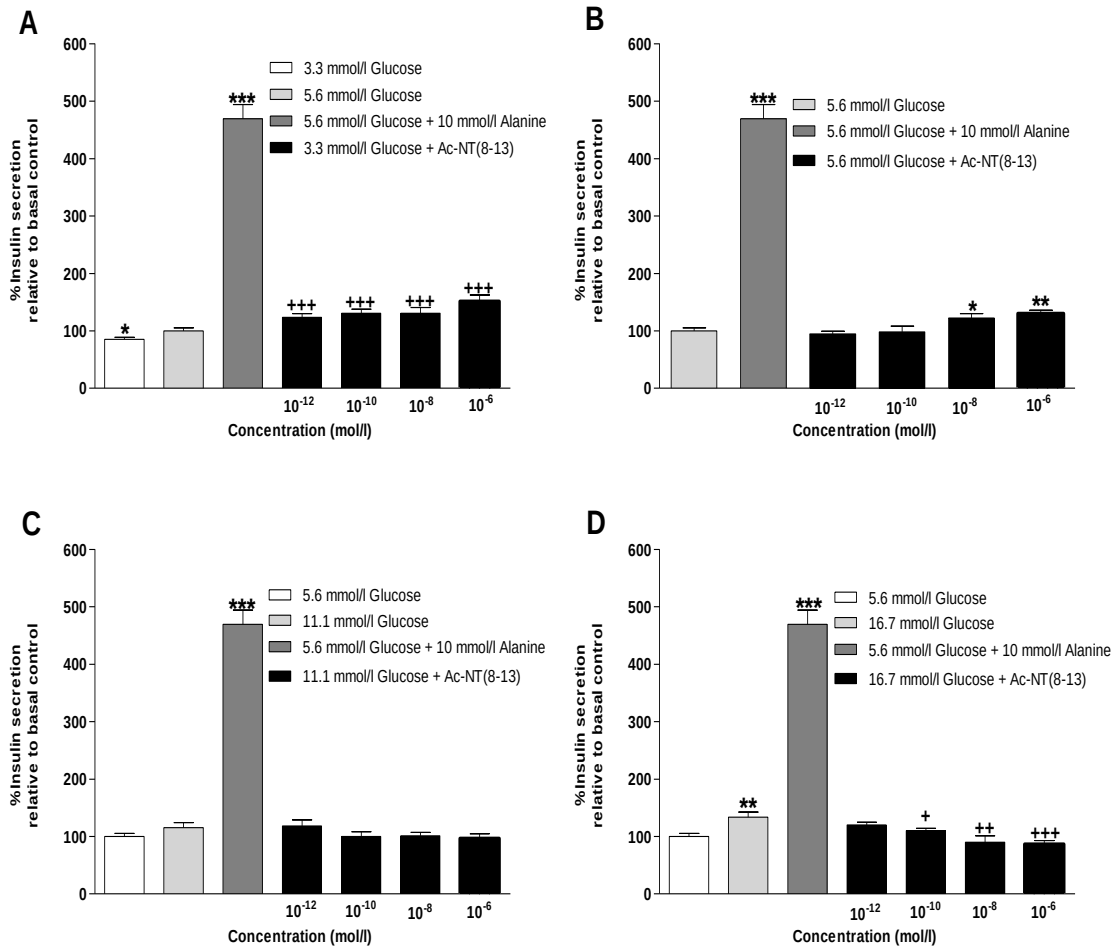

BRIN-BD11 cells were incubated (20 min) with test peptide (10^{-12} to 10^{-6} mol/l) in the presence of (A) 3.3, (B) 5.6, (C) 11.1 and (D) 16.7 mmol/l glucose. Insulin was measured by RIA. Values are mean ± SEM (n=8) for insulin release. *P<0.05, **P<0.01 and ***P<0.001 compared to 5.6 mol/l glucose control. $^{+}$P<0.05, $^{++}$P<0.01 and $^{+++}$P<0.001 compared to respective glucose control.

Figure 5.6 Acute effects of acetyl-neurotensin(8-13) in the presence of GIP and GLP-1 on insulin release from BRIN-BD11 cells

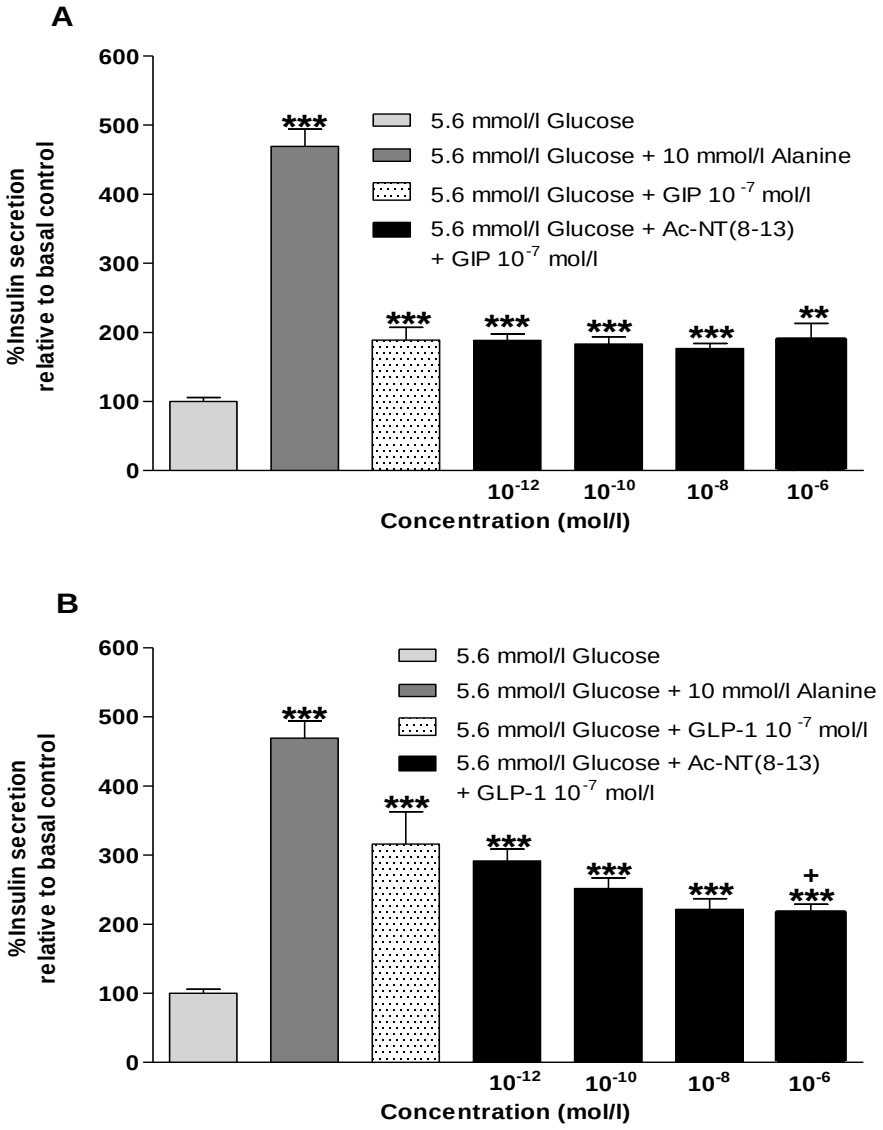

BRIN-BD11 cells were incubated (20 min) with test peptide (10^{-12} to 10^{-6} mol/l) in the presence of (A) GIP and (B) GLP-1 (both at 10^{-7} mol/l) at 5.6 mmol/l glucose. Insulin was measured by RIA. Values are mean ± SEM (n=8) for insulin release. **P<0.01 and ***P<0.001 compared to 5.6 mmol/l glucose alone. $^{+}$P<0.05 compared to respective GIP or GLP-1 control.

Figure 5.7 Acute effects of acetyl-neurotensin(8-13)-xenin-8-Gln on insulin release from BRIN-BD11 cells

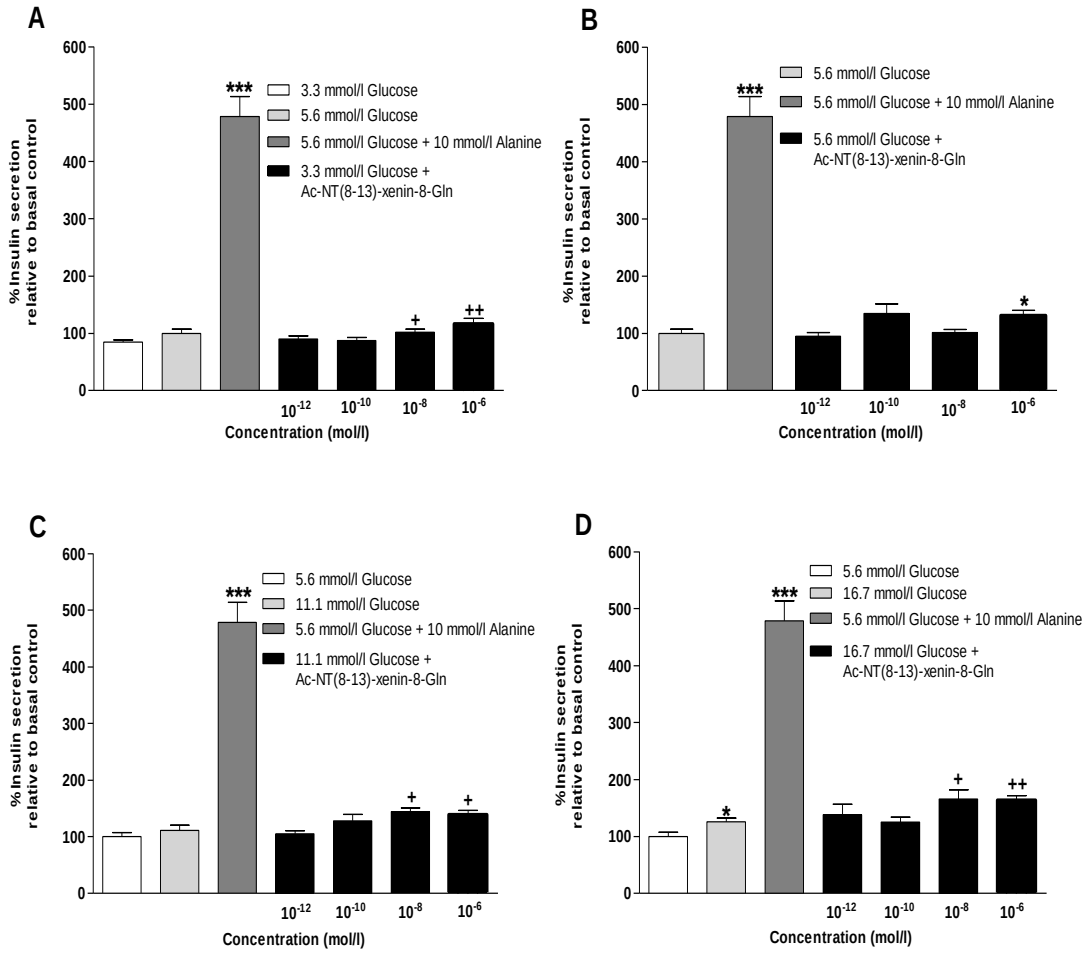

BRIN-BD11 cells were incubated (20 min) with test peptide (10^{-12} to 10^{-6} mol/l) in the presence of (A) 3.3, (B) 5.6, (C) 11.1 and (D) 16.7 mmol/l glucose. Insulin was measured by RIA. Values are mean ± SEM (n=8) for insulin release. *P<0.05 and ***P<0.001 compared to 5.6 mol/l glucose control. $^{+}$P<0.05 ang $^{++}$P<0.01 compared to respective glucose control.

Figure 5.8 Acute effects of acetyl-neurotensin(8-13)-xenin-8-Gln in the presence of GIP and GLP-1 on insulin release from BRIN-BD11 cells

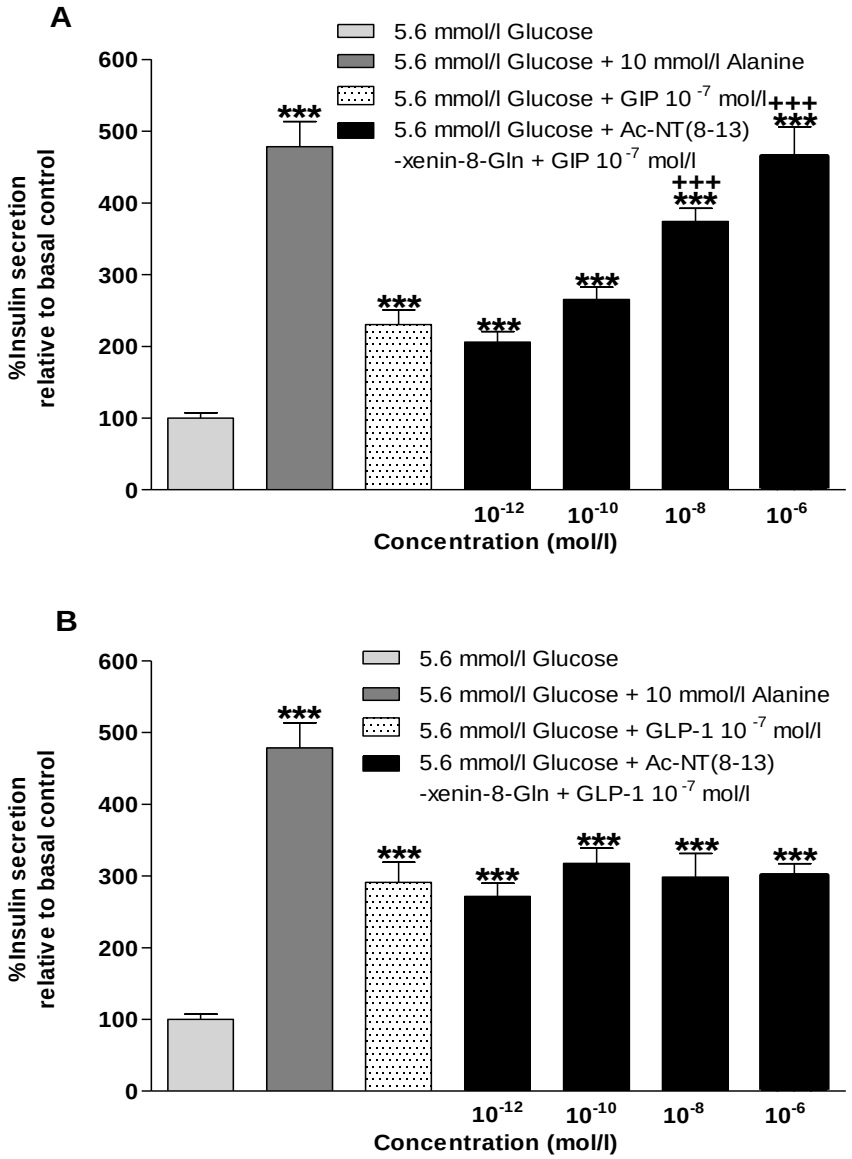

BRIN-BD11 cells were incubated (20 min) with test peptide (10^{-12} to 10^{-6} mol/l) in the presence of (A) GIP and (B) GLP-1 (both at 10^{-7} mol/.) at 5.6 mmol/l glucose. Insulin was measured by RIA. Values are mean ± SEM (n=8) for insulin release. ***P<0.001 compared to 5.6 mmol/l glucose alone. $^{+++}$P<0.001 compared to respective GIP or GLP-1 control.

Figure 5.9 Effects of neurotensin analogues and neurotensin-xenin-8-Gln hybrids on insulin release from isolated mouse islets

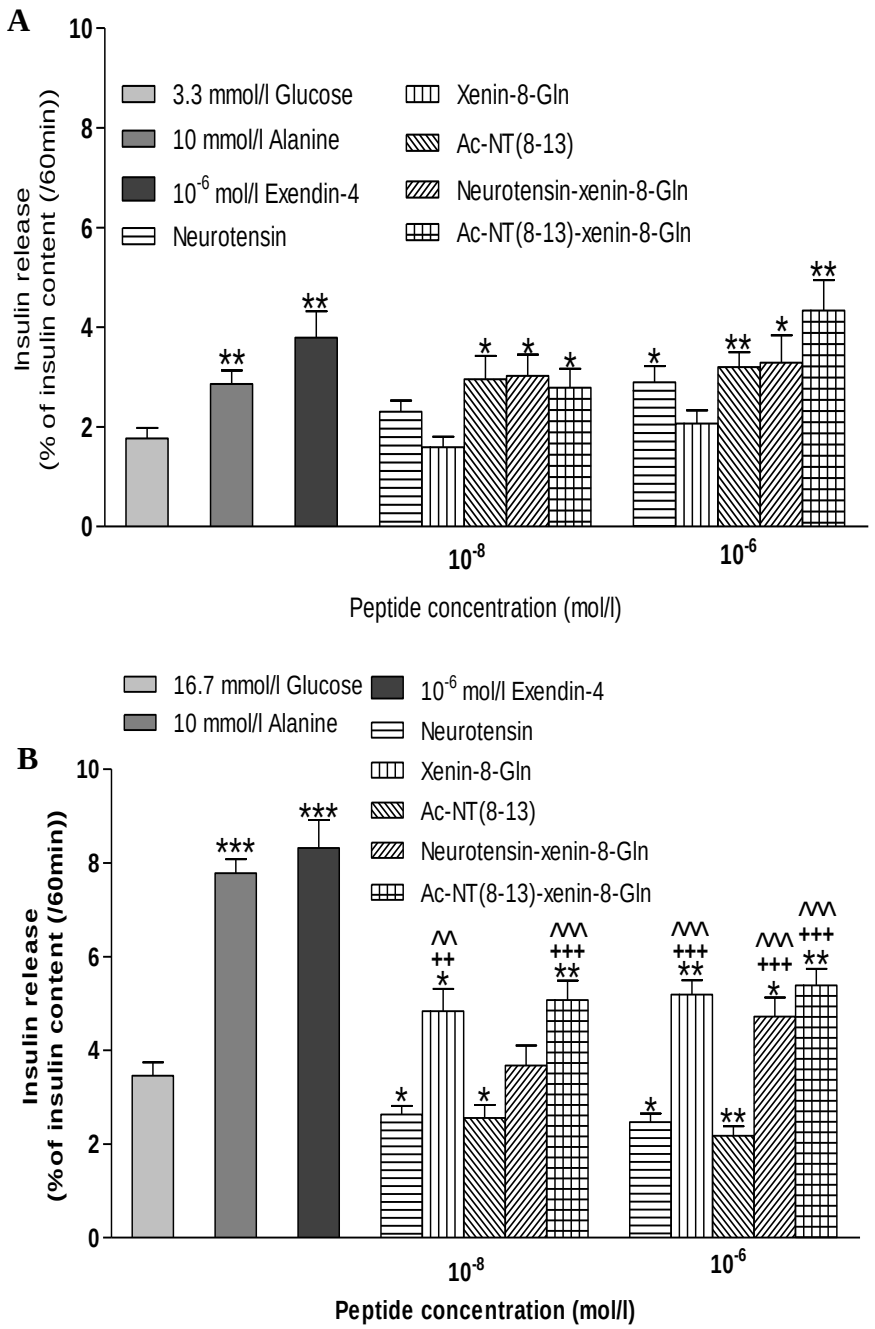

Isolated mice islets were incubated for 60 min with 10^{-6} or 10^{-8} mol/l of neurotensin, xenin-8-Gln, acetyl-neurotensin(8-13), neurotensin-xenin-8-Gln or acetyl-neurotensin(8-13)-xenin-8-Gln at (A) 3.3 and (B) 16.7 mmol/l glucose. Insulin release was measured using RIA. Values represent mean ± SEM (n=6). *P<0.05 and **P<0.01 compared to respective glucose control. $^{++}$P<0.01 and $^{++}$P<0.001 compared to neurotensin. ^^P<0.01 and ^^^P<0.001 compared to acetyl-neurotensin(8-13).

Figure 5.10 The effects of xenin-8-Gln, neurotensin(8-13), acetyl-neurotensin(8-13) and acetyl-neurotensin(8-13)-xenin-8-Gln on BRIN-BD11 cell proliferation

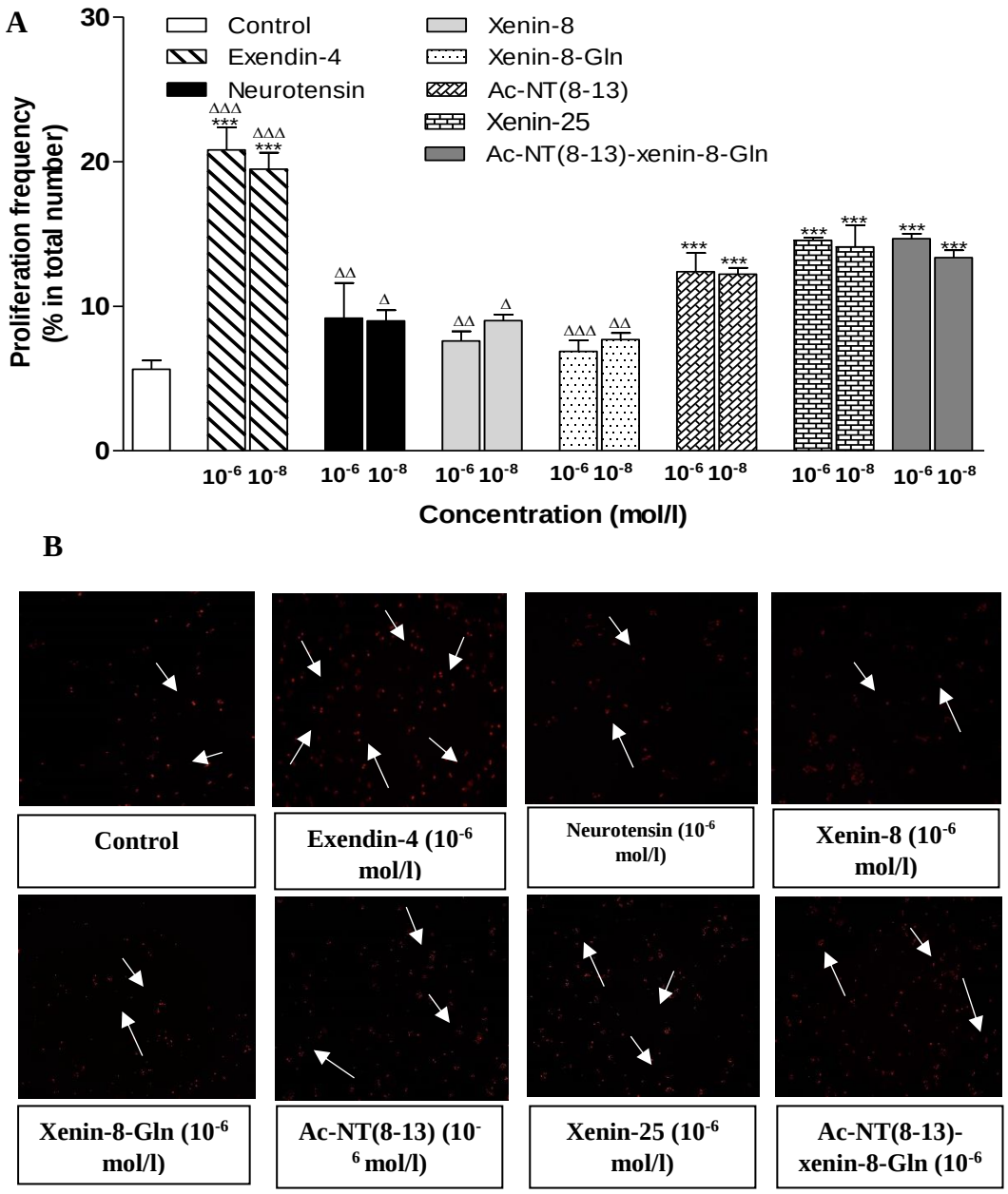

Proliferation frequency in BRIN-BD11 cells cultured with exendin-4, neurotensin, xenin-8, xenin-8-Gln, neurotensin(8-13), acetyl-neurotensin(8-13), xenin-25 and acetyl-neurotensin(8-13)-xenin-8-Gln (A) (at 10^{-6} or 10^{-8} mol/l) for 18 h. Representative images (B) showing proliferating beta cells, arrows indicate proliferating cells. Values are mean ± SEM (n=4). ***P<0.001 compared to control. $^{\Delta}$P<0.05, $^{\Delta\Delta}$P<0.01 and $^{\Delta\Delta\Delta}$P<0.001 compared to respective acetyl-neurotensin(8-13)-xenin-8-Gln.

Figure 5.11 The effects of exendin-4, xenin-8, xenin-8-Gln, neurotensin(8-13), acetyl-neurotensin(8-13) and acetyl-neurotensin(8-13)-xenin-8-Gln on BRIN-BD11 cell apoptosis

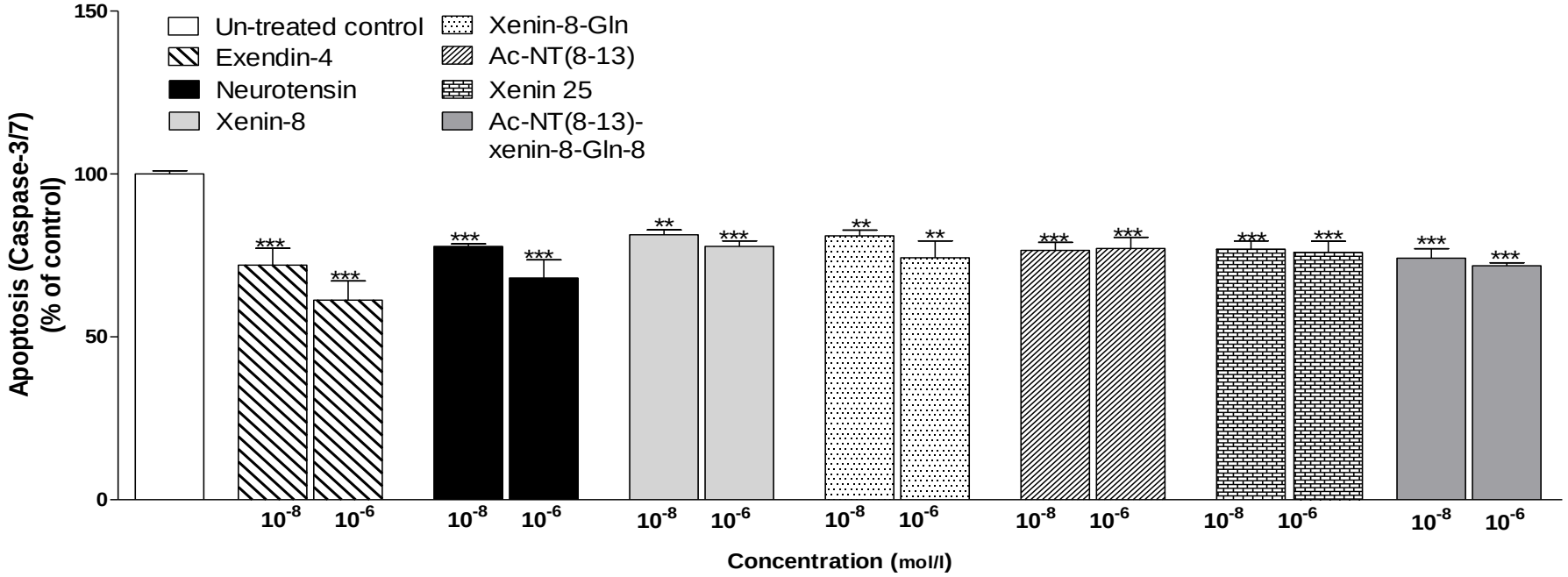

Apoptosis frequency in BRIN-BD11 cells cultured with exendin-4, neurotensin, xenin-8, xenin-8-Gln, neurotensin(8-13), acetyl-neurotensin(8-13), xenin-25 or acetyl-neurotensin(8-13)-xenin-8-Gln (at 10^{-6} or 10^{-8} mol/l) for 18 h. Caspase-3/7 activation was detected by luminescence. Values are mean ± SEM (n=3). **P<0.01 and ***P<0.001 compared to untreated control culture.

Figure 5.12 Effects of twice-daily administration of exendin-4, acetyl-neurotensin(8-13)-xenin-8-Gln or a combination of both peptides on cumulative energy intake, body weight and % fat in HFF mice

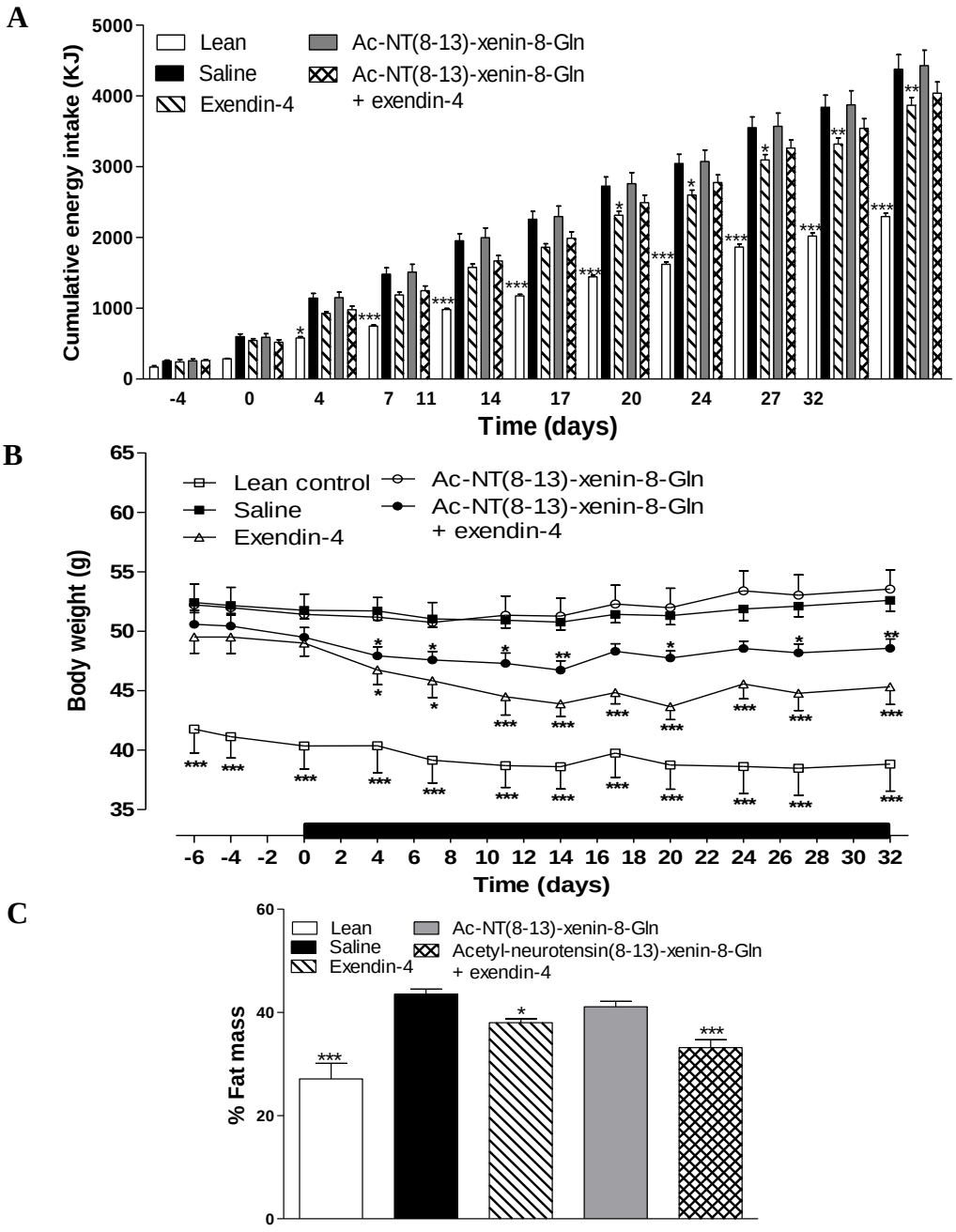

Parameters were measured for 6 days before and 32 days during (indicated by black horizontal line (B)) twice-daily treatment with saline, exendin-4, acetyl-neurotensin(8-13)-xenin-8-Gln or a combination of both (each at 25 nmol/kg) on cumulative energy intake (A) and body weight (B) and % fat mass (C), in HFF mice. Values represent mean ± SEM (n=6-8). *P<0.05, **P<0.01 and ***P<0.001 in comparison with saline control.

Figure 5.13 Effects of twice-daily administration of exendin-4, acetyl-neurotensin(8-13)-xenin-8-Gln or a combination of both peptides on non-fasted glucose and insulin in HFF mice

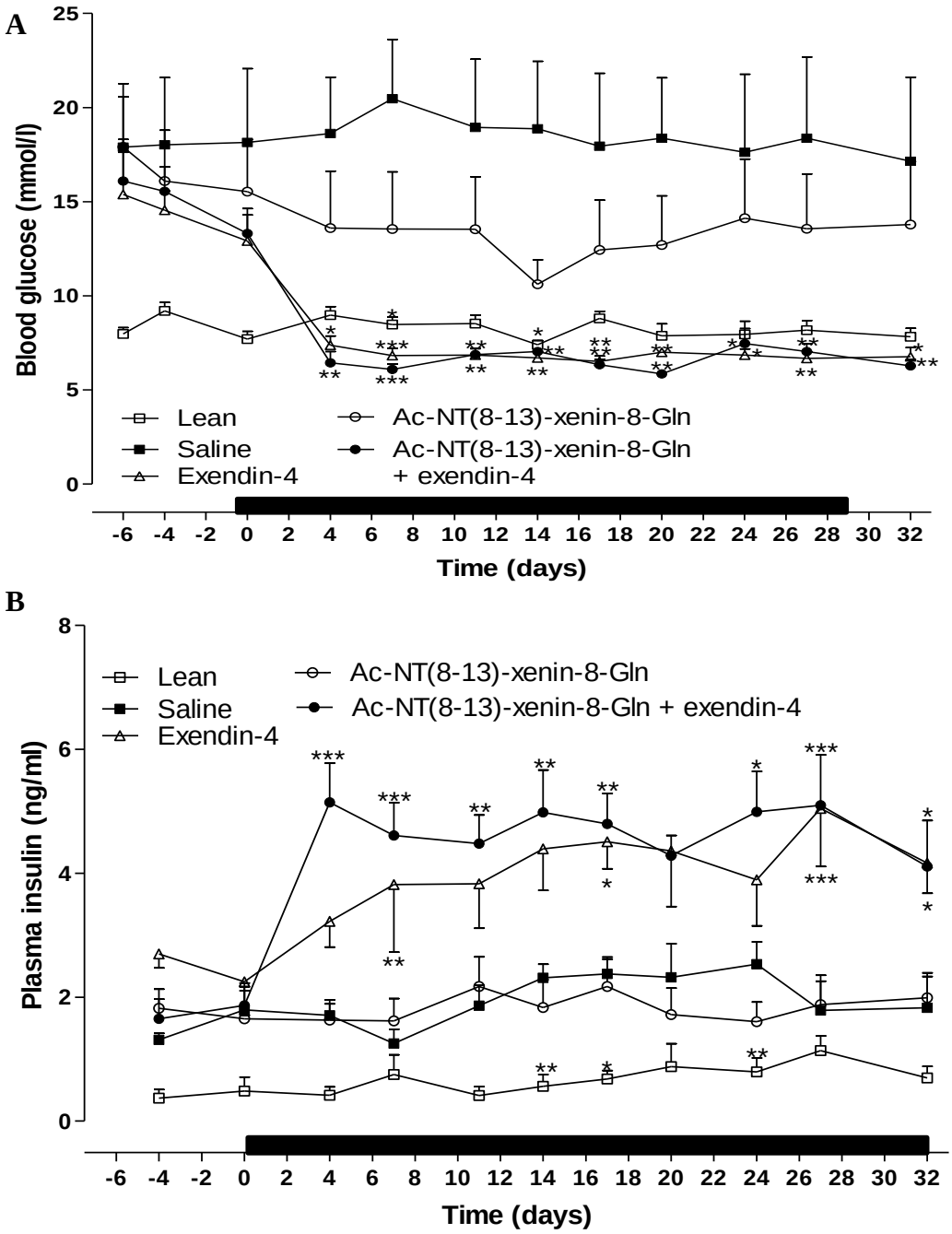

(A) Blood glucose and (B) plasma insulin was measured for 6 days before and 32 days during (indicated by black horizontal line) twice-daily treatment with saline, exendin-4, acetyl-neurotensin(8-13)-xenin-8-Gln or a combination of both peptides (each at 25 nmol/kg) in HFF mice. Values represent mean ± SEM (n=6-8). *P<0.05, **P<0.01 and ***P<0.001 compared with saline control.

Figure 5.14 Effects of twice daily administration of exendin-4, acetyl-neurotensin(8-13)-xenin-8-Gln or a combination of both peptides on 24 hour blood glucose profile and %HbA1c in HFF mice

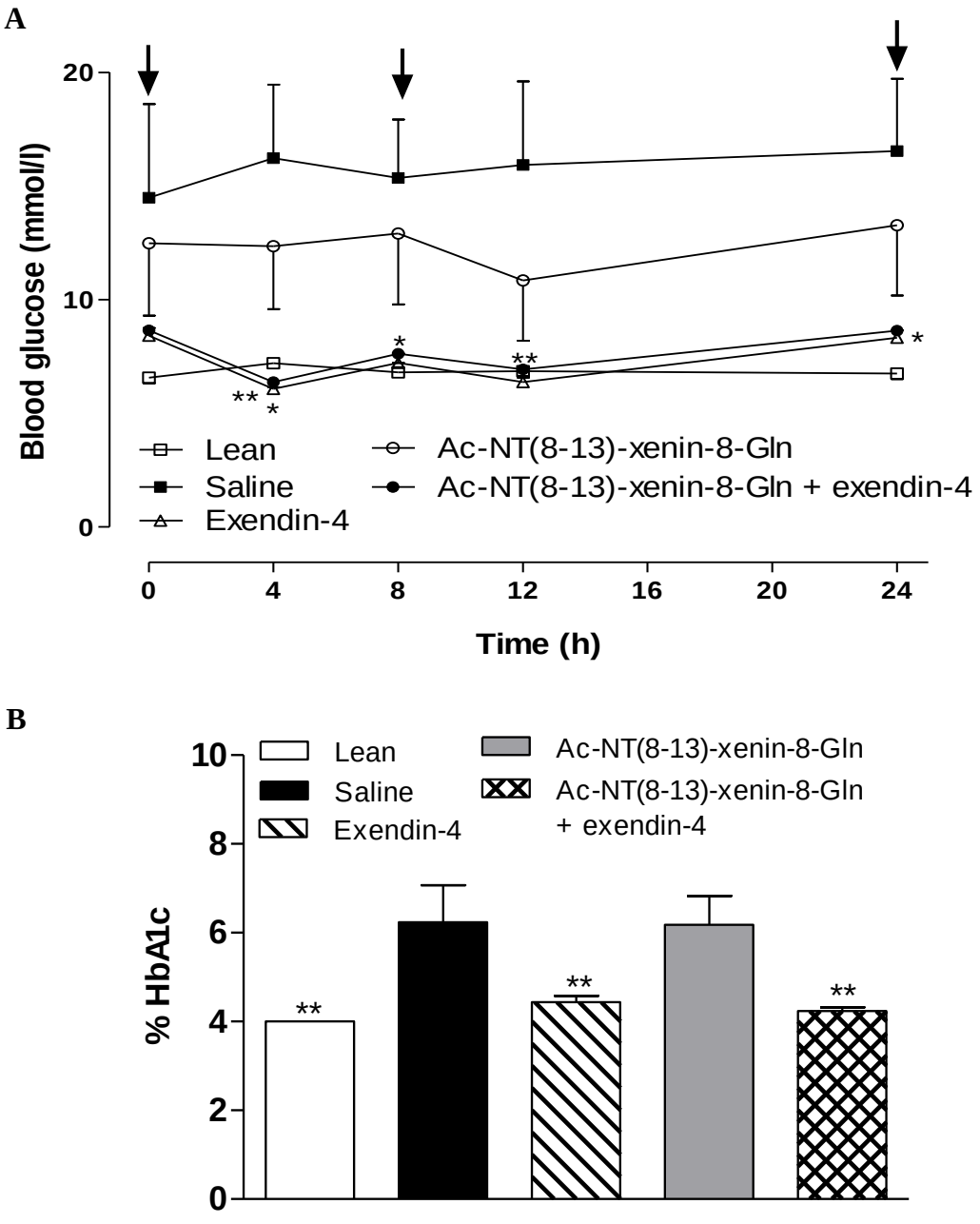

The 24 hour blood glucose profile (A) and %HbA1c (B) were assessed following 32 days of twice daily i.p. administration of saline, exendin-4, acetyl-neurotensin(8-13)-xenin-8-Gln or a combination of both peptides (each at 25 nmol/kg bw) in HFF mice. Arrows are indicative of treatment administration. Values represent mean ± SEM (n=6-8). *P<0.05 and **P<0.01 compared with saline control.

Figure 5.15 Effects of twice daily administration of exendin-4, acetyl-neurotensin(8-13)-xenin-8-Gln or a combination of both peptides on glucose and insulin in response to an oral glucose challenge in HFF mice

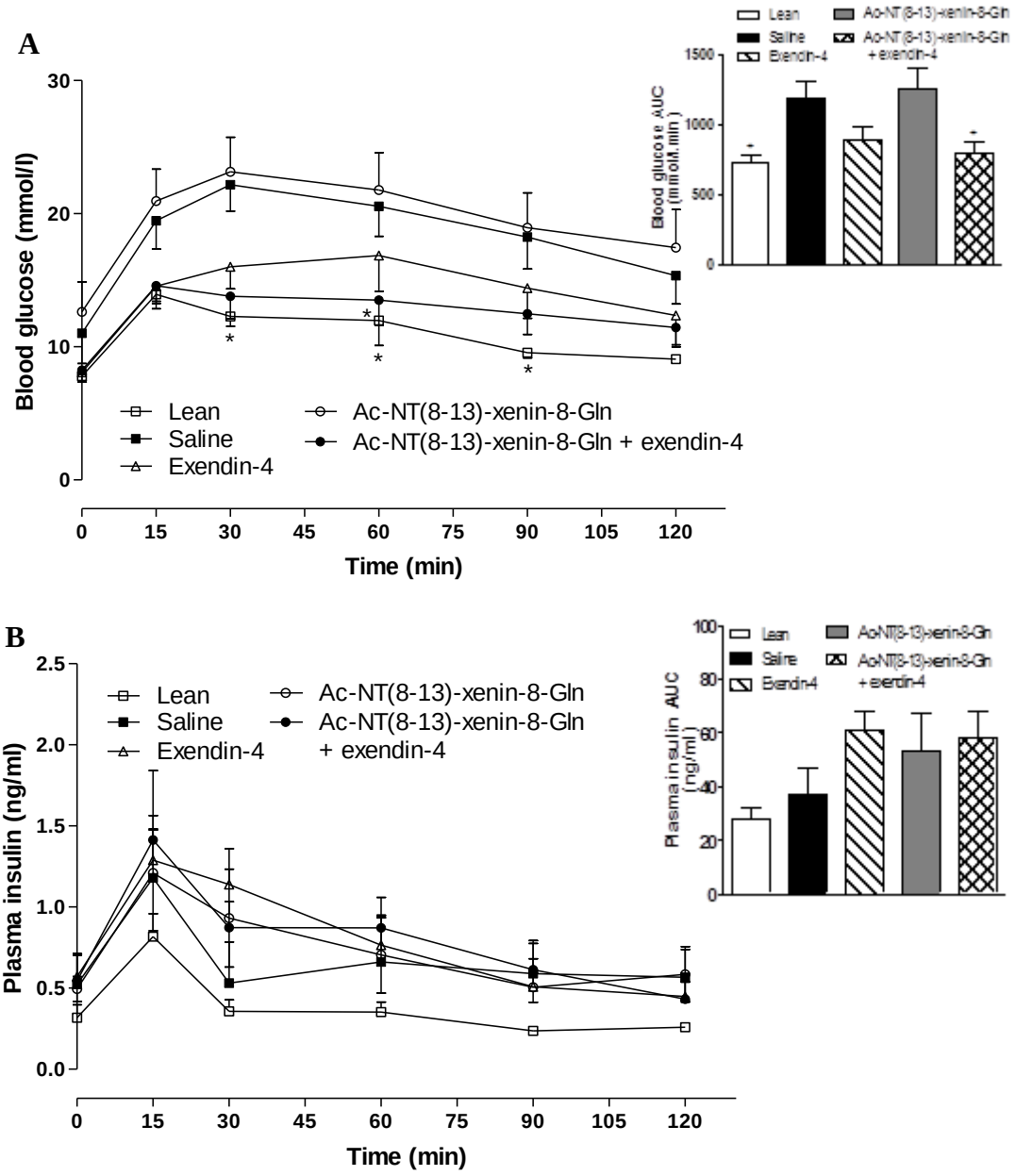

Test were performed following 32 days twice-daily i.p. administration of saline, exendin-4, acetyl-neurotensin(8-13)-xenin-8-Gln or a combination of both peptides (each at 25 nmol/kg bw). Mice were fasted for 10 h previously. Blood glucose (A) and plasma insulin (B) was measured prior to and after oral administration of glucose alone (18 mmol/kg bw). Blood AUC values for 0-120min are also included. Values represent mean ± SEM (n=6-8). *P<0.05 compared with saline control. $^{+}$P<0.05 compared with acetyl-neurotensin(8-13)-xenin-8-Gln.

Figure 5.16 Effects of twice daily administration of exendin-4, acetyl-neurotensin(8-13)-xenin-8-Gln or a combination of both peptides on glucose and insulin in response to a GIP tolerance test in HFF mice

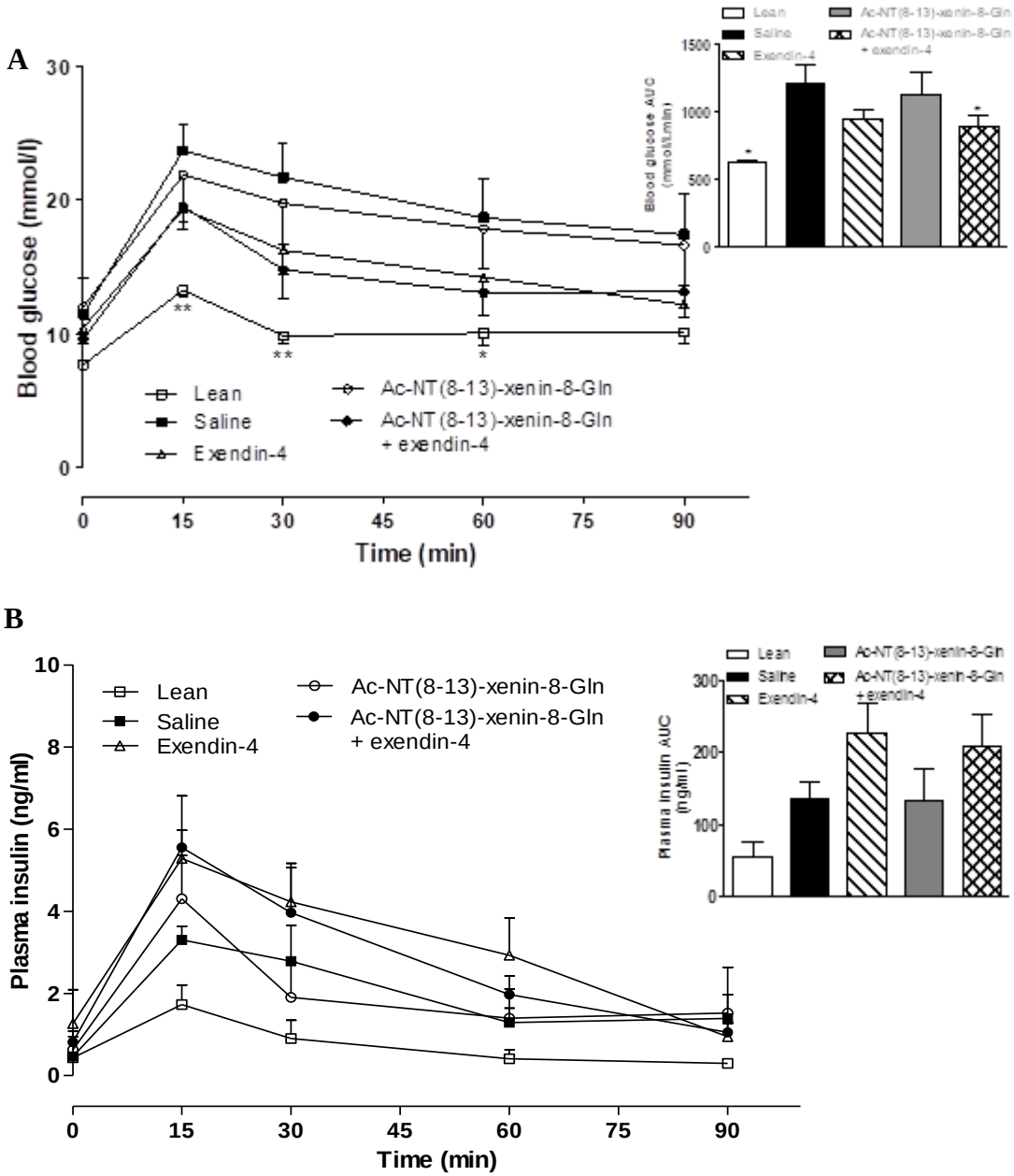

Test were performed following 32 days twice-daily i.p. administration of saline, exendin-4, acetyl-neurotensin(8-13)-xenin-8-Gln or a combination of both peptides (each at 25 nmol/kg bw) in HFF mice. Mice were fasted for 10 h previously. Blood glucose (A) and plasma insulin (B) was measured prior to and after i.p. administration of glucose (18 mmol/kg bw) in combination with GIP (25 nmol/kg bw). Blood AUC values for 0-90min are also included. Values represent mean ± SEM (n=6-8). *P<0.05 and **P<0.01 compared with saline control.

Figure 5.17 Effects of twice-daily administration of exendin-4, acetyl-neurotensin(8-13)-xenin-8-Gln or a combination of both peptides on insulin sensitivity and pancreatic insulin content in HFF mice

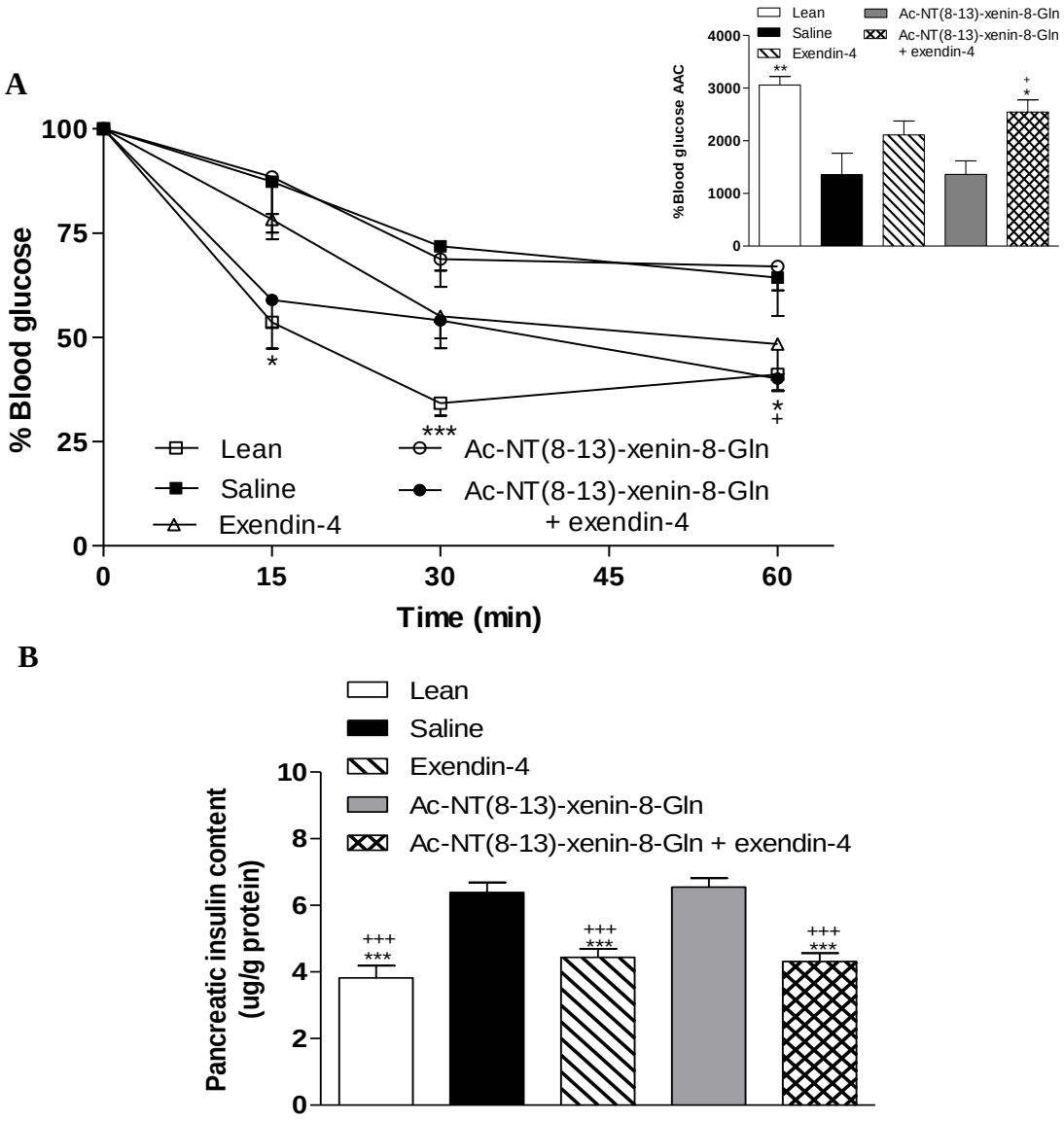

Test were performed following 32 days twice-daily i.p. administration of saline, exendin-4, acetyl-neurotensin(8-13)-xenin-8-Gln or a combination of both peptides (each at 25 nmol/kg bw) in HFF mice. Blood glucose was measured prior to and after i.p. administration of insulin (25 U/kg bw). Blood AAC values for 0-60 min are also included. Pancreatic insulin content (B) was measured by RIA following pancreatic hormone extraction. Values represent mean ± SEM (n=6-8). *P<0.05, **P<0.01 and ***P<0.001 compared with saline control. $^{+}$P<0.05 and $^{+++}$P<0.001 compared with acetyl-neurotensin(8-13)-xenin-8-Gln.

Figure 5.18 Effects of twice daily administration of exendin-4, acetyl-neurotensin(8-13)-xenin-8-Gln or a combination of both peptides on bone mineral density and bone mineral content in high fat fed mice

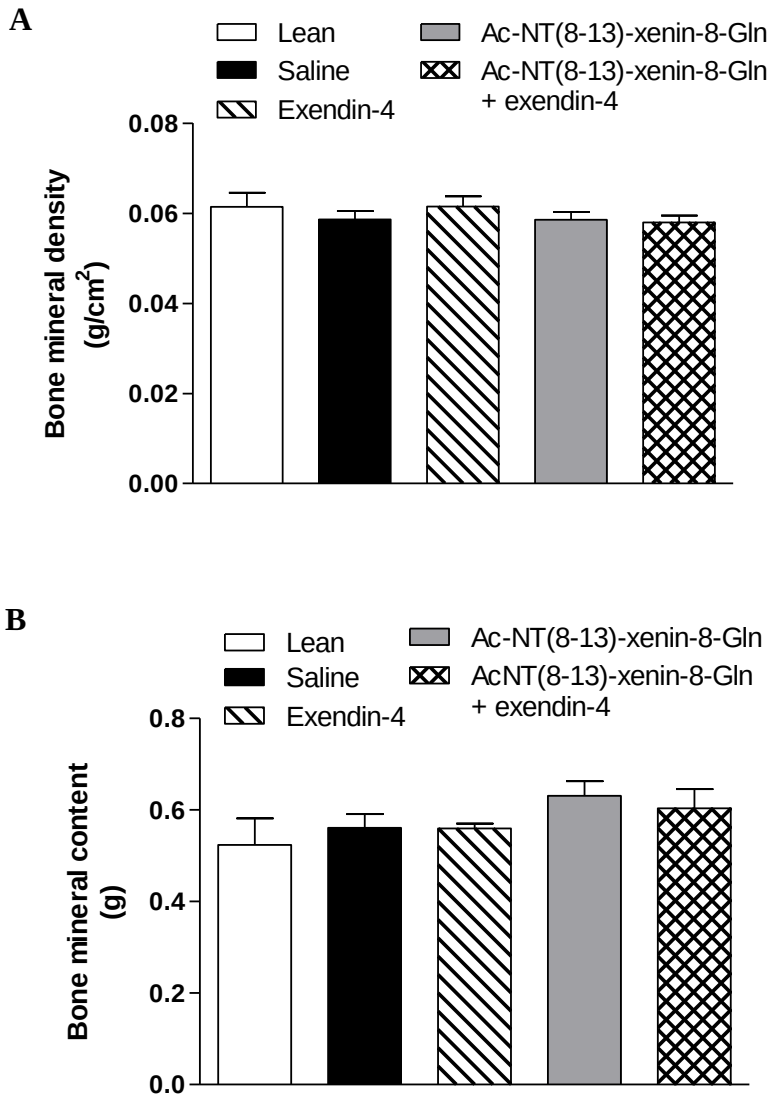

Effect of twice daily administration of exendin-4, acetyl-neurotensin(8-13)-xenin-8-Gln or a combination of both peptides on bone mineral density (A) and bone mineral content (B) measured by DEXA scanning in HFF and lean mice. Values represent mean ± SEM (n-6-8).

Figure 5.19 Effects of twice daily administration of exendin-4, acetyl-neurotensin(8-13)-xenin-8-Gln or a combination of both peptides on total cholesterol, triglycerides, HDL and LDL in high fat fed mice

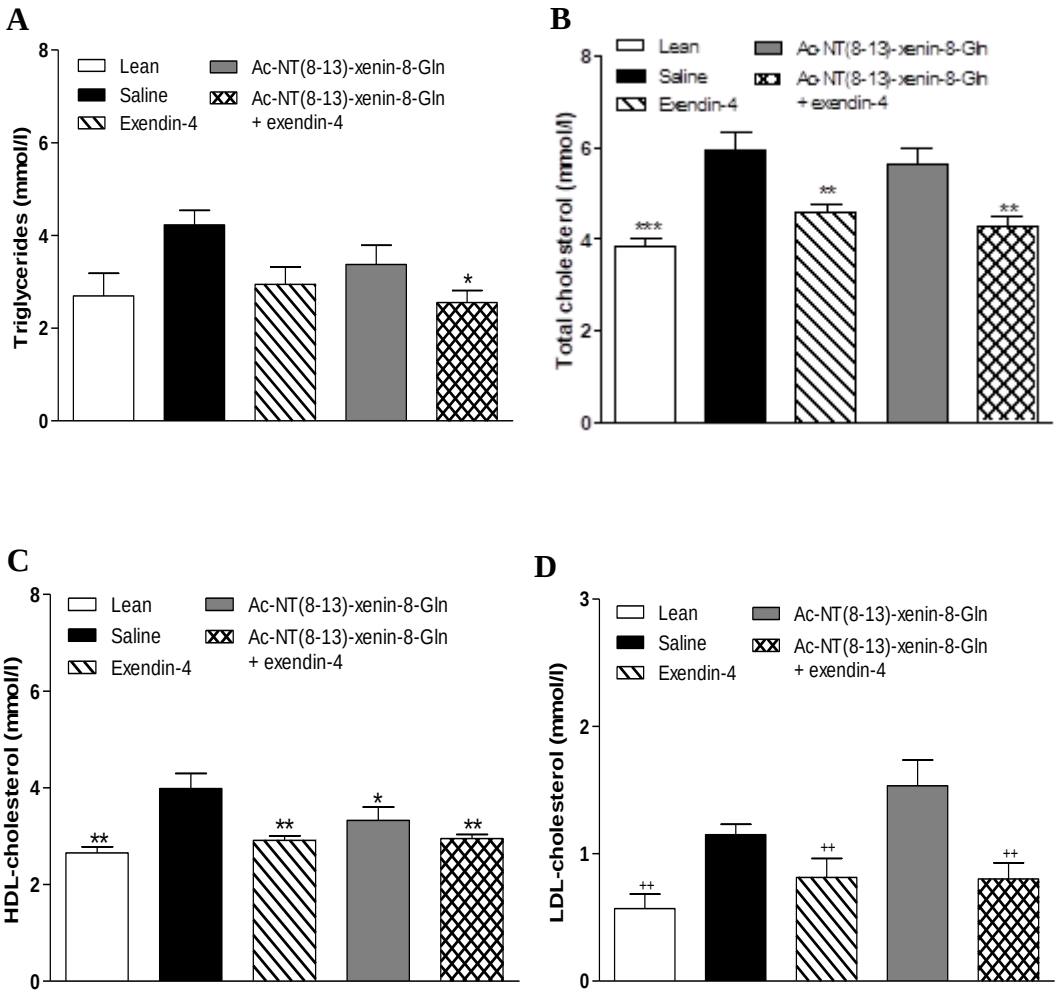

Effects of twice-daily i.p. administration of exendin-4, acetyl-neurotensin(8-13)-xenin-8-Gln or a combination of both peptides (each at 25 nmol/kg bw) following 32 day administration on total cholesterol (A), triglycerides (B), HDL (C) and LDL (D) in HFF mice. LDL was calculated as total cholesterol - HDL - (triglycerides /5). Values are mean ± SEM (n=6-8). *P<0.05 **P<0.01 and ***P<0.001 compared with saline treated control. $^{++}$P<0.01 compared with acetyl-neurotensin(8-13)-xenin-8-Gln.

Figure 5.20 Effects of twice daily administration of exendin-4, acetyl-neurotensin(8-13)-xenin-8-Gln or a combination of both peptides on pancreatic histology in HFF mice

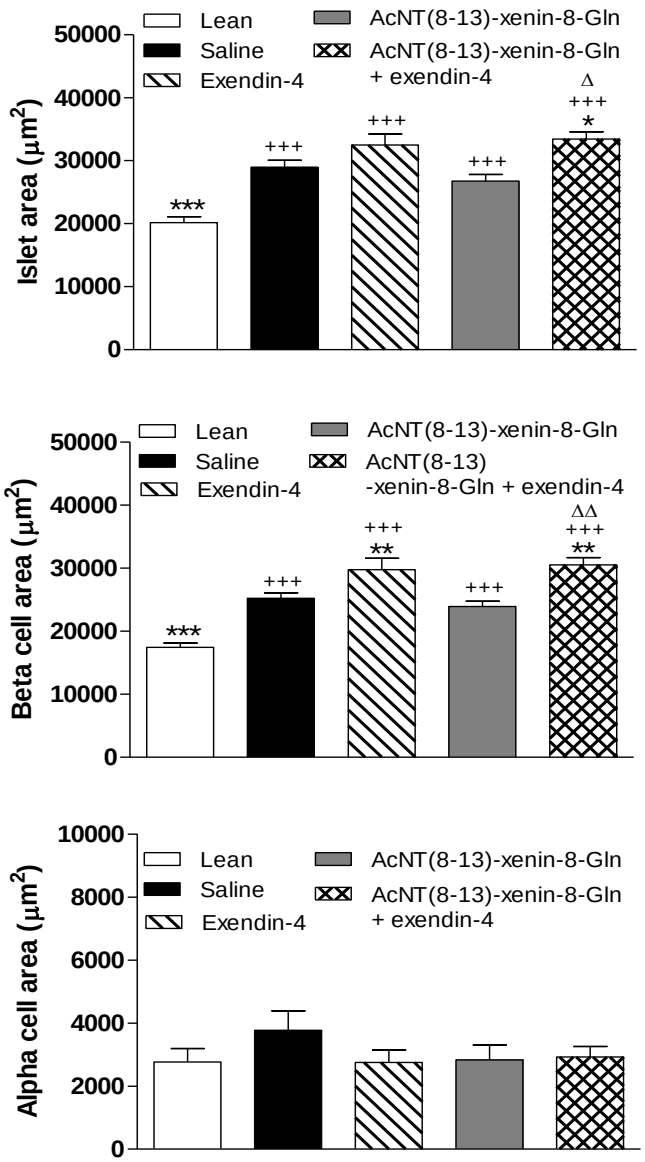

Effects of twice-daily i.p. administration of exendin-4, acetyl-neurotensin(8-13)-xenin-8-Gln or a combination of both peptides for 32 days (each at 25 nmol/kg bw) on islet area (A), beta cell area (B), and alpha cell area (C) in HFF mice. Values are mean ± SEM (n=6-8). *P<0.05, **P<0.01 and ***P<0.001 compared with saline treated control. $^{+++}$P<0.001 compared to lean control. $^{\Delta}$P<0.05 and $^{\Delta\Delta}$P<0.01 compared to neurotensin alone.

Figure 5.21 Effects of twice daily administration of exendin-4, acetyl-neurotensin(8-13)-xenin-8-Gln or a combination of both peptides on pancreatic islet histology in HFF mice

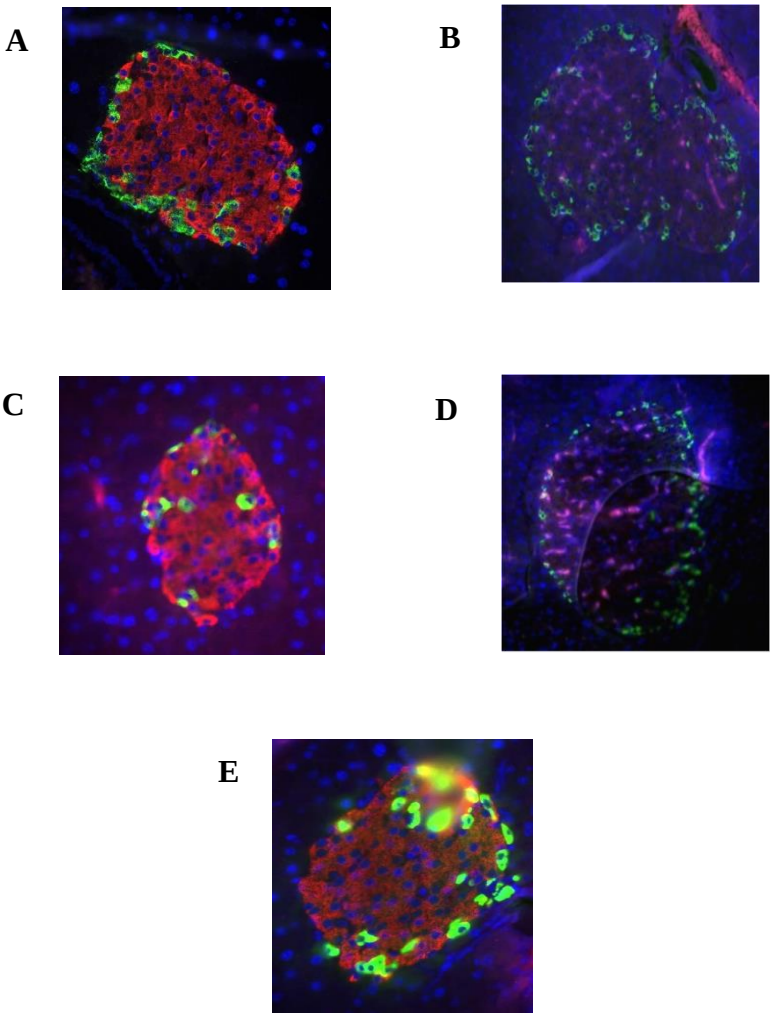

Images were captured by an Olympus System Microscope BX51 (Olympus instruments, UK) and a DP70 camera adapter. Cell^F image analysis software was used to assess parameters, magnification was X40. Insulin (red), glucagon (green) and DAPI (blue) in pancreatic tissue harvested from lean control (A) and HFF mice treated twice-daily with saline (B), exendin-4 (C), acetyl-neurotensin(8-13)-xenin-8-Gln (D) and a combination of both peptides (E) (each at 25 nmol/kg bw) for 32 days.

Chapter 6

Attempts to optimise an unambiguous GIP receptor antagonist with potential for translation as an anti-obesity-T2DM therapeutic

6.1 Summary

The prevalence of obesity is at an all time high with around 1 in 4 UK adults classified as obese. Obesity and associated insulin resistance is linked to the development of T2DM, but not all individuals go on to develop overt T2DM. Research suggests that hyper-secretion of the incretin hormone GIP has a key role to play in the development of obesity-T2DM. GIP is a key regulator of insulin secretion and lipid metabolism and these beneficial actions appear to be lost in individuals with obesity-T2DM. Studies with bariatric surgery show decreased GIP secretion and action as a main metabolic outcome which results in significant, long-term weight loss in these patients. Thus, there is an increasing interest in the less invasive approaches of GIP antagonism and/or disruption of GIPR action utilising peptide-based GIPR antagonists. However, it appears not to be essential to completely diminish GIP signalling, as reduction or partial reduction in GIP can produce beneficial anti-obesity effects. Yet, a specific GIPR antagonist continues to elude us. N- and C-terminally truncated GIP(3-30) and GIP(5-30) have recently been identified as competitive antagonists of the GIPR and questioned the efficacy of peer reviewed Pro^3GIP antagonist. This study attempts to uncover a true GIPR antagonist utilising human and mouse sequences. Initial *in vitro* analysis at low and high glucose concentrations in BRIN-BD11 cells shows human GIP(3-30), human Pro^3(3-30)GIP and mouse GIP(3-30) weakly stimulated insulin secretion, and significantly ($P<0.01$ to $P<0.001$) inhibited GIP-stimulated insulin secretion. *In vivo* analysis showed all peptides, with varying degrees had reduced ($P<0.01$) glucose lowering abilities when administered alone or in combination with human GIP (1-42). Interestingly, in those peptides with their C-terminus intact (position 31–42) the GIP receptor antagonistic quality was decreased. Further *in vivo* evaluation of human GIP(3-30) and GIP(5-30) and human Pro^3GIP(3-30) demonstrated that the latter had superior antagonistic abilities (1.3-fold, $P<0.05$), with human GIP(5-30) marginally behind. Additionally, to evaluate the receptor blockading capacity the peptides were administered 30 min prior to a glucose plus GIP challenge. Human Pro^3GIP(3-30) (1.4-fold, $P<0.001$), showed superior GIPR antagonistic activity in this system. These data concur with previous work on Pro^3GIP and further evidence it as a GIPR antagonist warranting further analysis with potential for translation as an antiobesity-T2DM therapeutic.

6.2 Introduction

In recent years the development of T2DM has been linked to obesity and associated insulin resistance and aging (Al-Goblan, Al-Alfi and Khan, 2014). This increased risk is thought to occur when, over time, pancreatic beta cell function declines and can no longer compensate for increased insulin demand and decreased peripheral sensitivity to insulin. However, surprisingly many obese individuals do not go on to develop T2DM, as obesity has been shown to increase in beta cell mass by 50%, thus enhancing insulin response to glucose (Cantley and Ashcroft, 2015). However, it is when this compensatory mechanism fails that subsequently leads to the development of T2DM (Cantley and Ashcroft, 2015). The prevalence of obesity is at an all time high, with around 1 in 4 UK adults classified as obese and these figures are projected to rise from 26% to 41–48% in men and from 26% to 35–43% in women by 2030 (Cantley and Ashcroft, 2015; Wang *et al.,* 2011). Thus, the likelihood of developing T2DM is also increased.

The incretin hormone GIP secreted in response to elevated glucose levels, has also been linked to obesity-T2DM through its actions as a key regulator of lipid metabolism (Al-Sabah, 2015; Seino and Yabe, 2010). Interestingly, patients with T2DM exhibit a decreased insulinotropic response to GIP and at the molecular level, and the loss of the incretin effect is a possible early pathophysiological indicator of T2DM (Al-Sabah, 2015). Moreover, it is the associated overnutrition, primarily by chronic consumption of dietary fats, that is thought to increase the circulating levels of GIP. Thus, ingested fat is known to be a potent stimulus for GIP secretion (Al-Sabah, 2015). Therefore, it appears that circulating GIP levels are elevated in obesity and T2DM resulting in excessive accumulation of visceral and subcutaneous fat deposition (Irwin and Flatt, 2009). Thus, increased action or secretion of GIP can predispose individuals to obesity (Irwin and Flatt, 2009; Paschetta, Hvalrug & Musso, 2011; Nakamura *et al.,* 2018).

A study by Zhou and colleagues (2005) provides further evidence for the link between GIP and obesity through studies using insulin receptor substrate (IRS)-1-deficient knockout mice. They observed that if the action of insulin was diminished, as is the case in T2DM, then GIP could switch from fat oxidation to fat accumulation, which ultimately resulted in increased triglyceride storage (Zhou *et al.,* 2005). Genetic studies also provided evidence that links GIP to obesity. Vogel and colleagues (2009) analysed

the GIPR gene and found polymorphisms, single nucleotide repeats (SNPs) within the coding regions or regions adjacent to these which could attribute to genetic predisposition to obesity (Vogel *et al.,* 2009). This is significant because the major causative factor of insulin resistance in obesity-related diabetes is found in those individuals with centrally distributed body fat and associated metabolic dysregulation. This includes increased levels of circulating free fatty acids (FFA), as this type of fat is more lipolytic and results in lipid toxicity, initiating an inflammatory response (Boden, 2011; Al-Goblan, Al-Alfi and Khan, 2014). This metabolic dysfunction results in insulin resistance that creates a hyperglycaemic state further exacerbating the T2DM disease state (Al-Goblan, Al-Alfi and Khan, 2014).

With accumulating evidence linking elevated GIP levels to development of obesity and insulin resistance, there is growing interest in research surrounding GIP antagonism, and/or disruption of GIPR action and how it could be exploited to potential treat obesity-T2DM (Gasbjerg *et al.,* 2018a). Currently, it is primarily bariatric surgery that results in significant long-term weight loss in patients with obesity-T2DM (Mingrone *et al.,* 2012; 2015). Interestingly, a number of these studies point to decreased GIP secretion and action as a main metabolic outcome of the surgical process (Mingrone *et al.,* 2009; Xiong *et al.,* 2015). Until recently, the most widely used pharmacological agent for obesity was orlistat, but current clinical recommendations have seen the introduction of liraglutide, the GLP-1 agonist, as an adjunct therapeutic with diet and physical activity for weight management (Mehta, Marso and Neeland, 2017; Nakamura *et al.,* 2018; Troke *et al.,* 2014). Liraglutide has been shown in several clinical trials to offer superior and sustainable weight loss, with 5-10%, at the higher therapeutic dosage of 3 mg than at the normal therapeutic range (1.8 mg). However, the long-term efficacy of liraglutide has yet to be established for obesity, and adverse effects such as gastrointestinal disturbances and hypoglycaemia along with an increased risk of medullary thyroid carcinoma should not be overlooked (Mehta, Marso and Neeland, 2017).

GIP antagonism studies have included work in animal models with genetic deletions of the GIPR (Zhou *et* a*l.,* 2008; Naitoh *et al.,* 2008), small molecules that block the GIP receptor (Irwin *et al.,* 2006; Nakamura *et al.,* 2012), immunisation against GIP (Irwin *et al.,* 2009; Ravn *et al.,* 2013), and peptide-based antagonists (Gault *et al.,* 2007a; Kerr *et al.,* 2011). Importantly, an interesting study has suggested that it is not

entirely necessary to completely obliterate GIP signalling to gain anti-obesity benefits, and a reduction or even a partial reduction in GIP secretion has been shown to yield the anti-obesity effect (Nasteska *et al.,* 2014). Indeed, this approach would also be considered to have a less detrimental effect on GIP-induced insulin secretion, that would be beneficial in T2DM. Thus, development of an efficacious GIP antagonist could mimic positive results from bariatric surgeries, without the need for major surgery or adverse effects.

The Diabetes Research Group (DRG) at Ulster have generated and developed several peptide antagonists of GIP. Key approaches have examined N-terminally truncated GIP peptides (Kerr *et al.,* 2011), amino acid substituted analogues such as Pro^3GIP (Gault *et al.,* 2007b; McClean *et al.,* 2007; McClean *et al.,* 2008) and N- and C-terminally truncated palmitoylated GIP peptides (Pathak *et al.,* 2015a). These studies have shown beneficial effects on normalising glucose tolerance, improving insulin sensitivity and energy intake, reversing obesity and associated metabolic disturbances. Furthermore, adipocyte hypertrophy, adipose tissue mass and triglyceride deposition in the liver and muscle of high-fat fed mice were significantly reduced along with a significant reduction in circulating triglycerides, cholesterol and glucagon levels (Gault *et al.,* 2007b; Gault *et al.,* 2008; McClean *et al.,* 2007; McClean *et al.,* 2008; Pathak *et al.,* 2015a). Pro^3GIP has also been shown to prevent diabetes and the associated metabolic disturbances in mice with early administration (Irwin *et al.,* 2007). However, recent research has refuted Pro^3GIP as full antagonist at the human GIPR but rather suggesting it is a partial GIP agonist, that is linked to interspecies variation at receptors and ligands between humans and rodents (Hansen *et al.,* 2015; Nakamura *et al.,* 2018; Sparre-Ulrich *et al.,* 2015). Therefore, we sought to build upon our work and recent work of others to optimise truncated GIP peptides and assess their potential antagonist properties *in vitro* and *in vivo*. Whilst availability of a potent GIP antagonist would be invaluable in determining full spectrum of GIP physiology there is also much opportunity that GIP antagonism could actually be beneficial as a potential therapeutic.

6.3 Materials and Methods

6.3.1 Peptides

All peptides were purchased from Syn Peptide Shanghai, China. Purity was confirmed by RP-HPLC and characterised by MALDI-TOF MS (Table 6.1), as previously described in Sections 2.2.2 to 2.2.4. For all experimental materials and methods please refer to Section 2.1, and the relevant subsections.

6.3.2 Acute effects of peptides on *in vitro* insulin secretion from BRIN-BD11 cells

The *in vitro* insulin secretory activity of test peptides was examined in BRIN-BD 11 cells as described in Section 2.5.2. BRIN-BD11 cells were incubated with test peptides (10^{-6} – 10^{-12} mol/l) alone or in the presence of native GIP (1-42) at 5.6 and 16.7 mmol/l glucose for 20 min. Following test incubations, insulin was measured by RIA, as previously described in Sections 2.5.2 and 2.5.4.

6.3.3 Animals

Acute studies used male Swiss mice as described in Section 2.9.1-2.10.2. Experiments for glucose tolerance studies were conducted using test peptides in overnight fasted mice, as outlined in Sections 2.10.1-2.10.2.

6.3.4 Biochemical analysis

Blood glucose was measured directly by the Ascencia Contour glucose meter (Bayer, Newbury, UK), as described in Section 2.10.

6.3.5 Statistical analysis

As described in Section 2.12

6.4 Results

6.4.1 Acute effects of human GIP(1-42), human GIP(1-30) and mouse GIP(1-30) on insulin release from BRIN-BD11 cells

Figure 6.1(A-B) demonstrate the abilities of native human GIP(1-42) and C-terminally truncated human and mouse GIP(1-30) to increase insulin secretion from BRIN-BD11 cells at both 5.6 and 16.7 mmol/l glucose in a dose-dependent (10^{-12} – 10^{-6} mol/l) manner compared to glucose control. However, human and mouse GIP(1-30) only significantly increase ($P<0.01$ to $P<0.001$) insulin secretion at higher peptide concentrations (10^{-8} mol/l to 10^{-6} mol/l) in 5.6 (Figure 6.1A) and 16.7 (Figure 6.1B) mmol/l glucose. Furthermore, the potency of human GIP(1-42) and (1-30) is significantly less ($P<0.05$ to $P<0.01$) in comparison to mouse GIP(1-30) at concentrations 10^{-10} mol/l and 10^{-8} mol/l at 16.7 mmol/l glucose (Figure 6.1B).

6.4.2 Acute effects of human GIP(3-30) and mouse GIP(3-30) alone or in combination with native human GIP(1-42) on insulin release from BRIN-BD11 cells

Figure 6.2(A-D) shows human and mouse GIP(3-30), at 10^{-7} mol/l, significantly reduced ($P<0.001$) GIP-induced (10^{-12} to 10^{-6} mol/l) insulin secretion from BRIN-BD11 cells at both 5.6 and 16.7 mmol/l glucose. Importantly, neither human nor mouse GIP(3-30) had any effect on insulin secretion from BRIN-BD11 cells at either 5.6 or 16.7 mmol/l glucose (Figure 6.2A-D).

6.4.3 Acute effects of human Pro^3GIP(3-30) and human GIP(5-30) alone or in combination with native human GIP(1-42) on insulin release from BRIN-BD11 cells

Human Pro^3GIP(3-30) significantly decreased ($P<0.01$ to $P<0.001$) GIP-induced (10^{-12} mol/l to 10^{-6} mol/l) insulin secretion from BRIN-BD11 at both 5.6 and 16.7 mmol/l glucose (Figure 6.3A-B). However, human GIP(5-30) was unable to impede the insulinotropic action of GIP(1-42) (Figure 6.3C-D). Indeed, at 16.7 mmol/l glucose, human GIP(5-30) actually stimulated ($P<0.01$) insulin release when compared to glucose alone control (Figure 6.3D).

6.4.4 Acute effects of human GIP(3-42) and human GIP(5-42) alone or in combination with native human GIP(1-42) on insulin release from BRIN-BD11 cells

Human GIP(3-42) was unable to block GIP-induced (10^{-12} to 10^{-6} mol/l) insulin secretion at 5.6 mmol/l glucose (Figure 6.4A), but was a moderately effective GIP blocker at 16.7 mmol/l glucose (Figure 6.4B). However, human GIP(5-42) did not impede the insulinotropic action of GIP at 5.6 or 16.7 mmol/l glucose (Figure 6.4C-D), and actually evoked significant ($P<0.05$) insulin release when incubated alone with BRIN-BD11 cells at 16.7 mmol/l glucose (Figure 6.4D).

6.4.5 Acute effects of native human GIP(1-42), human GIP(1-30) and mouse GIP(1-30) on glucose tolerance in lean mice

The acute effects of native human GIP(1-42) and human and mouse GIP(1-30) on blood glucose in overnight fasted mice is shown in Figure 6.4. Human GIP(1-42) significantly lowered ($P<0.05$ to $P<0.01$) glucose levels (at 15, 30 and 60 min) and human GIP(1-30) at the 60 min time point compared to glucose control (Figure 6.5A). Mouse GIP(1-30) had no significant effect on glucose-lowering (Figure 6.5A). These observations correlate with the 0-60 min overall AUC values showing a reduction ($P<0.05$) in glucose by human GIP(1-42) and (1-30), but not mouse GIP(1-30) (Figure 6.5B). No differences in efficacy were noted between human GIP(1-42) and human GIP(1-30).

6.4.6 Acute effects of human GIP(3-30) alone or in combination with native human GIP(1-42) on glucose tolerance in lean mice

Human GIP(3-30) alone or in combination with human GIP(1-42) demonstrated no significant effects on glucose levels in overnight fasted mice (Figure 6.6A-B). However, human GIP(3-30) blocked the ability of human GIP(1-42) ability to ($P<0.05$) reduce glucose levels (Figure 6.6A-B).

6.4.7 Acute effects of mouse GIP(3-30) alone or in combination with native human GIP(1-42) on glucose tolerance in le

an mice

Mouse GIP(3-30) in combination with human GIP(1-42) demonstrated a significant blocking (1.3-fold; $P<0.05$) effect on the ability of human GIP(1-42) to reduce glucose levels (Figure 6.7A-B). When administered alone, mouse GIP(3-30) had no effects on glucose levels, being similar to that of the glucose control (Figure 6.7A-B).

6.4.8 Acute effects of human Pro^3GIP(3-30) alone or in combination with native human GIP(1-42) on glucose tolerance in lean mice

Human Pro^3GIP(3-30**)** alone displayed no significant effects on overall AUC blood glucose levels, but did decrease ($P<0.05$) individual glucose levels at 60 min post-injection compared to glucose alone (Figure 6.8A-B). However, when human Pro^3GIP(3-30) was combined with human GIP(1-42), the glucose-lowering effects of native GIP were lost (Figure 6.8A-B).

6.4.9 Acute effects of human GIP(5-30) alone or in combination with native human GIP(1-42) on glucose tolerance in lean mice

Human GIP(5-30) alone had no impact on glucose lowering in overnight fasted mice (Figure 6.9A-B). However, in combination with human GIP(1-42) there was a significant ($P<0.05$ to $P<0.01$) hindering effect on the glucose-lowering action of GIP, both in terms of individual and AUC values (Figure 6.9A-B).

6.4.10 Acute effects of human GIP(3-42) alone or in combination with native human GIP(1-42) on glucose tolerance in lean mice

Figure 6.10 reveals that human GIP(3-42**)** alone no effect on glucose homeostasis in mice (Figure 6.10A-B). In addition, human GIP(3-42) was unable to impede the glucose-lowering action of human GIP(1-42) (Figure 6.10A-B).

6.4.11 Acute effects of human GIP(5-42) alone or in combination with native human GIP(1-42) on glucose tolerance in lean mice

Similar to human GIP(3-42), glucose-homeostatic actions of human GIP(5-42) were not apparent in overnight fasted mice, either when injected alone or in combination with human GIP(1-42) Figure 6.11A-B).

6.4.12 Acute effects of high dose human GIP(3-30), human Pro^{3}GIP(3-30) or human GIP(5-30) on glucose tolerance in lean mice

Higher dose (100 nmol/kg) of human GIP(3-30), human Pro^{3}GIP(3-30) or human GIP(5-30) had a significant glucose-lowering ($P<0.01$) ability at least one observation point during the 60 min test (Figure 6.12A). Overall glucose AUC confirmed glucose-lowering actions of all three peptides, similar to native GIP (Figure 6.12B; Table 6.2). However, the efficacy of human Pro^{3}GIP(3-30) or human GIP(5-30) was significantly ($P<0.05$) reduced when compared to native GIP (Figure 6.12B; Table 6.2).

6.4.13 Acute effects of early administration of high dose human GIP(3-30), human Pro^{3}GIP(3-30) and human GIP(5-30) on glucose tolerance in lean mice

The effects of early administration (at -30 min) of 100 nmol/kg human GIP(3-30), human Pro^{3}GIP(3-30) and human GIP(5-30) are shown in Figure 6.13. Interestingly, only human Pro^{3}GIP(3-30) was able to block the glucose-lowering action of native GIP when injected 30 mins prior to GIP challenge (Figure 6.13A-B; Table 6.2). As such, both human GIP(3-30) and human GIP(5-30) were ineffective (Figure 6.13A-B; Table 6.2).

6.5 Discussion

Research by Hansen and colleagues (2016), has identified N- and C-terminally truncated GIP(3-30) and GIP(5-30) as competitive antagonists of the GIPR. However, further research demonstrated that efficacy and possible therapeutic translatability of GIP based peptides is underpinned by interspecies variation in the structure/function of GIP (Gasbjerg *et al.,* 2018b; Hansen *et al.,* 2016; Sparre-Ulrich *et al*., 2015). The

data infers that alteration in amino sequence structure of GIP between species, even by just one amino acid, can cause a significant difference in potency and receptor binding affinity (Sparre-Ulrich *et al*., 2015). The GIPR is 81% conserved between human and rodent species, along with some variations within the ligand sequence (Sparre-Ulrich *et al*., 2016). This is more apparent within mouse GIP, as it has three substitutions compared to human GIP, whereas rat has two amino acid substitutions (Sparre-Ulrich *et al*., 2015). Both rodent species have substitutions that occur at position 18, where arginine present in human GIP is substituted with histidine (Sparre-Ulrich *et al*., 2015). In mouse, at position 30, lysine is substituted to arginine and at position 34, asparagine to serine when compared to human GIP (Sparre-Ulrich *et al*., 2016). In rat, the second amino acid substitution is isoleucine for leucine at position 40 (Sparre-Ulrich *et al*., 2015).

In addition, the present work reaffirms understanding that N- and C- terminals of GIP are a key consideration when designing potential therapeutics. GIP receptors are from the class B family of G-protein coupled receptors (GPCRs) and have a large extracellular N-terminal domain (NTD) linked to a 7-transmembrane helical domain (Al-Sabah, 2015). The C-terminal region of the peptide ligand binds to the receptors NTD, and this allows for secondary interaction between the N-terminus of the peptide and transmembrane domain (TMD). Research suggests that the first two amino acids of the GIP N-terminus are essential for agonist properties, and that if truncated, receptor activation does not occur (Hansen *et al.,* 2016). Moreover, it has been determined that only amino acids from position 3-30 in GIP are essential for receptor binding (Hansen *et al.,* 2016). The present study utilised this information to investigate the impact of truncating the N- and C- terminals of GIP and substituting a proline at position 3, thus Pro^3GIP(3-30), and comparing this effect on both human and mouse GIP counterparts.

The *in vitro* and *in vivo* assessment of human GIP(1-42) and GIP(1-30) revealed that they had equal potency to stimulate insulin secretion. This is in line with previous work by the DRG and the study by Hansen and colleagues (2016), which assessed functionality and showed both peptides to have full agonist properties with equal affinity for the GIPR (Gault *et al.,* 2011; Hansen *et al.,* 2016). Moreover, mouse GIP(1-30) enhanced insulin secretion from BRIN-BD11 cells. This contrasts with the study by Sparre-Ulrich and colleagues (2015) on interspecies variation regarding receptor

and ligand binding. Both human and rat GIP(1-30) have a lysine at position 30, whereas the mouse sequence has an arginine at position 30. Therefore, if this interspecies variation was a factor influencing translatability to humans, a larger impact in terms of insulin secretion from a rat cell-line and glucose lowering in rodents would be expected (Sparre-Ulrich *et al.*, 2015). In terms of biochemical structure, it is somewhat surprising that lysine to arginine substitution would have such a profound effect. It would seem unlikely that charge is the key factor here and more likely resides in orientation within the peptide. At both low and high glucose concentrations, human GIP(3-30), human Pro^3(3-30)GIP and mouse GIP(3-30) weakly stimulated insulin secretion, but significantly inhibited GIP-stimulated insulin secretion. However, GIP-stimulated insulin secretion was unaffected in combination with human GIP(5-30), GIP(3-42) or GIP(5-42). This result contrasts with previous work using related analogues and GIP(3-42) (Gault *et al.*, 2002). It is not clear why this would be the case but could reside in peptide quality and/or precise application in the model system in BRIN-BD11 which differed in passage.

Further *in vivo* analysis established that all peptide analogues, some more significant than others, had reduced glucose-lowering abilities when administered alone or in combination with human GIP (1-42). Effects on glucose control were possibly more apparent when administered at a higher dose (100 nmol/kg bw), but even at this dose, none of the peptides were as effective as native GIP to lower glucose. Interestingly, the GIP receptor antagonistic quality was decreased in peptides with their C-terminus intact (position 31–42), namely human GIP(3-42) and GIP(5-42), correlating with recent findings by Hansen and colleagues (Hansen *et al.*, 2016). Converse to the early suggested interspecies variation discrepancies of mouse and human GIP(1-30), it was mouse GIP(3-30) that displayed the most superior GIP antagonistic abilities *in vivo* (Hansen *et al.*, 2016; Sparre-Ulrich *et al.*, 2015). This could well be due to the models used between the two studies.

Interestingly, following evaluation of human, rat and mouse Pro^3GIP, Sparre-Ulrich and colleagues (2015) noted that there was lower bioactivity within the rodent system than in humans. The same research team noted that human Pro^3GIP at the human receptor had full agonism activity, and rodent ligands having a similar effect. However, on rodent GIPRs they suggested that Pro^3GIP ligands act as partial agonists with competitive antagonistic properties (Sparre-Ulrich *et al.*, 2015). Yet, it was the

human sequence of GIPR agonist, namely native GIP(1-42), that had a lower potency and efficacy on all three GIPRs in these same studies, with both rodent GIP demonstrating equal potency and efficacy on all GIPRs (Sparre-Ulrich *et al.,* 2015). Furthermore, binding studies showed that these functional differences were not due to binding affinity (Sparre-Ulrich *et al.,* 2015). Thus, with this confliction of reduced efficacy and potency of human GIP on all receptors compared to rodent ligands, further studies are required to confirm the exact consequences of different species of the GIP ligand on receptor activation. It could be possible that position 18 of GIP may have an important mechanistic activation role for the GIPR, and it has been shown that position 18 arginine substitution can produce a much more formidable antagonistic effect than histidine (Sparre-Ulrich *et al.,* 2017). Taking this, and related studies on truncated human GIP(3-30) and GIP(5-30) into account, it seems inappropriate to completely rule out Pro^3GIP as a competitive GIPR antagonist (Hansen *et al.,* 2016; Sparre-Ulrich *et al*., 2015; Sparre-Ulrich *et al*., 2017).

Thus, the remainder of this study focused on the further assessment of human GIP(3-30), GIP(5-30), and Pro^3GIP(3-30) *in vivo*. Indeed, in the current study it was human Pro^3GIP(3-30) that yielded superior antagonistic abilities over human GIP(3-30) and GIP(5-30), in terms of annulling the glucose-lowering ability of human GIP(1-42). The data shows that although the margin of superiority is slight, the modification of human Pro^3GIP(3-30) augments the effects of the N- an C- terminal truncations further. Additionally, to further assess the receptor blockading capacity of these analogues they were administered 30 min prior to a glucose plus GIP challenge. Once again it was human Pro^3GIP(3-30) that had superior GIPR antagonistic activity over both human GIP(3-30) and GIP(5-30) confirming superior biological effects. Thus, human Pro^3GIP(3-30) may have a greater affinity to the GIPR and/or a prolonged circulating half-life, perhaps due to the amino acid substitution resulting in increased efficacy as a GIPR antagonist and potential as a novel functional GIP antagonist. However, further studies would be required to confirm this. In support of these findings a subsequent study by Sparre-Ulrich and colleagues (2017), determined that even though rat GIP(3-30) had superior affinity as a competitive antagonist on the rat GIPR *in vitro* and in perfused rat pancreas, human GIP(3-30) still displayed antagonistic qualities (Sparre-Ulrich *et al.,* 2017). There are some limitations within the current study, particularly related to the glucose homeostatic mechanism(s) of

action in the *in vivo* studies. Thus, GIP is known to potently augment insulin secretion (Campbell and Drucker, 2013), and this was not measured in the current study. In addition to this, GIP also has notable extrapancreatic glucose-lowering actions (Al-Sabah, 2015; Baggio and Drucker, 2007), that would also need to be considered. However, it is clear that these peptides, and especially human Pro^3GIP(3-30) had GIP blocking actions.

Overall, these studies have called in to question some of the recent previous work on GIPR antagonists, and in particular, the impact of species variation in the amino acid sequences of both the GIP ligand and receptor (Hansen *et al.,* 2016; Sparre-Ulrich *et al*., 2015; Sparre-Ulrich *et al.,* 2017). In agreement with previous work on Pro^3GIP(1-42) (Gault *et al*., 2007ab; McClean *et al.,* 2007; McClean *et al*., 2008), the current data confirms GIPR blocking ability of human Pro^3GIP(3-30). Given that GIPR blockade has been suggested as a useful treatment option for obesity and obesity-driven forms of T2DM (Irwin *et al*., 2006; Irwin *et al*., 2009; Kerr *et al*., 2011; Naitoh *et al*., 2008; Nakamura *et al*., 2012; Pathak *et al.,* 2015a; Ravn *et al*., 2013; Zhou *et al.,* 2008) further detailed analysis is warranted to explore human Pro^3GIP(3-30) as a potential obesity-T2DM therapeutic.

Table 6.1 Summary of purified native human GIP(1-42) and N- and C-terminally truncated GIP peptides; RP-HPLC retention times and MALDI-TOF MS of peptides

Peptides	Name	Sequence	Theoretical Mass (Da)	Experimental Mass (Da)	Retention Time (min)
1	Human GIP(1-42)	YAEGTFISDYSIAMDKIHQQDFVNWLLAQKGKKNDWKHNITQ	4983.6	4982.8	19.8
2	Human GIP(1-30)	YAEGTFISDYSIAMDKIHQQDFVNWLLA QK-NH_2	3531.9	3530.6	21.0
3	Mouse GIP(1-30)	YAEGTFISDYSIAMDKIRQQDFVNWLLA QR-NH_2	3579.0	3578.4	21.3
4	Human GIP(3-30)	EGTFISDYSIAMDKIHQQDFVNWLLAQ K-NH_2	3297.7	3296.3	20.7
5	Mouse GIP(3-30)	EGTFISDYSIAMDKIRQQDFVNWLLAQR-NH_2	3344.7	3342.5	21.0
6	Human Pro^3GIP(3-30)	PGTFISDYSIAMDKIHQQDFVNWLLAQK-NH_2	3265.7	3263.4	20.9
7	Human GIP(3-42)	EGTFISDYSIAMDKIHQQDFVNWLLAQKGKKNDWKHNITQ	4749.3	4749.2	19.3
8	Human GIP(5-30)	TFISDYSIAMDKIHQQDFVNWLLAQK-NH_2	3111.5	3110.2	20.6
9	Human GIP(5-42)	TFISDYSIAMDKIHQQDFVNWLLAQKGKKNDWKHNITQ	4563.1	4562.3	19.4

Peptide was purified by injecting (1ml) into a Phenomenex Aeris peptide 3.6µ XB-C18 250*15mm HPLC column equilibrated with 0.12% (TFA)/H_20 at a rate of 6 ml/min using 0.1% TFA in 70% acetonitrile/H_20. Surveyor Plus Liquid Chromatograph/HPLC (Thermo Finnigan ,San Jose, California, USA). Absorbance was measured at 214 nm, retention times recorded using ChromQuest software. Molecular mass confirmed using MALDI-ToF, Voyager-DE BioSpectrometry Workstation and m/z ratio *vs* peak intensity.

Figure 6.1 Acute effects of human GIP(1-42), human GIP(1-30) and mouse GIP(1-30) on insulin release from BRIN-BD11 cells

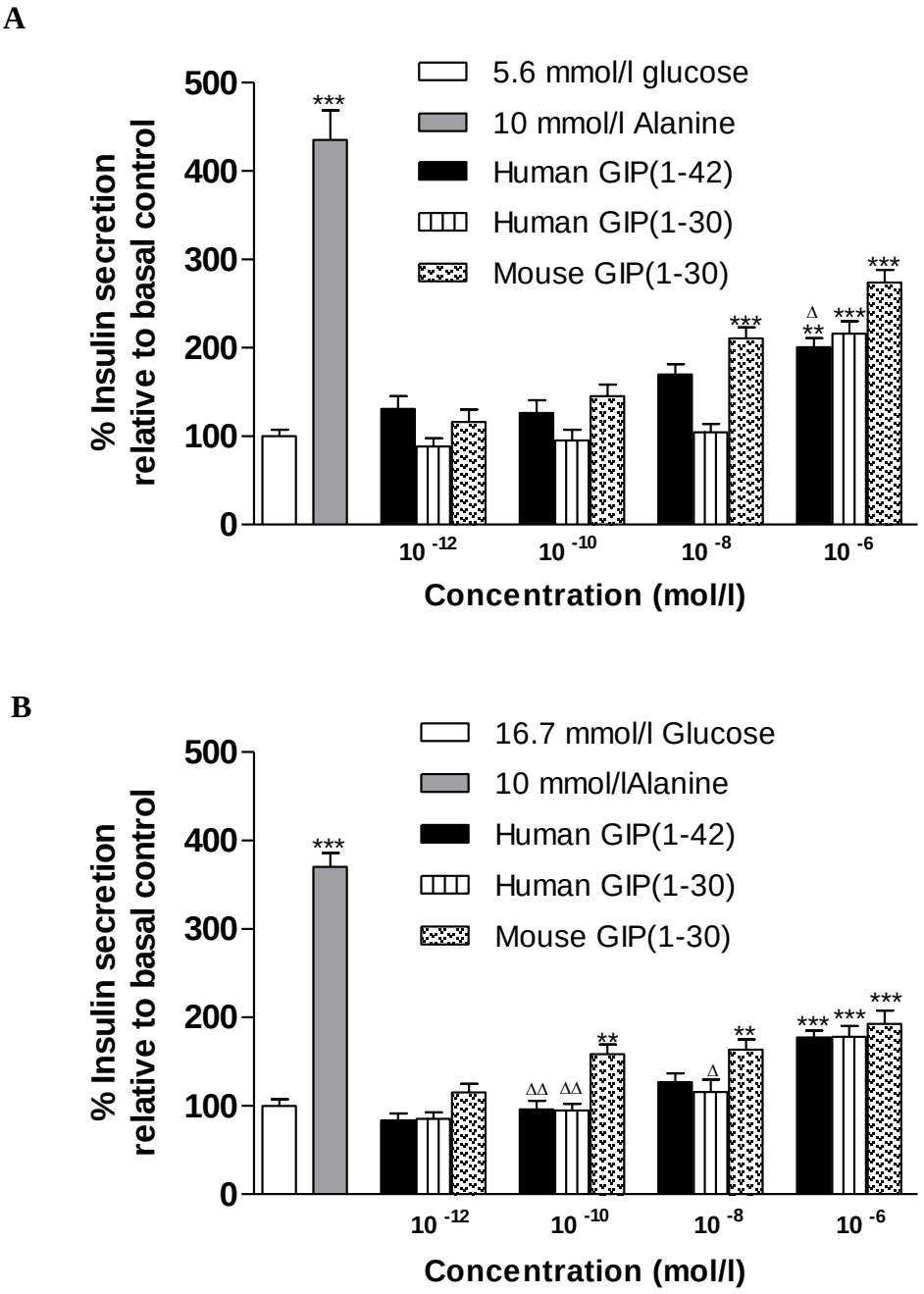

BRIN-BD11 cells were incubated (20 min) with test peptides (10^{-12} to 10^{-6} mol/l) in the presence of (A) 5.6, or (B) 16.7 mmol/l glucose. Insulin was measured by RIA. Values are mean ± SEM (n=8) for insulin release. *P<0.05, **P<0.01 and ***P<0.001 compared to 5.6 mmol/l glucose alone. $^{\Delta}$P<0.05 and $^{\Delta\Delta}$P<0.01 compared to mouse GIP(1-30).

Figure 6.2 Acute effects of human GIP(3-30) and mouse GIP(3-30) alone or in combination with native human GIP(1-42) on insulin release from BRIN-BD11 cells

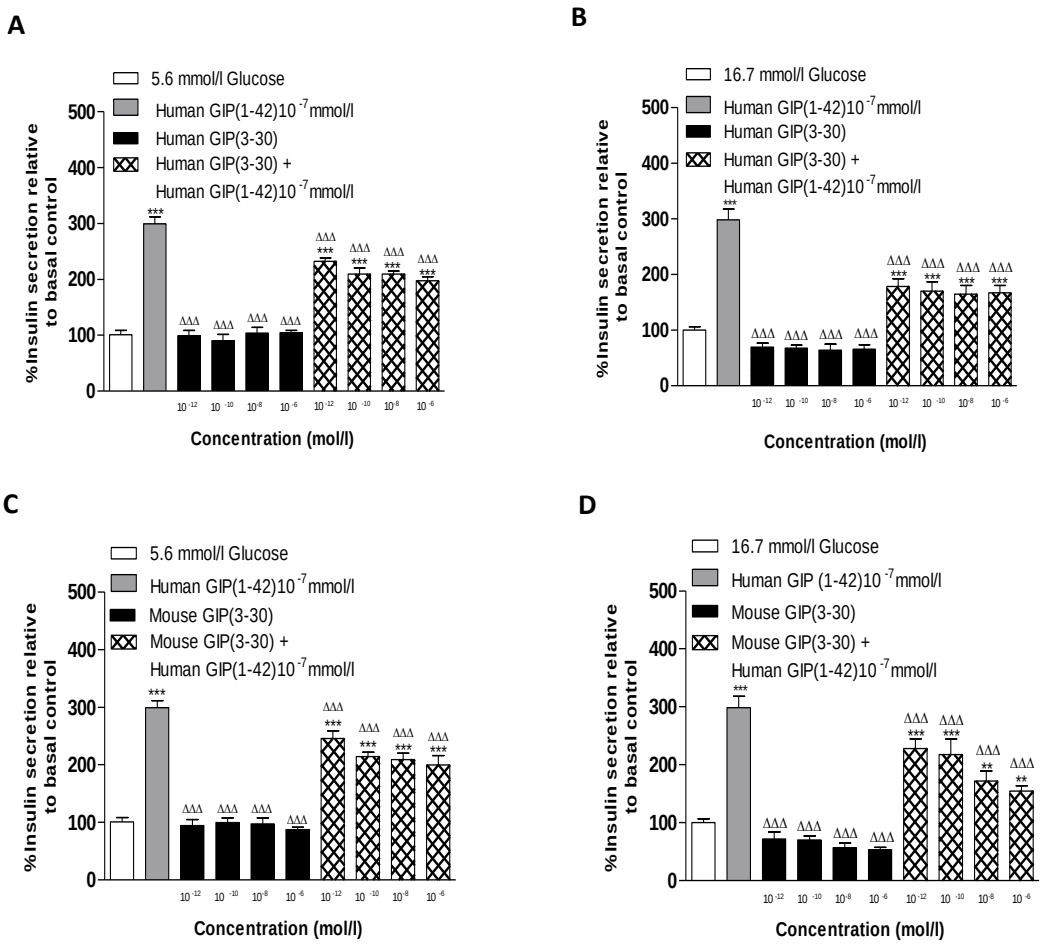

BRIN-BD11 cells were incubated (20 min) with test peptides (10^{-12} to 10^{-6} mol/l) alone or in combination with native human GIP(1-42) (10^{-7} mol/l) in the presence of (A & C) 5.6 or (B & D) 16.7 mmol/l glucose. Insulin was measured by RIA. Values are mean ± SEM (n=8) for insulin release. *P<0.05, **P<0.01 and ***P<0.001 compared to relevant glucose alone. $^{\Delta}$P<0.05 and $^{\Delta\Delta}$P<0.01 $^{\Delta\Delta\Delta}$P<0.001 compared to human GIP(1-42).

Figure 6.3 Acute effects of human Pro^{3}GIP(3-30) and human GIP(5-30) alone or in combination with native human GIP(1-42) on insulin release from BRIN-BD11 cells

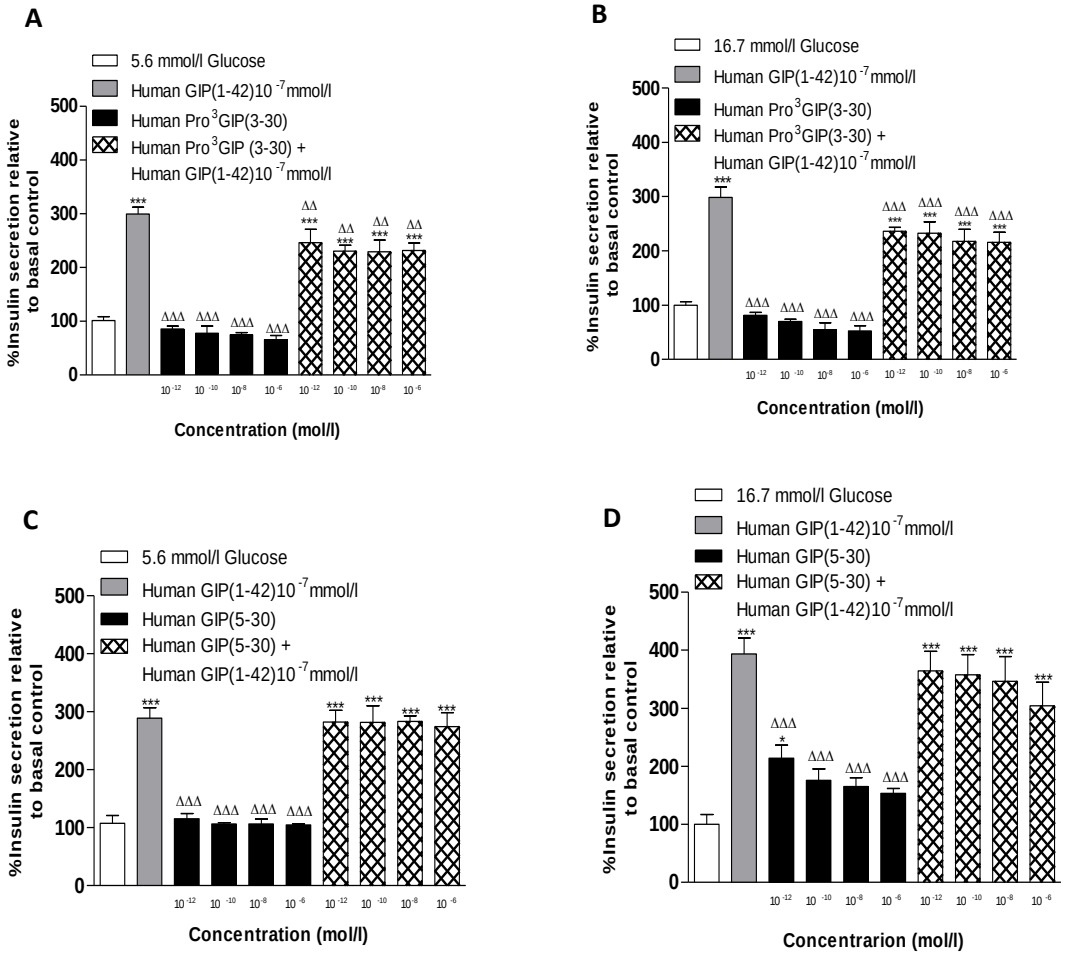

BRIN-BD11 cells were incubated (20 min) with test peptides (10^{-12} to 10^{-6} mol/l) alone or in combination with native human GIP(1-42) (10^{-7} mol/l) in the presence of (A & C) 5.6 or (B & D) 16.7 mmol/l glucose. Insulin was measured by RIA. Values are mean ± SEM (n=8) for insulin release. *P<0.05, **P<0.01 and ***P<0.001 compared to relevant glucose alone. $^{\Delta}$P<0.05 and $^{\Delta\Delta}$P<0.01 $^{\Delta\Delta\Delta}$P<0.001 compared to human GIP(1-42).

Figure 6.4 Acute effects of human GIP(3-42) and human GIP(5-42) alone or in combination with native human GIP(1-42) on insulin release from BRIN-BD11 cells

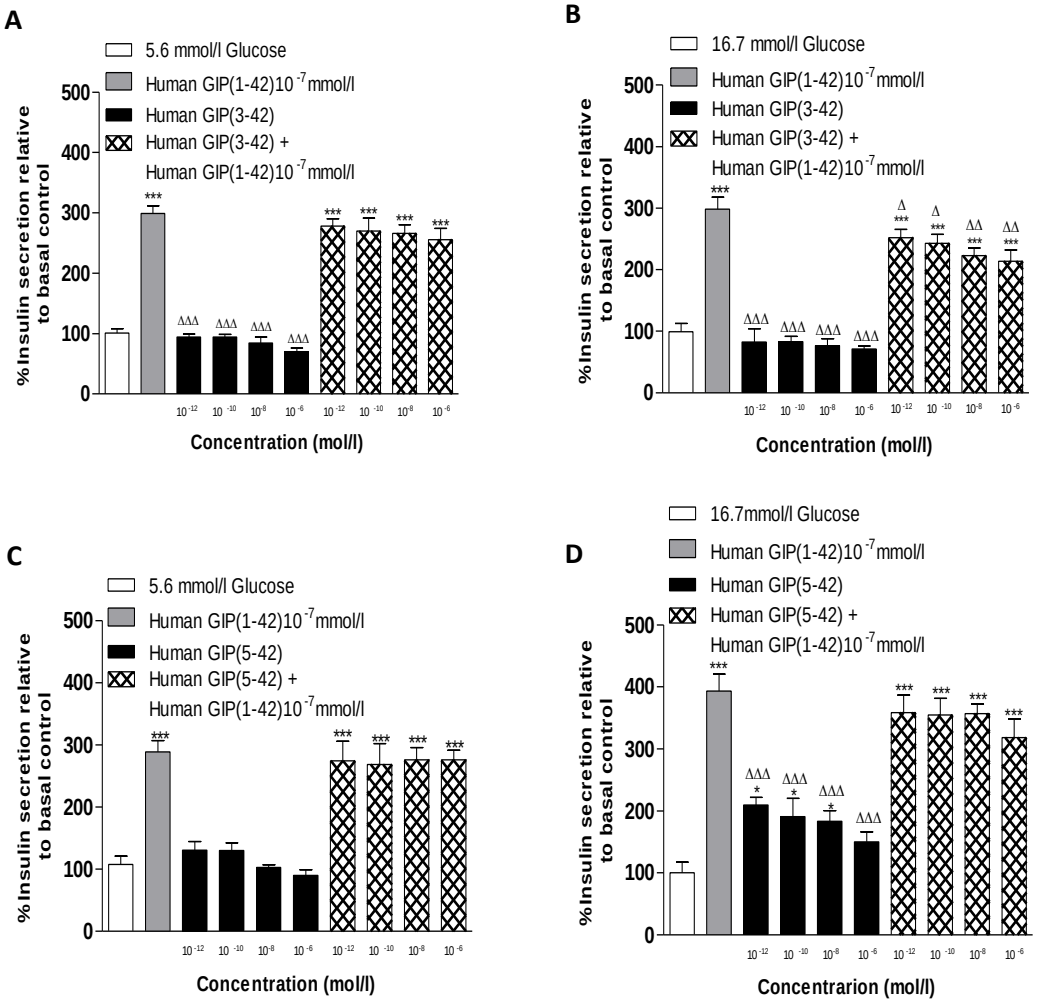

BRIN-BD11 cells were incubated (20 min) with test peptides (10^{-12} to 10^{-6} mol/l) alone or in combination with native human GIP(1-42) (10^{-7} mol/l) in the presence of (A & C) 5.6 or (B & D) 16.7 mmol/l glucose. Insulin was measured by RIA. Values are mean ± SEM (n=8) for insulin release. *P<0.05, **P<0.01 and ***P<0.001 compared to relevant glucose alone. $^{\Delta}$P<0.05 and $^{\Delta\Delta}$P<0.01 $^{\Delta\Delta\Delta}$P<0.001 compared to human GIP(1-42).

Figure 6.5 Acute effects of native human GIP(1-42), human GIP(1-30) and mouse GIP(1-30) on glucose tolerance in lean mice

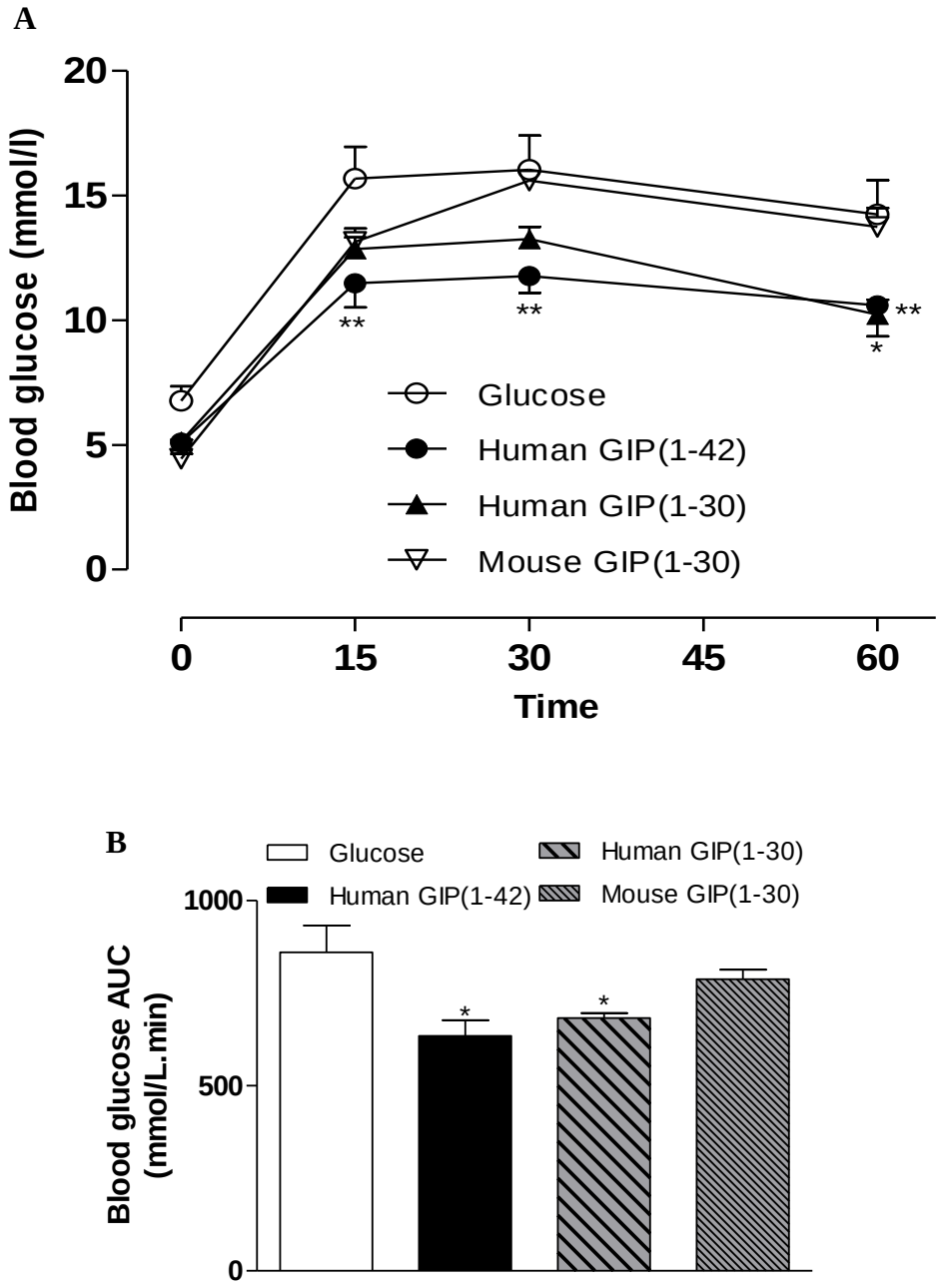

Blood glucose (A) concentrations were measured before and after intraperitoneal injection of glucose alone (18 mmol/kg bw), or in combination with native human GIP(1-42), human GIP(1-30) or mouse GIP(1-30) (each at 50 nmol/kg bw) in fasted mice. Glucose area under the curve (AUC) (B). Values for 0-60 min post injection are also shown. Values represent mean ± SEM (n=5-6). *P<0.05 and **P<0.01 compared with glucose alone.

Figure 6.6 Acute effects of human GIP(3-30) alone or in combination with native human GIP(1-42) on glucose tolerance in lean mice

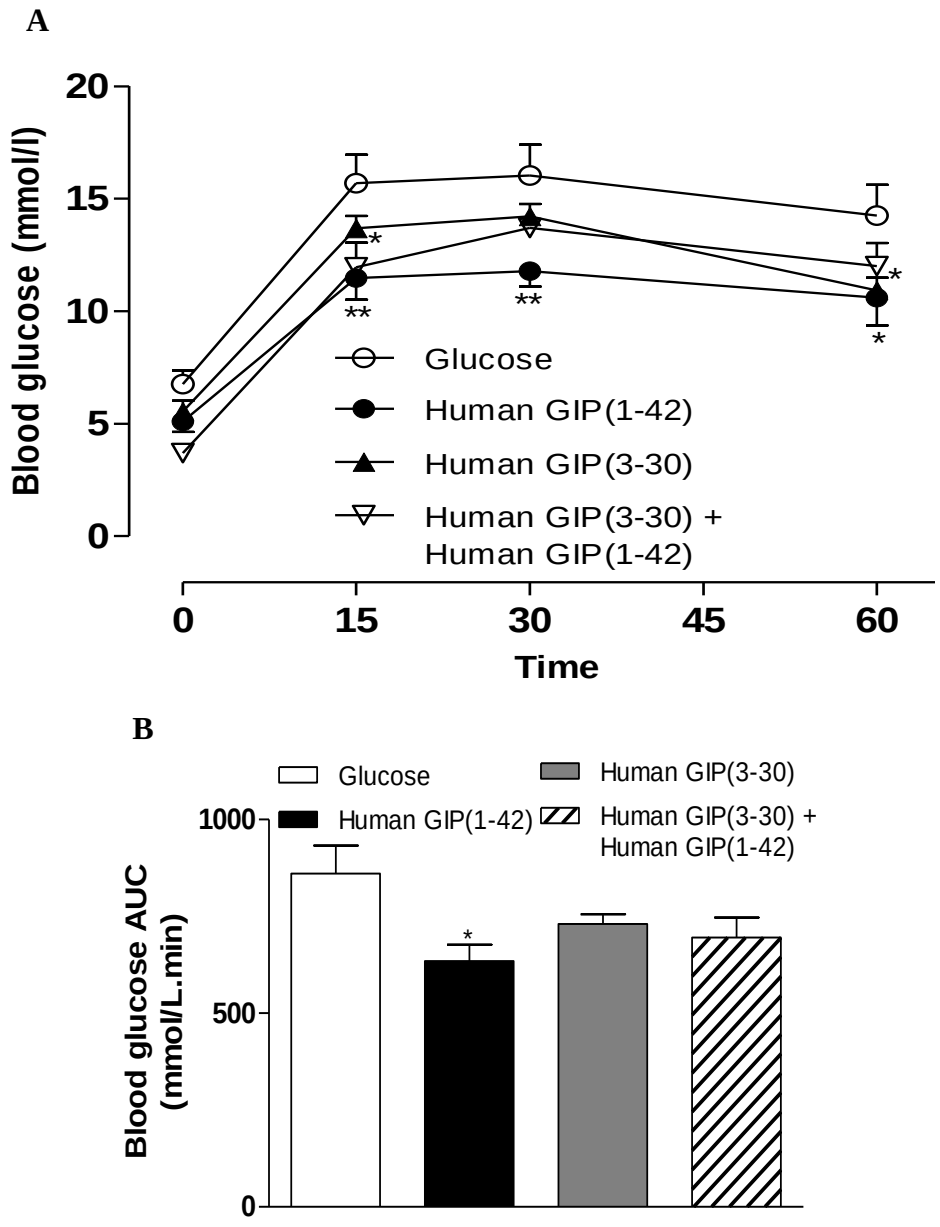

Blood glucose (A) concentrations were measured before and after intraperitoneal injection of glucose alone (18 mmol/kg bw), or in combination with native human GIP(1-42), human GIP(3-30), or human GIP(3-30) and native human GIP(1-42) combined (each at 50 nmol/kg bw) in fasted mice. Glucose area under the curve (AUC) (B) values for 0-60 min post injection are also shown. Values represent mean ± SEM (n=5-6). *P<0.05 and **P<0.01 compared with glucose alone.

Figure 6.7 Acute effects of mouse GIP(3-30) alone or in combination with native human GIP(1-42) on glucose tolerance in lean mice

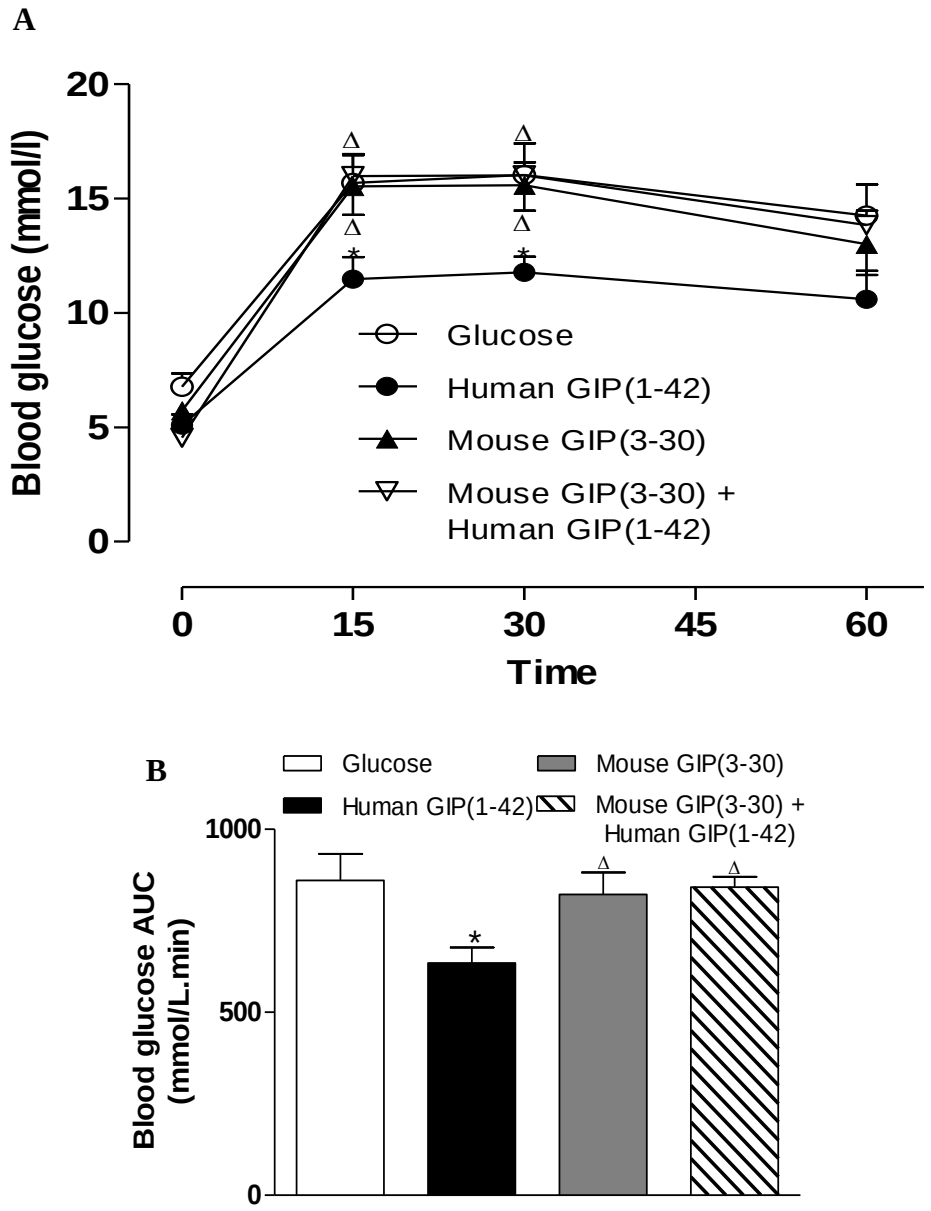

Blood glucose (A) concentrations were measured before and after intraperitoneal injection of glucose alone (18 mmol/kg bw), or in combination with native human GIP(1-42), mouse GIP(3-30), or mouse GIP(3-30) and native human GIP(1-42) combined (each at 50 nmol/kg bw) in fasted mice. Glucose area under the curve (AUC) (B) values for 0-60 min post injection are also shown. Values represent mean ± SEM (n=5-6). *P<0.05 compared with glucose alone or $^{\Delta}$P<0.05 compared to human GIP(1-42).

Figure 6.8 Acute effects of human Pro^{3}GIP(3-30) alone or in combination with native human GIP(1-42) on glucose tolerance in lean mice

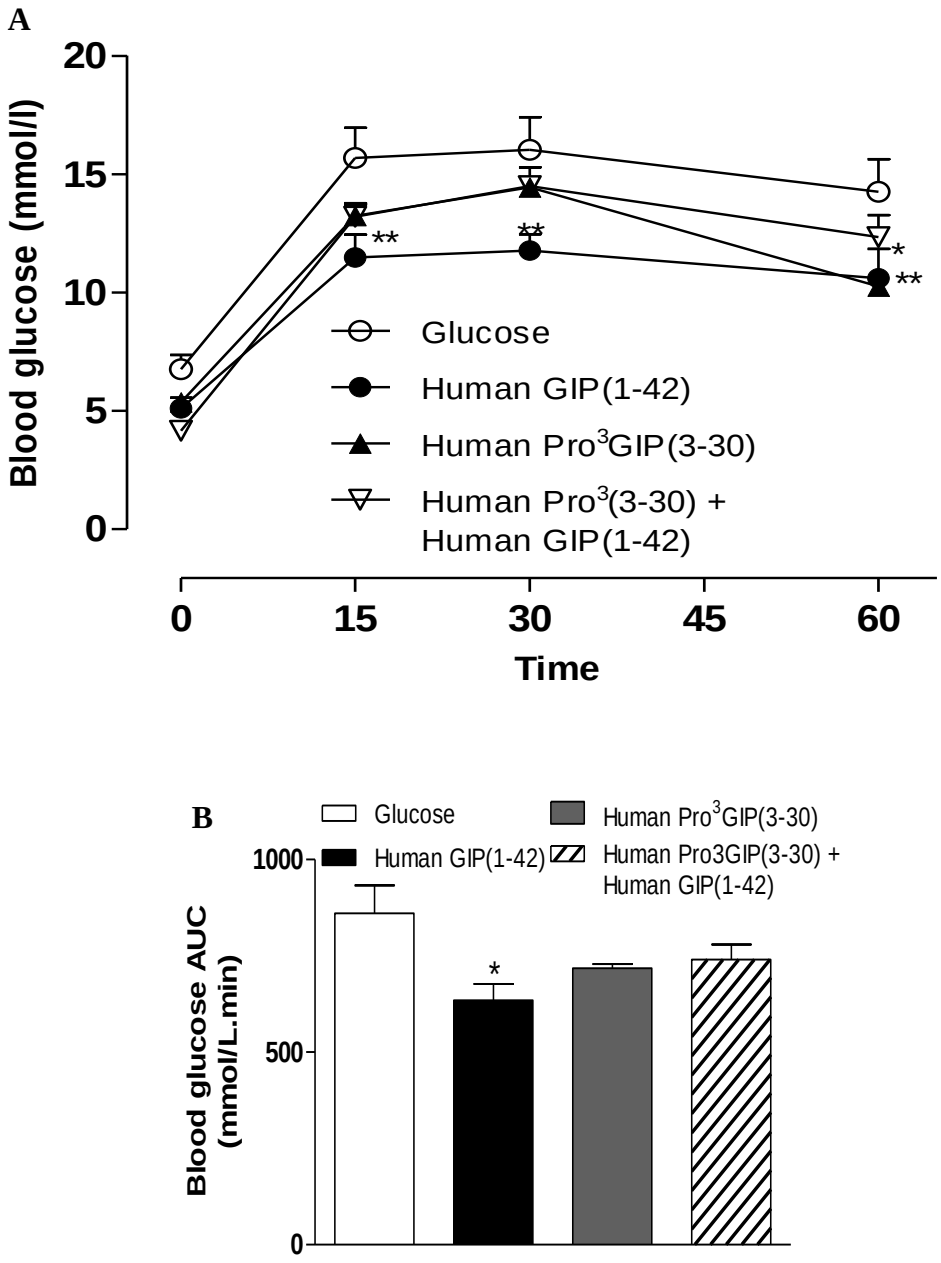

Blood glucose (A) concentrations were measured before and after intraperitoneal injection of glucose alone (18 mmol/kg bw), or in combination with native human GIP(1-42), human Pro^{3}GIP(3-30), or human Pro^{3}GIP(3-30) and native human GIP(1-42) combined (each at 50 nmol/kg bw) in fasted mice. Glucose area under the curve (AUC) (B) values for 0-60 min post injection are also shown. Values represent mean ± SEM (n=5-6). *P<0.05 and **P<0.01 compared with glucose alone.

Figure 6.9 Acute effects of human GIP(5-30) alone or in combination with native human GIP(1-42) on glucose tolerance in lean mice

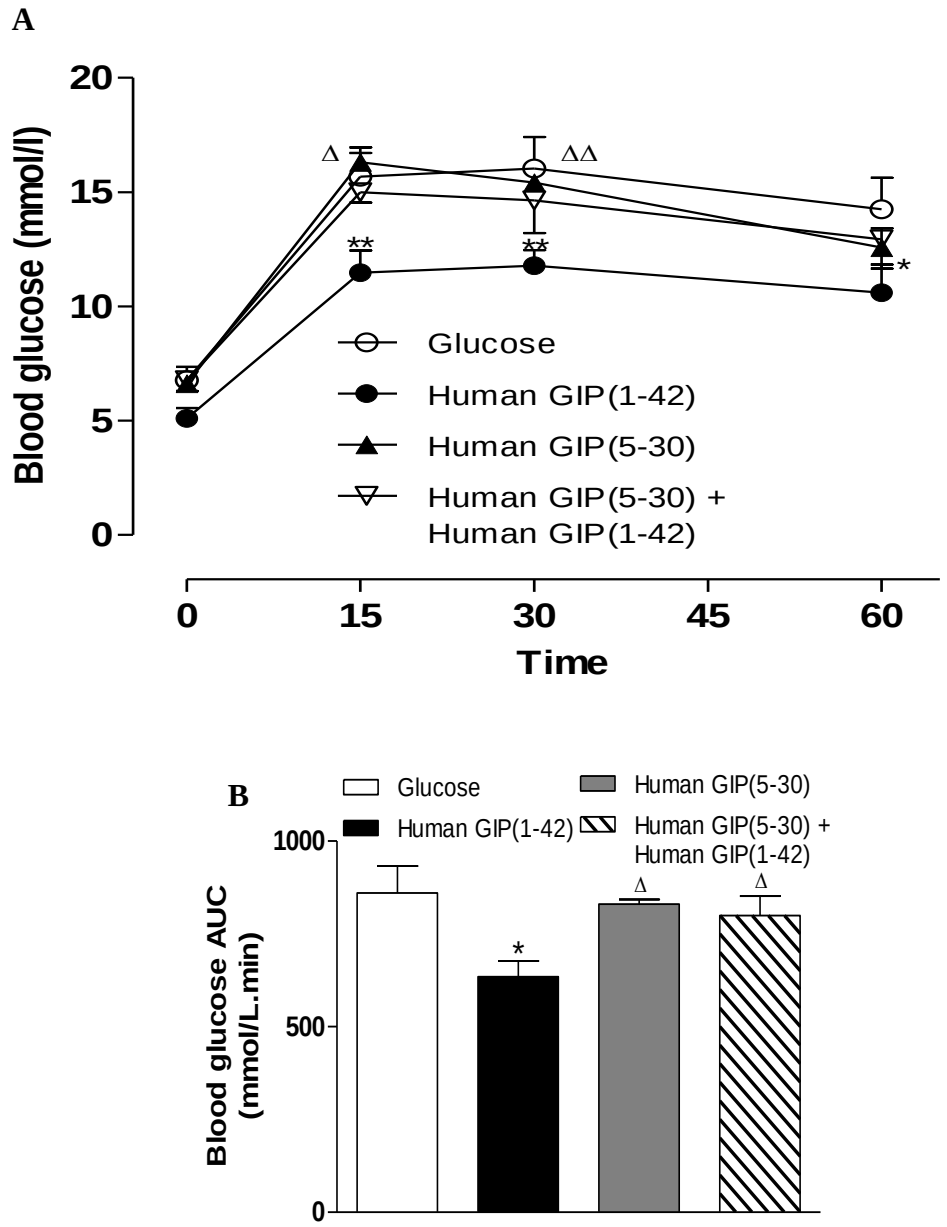

Blood glucose (A) concentrations were measured before and after intraperitoneal injection of glucose alone (18 mmol/kg bw), or in combination with native human GIP(1-42), human GIP(5-30), or human GIP(5-30) and native human GIP(1-42) combined (each at 50 nmol/kg bw) in fasted mice. Glucose area under the curve (AUC) (B) values for 0-60 min post injection are also shown. Values represent mean ± SEM (n=5-6). *P<0.05 and **P<0.01 compared with glucose alone or $^{\Delta}$P<0.05 and $^{\Delta\Delta}$P<0.01 compared to human GIP(1-42).

Figure 6.10 Acute effects of human GIP(3-42) alone or in combination with native human GIP(1-42) on glucose tolerance in lean mice

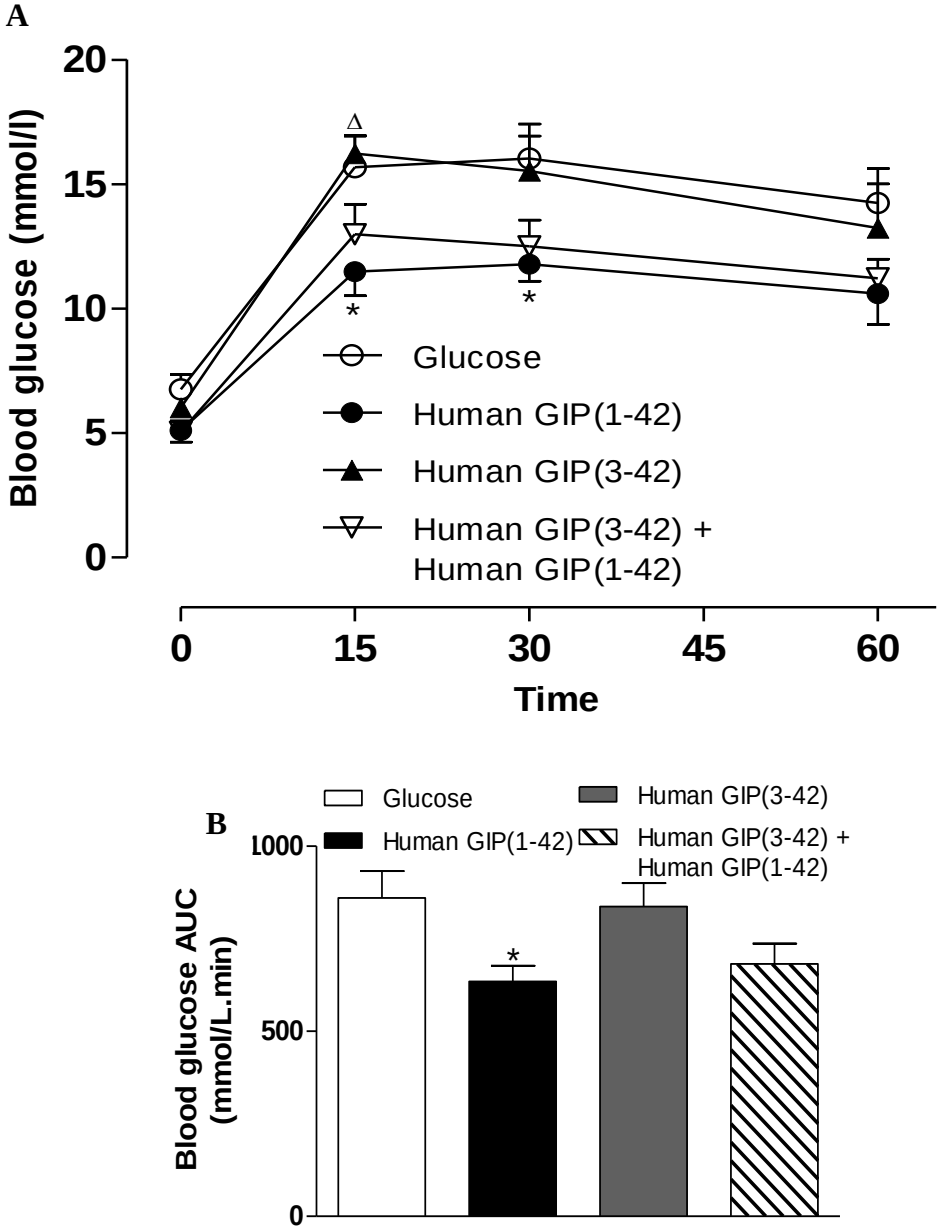

Blood glucose (A) concentrations were measured before and after intraperitoneal injection of glucose alone (18 mmol/kg bw), or in combination with native human GIP(1-42), human GIP(3-42), or human GIP(3-42) and native human GIP(1-42) combined (each at 50 nmol/kg bw) in fasted mice. Glucose area under the curve (AUC) (B) values for 0-60 min post injection are also shown. Values represent mean ± SEM (n=5-6). *P<0.05 and **P<0.01 compared with glucose alone.

Figure 6.11 Acute effects of human GIP(5-42) alone or in combination with native human GIP(1-42) on glucose tolerance in lean mice

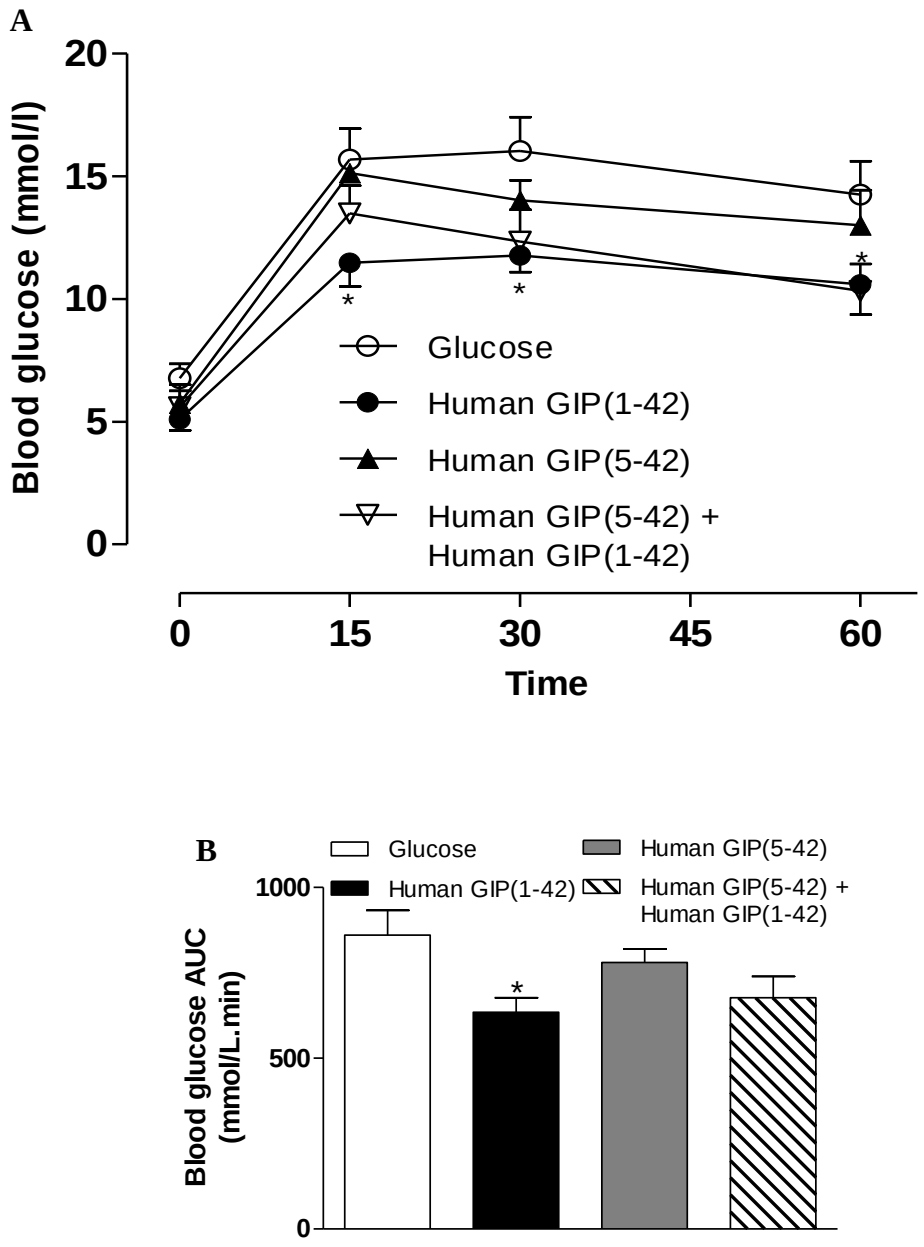

Blood glucose (A) concentrations were measured before and after intraperitoneal injection of glucose alone (18 mmol/kg bw), or in combination with native human GIP (1-42), human GIP (3-42), or human GIP (3-42) and native human GIP (1-42) combined (each at 50 nmol/kg bw) in fasted mice. Glucose area under the curve (AUC) (B) values for 0-60 min post injection are also shown. Values represent mean ± SEM (n=5-6). *P<0.05 compared with glucose alone.

Figure 6.12 Acute effects of high dose human GIP(3-30), human Pro^{3}GIP(3-30) or human GIP(5-30) on glucose tolerance in lean mice

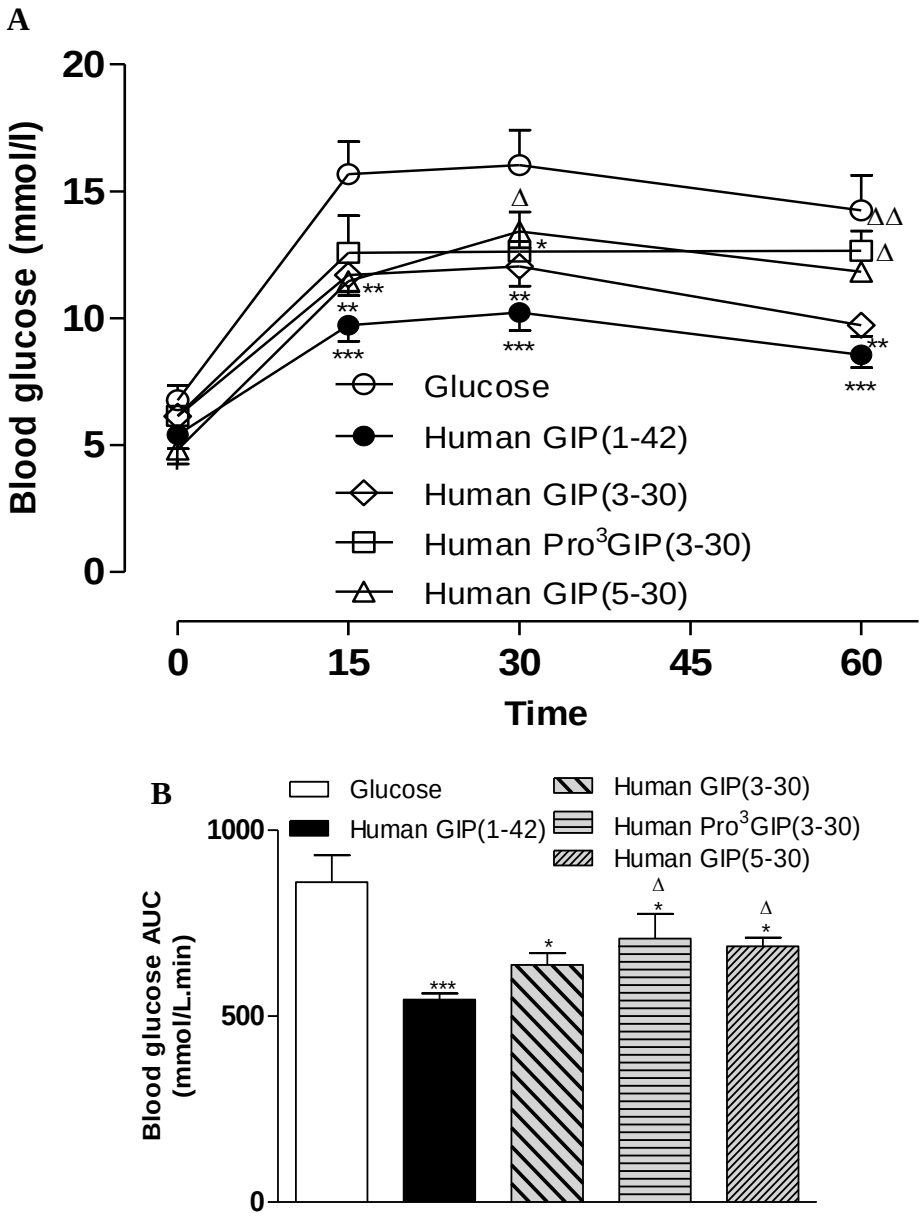

Blood glucose (A) concentrations were measured before and after intraperitoneal injection of glucose alone (18 mmol/kg bw), or in combination with native human GIP(1-42), human GIP(3-30), or human Pro^{3}GIP (3-30) and native human GIP(1-42) combined (each at 100 nmol/kg bw) in fasted mice. Glucose area under the curve (AUC) (B) values for 0-60 min post injection are also shown. Values represent mean ± SEM (n=5-6). *P<0.05, **P<0.01, ***P<0.001 compared with glucose alone or $^{\Delta}$P<0.05 and $^{\Delta\Delta}$P<0.01 compared to human GIP(1-42).

Figure 6.13 Acute effects of early administration of high dose human GIP (3-30), human Pro^{3}GIP (3-30) and human GIP(5-30) on glucose tolerance in lean mice

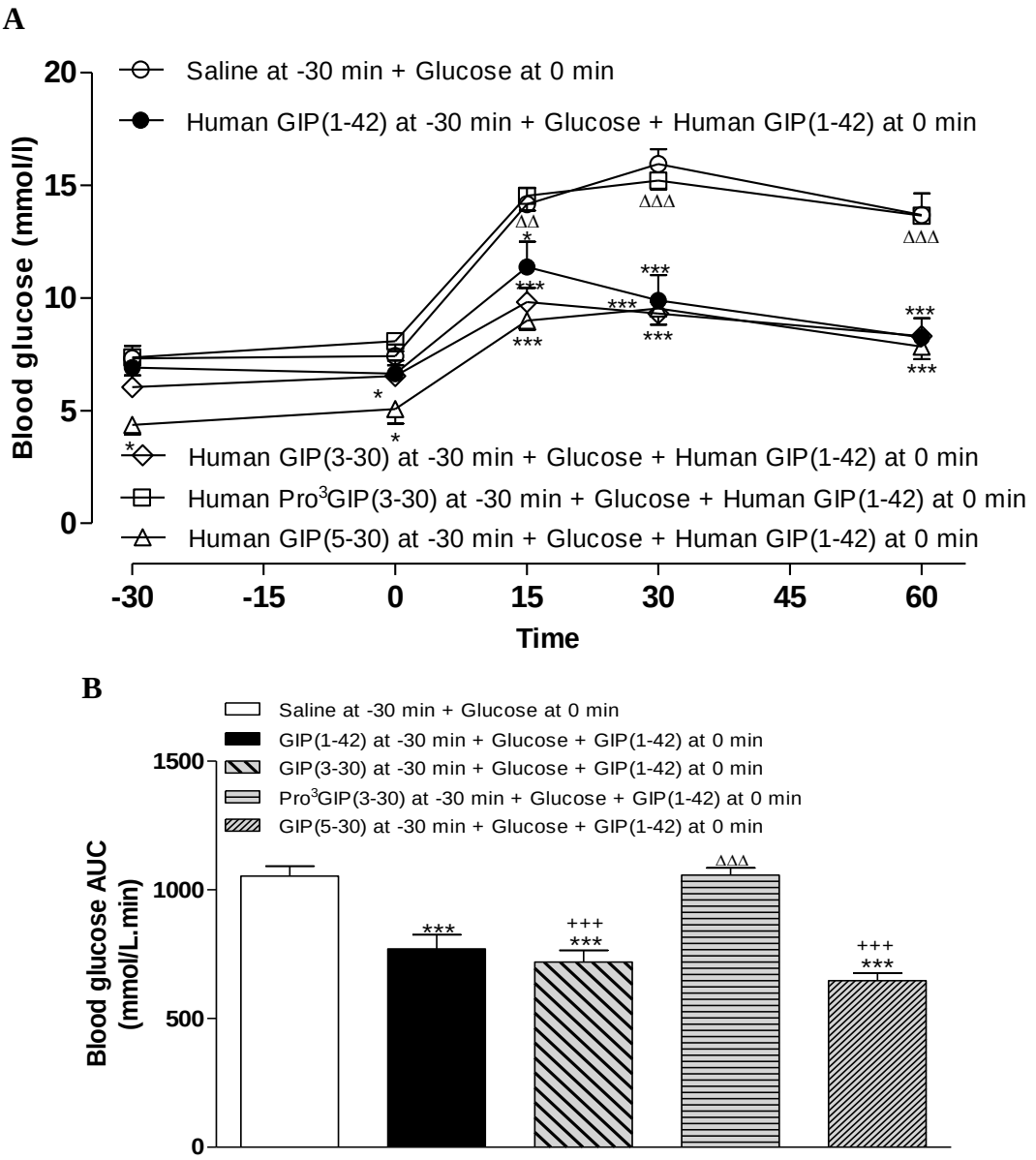

Blood glucose (A) concentrations after early intraperitoneal injection of saline vehicle (0.9% (w/v), NaCl) or saline in combination with native human GIP(1-42), human GIP(3-30), human Pro^{3}GIP(3-30) or human GIP(5-30), 30 min prior to administration of a glucose load (18 mmol/kg bw), alone or in combination with human GIP(1-42) (100 nmol/kg bw) in fasted mice. Glucose area under the curve (AUC) (B) values for -30-60 min post injection are also shown. Values represent mean ± SEM (n=5-6). *P<0.05, **P<0.01, ***P<0.001 compared with glucose alone or $^{\Delta}$P<0.05, $^{\Delta\Delta}$P<0.01 and $^{\Delta\Delta\Delta}$P<0.001 compared to human GIP(1-42) or $^{+++}$P<0.001 compared to human Pro^{3}GIP(3-30).

Table 6.2 Summary of acute effects of high dose and early administration of human GIP (3-30), human Pro^{3}GIP (3-30) and human GIP(5-30) on glucose tolerance in lean mice

Glucose tolerance test	
Treatment group	**Blood glucose AUC (mmol/l.min)**
Glucose	860.5 ± 72.29
High dose human GIP(1-42)	544.9 ± 16.62***
High dose human GIP(3-30)	638.3 ± 31.22*
High dose human Pro3GIP(3-30)	708.8 ± 66.84*$^{\Delta}$
High dose human GIP(5-30)	687.7 ± 23.75*$^{\Delta}$
Early administration glucose	1053 ± 39.25
Early administration human GIP(1-42)	770.3 ± 55.18***
Early administration human GIP(3-30)	719.2 ± 45.42*** $^{+++}$
Early administration human Pro3GIP(3-30)	1058 ± 28.10$^{\Delta\Delta\Delta}$
Early administration human GIP(5-30)	646.8 ± 29.73*** $^{+++}$

Summary of blood glucose concentrations measured before and after high dose intraperitoneal injection of glucose alone (18 mmol/kg bw), or in combination with native human GIP(1-42), human GIP(3-30), or human Pro^{3}GIP (3-30) and native human GIP(1-42) combined (each at 100 nmol/kg bw) AUC values 0-60 min post injection (Figure 6.12) and early intraperitoneal injection of saline vehicle (0.9% (w/v), NaCl) or saline in combination with native human GIP(1-42), human GIP(3-30), human Pro^{3}GIP(3-30) or human GIP(5-30), 30 min prior to administration of a glucose load (18 mmol/kg bw), alone or in combination with human GIP(1-42) (100 nmol/kg bw) in fasted mice AUC values -30-60 min post injection (Figure 6.13). Values represent mean ± SEM (n=5-6). *P<0.05, **P<0.01, ***P<0.001 compared with glucose alone or $^{\Delta}$P<0.05, $^{\Delta\Delta}$P<0.01 and $^{\Delta\Delta\Delta}$P<0.001 compared to human GIP(1-42) or $^{+++}$P<0.001 compared to human Pro^{3}GIP(3-30).

Chapter 7

General Discussion

7.1 Treating Type 2 diabetes

T2DM is the major non-communicable disease pandemic that accounts for 90% of all diabetes cases (Public Health England, 2018). Presently, the risk prevalence of T2DM is exacerbated and driven forward by high calorific diets and obesity that today is considered a societal 'norm' (Public Health England, 2018). T2DM was ranked as the 6th leading cause of death in 2015 and is a priority non-communicable disease targeted by world leaders across the globe (Public Health England, 2018; WHO, 2016). In the UK alone, 3.8 million people live with T2DM and 200,000 people are newly diagnosed every year (Public Health England, 2018). T2DM is not only a major public health problem but also a financial burden, both directly and indirectly (Diabetes UK, 2014; NHS, 2018). Therefore, development of novel T2DM therapeutics is not only relevant, but essential in the management of T2DM. With all cases of T2DM and obesity, those who are detected and appropriately managed can generally prevent and/or delay the onset of associated complications and go on to live longer, better quality, healthier lives (Davies *et al.*, 2018; WHO, 2016).

The primary aim when treating T2DM is to develop safe and efficacious pharmaceuticals that are effective in terms of glycaemic control and maintaining HbA1c at or below target levels. Thus, reducing long-term microvascular and macrovascular risks associated with the disease (Davies *et al.*, 2018; Marchetti *et al.*, 2009). Additionally, associated risk of atherosclerotic cardiovascular disease (ASCVD) and chronic kidney disease are now recommended to be considered for all T2DM therapeutic regimens (Davies *et al.*, 2018). Currently, pharmaceutical agents such as biguanides, sulfonylureas, thiazolidinediones, SGLT2, DPP IV inhibitors and incretin mimetics aim to not only reduce glucose levels but assist in protecting and/or preventing pancreatic beta cell dysregulation and reduced sensitivity to insulin (Brandt *et al.*, 2018; Marchetti *et al.*, 2009). However, available agents for T2DM all have varying efficacy and adverse effects including increased risk of hypoglycaemia and weight gain, thus limiting their merit in being safe and effective.

Additionally, in comparison to notable benefits of certain types of bariatric surgery that can restore metabolic control and sustain long-term weight loss (Irwin and Flatt, 2015; Meek *et al.*, 2016; Singh *et al.*, 2015), none of the currently approved pharmaceutical agents are able to fully replicate this scenario (Capozzi *et al.*, 2018). It

is postulated the metabolic changes in bariatric surgeries, such as Roux-en-Y Gastric Bypass (RYGB), are due to complex, multifaceted mechanisms and that pharmacological manipulation of a single metabolic pathway is unable to replicate this fully Currently, lifestyle changes and weight loss induced by very low calorie diets (624–700 kcal/day) is the only regimen that even come close to the success of bariatric surgery (Capozzi *et al.,* 2018; Mehta, Marso and Neeland, 2017; Steven *et al.,* 2016). However, compliance to these extreme lifestyle changes remains a key challenge to long-term sustainability and the regimes may not be applicable to all cases (Mehta, Marso and Neeland, 2017; Steven *et al.,* 2016). The idea of targeting multiple receptors, rather than lone metabolic pathways, could represent one way to better replicate the benefits of bariatric surgeries for patients with T2DM (Brandt *et al.,* 2018).

7.2 Single hybrid peptide multiple receptor agonists

In recent times the beneficial antidiabetic actions of novel incretin-based therapies have been demonstrated, and these therapies have been suggested to protect beta cells against apoptosis and promote differentiation and proliferation (Brandt *et al.,* 2018; Marchetti *et al.,* 2009). As the variety of available incretin-based agents continues to grow, including pronounced longer-lasting action (for example formulations allowing for once weekly injection), the benefit to people living with T2DM should also dramatically increase (Bhat *et al.,* 2013; Brandt *et al.,* 2018; Finan *et al.,* 2014; Rosenstock *et al.,* 2015). However, these GLP-1 based therapies are still limited to modulation of a single receptor mediated pathway.

As such, novel forms of incretin-based and incretin-like therapies are now being engineered as dual and triple monomeric/hybrid peptides (Bhat *et al.,* 2013; Brandt *et al.,* 2018; Finan *et al.,* 2014; Rosenstock *et al.,* 2015). Furthermore, utilising non-classic intestinal and neuronal hormones has become increasingly popular within this paradigm, as it is now understood that neural/hormonal signals between the gut and brain have a major role in development of T2DM and obesity (Capozzi *et al.,* 2018). Thus, novel hybrid peptide therapies aim to have an extended therapeutic scope in comparison to their single target counterparts as the receptors targets are extensively disseminated across tissues (Irwin and Flatt, 2015). Ultimately, this would lead to

improved therapeutic efficacy, with the potential for lower dosage, thereby reducing or eliminating adverse effects (Capozzi *et al.,* 2018; Irwin and Flatt, 2015). There have been several proof-of-concept studies with dual acting peptide hormone agonists, and these include but not limited to GLP-1-GIP, GLP-1-oxyntomodulin and GLP-1-gastrin agonists (Capozzi *et al.,* 2018; Fosgerau and Hoffmann, 2015). Interestingly, a very recent study has documented the remarkable benefits of a dual GIP and GLP-1 receptor agonist, LY3298176, in T2DM patients (Frias *et al.,* 2018), that further promotes the usefulness of this avenue of therapeutics.

This thesis has applied the principles of dual agonist technology to provide further proof of concept. In Chapters 3-5, the incretin hormone GIP was fused to the non-classical xenin peptide hormone, as well as creation and characterisation of xenin-neurotensin based hybrids. Initially, the studies built on work by Hasib *et al.,* (2017), to augment therapeutic ability of GIP-xenin by combined treatment with the established GLP-1 agonist, exendin-4, in different models of T2DM (Capozzi *et al.,* 2018; Hasib *et al.,* 2017). This work was progressed to establishing antidiabetic effects and anorectic benefits of xenin and neurotensin, as well as related hybrid peptides in a mouse model of T2DM-obesity. Finally, the focus in Chapter 6 was to further investigate an alternative approach to GIP therapeutics by development of a specific GIPR antagonist that has the potential to be utilised as a therapeutic in obesity-diabetes. These studies also build from previous positive work on GIPR antagonism at Ulster (Gault *et al.,* 2007a; Gault *et al.,* 2008; Irwin *et al.,* 2007; Kerr *et al.,* 2011; McClean *et al.,* 2007; McClean *et al.,* 2008; Pathak *et al.,* 2015a).

7.3 GIP-xenin hybrid

It is now well understood that under hyperglycaemic conditions of T2DM in humans, the insulin releasing action of GIP is reduced, even with exogenous administration of large doses (Capozzi *et al.,* 2018). It is only when the hyperglycaemia is alleviated that the insulinotropic action of GIP is restored (Capozzi *et al.,* 2018). Thus, a single targeting GIP therapy may not provide prominent therapeutic value in the treatment of T2DM (Capozzi *et al.,* 2018; Hasib *et al.,* 2017). Therefore, the rationale that augmenting GIP action, using the co-secreted hormone xenin known to potentiate GIP effects, was demonstrated by Hasib *et al.,* (2017) by the dual agonist hybrid,

(DAla^2)GIP/xenin-8-Gln. Chapters 3 and 4 have assessed (DAla^2)GIP/xenin-8-Gln alone, and in combination with exendin-4, in two separate mouse models of contrasting T2DM aetiology, namely diet-induced HFF and genetically induced *db/db* mice (Faitia *et al.,* 2018; Katsuda *et al.,* 2013; King, 2012; Winzell and Ahren, 2004). Thus, it has already been established that the loss of endogenous GLP-1 and its glucose-lowering effects can be overcome in T2DM by exogenous administration of stable GLP-1 analogues such as exendin-4 (Nauck, 2016). This combined treatment approach could potentially enhance the effects of the GIP-xenin hybrid by activation of an additional signalling pathway and by concomitantly reducing hyperglycaemia (Capozzi *et al.,* 2018; Hasib *et al.,* 2017). Comparatively, Chapters 3 and 4 had some similar outcomes, but there was also evidence of contrasting effects, likely related to the mouse model employed.

To summarise, over the treatment period used, circulating glucose and HbA1c levels were lowered in both mouse models by (DAla^2)GIP-xenin-8-Gln in combination with exendin-4. Notably, circulating insulin were much greater in response to treatments in HFF mice than *db/db* mice, and this likely reflects the beta cell dysfunction that is apparent in *db/db* mice (Faita *et al.,* 2018). Thus, it could suggest that the benefits of (DAla^2)GIP-xenin-8-Gln and exendin-4 are both somewhat dependent on intact beta cell function. Assessment of insulin secretion from islets isolated from HFF mice at the end of the study confirmed this view. However, glucose tolerance in the HFF model was not improved by either treatment group, yet benefits were apparent in the *db/db* model, especially in mice treated with (DAla^2)GIP-xenin-8-Gln in combination with exendin-4. This could imply that activation of multiple target pathways results in glucose-lowering actions independent of insulin. Indeed, it is well known that GIP and GLP-1 possess important extrapancreatic antihyperglycaemic actions (Al-Sabah, 2015; Campbell and Drucker, 2013; Capozzi *et al.,* 2018; Marín-Penalver *et al.,* 2016). In relation to this, insulin sensitivity was unaffected in the *db/db* model, whereas the HFF had improvement in the (DAla^2)GIP-xenin-8-Gln treatment group and more so in the combination group. In addition, lipid metabolism, as evidenced by total cholesterol and triglycerides levels, was improved by treatment regimens in HFF mice, possibly by augmentation of GIP action and/or sensitivity facilitated or enhanced by xenin, as it too plays a role in lipid metabolism (Capozzi *et al.,* 2018; Craig, Gault and Irwin, 2018; Hasib *et al.,* 2017). Finally, both the HFF single treatment groups had

improved sensitivity to GIP with the combination group most improved, contrary to the *db/db* model as this parameter was unaffected by either treatment. This may well be linked to differences in disease severity and ambient glucose levels between the two mouse models. Histological staining and assessment of pancreatic architecture would also conform to this viewpoint.

Comparatively, these two contrasting models of T2DM show the strengths and limitations of (DAla^2)GIP-xenin-8-Gln as a single dual agonist treatment option and as a combined therapeutic approach with exendin-4. In the less severe HFF model with intact beta cell function, (DAla^2)GIP-xenin-8-Gln alone, was as effective as (DAla^2)GIP-xenin-8-Gln in combination with exendin-4. However, the main benefits in *db/db* mice were largely observed only when (DAla^2)GIP-xenin-8-Gln was combined with exendin-4. This is suggestive that hyperglycaemia in this model is so severe, that GLP-1 is required to reduce hyperglycaemia to allow (DAla^2)GIP-xenin-8-Gln to exert positive effects. Indeed, a number of studies in animals and humans have shown that the antidiabetic effects of GIP can be restored by concomitant reductions of hyperglycaemic (Frias *et al.,* 2017; Gault, 2018; Skow, Bergmann, and Knop, 2016). It is presumed that the same scenario is important in *db/db* mice.

Overall Chapters 3 and 4 have demonstrated that (DAla^2)GIP-xenin-8-Gln alone or in combination with exendin-4 is primarily suited as a T2DM therapeutic in less severe presentations of the disease. Whereas the more severe manifestation of T2DM, the *db/db* model, it was clear that (DAla^2)GIP-xenin-8-Gln therapeutic action was only enhanced by the addition of exendin-4 and significantly inhibited alone even with its dual agonist attributes (Hasib *et al.,* 2017). Thus, possible pharmacological intervention with (DAla^2)GIP-xenin-8-Gln alone or in combination with exendin-4 may need to be further considered in relation to disease status of the patient.

7.4 Neurotensin-xenin hybrid

With the premise that novel xenin-containing hybrid peptides are effective antidiabetic agents, neurotensin was considered a good candidate for development into a hybrid peptide. Neurotensin (NT) has several antidiabetic actions and is known to facilitate absorption of fatty acids in the small intestine (Barchetta *et al.,* 2018; Mazella *et al.,*

2012). Additionally, xenin is structurally related to neurotensin (NT), with similar biological actions including appetite suppression, modulation of lipid metabolism and glucose homeostasis (Anlauf *et al.*, 2000; Craig, Gault and Irwin, 2018; Khan *et al.*, 2017; Mazella *et al.*, 2012). Thus, combining elements of these two peptides, forming acetyl-neurotensin(8-13)-xenin-8-Gln, had the potential to modulate several regulatory pathways including glucose and energy balance, and as with (DAla^2)GIP-xenin-8-Gln, this may also be augmented by addition of exendin-4 to the regimen.

Preliminary studies with acetyl-neurotensin(8-13)-xenin-8-Gln established that receptor binding and activation was intact, an important quality when developing and fusing novel hybrid peptides (Al-Sabah, 2015; Capozzi *et al.*, 2018; Fosgerau and Hoffmann, 2015). Acetyl-neurotensin(8-13)-xenin-8-Gln *in vitro*, and *ex vivo* in isolated islets, greatly increased insulin secretion at higher glucose levels compared to acetyl-neurotensin(8-13) and native NT, which only enhanced at lower concentrations. This is consistent with published literature (Khan *et al.*, 2017). Furthermore, acetyl-neurotensin(8-13)-xenin-8-Gln maintained the proliferative and anti-apoptotic qualities shown by both parent peptides (Khan *et al.*, 2017). Thus, these data confirm that the key antidiabetic actions for the NT/xenin hybrid remain, and further *in vivo* assessment was warranted.

The model of choice was HFF mice, based on previous observations in Chapters 3 and 4. Biological assessment revealed that acetyl-neurotensin(8-13)-xenin-8-Gln had reduced efficacy in terms of glucose-lowering and insulin secretion capabilities when compared to exendin-4 alone, or both drugs in combination, following sub-chronic injection regimens. However, more importantly, in some instances acetyl-neurotensin(8-13)-xenin-8-Gln in combination with exendin-4 outperformed exendin-4 alone in terms of antidiabetic benefits, particularly in relation to glucose tolerance and insulin sensitivity. Interestingly, it was exendin-4 alone that had superior effects on satiety and body weight, even though both NT and xenin are known to have roles in regulating energy balance pathways (Barchetta *et al.*, 2018; Craig, Gault and Irwin, 2018; Mazella *et al.*, 2012). However, acetyl-neurotensin(8-13)-xenin-8-Gln in combination with exendin-4 did positively modulate lipid metabolism as both triglycerides and fat mass were reduced in this group of mice. It is also postulated that NT modulates leptin concentrations and signalling in the periphery as well as in the

central nervous system (Barchetta *et al.,* 2018), and assessment of leptin action may have been a useful addition to these studies.

To summarise, initial *in vitro* actions of acetyl-neurotensin(8-13)-xenin-8-Gln suggested promise as an antidiabetic, but these were not fully translated to the *in vivo* setting in HFF mice. Although there does seem to be potential if acetyl-neurotensin(8-13)-xenin-8-Gln is utilised as a combined therapeutic, as shown in this study with exendin-4. When in combination with exendin-4, acetyl-neurotensin(8-13)-xenin-8-Gln proved to have equally desirable or superior therapeutic attributes than exendin-4 alone, and thus may still have potential as a T2DM therapeutic. More detailed studies using this molecule and in particular, effects on other physiological parameters are warranted.

7.5 GIP antagonism

As previously discussed, under T2DM conditions GIP action becomes dysregulated, with GIPR signalling linked to obesity development as elevated GIP levels increase fat deposition (Al-Sabah, 2015; Capozzi *et al.,* 2018; Gasbjerg *et al.,* 2018a). This is further evidenced by decreased GIP secretion and action being suggested as a primary metabolic benefit associated with bariatric surgery (Mingrone *et al.,* 2009; Xiong *et al.,* 2015). The focus of Chapter 7 was therefore to elucidate a GIPR antagonist as the validity of currently characterised GIPR antagonistic have been called into question (Gasbjerg *et al.,* 2018a; Gasbjerg *et al.,* 2018b; Hansen *et al.,* 2016; Sparre-Ulrich *et al.,* 2017).

The study utilised GIP-based peptides with various amino acid substitutions and N- and C-terminus variations from the native sequence. As with the previous studies, it was essential to uncover which peptides maintained receptor binding, but on this occasion have lost activation capabilities, ensuring receptor antagonistic qualities (Hansen *et al.,* 2016). Keeping in mind that to procure benefits from GIPR antagonism, it is not entirely necessary to fully eliminate GIPR signalling, as a partial reduction of GIP signalling can yield the beneficial in obesity (Nasteska *et al.,* 2014). Moreover, the GIPR antagonist, (Pro^3)GIP, that was shown to have various benefits in rodent models obesity and T2DM (Gault *et al*., 2007a; Gault *et al*., 2008; Irwin *et al*., 2007;

Kerr *et al.,* 2011; McClean *et al.,* 2007; McClean *et al.,* 2008; Pathak *et al.,* 2015a), has now been confirmed as a weak partial GIPR agonist rather than a full GIPR antagonist (Sparre-Ulrich *et al.,* 2017; Pathak *et al.,* 2015a).

Initial *in vitro* assessment identified human GIP(3-30), human Pro^3(3-30)GIP and mouse GIP(3-30) to significantly inhibit GIP-stimulated insulin secretion, which was unaffected by human GIP(5-30), GIP(3-42) or GIP(5-42). As would be expected, all peptides had reduced glucose-lowering ability when compared to native GIP, although peptides with their C-terminus intact, namely human GIP(3-42) or GIP(5-42) were less potent as GIPR antagonists. The findings were indicative of the C-termini importance in receptor activation and consistent with published literature (Hansen *et al.,* 2016). This was further supported by findings that at higher dosages, the C-terminally truncated human GIP(3-30), Pro^3(3-30)GIP and GIP(5-30) displayed superior GIP antagonistic properties. Although further assessment would be required to be definitive, the data suggest that human Pro^3(3-30)GIP has greater ligand affinity without receptor activation, which could be attributed to addition of a proline at position 3, as these attributes are not displayed by human GIP(3-30). Therefore, human Pro^3(3-30)GIP appeared to represent the most useful GIPR antagonist.

The findings of this study further support the previous literature on Pro^3GIP as a tool to block full GIP receptor activation (Gault *et al.,* 2007a; Irwin *et al.,* 2007; McClean *et al.,* 2007; Pathak *et al.,* 2015a). However, more in depth analysis including insulin secretion analysis, binding studies and assessment of longer-term biological effects in a suitable *in vivo* model would be required to be totally definitive. In addition, use of CRISPR/Cas9 and targeted genome editing (Nishimura and Fukagawa, 2017) to create a cell-line with specific knockout of the GIPR would also be useful to confirm specificity of these peptides.

7.6 Advancements of work and related limitations

The dual agonist peptides assessed in this thesis have shown that, under certain instances, there are major advantages of modulating naturally occurring peptides into multifunctional, dual receptor agonists. This approach broadens therapeutic applicability, which can be further enhanced by combining the dual agonist with another treatment option, such as a GLP-1 mimetic. However, it must also be noted

that there are limitations when developing monomeric peptides in comparison to the predictability of single receptor agents. This would include prediction of translation of benefits from the *in vitro* to the *in vivo* setting, as noted with acetyl-neurotensin(8-13)-xenin-8-Gln hybrid. More significantly, this may also raise the question of applicability of translation from the animal model to the clinical setting, due to the multifaceted mechanisms of T2DM (Fosgerau and Hoffmann, 2015). However, the data also encourage the premise of enhanced therapeutic applicability with triple gut hormone receptor agonism, by use of a GLP-1 mimetic in combination with either the GIP/xenin of NT/xenin hybrid peptides. This does raise the possibility of potential for generation of a single tri-agonist peptide for diabetes. Indeed, of late there has been some headway made in terms of generating and characterising triple-acting hybrid peptides that show clear antidiabetic promise (Capozzi *et al.,* 2018; Finan *et al.,* 2015; Fosgerau and Hoffmann, 2015), and this could be considered as a future avenue for the dual acting hybrids described here.

In addition, the work from this thesis also highlights the issues of interpretation and understanding of data derived from different established mouse models of diabetes. Thus, despite best efforts, no animal model can completely and accurately mimic the complex aetiology of human T2DM. Despite this obvious limitation, it is still noteworthy that for new T2DM drugs to make it towards human use, they must first show efficacy and safety in such rodent models. Further to this, modulation of GIP structure to produce a specific GIPR antagonist demonstrated how N- and C- termini truncations of the native peptide can dramatically alter the biological action. This could, as evidenced in Chapter 6, lead to generation of a suitable GIPR antagonist for the treatment of obesity and related diabetes (Irwin and Flatt, 2015). The limitations of currently characterised GIPR antagonists has been aptly described in a number of recent publications (Gasbjerg *et al.,* 2018ab; Hansen *et al*., 2016; Pathak *et al.,* 2015a; Sparre-Ulrich *et al.,* 2017). However, it should also be noted that a recently characterised dual GIP and GLP-1 receptor antagonist evoked significant reductions in body weight in T2DM patients (Frias *et al.,* 2018). Thus, the full impact of GIPR signalling on the development of obesity and related T2DM may well require further characterisation. Nonetheless, taken together, the current studies would suggest that whilst manipulating and integrating peptide structures to produce multi-acting hybrid peptides is encouraging, care is required to ensure that the overall impact on each

individual receptor binding and activation is not compromised. As such, small alterations in the structure of GIP can result in generation of potent GIPR antagonists. The timing of peptide administration could be another consideration as inducing beta cell rest during the light phase in mice and beta cell stimulation during their active dark phase has been shown to improved treatment effects such as reducing glucose concentrations and enhancing insulin sensitivity compared to other dosing regimens (Pathak *et al.,* 2017b). A final obvious limitation of peptide based therapies is the route of administration in humans, and the need for subcutaneous injection as opposed to oral delivery (Scheen *et al.,* 2017). However, recent advancements with possible oral delivery of the GLP-1 mimetic, semaglutide (Scheen, 2017), could dramatically change the landscape of incretin based therapies for diabetes.

7.7 Future work

This thesis has provided invaluable data and evidence of the therapeutic utility of gut-derived peptides with regards to T2DM and obesity therapy. However, further analysis is warranted to fully elucidate their treatment potential, including assessment of safety and testing in humans. In addition, investigation of the sustainability of therapeutic effects of the hybrids when the treatment regimen has ceased would be interesting, thus determining their potential treatment longevity. Essentially, long-lived benefits would suggest disease altering effects of the hybrid peptides would certainly be considered as a benefit. Additionally, a lipid challenge test as a supplementary assessment parameter following treatment would also be helpful with further understanding of lipid metabolism and flow cytometry to analyse *ex vivo* adipose tissue to assess inflammatory response variation amongst treatment groups. With molecular targets now a major focus in drug therapy, the analysis of peptides effects on micro RNAs (miRNAs) should also not be neglected. As such, miRNAs are now considered to be key regulators of gene expression within T2DM disease pathology including pancreatic beta cell dysfunction, proliferation and apoptosis as well as adipocyte regulation and related cardiovascular pathophysiology (Ding, Sun and Shan, 2017; Feng, Xing and Xie, 2016; Shantikumar *et al.,* 2012). Furthermore, knockout mice could be utilised to understand receptor activation as well as the utility of CRISPR/Cas9 technology to knockout specific receptors within cell-lines to establish

receptor balance of each hybrid is also of importance. In addition, an assay to directly assess the pharmacokinetic profile of each of the novel peptides would also provide valuable information for future work with experimental drugs, by offering more information in relation to optimum dosing schedules. With these additional studies, the ultimate aim would be to generate a scientific rationale for progression of these novel peptide therapies towards studies in humans.

7.8 Overall conclusion

Collectively the data accumulated from this thesis demonstrates that designer hybrid peptides and combination therapy can elicit positive biological effects and improved therapeutic efficacy in T2DM. The observed benefits on glycaemic control and circulating lipids are directly in line with the new 2018 treatment goals published by the American Diabetes Association (ADA) and the European Association for the study of Diabetes (EASD). This consortium have noted that antidiabetic drugs should reduce hyperglycaemia, minimise weight gain and lower cardiovascular risk (Davies *et al.*, 2018). It is clear that the novel drugs described within this thesis warrant further investigation as potential T2DM treatments based on these recognised and approved treatment goals.

Chapter 8

References

Al-Sabah, S. (2015) Molecular Pharmacology of the Incretin Receptors. *Medical Principles and Practic: International Journal of the Kuwait University, Health Science Centre,* **25, Suppl 1** S15-21

Al Tulaihi, B. and Alhabib, S. (2017) Uncertainties around incretin-based therapies: A literature review. *Saudi Pharmaceutical Journal: SPJ: The Official Publication of the Saudi Pharmaceutical Society,* **25**, 1-7.

Alarcon, C., Boland, B.B., Uchizono, Y., Moore, P.C., Peterson, B., Rajan, S., Rhodes, O.S., Noske, A.B., Haataja, L., Arvan, P., Marsh, B.J., Austin, J. and Rhodes, C.J. (2016) Pancreatic beta-Cell Adaptive Plasticity in Obesity Increases Insulin Production but Adversely Affects Secretory Function. *Diabetes,* **65**, 438-450.

Al-Goblan, A.S., Al-Alfi, M.A. and Khan, M.Z. (2014) Mechanism linking diabetes mellitus and obesity. *Diabetes, Metabolic Syndrome and Obesity: Targets and Therapy,* **7**, 587-591.

Anlauf, M., Weihe, E., Hartschuh, W., Hamscher, G. and Feurle, G.E. (2000) Localization of xenin-immunoreactive cells in the duodenal mucosa of humans and various mammals. *The Journal of Histochemistry and Cytochemistry: Official Journal of the Histochemistry Society,* **48**, 1617-1626.

Baggio, L.L. and Drucker, D.J. (2007) Biology of Incretins: GLP-1 and GIP. *Gastroenterology,* **132**, 2131-2157.

Barchetta, I., Cimini, F.A., Capoccia, D., Bertoccini, L., Ceccarelli, V., Chiappetta, C., Leonetti, F., Di Cristofano, C., Silecchia, G., Orho-Melander, M., Melander, O. and Cavallo, M.G. (2018) Neurotensin Is a Lipid-Induced Gastrointestinal Peptide Associated with Visceral Adipose Tissue Inflammation in Obesity. *Nutrients,* **10**, 526.

Bhat, V.K., Kerr, B.D., Flatt, P.R. and Gault, V.A. (2013) A novel GIP-oxyntomodulin hybrid peptide acting through GIP, glucagon and GLP-1 receptors exhibits weight reducing and anti-diabetic properties. *Biochemical Pharmacology,* **85**, 1655-1662.

Bhavya, S., Lew, P.S. and Mizuno, T.M. (2018) Stimulation of white adipose tissue lipolysis by xenin, a neurotensin-related peptide. *Biochemical and Biophysical Research Communications,* **498**, 842-848.

Boden, G. (2008) Obesity and free fatty acids. *Endocrinology and Metabolism Clinics of North America,* **37**, 635-46.

Boden, G. (2011) Obesity, insulin resistance and free fatty acids. *Current Opinion in Endocrinology, Diabetes, and Obesity,* **18**, 139-143.

Boules, M., Li, Z., Smith, K., Fredrickson, P. and Richelson, E. (2013) Diverse roles of neurotensin agonists in the central nervous system. *Frontiers in Endocrinology,* **4**, 36.

Brereton, M.F., Vergari, E., Zhang, Q. and Clark, A. (2015) Alpha-, Delta- and PP-cells: Are They the Architectural Cornerstones of Islet Structure and Co-ordination? *The Journal of Histochemistry and Cytochemistry: Official Journal of the Histochemistry Society,* **63**, 575-591.

Campbell, J.E. and Drucker, D.J. (2013) Pharmacology, physiology, and mechanisms of incretin hormone action. *Cell Metabolism,* **17**, 819-837.

Cantley, J. and Ashcroft, F.M. (2015) Q&A: insulin secretion and type 2 diabetes: why do beta-cells fail? *BMC Biology,* **13**, 33.

Capozzi, M.E., DiMarchi, R.D., Tschop, M.H., Finan, B. and Campbell, J.E. (2018) Targeting the Incretin/Glucagon System with Triagonists to Treat Diabetes. *Endocrine Reviews,* **39**, 719-738.

Chaudhury, A., Duvoor, C., Reddy Dendi, V.S., Kraleti, S., Chada, A., Ravilla, R., Marco, A., Shekhawat, N.S., Montales, M.T., Kuriakose, K., Sasapu, A., Beebe, A., Patil, N., Musham, C.K., Lohani, G.P. and Mirza, W. (2017) Clinical Review of Antidiabetic Drugs: Implications for Type 2 Diabetes Mellitus. Management. *Frontiers in Endocrinology,* **8**, 6.

Cheng, A.Y. and Fantus, I.G. (2005) Oral antihyperglycemic therapy for type 2 diabetes mellitus. *CMAJ: Canadian Medical Association Journal,* **172**, 213-226.

Chowdhury, S., Wang, S., Patterson, B.W., Reeds, D.N. and Wice, B.M. (2013) The combination of GIP plus xenin-25 indirectly increases pancreatic polypeptide release in humans with and without type 2 diabetes mellitus. *Regulatory Peptides,* **187**, 42-50.

Cooke, J.H., Patterson, M., Patel, S.R., Smith, K.L., Ghatei, M.A., Bloom, S.R. and Murphy, K.G. (2009) Peripheral and central administration of xenin and neurotensin suppress food intake in rodents. *Obesity (Silver Spring, Md.),* **17**, 1135-1143.

Coppola, T., Beraud-Dufour, S., Antoine, A., Vincent, J.P. and Mazella, J. (2008) Neurotensin protects pancreatic beta cells from apoptosis. *The International Journal of Biochemistry & Cell Biology,* **40**, 2296-2302.

Craig, S.L., Gault, V.A. and Irwin, N. (2018) Emerging therapeutic potential for xenin and related peptides in obesity and diabetes. *Diabetes/metabolism Research and Reviews,* **34**, e3006.

Creutzfeldt, W. (2005) The [pre-] history of the incretin concept. *Regulatory Peptides,* **128**, 87-91.

Dalvi, P.S., Nazarians-Armavil, A., Purser, M.J. and Belsham, D.D. (2012) Glucagon-like peptide-1 receptor agonist, exendin-4, regulates feeding-associated neuropeptides in hypothalamic neurons in vivo and in vitro. *Endocrinology,* **153**, 2208-2222.

Deacon, C.F. and Ahren, B. (2011) Physiology of incretins in health and disease. *The Review of Diabetic Studies: RDS,* **8**, 293-306.

Dendup, T., Feng, X., Clingan, S. and Astell-Burt, T. (2018) Environmental Risk Factors for Developing Type 2 Diabetes Mellitus: A Systematic Review. *International Journal of Environmental Research and Public Health,* **15(1)**, 78.

Devader, C., Beraud-Dufour, S., Coppola, T. and Mazella, J. (2013) The anti-apoptotic role of neurotensin. *Cells,* **2**, 124-135.

Diabetes UK (2014) *Diabetes: Facts and Stats.* [Online] Available from: https://www.diabetes.org.uk/Documents/About%20Us/Statistics/Diabetes-key-stats-guidelines-April2014.pdf [Accessed 18/07/18].

Diabetes UK (2018) *Diagnostic criteria for diabetes* [Online] Available from: https://www.diabetes.org.uk/professionals/position-statements-reports/diagnosis-

ongoing-management-monitoring/new_diagnostic_criteria_for_diabetes [Accessed 18/7/18].

Ding, Y., Sun, X. and Shan, P.F. (2017) MicroRNAs and Cardiovascular Disease in Diabetes Mellitus. *BioMed Research International*, **2017**, 4080364.

Evans, J.L., Balkan, B., Chuang E., Chuang, E. and Rushakoff. R.J. (2016) *Oral and Injectable (Non-insulin) Pharmacological Agents for Type 2 Diabetes*. Endotext.org. [Online] Available from: https://www.ncbi.nlm.nih.gov/books/NBK279141/ [Accessed 20/7/18].

Faita, F., Di Lascio, N., Rossi, C., Kusmic, C. and Solini, A. (2018) Ultrasonographic Characterization of the db/db Mouse: An Animal Model of Metabolic Abnormalities. *Journal of Diabetes Research*, **2018**, 4561309.

Feifel, D., Goldenberg, J., Melendez, G. and Shilling, P.D. (2010) The acute and subchronic effects of a brain-penetrating, neurotensin-1 receptor agonist on feeding, body weight and temperature. *Neuropharmacology*, **58**, 195-198.

Feng, J., Xing, W. and Xie, L. (2016) Regulatory Roles of MicroRNAs in Diabetes. *International Journal of Molecular Sciences*, **17**, 10.3390/ijms17101729.

Ferrannini, E. and Solini, A. (2012) SGLT2 inhibition in diabetes mellitus: rationale and clinical prospects. *Nature Reviews. Endocrinology*, **8**, 495-502.

Feurle, G.E., Hamscher, G., Kusiek, R., Meyer, H.E. and Metzger, J.W. (1992) Identification of xenin, a xenopsin-related peptide, in the human gastric mucosa and its effect on exocrine pancreatic secretion. *The Journal of Biological Chemistry*, **267**, 22305-22309.

Feurle, G.E., Heger, M., Niebergall-Roth, E., Teyssen, S., Fried, M., Eberle, C., Singer, M.V. and Hamscher, G. (1997) Gastroenteropancreatic effects of xenin in the dog. *The Journal of Peptide Research: Official Journal of the American Peptide Society*, **49**, 324-330.

Feurle, G.E. (1998) Xenin--a review. *Peptides*, **19**, 609-615.

Feurle, G.E., Metzger, J.W., Grudinski, A. and Hamscher, G. (2002) Interaction of xenin with the neurotensin receptor of guinea pig enteral smooth muscles. *Peptides*, **23(3)**, 523-529.

Finan, B., Ma, T., Ottaway, N., Muller, T.D., Habegger, K.M., Heppner, K.M., Kirchner, H., Holland, J., Hembree, J., Raver, C., Lockie, S.H., Smiley, D.L., Gelfanov, V., Yang, B., Hofmann, S., Bruemmer, D., Drucker, D.J., Pfluger, P.T., Perez-Tilve, D., Gidda, J., Vignati, L., Zhang, L., Hauptman, J.B., Lau, M., Brecheisen, M., Uhles, S., Riboulet, W., Hainaut, E., Sebokova, E., Conde-Knape, K., Konkar, A., DiMarchi, R.D. and Tschop, M.H. (2013) Unimolecular dual incretins maximize metabolic benefits in rodents, monkeys, and humans. *Science Translational Medicine*, **5**, 151.

Finan, B., Yang, B., Ottaway, N., Smiley, D.L., Ma, T., Clemmensen, C., Chabenne, J., Zhang, L., Habegger, K.M., Fischer, K., Campbell, J.E., Sandoval, D., Seeley, R.J., Bleicher, K., Uhles, S., Riboulet, W., Funk, J., Hertel, C., Belli, S., Sebokova, E., Conde-Knape, K., Konkar, A., Drucker, D.J., Gelfanov, V., Pfluger, P.T., Muller, T.D., Perez-Tilve, D., DiMarchi, R.D. and Tschop, M.H. (2015) A rationally designed

monomeric peptide triagonist corrects obesity and diabetes in rodents. *Nature Medicine,* **21**, 27-36.

Flatt, P.R. and Bailey, C.J. (1981) Abnormal plasma glucose and insulin responses in heterozygous lean (ob/+) mice. *Diabetologia,* **20**, 573-577.

Fonseca, V.A. (2009) Defining and characterizing the progression of type 2 diabetes. *Diabetes Care,* **32**, **Suppl 2** S151-6.

Fosgerau, K. and Hoffmann, T. (2015) Peptide therapeutics: current status and future directions. *Drug Discovery Today,* **20**, 122-128.

Fowler, M., J. (2007) Diabetes Treatment, Part 2: Oral Agents for Glycemic Management. *Clinical Diabetes,* **25**, 131-134.

Fraker, P.J. and Speck, J.C., Jr. (1978) Protein and cell membrane iodinations with a sparingly soluble chloroamide, 1,3,4,6-tetrachloro-3a,6a-diphrenylglycoluril. *Biochemical and Biophysical Research Communications,* **80**, 849-857.

Freeman, J.S. (2009) Role of the incretin pathway in the pathogenesis of type 2 diabetes mellitus. *Cleveland Clinic Journal of Medicine,* **76**, **Suppl 5** S12-9.

Frias, J.P., Bastyr, E.J.,3rd, Vignati, L., Tschop, M.H., Schmitt, C., Owen, K., Christensen, R.H. and DiMarchi, R.D. (2017) The Sustained Effects of a Dual GIP/GLP-1 Receptor Agonist, NNC0090-2746, in Patients with Type 2 Diabetes. *Cell Metabolism,* **26**, 343-352.e2.

Frias, J.P., Nauck, M.A., Van, J., Kutner, M.E., Cui, X., Benson, C., Urva, S., Gimeno, R.E., Milicevic, Z., Robins, D. and Haupt, A. (2018) Efficacy and safety of LY3298176, a novel dual GIP and GLP-1 receptor agonist, in patients with type 2 diabetes: a randomised, placebo-controlled and active comparator-controlled phase 2 trial. *Lancet (London, England),* **18**, 32260-8.

Fusco, J., Xiao, X., Prasadan, K., Sheng, Q., Chen, C., Ming, Y.C. and Gittes, G. (2017) GLP-1/Exendin-4 induces beta-cell proliferation via the epidermal growth factor receptor. *Scientific Reports,* **7**, 9100-017-09898-4.

Gasbjerg, L.S., Gabe, M.B.N., Hartmann, B., Christensen, M.B., Knop, F.K., Holst, J.J. and Rosenkilde, M.M. (2018a) Glucose-dependent insulinotropic polypeptide (GIP) receptor antagonists as anti-diabetic agents. *Peptides,* **100**, 173-181.

Gasbjerg, L.S., Christensen, M.B., Hartmann, B., Lanng, A.R., Sparre-Ulrich, A.H., Gabe, M.B.N., Dela, F., Vilsboll, T., Holst, J.J., Rosenkilde, M.M. and Knop, F.K. (2018b) GIP(3-30)NH2 is an efficacious GIP receptor antagonist in humans: a randomised, double-blinded, placebo-controlled, crossover study. *Diabetologia,* **61**, 413-423.

Gault, V.A., Parker, J.C., Harriott, P., Flatt, P.R. and O'Harte, F.P. (2002) Evidence that the major degradation product of glucose-dependent insulinotropic polypeptide, GIP(3-42), is a GIP receptor antagonist in vivo. *The Journal of Endocrinology,* **175**, 525-533.

Gault, V.A., O'Harte, F.P., Harriott, P., Mooney, M.H., Green, B.D. and Flatt, P.R. (2003) Effects of the novel (Pro3)GIP antagonist and exendin(9-39)amide on GIP- and GLP-1-induced cyclic AMP generation, insulin secretion and postprandial insulin

release in obese diabetic (ob/ob) mice: evidence that GIP is the major physiological incretin. *Diabetologia*, **46**, 222-230.

Gault, V.A., McClean, P.L., Cassidy, R.S., Irwin, N. and Flatt, P.R. (2007a) Chemical gastric inhibitory polypeptide receptor antagonism protects against obesity, insulin resistance, glucose intolerance and associated disturbances in mice fed high-fat and cafeteria diets. *Diabetologia,* **50**, 1752-1762.

Gault, V.A., Hunter, K., Irwin, N., Green, B.D., Greer, B., Harriott, P., O'Harte, F.P.M. and Flatt, P.R. (2007b) Characterisation and biological activity of Glu3 amino acid substituted GIP receptor antagonists. *Archives of Biochemistry and Biophysics,* **461**, 263-274.

Gault, V.A., Kerr, B.D., Irwin, N. and Flatt, P.R. (2008) C-terminal mini-PEGylation of glucose-dependent insulinotropic polypeptide exhibits metabolic stability and improved glucose homeostasis in dietary-induced diabetes. *Biochemical Pharmacology,* **75**, 2325-2333.

Gault, V.A., Porter, D.W., Irwin, N. and Flatt, P.R. (2011) Comparison of sub-chronic metabolic effects of stable forms of naturally occurring GIP(1-30) and GIP(1-42) in high-fat fed mice. *The Journal of Endocrinology,* **208**, 265-271.

Gault, V.A., Martin, C.M., Flatt, P.R., Parthsarathy, V. and Irwin, N. (2015) Xenin-25[Lys13PAL]: a novel long-acting acylated analogue of xenin-25 with promising antidiabetic potential. *Acta Diabetologica*, **52**, 461-471.

Gault, V.A. (2018) RD Lawrence Lecture 2017 Incretins: the intelligent hormones in diabetes. *Diabetic Medicine: A Journal of the British Diabetic Association,* **35**, 33-40.

Good, D.J. (2012) Extending the reach of Exendin-4: new pathways in the control of body weight and glucose homeostasis. *Endocrinology*, **153**, 2051-2053.

Greenberg, A.S. and Obin, M.S. (2006) Obesity and the role of adipose tissue in inflammation and metabolism. *The American Journal of Clinical Nutrition*, **83**, 461S-465S.

Grunddal, K.V., Ratner, C.F., Svendsen, B., Sommer, F., Engelstoft, M.S., Madsen, A.N., Pedersen, J., Nohr, M.K., Egerod, K.L., Nawrocki, A.R., Kowalski, T., Howard, A.D., Poulsen, S.S., Offermanns, S., Backhed, F., Holst, J.J., Holst, B. and Schwartz, T.W. (2016) Neurotensin Is Coexpressed, Coreleased, and Acts Together With GLP-1 and PYY in Enteroendocrine Control of Metabolism. *Endocrinology,* **157**, 176-194.

Halban, P.A., Polonsky, K.S., Bowden, D.W., Hawkins, M.A., Ling, C., Mather, K.J., Powers, A.C., Rhodes, C.J., Sussel, L. and Weir, G.C. (2014) Beta-Cell Failure in Type 2 Diabetes: Postulated Mechanisms and Prospects for Prevention and Treatment. *The Journal of Clinical Endocrinology and Metabolism,* **99**, 1983-1992.

Hansen, K.B., Vilsboll, T. and Knop, F.K. (2010) Incretin mimetics: a novel therapeutic option for patients with type 2 diabetes - a review. *Diabetes, Metabolic Syndrome and Obesity: Targets and Therapy,* **3,** 155-163.

Hansen, L.S., Sparre-Ulrich, A.H., Christensen, M., Knop, F.K., Hartmann, B., Holst, J.J. and Rosenkilde, M.M. (2015) N- and C-terminally truncated forms of glucose-dependent insulinotropic polypeptide are high-affinity competitive antagonists of the human GIP receptor. *British Journal of Pharmacology,* **173**, 826-38.

Hasib, A., Ng, M.T., Gault, V.A., Khan, D., Parthsarathy, V., Flatt, P.R. and Irwin, N. (2017) An enzymatically stable GIP/xenin hybrid peptide restores GIP sensitivity, enhances beta cell function and improves glucose homeostasis in high-fat-fed mice. *Diabetologia,* **60**, 541-552.

Hasib, A., Ng, M.T., Khan, D., Gault, V.A., Flatt, P.R. and Irwin, N. (2018a) A novel GLP-1/xenin hybrid peptide improves glucose homeostasis, circulating lipids and restores GIP sensitivity in high fat fed mice. *Peptides,* **100**, 202-211.

Hasib, A., Ng, M.T., Khan, D., Gault, V.A., Flatt, P.R. and Irwin, N. (2018b) Characterisation and antidiabetic utility of a novel hybrid peptide, exendin-4/gastrin/xenin-8-Gln. *European Journal of Pharmacology,* **834**, 126-135.

Hinke, S.A., Gelling, R.W., Pederson, R.A., Manhart, S., Nian, C., Demuth, H.U. and McIntosh, C.H. (2002) Dipeptidyl peptidase IV-resistant [D-Ala(2)]glucose-dependent insulinotropic polypeptide (GIP) improves glucose tolerance in normal and obese diabetic rats. *Diabetes,* **51**, 652-661.

Hinke, S.A., Manhart, S., Speck, M., Pederson, R.A., Demuth, H.U. and McIntosh, C.H. (2004) In depth analysis of the N-terminal bioactive domain of gastric inhibitory polypeptide. *Life Sciences,* **75(15)**, 1857-1870.

Irwin, N., Green, B.D., Parker, J.C., Gault, V.A., O'Harte, F.P. and Flatt, P.R. (2006) Biological activity and antidiabetic potential of synthetic fragment peptides of glucose-dependent insulinotropic polypeptide, GIP(1-16) and (Pro3)GIP(1-16). *Regulatory Peptides,* **135**, 45-53.

Irwin, N., McClean, P.L., O'Harte, F.P., Gault, V.A., Harriott, P. and Flatt, P.R. (2007) Early administration of the glucose-dependent insulinotropic polypeptide receptor antagonist (Pro3)GIP prevents the development of diabetes and related metabolic abnormalities associated with genetically inherited obesity in ob/ob mice. *Diabetologia,* **50**, 1532-1540.

Irwin, N. and Flatt, P.R. (2009) Evidence for beneficial effects of compromised gastric inhibitory polypeptide action in obesity-related diabetes and possible therapeutic implications. *Diabetologia,* **52**, 1724-1731.

Irwin, N., McClean, P.L., Patterson, S., Hunter, K. and Flatt, P.R. (2009) Active immunisation against gastric inhibitory polypeptide (GIP) improves blood glucose control in an animal model of obesity-diabetes. *Biological Chemistry,* **390**, 75-80.

Irwin, N. and Flatt, P.R. (2015) New perspectives on exploitation of incretin peptides for the treatment of diabetes and related disorders. *World Journal of Diabetes,* **6**, 1285-1295.

Jackson, S.H., Martin, T.S., Jones, J.D., Seal, D. and Emanuel, F. (2010) Liraglutide (victoza): the first once-daily incretin mimetic injection for type-2 diabetes. *P & T: A Peer-Reviewed Journal for Formulary Management,* **35**, 498-529.

Kaku, K. (2010) Pathophysiology of Type 2 Diabetes and Its Treatment Policy. *Japan Medical Association Journal, **53***, 41-46.

Kanoski, S.E., Hayes, M.R. and Skibicka, K.P. (2016) GLP-1 and weight loss: unraveling the diverse neural circuitry. *American Journal of Physiology, Regulatory, Integrative and Comparative Physiology,* **310**, 885-95.

Katsuda, Y., Ohta, T., Shinohara, M., Bin, T. and Yamada, T. (2013) Diabetic mouse models. *Open Journal of Animal Sciences*, **3**, 334-342.

Kerbel, B., Badal, K., Sundarrajan, L., Blanco, A. and Unniappan, S. (2018) Xenin is a novel anorexigen in goldfish (Carassius auratus). *PloS One,* **13**, e0197817.

Kerr, B.D., Flatt, A.J., Flatt, P.R. and Gault, V.A. (2011) Characterization and biological actions of N-terminal truncated forms of glucose-dependent insulinotropic polypeptide. *Biochemical and Biophysical Research Communications,* **404**, 870-876.

Khan, D., Vasu, S., Moffett, R.C., Gault, V.A., Flatt, P.R. and Irwin, N. (2017) Locally produced xenin and the neurotensinergic system in pancreatic islet function and beta-cell survival. *Biological Chemistry,* **399**, 79-92.

Kim, E.R., Lew, P.S., Spirkina, A. and Mizuno, T.M. (2016) Xenin-induced feeding suppression is not mediated through the activation of central extracellular signal-regulated kinase signalling in mice. *Behavioural Brain Research,* **312**, 118-126.

King, A.J. (2012) The use of animal models in diabetes research. *British Journal of Pharmacology,* **166**, 877-894.

Kitabgi, P. (2006) Differential processing of pro-neurotensin/neuromedin N and relationship to pro-hormone convertases. *Peptides,* **27**, 2508-2514.

Kooijman, S., Wang, Y., Parlevliet, E.T., Boon, M.R., Edelschaap, D., Snaterse, G., Pijl, H., Romijn, J.A. and Rensen, P.C. (2015) Central GLP-1 receptor signalling accelerates plasma clearance of triacylglycerol and glucose by activating brown adipose tissue in mice. *Diabetologia,* **58**, 2637-2646.

Lacy, P.E. and Kostianovsky, M. (1967) Method for the isolation of intact islets of Langerhans from the rat pancreas. *Diabetes,* **16**, 35-39.

Leckstrom, A., Kim, E.R., Wong, D. and Mizuno, T.M. (2009) Xenin, a gastrointestinal peptide, regulates feeding independent of the melanocortin signaling pathway. *Diabetes,* **58**, 87-94.

Leinninger, G.M., Opland, D.M., Jo, Y.H., Faouzi, M., Christensen, L., Cappellucci, L.A., Rhodes, C.J., Gnegy, M.E., Becker, J.B., Pothos, E.N., Seasholtz, A.F., Thompson, R.C. and Myers, M.G., Jr. (2011) Leptin action via neurotensin neurons controls orexin, the mesolimbic dopamine system and energy balance. *Cell Metabolism,* **14**, 313-323.

Mabilleau, G., Gobron, B., Bouvard, B. and Chappard, D. (2018) Incretin-based therapy for the treatment of bone fragility in diabetes mellitus. *Peptides,* **100**, 108-113.

MacDonald, P.E., El-Kholy, W., Riedel, M.J., Salapatek, A.M., Light, P.E. and Wheeler, M.B. (2002) The multiple actions of GLP-1 on the process of glucose-stimulated insulin secretion. *Diabetes,* **51**, **Suppl 3** S434-42.

Marchetti, P., Lupi, R., Del Guerra, S., Bugliani, M., D'Aleo, V., Occhipinti, M., Boggi, U., Marselli, L. and Masini, M. (2009) Goals of treatment for type 2 diabetes: beta-cell preservation for glycemic control. *Diabetes Care,* **32**, **Suppl 2** S178-83.

Marin-Penalver, J.J., Martin-Timon, I. and Del Canizo-Gomez, F.J. (2016) Management of hospitalized type 2 diabetes mellitus patients. *Journal of Translational Internal Medicine,* **4**, 155-161.

Martin, C.M., Gault, V.A., McClean, S., Flatt, P.R. and Irwin, N. (2012) Degradation, insulin secretion, glucose-lowering and GIP additive actions of a palmitate-derivatised analogue of xenin-25. *Biochemical Pharmacology,* **84**, 312-319.

Martin, C.M., Irwin, N., Flatt, P.R. and Gault, V.A. (2013) A novel acylated form of (d-Ala(2))GIP with improved antidiabetic potential, lacking effect on body fat stores. *Biochimica Et Biophysica Acta,* **1830**, 3407-3413.

Martin, C.M., Parthsarathy, V., Pathak, V., Gault, V.A., Flatt, P.R. and Irwin, N. (2014) Characterisation of the biological activity of xenin-25 degradation fragment peptides. *The Journal of Endocrinology,* **221**, 193-200.

Martin, C.M., Parthsarathy, V., Hasib, A., Ng, M.T., McClean, S., Flatt, P.R., Gault, V.A. and Irwin, N. (2016) Biological Activity and Antidiabetic Potential of C-Terminal Octapeptide Fragments of the Gut-Derived Hormone Xenin. *PloS One,* **11**, e0152818.

Mayo Clinic (2014) *Diabetes: Complications* [Online] Available from: http://www.mayoclinic.org/diseases-conditions/diabetes/basics/complications/con-20033091 [Accessed 18/07/18].

Mazella, J., Beraud-Dufour, S., Devader, C., Massa, F. and Coppola, T. (2012) Neurotensin and its receptors in the control of glucose homeostasis. *Frontiers in Endocrinology,* **3**, 143.

McClean, P.L., Irwin, N., Cassidy, R.S., Holst, J.J., Gault, V.A. and Flatt, P.R. (2007) GIP receptor antagonism reverses obesity, insulin resistance, and associated metabolic disturbances induced in mice by prolonged consumption of high-fat diet. *American Journal of Physiology, Endocrinology and Metabolism,* **293**, 1746-55.

McClean, P.L., Irwin, N., Hunter, K., Gault, V.A. and Flatt, P.R. (2008) (Pro(3))GIP[mPEG]: novel, long-acting, mPEGylated antagonist of gastric inhibitory polypeptide for obesity-diabetes (diabesity) therapy. *British Journal of Pharmacology,* **155**, 690-701.

McClenaghan, N.H., Barnett, C.R., Ah-Sing, E., Abdel-Wahab, Y.H., O'Harte, F.P., Yoon, T.W., Swanston-Flatt, S.K. and Flatt, P.R. (1996a) Characterization of a novel glucose-responsive insulin-secreting cell line, BRIN-BD11, produced by electrofusion. *Diabetes,* **45**, 1132-1140.

McClenaghan, N.H., Barnett, C.R., O'Harte, F.P. and Flatt, P.R. (1996b) Mechanisms of amino acid-induced insulin secretion from the glucose-responsive BRIN-BD11 pancreatic B-cell line. *The Journal of Endocrinology,* **151**, 349-357.

McCreight, L.J., Bailey, C.J. and Pearson, E.R. (2016) Metformin and the gastrointestinal tract. *Diabetologia,* **59**, 426-435.

Meek, C.L., Lewis, H.B., Reimann, F., Gribble, F.M. and Park, A.J. (2016) The effect of bariatric surgery on gastrointestinal and pancreatic peptide hormones. *Peptides,* **77**, 28-37.

Mehta, A., Marso, S.P. and Neeland, I.J. (2017) Liraglutide for weight management: a critical review of the evidence. *Obesity Science & Practice,* **3**, 3-14.

Miller, R.A., Chu, Q., Xie, J., Foretz, M., Viollet, B. and Birnbaum, M.J. (2013) Biguanides suppress hepatic glucagon signalling by decreasing production of cyclic AMP. *Nature,* **494**, 256-260.

Mingrone, G., Nolfe, G., Gissey, G.C., Iaconelli, A., Leccesi, L., Guidone, C., Nanni, G. and Holst, J.J. (2009) Circadian rhythms of GIP and GLP1 in glucose-tolerant and in type 2 diabetic patients after biliopancreatic diversion. *Diabetologia,* **52**, 873-881.

Mingrone, G., Panunzi, S., De Gaetano, A., Guidone, C., Iaconelli, A., Leccesi, L., Nanni, G., Pomp, A., Castagneto, M., Ghirlanda, G. and Rubino, F. (2012) Bariatric surgery versus conventional medical therapy for type 2 diabetes. *The New England Journal of Medicine,* **366**, 1577-1585.

Mingrone, G., Panunzi, S., De Gaetano, A., Guidone, C., Iaconelli, A., Nanni, G., Castagneto, M., Bornstein, S. and Rubino, F. (2015) Bariatric-metabolic surgery versus conventional medical treatment in obese patients with type 2 diabetes: 5 year follow-up of an open-label, single-centre, randomised controlled trial. *Lancet (London, England),* **386**, 964-973.

Moffett, R.C., Patterson, S., Irwin, N. and Flatt, P.R. (2015) Positive effects of GLP-1 receptor activation with liraglutide on pancreatic islet morphology and metabolic control in C57BL/KsJ db/db mice with degenerative diabetes. *Diabetes/metabolism Research and Reviews,* **31**, 248-255.

Naitoh, R., Miyawaki, K., Harada, N., Mizunoya, W., Toyoda, K., Fushiki, T., Yamada, Y., Seino, Y. and Inagaki, N. (2008) Inhibition of GIP signaling modulates adiponectin levels under high-fat diet in mice. *Biochemical and Biophysical Research Communications,* **376**, 21-25.

Nakamura, T., Tanimoto, H., Mizuno, Y., Tsubamoto, Y. and Noda, H. (2012) Biological and functional characteristics of a novel low-molecular weight antagonist of glucose-dependent insulinotropic polypeptide receptor, SKL-14959, in vitro and in vivo. *Diabetes, Obesity & Metabolism,* 14, 511-517.

Nakamura, T., Tanimoto, H., Mizuno, Y., Okamoto, M., Takeuchi, M., Tsubamoto, Y. and Noda, H. (2018) Gastric inhibitory polypeptide receptor antagonist, SKL-14959, suppressed body weight gain on diet-induced obesity mice. *Obesity Science & Practice,* **4**, 194-203.

Nasteska, D., Harada, N., Suzuki, K., Yamane, S., Hamasaki, A., Joo, E., Iwasaki, K., Shibue, K., Harada, T. and Inagaki, N. (2014) Chronic reduction of GIP secretion alleviates obesity and insulin resistance under high-fat diet conditions. *Diabetes*, **63**, 2332-2343.

Nauck, M. (2016) Incretin therapies: highlighting common features and differences in the modes of action of glucagon-like peptide-1 receptor agonists and dipeptidyl peptidase-4 inhibitors. *Diabetes, Obesity & Metabolism,* **18**, 203-216.

NHS UK (2012) *Diabetes: cases and costs predicted to rise* [Online] Available from: http://www.nhs.uk/news/2012/04april/Pages/nhs-diabetes-costs-cases-rising.aspx [Accessed 18/07/18].

Nishimura, K. and Fukagawa, T. (2017) An efficient method to generate conditional knockout cell lines for essential genes by combination of auxin-inducible degron tag and CRISPR/Cas9. *Chromosome Research: An International Journal on the*

Molecular, Supramolecular and Evolutionary Aspects of Chromosome Biology, **25**, 253-260.

O'Brien, P.D., Sakowski, S.A. and Feldman, E.L. (2014) Mouse models of diabetic neuropathy. *ILAR Journal,* **54**, 259-272.

Olokoba, A.B., Obateru, O.A. and Olokoba, L.B. (2012) Type 2 diabetes mellitus: a review of current trends. *Oman Medical Journal,* **27**, 269-273.

Parthsarathy, V., Irwin, N., Hasib, A., Martin, C.M., McClean, S., Bhat, V.K., Ng, M.T., Flatt, P.R. and Gault, V.A. (2016) A novel chemically modified analogue of xenin-25 exhibits improved glucose-lowering and insulin-releasing properties. *Biochimica Et Biophysica Acta,* **1860**, 757-764.

Paschetta, E., Hvalryg, M. and Musso, G. (2011) Glucose-dependent insulinotropic polypeptide: from pathophysiology to therapeutic opportunities in obesity-associated disorders. *Obesity Reviews,* **12**, 813-828.

Pathak, V., Vasu, S., Flatt, P.R. and Irwin, N. (2014) Effects of chronic exposure of clonal beta-cells to elevated glucose and free fatty acids on incretin receptor gene expression and secretory responses to GIP and GLP-1. *Diabetes, Obesity & Metabolism,* **16**, 357-365.

Pathak, V., Gault, V.A., Flatt, P.R. and Irwin, N. (2015a) Antagonism of gastric inhibitory polypeptide (GIP) by palmitoylation of GIP analogues with N- and C-terminal modifications improves obesity and metabolic control in high fat fed mice. *Molecular and Cellular Endocrinology,* **401**, 120-129.

Pathak, V., Vasu, S., Gault, V.A., Flatt, P.R. and Irwin, N. (2015b) Sequential induction of beta cell rest and stimulation using stable GIP inhibitor and GLP-1 mimetic peptides improves metabolic control in C57BL/KsJ db/db mice. *Diabetologia,* **58**, 2144-2153.

Pathak, N.M., Millar, P.J.B., Pathak, V., Flatt, P.R. and Gault, V.A. (2018) Beneficial metabolic effects of dietary epigallocatechin gallate alone and in combination with exendin-4 in high fat diabetic mice. *Molecular and Cellular Endocrinology,* **460**, 200-208.

Pok, E.H. and Lee, W.J. (2014) Gastrointestinal metabolic surgery for the treatment of type 2 diabetes mellitus. *World Journal of Gastroenterology,* **20**, 14315-14328.

Pories, W.J. (2008) Bariatric surgery: risks and rewards. *The Journal of Clinical Endocrinology and Metabolism,* **93**, **Suppl 1** S89-96.

Psichas, A., Reimann, F. and Gribble, F.M. (2015) Gut chemosensing mechanisms. *The Journal of Clinical Investigation,* **125**, 908-917.

Public Health England (2018) *Health matters: preventing Type 2 Diabetes* [Online] Available from: https://www.gov.uk/government/publications/health-matters-preventing-type-2-diabetes/health-matters-preventing-type-2-diabetes [Accessed 18/07/18].

Qatanani, M. and Lazar, M.A. (2007) Mechanisms of obesity-associated insulin resistance: many choices on the menu. *Genes & Development,* **21**, 1443-1455.

Randle, P.J., Garland, P.B., Hales, C.N. and Newsholme, E.A. (1963) The glucose fatty-acid cycle. Its role in insulin sensitivity and the metabolic disturbances of diabetes mellitus. *Lancet (London, England)*, **281**, 785-789.

Ratner, C., Skov, L.J., Raida, Z., Bachler, T., Bellmann-Sickert, K., Le Foll, C., Sivertsen, B., Dalboge, L.S., Hartmann, B., Beck-Sickinger, A.G., Madsen, A.N., Jelsing, J., Holst, J.J., Lutz, T.A., Andrews, Z.B. and Holst, B. (2016) Effects of Peripheral Neurotensin on Appetite Regulation and Its Role in Gastric Bypass Surgery. *Endocrinology*, **157**, 3482-3492.

Ravn, P., Madhurantakam, C., Kunze, S., Matthews, E., Priest, C., O'Brien, S., Collinson, A., Papworth, M., Fritsch-Fredin, M., Jermutus, L., Benthem, L., Gruetter, M. and Jackson, R.H. (2013) Structural and pharmacological characterization of novel potent and selective monoclonal antibody antagonists of glucose-dependent insulinotropic polypeptide receptor. *The Journal of Biological Chemistry*, **288**, 19760-19772.

Redinger, R.N. (2007) The pathophysiology of obesity and its clinical manifestations. *Gastroenterology & Hepatology*, **3**, 856-863.

Rehfeld, J.F. (2012) Beginnings: a reflection on the history of gastrointestinal endocrinology. *Regulatory Peptides*, **177**, **Suppl 1** S1-5.

Rehfeld, J.F. (2015) Gastrointestinal hormone research - with a Scandinavian annotation. *Scandinavian Journal of Gastroenterology*, **50**, 668-679.

Roder, P.V., Wu, B., Liu, Y. and Han, W. (2016) Pancreatic regulation of glucose homeostasis. *Experimental & Molecular Medicine*, **48**, e219.

Rohrborn, D., Wronkowitz, N. and Eckel, J. (2015) DPP4 in Diabetes. *Frontiers in Immunology*, **6**, 386.

Rosenstock, J., Hansen, L., Zee, P., Li, Y., Cook, W., Hirshberg, B. and Iqbal, N. (2015) Dual add-on therapy in type 2 diabetes poorly controlled with metformin monotherapy: a randomized double-blind trial of saxagliptin plus dapagliflozin addition versus single addition of saxagliptin or dapagliflozin to metformin. *Diabetes Care*, **38**, 376-383.

Sadry, S.A. and Drucker, D.J. (2013) Emerging combinatorial hormone therapies for the treatment of obesity and T2DM. *Nature Reviews. Endocrinology*, **9**, 425-433.

Schauer, P.R., Bhatt, D.L., Kirwan, J.P., Wolski, K., Aminian, A., Brethauer, S.A., Navaneethan, S.D., Singh, R.P., Pothier, C.E., Nissen, S.E., Kashyap, S.R. and STAMPEDE Investigators. (2017) Bariatric Surgery versus Intensive Medical Therapy for Diabetes - 5-Year Outcomes. *The New England Journal of Medicine*, **376**, 641-651.

Scheen, A.J. (2017) Semaglutide: a promising new glucagon-like peptide-1 receptor agonist. *The Lancet.Diabetes & Endocrinology*, **5**, 236-238.

Schroeder, L.E. and Leinninger, G.M. (2018) Role of central neurotensin in regulating feeding: Implications for the development and treatment of body weight disorders. *Biochimica et Biophysica Acta*, **1864**, 900-916.

Seino, Y., Fukushima, M. and Yabe, D. (2010) GIP and GLP-1, the two incretin hormones: Similarities and differences. *Journal of Diabetes Investigation*, **1**, 8-23.

Shah, M. and Vella, A. (2014) Effects of GLP-1 on appetite and weight. *Reviews in Endocrine & Metabolic Disorders,* **15**, 181-187.

Shantikumar, S., Caporali, A. and Emanueli, C. (2012) Role of microRNAs in diabetes and its cardiovascular complications. *Cardiovascular Research,* **93**, 583-593.

Silvestre, R.A., Rodriguez-Gallardo, J., Egido, E.M., Hernandez, R. and Marco, J. (2003) Stimulatory effect of xenin-8 on insulin and glucagon secretion in the perfused rat pancreas. *Regulatory Peptides,* **115**, 25-29.

Singh, A.K., Singh, R. and Kota, S.K. (2015) Bariatric surgery and diabetes remission: Who would have thought it? *Indian Journal of Endocrinology and Metabolism,* **19**, 563-576.

Skow, M.A., Bergmann, N.C. and Knop, F.K. (2016) Diabetes and obesity treatment based on dual incretin receptor activation: 'twincretins'. *Diabetes, Obesity & Metabolism,* **18**, 847-854.

Sparre-Ulrich, A.H., Hansen, L.S., Svendsen, B., Christensen, M., Knop, F.K., Hartmann, B., Holst, J.J. and Rosenkilde, M.M. (2015) Species-specific action of (Pro3)GIP - an efficacious agonist on human GIP receptor, but partial agonist and competitive antagonist on rat and mouse GIP receptors. *British Journal of Pharmacology,* **173**, 27-38.

Sparre-Ulrich, A.H., Gabe, M.N., Gasbjerg, L.S., Christiansen, C.B., Svendsen, B., Hartmann, B., Holst, J.J. and Rosenkilde, M.M. (2017) GIP(3-30)NH2 is a potent competitive antagonist of the GIP receptor and effectively inhibits GIP-mediated insulin, glucagon, and somatostatin release. *Biochemical Pharmacology,* **131**, 78-88.

Srinivasan, K. and Ramarao, P. (2007) Animal models in type 2 diabetes research: an overview. *The Indian Journal of Medical Research,* **125**, 451-472.

Steven, S., Hollingsworth, K.G., Al-Mrabeh, A., Avery, L., Aribisala, B., Caslake, M. and Taylor, R. (2016) Very Low-Calorie Diet and 6 Months of Weight Stability in Type 2 Diabetes: Pathophysiological Changes in Responders and Nonresponders. *Diabetes Care,* **39**, 808-815.

Taylor, A.I., Irwin, N., McKillop, A.M., Patterson, S., Flatt, P.R. and Gault, V.A. (2010) Evaluation of the degradation and metabolic effects of the gut peptide xenin on insulin secretion, glycaemic control and satiety. *The Journal of Endocrinology,* **207**, 87-93.

Track, N.S. (1980) The gastrointestinal endocrine system. *Canadian Medical Association Journal,* **122**, 287-292.

Troke, R.C., Tan, T.M. and Bloom, S.R. (2014) The future role of gut hormones in the treatment of obesity. *Therapeutic Advances in Chronic Disease,* **5**, 4-14.

Varol, C., Zvibel, I., Spektor, L., Mantelmacher, F.D., Vugman, M., Thurm, T., Khatib, M., Elmaliah, E., Halpern, Z. and Fishman, S. (2014) Long-acting glucose-dependent insulinotropic polypeptide ameliorates obesity-induced adipose tissue inflammation. *Journal of Immunology,* **193**, 4002-4009.

Vasu, S., Moffett, R.C., Thorens, B. and Flatt, P.R. (2014) Role of endogenous GLP-1 and GIP in beta cell compensatory responses to insulin resistance and cellular stress. *PloS One,* **9**, e101005.

Vogel, C.I., Scherag, A., Bronner, G., Nguyen, T.T., Wang, H.J., Grallert, H., Bornhorst, A., Rosskopf, D., Volzke, H., Reinehr, T., Rief, W., Illig, T., Wichmann, H.E., Schafer, H., Hebebrand, J. and Hinney, A. (2009) Gastric inhibitory polypeptide receptor: association analyses for obesity of several polymorphisms in large study groups. *BMC Medical Genetics,* **10**, 19.

Wang, Y.C., McPherson, K., Marsh, T., Gortmaker, S.L. and Brown, M. (2011) Health and economic burden of the projected obesity trends in the USA and the UK. *Lancet (London, England),* **378**, 815-825.

Weir, G.C. and Bonner-Weir, S. (2004) Five stages of evolving beta-cell dysfunction during progression to diabetes. *Diabetes,* **53**, **Suppl 3** S16-21.

World Health Organization (2016) *Global report on diabetes.* [Online] Available from: http://apps.who.int/iris/bitstream/handle/10665/204871/9789241565257_eng.pdf;jsessionid=9945BC56A16AD40EE19856A355CDDB63?sequence=1 [Accessed 18/7/18].

Winzell, M.S. and Ahren, B. (2004) The high-fat diet-fed mouse: a model for studying mechanisms and treatment of impaired glucose tolerance and type 2 diabetes. *Diabetes,* **53**, **Suppl 3** S215-9.

Xiong, S.W., Cao, J., Liu, X.M., Deng, X.M., Liu, Z. and Zhang, F.T. (2015) Effect of Modified Roux-en-Y Gastric Bypass Surgery on GLP-1, GIP in Patients with Type 2 Diabetes Mellitus. *Gastroenterology Research and Practice,* **2015**, 625196.

Yabe, D. and Seino, Y. (2011) Two incretin hormones GLP-1 and GIP: comparison of their actions in insulin secretion and beta cell preservation. *Progress in Biophysics and Molecular Biology,* **107**, 248-256.

Zhou, G., Myers, R., Li, Y., Chen, Y., Shen, X., Fenyk-Melody, J., Wu, M., Ventre, J., Doebber, T., Fujii, N., Musi, N., Hirshman, M.F., Goodyear, L.J. and Moller, D.E. (2001) Role of AMP-activated protein kinase in mechanism of metformin action. *The Journal of Clinical Investigation,* **108**, 1167-1174.

Zhou, H., Yamada, Y., Tsukiyama, K., Miyawaki, K., Hosokawa, M., Nagashima, K., Toyoda, K., Naitoh, R., Mizunoya, W., Fushiki, T., Kadowaki, T. and Seino, Y. (2005) Gastric inhibitory polypeptide modulates adiposity and fat oxidation under diminished insulin action. *Biochemical and Biophysical Research Communications,* **335**, 937-942.